S

ENGINEERING CHANGE NOTICE

Page 1 of 2

1. ECN 656349

Proj. ECN

2. ECN Category (mark one)		3. Originator's Name, Organization, MSIN, and Telephone No.	4. USQ Required?	5. Date
Supplemental	[ ]	R. D. Crowe, Nuclear Safety, R3-26, 376-8028	[ ] Yes [x] No	3/22/00
Direct Revision	[x]	6. Project Title/No./Work Order No.	7. Bldg./Sys./Fac. No.	8. Approval Designator
Change ECN	[ ]	Spent Nuclear Fuel Project	W-379	S
Temporary	[ ]	9. Document Numbers Changed by this ECN (includes sheet no. and rev.)	10. Related ECN No(s).	11. Related PO No.
Standby	[ ]	SNF-3328, Rev. 1	N/A	N/A
Supersedure	[ ]			
Cancel/Void	[ ]			

12a. Modification Work	12b. Work Package No.	12c. Modification Work Complete	12d. Restored to Original Condition (Temp. or Standby ECN only)
[ ] Yes (fill out Blk. 12b)	N/A	N/A	N/A
[x] No (NA Blks. 12b, 12c, 12d)		Design Authority/Cog. Engineer Signature & Date	Design Authority/Cog. Engineer Signature & Date

13a. Description of Change

13b. Design Baseline Document? [ ] Yes [x] No

Revision 2 incorporates modifications to support the Canister Storage Basin Final Safety Analysis Report.

14a. Justification (mark one)

Criteria Change	[x]	Design Improvement	[ ]	Environmental	[ ]	Facility Deactivation	[ ]
As-Found	[ ]	Facilitate Const	[ ]	Const. Error/Omission	[ ]	Design Error/Omission	[ ]

14b. Justification Details

These revisions respond to DOE review comments to Revision 0. These revisions clarify and expand detail to more fully explain assumptions, bases, and results.

15. Distribution (include name, MSIN, and no. of copies)

See attached distribution coversheet.

RELEASE STAMP

DATE: MAR 23 2000

STA: 4

HANFORD RELEASE

ID: 2

A-7900-013-2 (05/96) GEF095

ENGINEERING CHANGE NOTICE

1. ECN (use no. from pg. 1): 656349

16. Design Verification Required	17. Cost Impact				18. Schedule Impact (days)		
	ENGINEERING		CONSTRUCTION				
[ ] Yes	Additional	[ ] N/A	Additional	[ ]	Improvement	[ ]	N/A
[x] No	Savings	[ ]	Savings	[ ]	Delay	[ ]	

19. Change Impact Review: Indicate the related documents (other than the engineering documents identified on Side 1) that will be affected by the change described in Block 13. Enter [illegible]

SDD/DD	[ ]	Seismic/Stress Analysis	[ ]	Tank Calibration Manual	[ ]
Functional Design Criteria	[ ]	Stress/Design Report	[ ]	Health Physics Procedure	[ ]
Operating Specification	[ ]	Interface Control Drawing	[ ]	Spares Multiple Unit Listing	[ ]
Criticality Specification	[ ]	Calibration Procedure	[ ]	Test Procedures/Specification	[ ]
Conceptual Design Report	[ ]	Installation Procedure	[ ]	Component Index	[ ]
Equipment Spec.	[ ]	Maintenance Procedure	[ ]	ASME Coded Item	[ ]
Const. Spec.	[ ]	Engineering Procedure	[ ]	Human Factor Consideration	[ ]
Procurement Spec.	[ ]	Operating Instruction	[ ]	Computer Software	[ ]
Vendor Information	[ ]	Operating Procedure	[ ]	Electric Circuit Schedule	[ ]
OM Manual	[ ]	Operational Safety Requirement	[ ]	ICRS Procedure	[ ]
FSAR/SAR	[x]	IEFD Drawing	[ ]	Process Control Manual/Plan	[ ]
Safety Equipment List	[ ]	Cell Arrangement Drawing	[ ]	Process Flow Chart	[ ]
Radiation Work Permit	[ ]	Essential Material Specification	[ ]	Purchase Requisition	[ ]
Environmental Impact Statement	[ ]	Fac. Proc. Samp. Schedule	[ ]	Tickler File	[ ]
Environmental Report	[ ]	Inspection Plan	[ ]		[ ]
Environmental Permit	[ ]	Inventory Adjustment Request	[ ]		[ ]

20. Other Affected Documents: (NOTE: Documents listed below will not be revised by this ECN.) Signatures below indicate that the signing organization has been notified of other affected documents listed below.

Document Number/Revision	Document Number/Revision	Document Number Revision
	N/A	

21. Approvals

	Signature	Date	Signature	Date
Design Authority n/a				
Cog. Eng. R. D. Crowe	[signature]	3/22/00		
Cog. Mgr. R. L. Garrett	[signature]	3/22/00		
QA n/a				
Safety L. J. Garvin	[signature]	3/22/00	DEPARTMENT OF ENERGY Signature or a Control Number that tracks the Approval Signature	
Environ. n/a			ADDITIONAL	

SNF-3328
Revision 2

Canister Storage Building Design Basis Accident Analysis Documentation

Prepared for the U.S. Department of Energy
Assistant Secretary for Environmental Management

Project Hanford Management Contractor for the
U.S. Department of Energy under Contract DE-AC06-96RL13200
Fluor Hanford
P.O. Box 1000
Richland, Washington

SNF-3328
Revision 2
ECN 656349

198 Total Pages

Canister Storage Building Design Basis Accident Analysis Documentation

R. D. Crowe
XWest Group, Inc.

M. G. Piepho
P. D. Rittmann
Fluor Federal Services, Inc.

Y. J. Liu
XWest Group, Inc.

Date Published
March 2000

Prepared for the U.S. Department of Energy
Assistant Secretary for Environmental Management

Project Hanford Management Contractor for the
U.S. Department of Energy under Contract DE-AC06-96RL13200

Fluor Hanford
P.O. Box 1000
Richland, Washington

Release Approval 3/23/00 Date

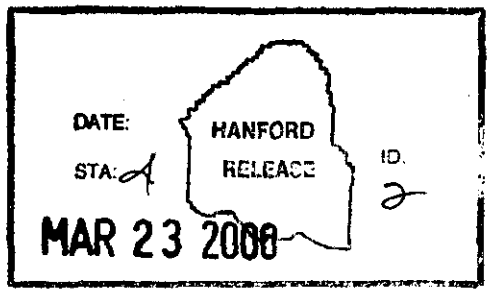

SNF-3328,
Revision 2

Abstract: This document provides the detailed accident analysis to support HNF-3553, *Spent Nuclear Fuel Project Final Safety Analysis Report*, Annex A, "Canister Storage Building Final Safety Analysis Report." All assumptions, parameters, and models used to provide the analysis of the design basis accidents are documented to support the conclusions in the Canister Storage Building Final Safety Analysis Report.

Key Words: Canister Storage Building, CSB, Accident Analysis, Design Basis Accident, DBA

RECORD OF REVISION	(1) Document Number SNF-3328, Rev. 2	Page 1
(2) Title Canister Storage Building Design Basis Accident Analysis Documentation		

CHANGE CONTROL RECORD			
(3) Revision	(4) Description of Change - Replace, Add, and Delete Pages	Authorized for Release	
		(5) Cog. Engr. Date	(6) Cog. Mgr. Date
	(7)		
0	**EDT: 624295**		
1	**ECN: 647516** *Revision 1 incorporates modifications to Revision 0 as a result of DOE review comments, dated August 1999.*	B. S. Lew	J. D. Carlson
2 RS	**ECN: 656349** *Revision 2 incorporates modifications to support the CSB FSAR Revision 0.*	R. D. Crowe 3/22/00	R. L. Garrett

CANISTER STORAGE BUILDING DESIGN BASIS ACCIDENT ANALYSIS DOCUMENTATION

SNF-3328
Revision 2

R. D. Crowe, XWest
Y. J. Liu, XWest
M. G. Piepho, Fluor Federal Services, Inc.
P. D. Rittmann, Fluor Federal Services, Inc.

March 2000

This page intentionally left blank.

CONTENTS

CONTENTS (Continued)

CONTENTS (Continued)

LIST OF FIGURES

LIST OF TABLES

LIST OF TABLES (Continued)

LIST OF TERMS

ALARA	as low as reasonably achievable
ARF	airborne release fraction
ARR	airborne release rate
BR	breathing rate
CSB	Canister Storage Building
CVDF	Cold Vacuum Drying Facility
DBA	design basis accident
DBE	design basis earthquake
DOE	U.S. Department of Energy
FFTF	Fast Flux Test Facility
HEPA	high-efficiency particulate air (filter)
LPF	leak path factor
MAR	material at risk
MCO	multi-canister overpack
MHM	multi-canister overpack handling machine
NRC	U.S. Nuclear Regulatory Commission
OSTA	overpack storage tube assembly
RF	respirable fraction
SNF	spent nuclear fuel
SSC	structure, system, and component
TSR	technical safety requirement
UD	dose per unit mass of uranium

This page intentionally left blank.

1.0 INTRODUCTION

The calculations in this document address the design basis accidents (DBAs) and beyond DBAs to support the analyses in the final safety analysis report for the Canister Storage Building (CSB). The objective is to determine the maximum quantity of radioactive particulate available at the CSB and to use that quantity to determine the amount of radioactive material that could be released during accidents. The radioactive material released is used to determine dose consequences to specific receptors. The dose consequences are compared with the appropriate evaluation guidelines and release limits to ascertain the need for preventive and mitigative controls.

1.1 DESIGN BASIS ACCIDENT SELECTION

The hazardous conditions identified by HNF-SD-SNF-HIE-001, *Canister Storage Building Hazard Analysis Report*, have been used to select candidate accidents for more detailed analysis. The general selection criteria used were consistent with the guidance provided in DOE-STD-3009-94, *Preparation Guide for U.S. Department of Energy Nonreactor Nuclear Facility Safety Analysis Reports*: "The range of accident scenarios analyzed in a SAR should be such that a complete set of bounding conditions to define the envelope of accident conditions to which the operation could be subjected are evaluated and documented."

The selection of candidate accidents was based on characterizing risk from, and developing controls for, a representative set of hazardous conditions. A hazardous condition is generally considered to be representative of other hazardous conditions if it has similar release characteristics and involves similar initiators. Hazardous conditions that represent the most severe consequences and the highest risk (a combination of frequency and consequences) within each set of representative hazards have been selected as candidate accidents for further analysis. The representative hazardous conditions bound conditions with lesser but similar potential consequences; represent the highest risk; or, while not necessarily bounding, present some unique but important phenomenological challenge to system safety. The accident selection process comprises five steps.

1. Initial screening. Hazardous conditions with unmitigated offsite consequences or onsite, collocated worker consequences are considered for representative accident selection through a ranking of relative, overall (frequency and consequences) risk.

2. Assignment of release attributes. Each hazardous condition is described with certain release attributes (event initiatives and release forms) related to uncontrolled release of the material at risk. At least one candidate accident is selected to represent each unique set of release conditions.

3. Creation of hazardous material release bins. After assigning release attributes, the hazardous conditions are collected to form release categories, or "bins." All hazardous

conditions with common initiators and release forms are grouped and ranked by estimated consequence and frequency. Representative and bounding accidents are chosen to represent all the hazardous conditions within a particular bin.

4. Selection of representative bounding hazardous conditions for each release attribute category. Within each release attribute bin, the most severe hazardous condition is selected. These accidents are the representative and bounding accidents selected for further quantitative analysis as DBAs.

5. Selection of unique hazardous conditions. Hazardous conditions are selected to represent additional unique causes within each release attribute bin. This is done to support development of controls for accidents with similar consequences but with different causes.

The hazardous conditions are grouped by candidate accident to facilitate incorporation of the information and conclusions from the accident analysis into the hazard analysis results when considering controls and hazard classification. An initial set of safety features that would serve to prevent or mitigate the postulated accident scenarios are identified in the hazard analysis, with a final set of safety features identified in the final safety analysis report. The hazard evaluation ranking performed in the hazard analysis identifies hazards and associated events that pose a challenge to offsite and onsite radiological dose evaluation guidelines. This ranking is used to select unique and representative accidents with sufficiently high risk estimates for further detailed quantitative evaluation as DBAs. Each of the DBAs analyzed represents a bounding case for a category of hazards and accidents. SNF-4042, *Evaluation of Accident Frequencies at the Canister Storage Building*, documents the derivation of the DBA frequency range.

The list of six candidate DBAs resulting from the hazards binning process for the CSB facility is presented in Table 1-1. Chapters 2.0 through 7.0 describe the analyses of these accidents.

Chapter 2.0 Mechanical Damage of Multi-Canister Overpack

An MCO, or the cask–MCO combination, subjected to an accidental drop, impact, or shear of sufficient magnitude could be damaged such that the MCO is breached or its internal geometry is compromised. Several potential accidents at the CSB that could damage the MCO with mechanical forces were identified in the hazard analysis. Three classifications of accidents were evaluated: drop of the MCO or cask–MCO, shear of the MCO by the MHM, and impacts to the MCO other than drops and shears. The unmitigated radiological offsite doses for all mechanical damage events are below the offsite release limits while the onsite doses are within evaluation guidelines for unlikely events.

Table 1-1. Binned Listing of Candidate Accidents. (2 sheets)

Candidate accident	Risk ranking[a]	Release or change energy[b]	Reference designator
Mechanical damage of MCO (Chapter 2.0)			
Possible mechanical damage of MCO due to a drop	5	Medium[c]	TV-G-13
	5	Medium[c]	SA-G-13a, -13b, -13c, -13d, -13e
	5	Medium[c]	OA-G-13c, 13d
	5	Medium[c]	WS-G-13a, 13b
	3	Medium[c]	SA-G-13f, 13g
	3	Medium[c]	OA G-13b
	–	Medium	OA-G-13a
Possible mechanical damage of MCO due to a shear	7	Low	SA-E-07
	7	Medium	SA-F-05
	7	Medium	SA-F-07b, -07c
	7	Low	OA-E-07
	7	Low	WS-E-07
	5	Low	SA-F-07d
	5	Low	SA-F-07e
	5	Low	OA-F-07a
	5	Low	OA-F-07b
	5	Low	WS-F-07a
	5	Low	WS-F-07b
Possible mechanical damage of MCO due to an impact other than drop or shear	5	Medium	SA-G-03a, -03c
	5	Medium	OA-G-03a
	5	Medium	WS-G-03a
	5	Low	SA-G-03d
	–	Medium	TV-G-03a, -03b
	–	Medium	SA-G-03b
	–	Medium	OA-G-03b
	–	Medium	OA-G-14a, -14b
	–	Medium	WS-G-03b
Gaseous release from the MCO (Chapter 3.0)			
Pressurized release from MCO	7	Medium	WS-G-04b, -06b, -07b
	5	Medium	WS-F-02, -05
	3	High	WS-H-06a, -07, -11
	–	High	WS-F-06
	–	Medium	WS-G-03b
MCO internal hydrogen deflagration (Chapter 4.0)			
Hydrogen deflagration	8	High	SA-J-06a
	5	High	OA-J-06a
	5	High	WS-J-06a
	5	High	WS-H-06b
	–	High	OA-J -06c

Table 1-1. Binned Listing of Candidate Accidents. (2 sheets)

Candidate accident	Risk ranking[a]	Release or change energy[b]	Reference designator
MCO external hydrogen deflagration (Chapter 5.0)			
External deflagration	7 –	High High	WS-L-11 OA-J-06b
Thermal runaway fuel reactions inside the MCO (Chapter 6.0)			
Runaway reaction	Note d	Note d.	WS-H-06b
Fuel reaction with water	8 6 6 6	Medium High High High	OU-R-01 SA-J-10b OA-J-10b WS-J-10b
Violations of design temperature criteria (Chapter 7.0)			
Violation of design temperature criteria	6	Medium	VL-B-07, -10, -11

[a]The risk ranking is derived from methodology found in DOE-STD-3009-94, *Preparation Guide for U.S. Department of Energy Nonreactor Nuclear Facility Safety Analysis Reports*, which correlates the consequence–frequency pairs assigned by HNF-SD-SNF-HIE-001, *Canister Storage Building Hazard Analysis Report*, to a single-scale risk ranking using a figure reproduced in Figure 3-1 of HNF-3553, *Spent Nuclear Fuel Project Final Safety Analysis Report*. Events identified by a dash (-) were considered S1 events in the hazard analysis but were initially considered of particular concern to the SNF Project and therefore were to be evaluated in more detail.

[b] Definition and use of energy release categories (high, medium, low) are based on guidance and examples in DOE-STD-3009-94.

[c]Energy was considered that could damage an MCO — falling onto the deck was viewed as higher energy than falling into the cask receiving or sampling/weld pit with impact absorbers present; falling into the tube with impact absorbers present was viewed as higher energy than falling into the cask receiving or sampling/weld pit with an impact absorber present.

[d]Before detailed analysis was performed, the hazard evaluation identified WS-H-06b as a serious hazard to be evaluated. Subsequent detailed analysis has shown that thermal runaway reactions are not possible at the CSB given limitation of water and resulting temperature.

MCO = multi-canister overpack.

Chapter 3.0 Calculations for Gaseous Release from the Multi-Canister Overpack

Events that may result in releases of radioactive material to the CSB facility from the uncontrolled release of the MCO's internal gas pressure were evaluated. A pressurized gaseous release would lead to entrainment and release of fuel particulate from the MCO and the creation of a radiological hazard. Several potential accidents at the CSB that could lead to a gaseous release were identified in the hazard analysis, including overpressurization caused by radiolytic decomposition and gaseous release caused by sampling system failure or operator error during sampling and backfilling operations. The unmitigated radiological offsite doses from all credible gaseous release events were calculated to be below the offsite release limits while the onsite doses were within evaluation guidelines for events in the anticipated category.

Chapter 4.0 Calculations for Multi-Canister Overpack Internal Hydrogen Explosion

Events were evaluated that could lead to the formation of flammable mixtures of hydrogen and oxygen within an MCO, which if ignited, could result in a deflagration inside the MCO. Several potential accidents at the CSB that could lead to an internal hydrogen deflagration were identified in the hazard analysis, including radiolytic decomposition of oxygen-containing compounds, introduction of oxygen into the MCO during recharging at the sampling/weld station, and ingress of oxygen following an MCO breach. The unmitigated radiological offsite doses from all internal hydrogen deflagration events were calculated to be below the offsite release limits while the onsite radiological doses were within evaluation guidelines for events in the unlikely category.

Chapter 5.0 Calculations for Multi-Canister Overpack External Hydrogen Explosion

Events were evaluated that could lead to the release of hydrogen from the MCO. The uncontrolled release of hydrogen could result in the formation of flammable mixtures of hydrogen and oxygen outside an MCO, which if ignited, could result in a deflagration. Several potential scenarios at the CSB that could lead to an external deflagration were identified in the hazard analysis, including deflagrations at the sampling/weld station, MHM, and storage tube. The unmitigated radiological offside doses from all credible external hydrogen deflagrations events were calculated to be below the offsite release limits while the onsite doses were within evaluation guidelines for events in the anticipated category.

Chapter 6.0 Calculations for Thermal Runaway Reactions Inside the Multi-Canister Overpack

A thermal runaway reaction is only possible in an MCO containing extremely high temperature fuel and excessive amounts of water. The accident evaluations for this DBA demonstrate that a thermal runaway accident is not credible at the CSB provided the fuel is properly loaded into the MCO at the K Basins and the dryness tests at the Cold Vacuum Drying Facility (CVDF) are satisfied. No release results from this event and the offsite release limits and onsite evaluation guidelines are satisfied.

Chapter 7.0 Calculations for Violation of Design Temperature Criteria

The hazard analysis identified the scenario for this accident as one in which the MCO and the safety-class CSB concrete structures could exceed their design temperatures due to a lack of cooling. The MCOs and CSB have been designed to provide sufficient heat transfer from the MCO so that unacceptable high temperatures will not be reached during normal handling and storage of the MCO at the CSB. Evaluation of the DBA demonstrates that situations in which a reduction in normal heat conduction causes overheating are precluded by the design of facility features such as the CSB vault and intake and exhaust structures. The accident is prevented and offsite release limits and onsite evaluation guidelines are satisfied

The consequences associated with each of the six bounding DBAs are summarized in Table 1-2. SNF-4042 contains frequency calculations for DBAs.

1.2 ACCIDENT ANALYSIS

This section presents the methodology used to develop the potential accidents that are described in Chapters 2.0 through 7.0. The accident analysis for each DBA starts with a description of the accident scenario with the major assumptions identified. The accident source term is then determined. Once a source term has been determined, onsite and offsite consequences are calculated for the atmospheric transport pathway. These consequences are then compared to evaluation guidelines for onsite consequences or release limits for offsite consequences for the identification of safety-class SSCs and TSRs.

Table 1-2. Summary of Consequences for Bounding Design Basis Accidents.

Accident category	Chapter	Offsite consequences		Onsite consequences	
		Release limit (rem) and frequency	Unmitigated (rem)	Evaluation guideline (rem) and frequency	Unmitigated (rem)
Mechanical damage of MCO	2.0	5.0 (unlikely)	2.2 E-03	10 (unlikely)	1.9
Gaseous release from MCO	3.0	0.5 (anticipated)	5.1 E-05	1.0 (anticipated)	4.5 E-02
MCO internal hydrogen deflagration	4.0	5.0 (unlikely)	3.4 E-03	10 (unlikely)	3.0
MCO external hydrogen deflagration	5.0	0.5 (anticipated)	4.3 E-04	1.0 (anticipated)	0.38
MCO thermal runaway reaction	6.0	—	Beyond extremely unlikely	—	Beyond extremely unlikely
Violation of design temperature criteria	7.0	—	Beyond extremely unlikely	—	Beyond extremely unlikely

Note: Offsite release limits and onsite evaluation guidelines cited are from Sellers, E.D., 1997, *Risk Evaluation Guidelines (REGs) to Ensure Inherently Safer Designs* (Letter 97-SFD-172 to H. J. Hatch, Fluor Daniel Hanford, Incorporated, August 26), U.S. Department of Energy, Richland Operations Office, Richland, Washington.

MCO = multi-canister overpack.

1.2.1 Source Term

The bounding source term used for the accident analyses is based on data for the fuel in the K East and K West Basins given in HNF-SD-SNF-TI-009, *105-K Basin Material Design Basis Feed Description for Spent Nuclear Fuel Project Facilities*. HNF-SD-SNF-TI-009 defines an inventory for safety analysis by considering inventories of Mark IV, Mark IA, and single-pass reactor fuel in the K Basins. High-burnup Mark IV fuel, the fuel type that results in the highest estimated radiological dose to people exposed to the material, was selected as the bounding inventory from the radiological dose perspective. Nuclear accountability records give the basis for the quantity, exposure variation, and decay time variation of the stored fuel. The radionuclide inventory was estimated from these data.

The MCO contains finely divided particulate material associated with oxidation of the fuel. This material includes an oxide layer on the fuel and particulate remaining on fuel surfaces and in crevices after fuel washing and racking into the MCO as well as expected increases in oxidation products that occur during queuing at the K Basins and processing at the CVDF. The particulate

inventory of the MCO dominates the airborne release. The radionuclide inventory of the sludge also is based on the high-burnup Mark IV fuel.

In calculating consequences in safety analysis, a number of phenomenological uncertainties are usually associated with the calculation factors. While it is not appropriate to ignore these uncertainties and use only best estimates, it also is not appropriate or meaningful to compound all the uncertainties and use an ultraconservative result that has no real practical meaning. The following approach has been developed to acknowledge the individual uncertainties in the calculation factors and to combine them into an overall uncertainty factor that can be applied to the best-estimate results to arrive at a bounding value at a predetermined confidence level.

Uncertainty (or error) factors and best estimates that are conservative but credible can be developed for many of the variables used in accident analyses. Multiplying each best estimate by an error factor yields a bounding value for that factor. If the uncertainties in all these factors are multiplied together, however, the result is unrealistically high because it is exceedingly unlikely that all these factors would simultaneously be at their most pessimistic bounding value. Therefore, a better approach is to calculate a source term using nominal (or median) values of the uncertain parameters and apply an appropriate uncertainty or error factor to the result. The method for combining uncertainty factors to arrive at an overall upper bound value is developed in the following paragraphs.

Assume a Lognormal Distribution for Each Variable. An upper bound value for a variable derived as the product of a number of other parameters can be determined using a simple sum-of-the-products-of-the-factors model. By using lognormal distributions, error factors for each of the individual variables can be combined into an overall error factor to obtain an upper bound value (e.g., 95th percentile).

The usefulness of the lognormal distribution comes from the central limit theorem, which states that the product of n independent random variables is a lognormally distributed random variable for large n (Apostolakis 1974). For example, the MAR is treated as the product of a number of processing parameters, such as fuel surface area, reaction rate, and processing time. It is therefore reasonable to describe the MAR as a variable with a lognormal distribution.

The ratio of the upper bound value to the median value (i.e., 50th percentile) is the error factor. The application of this type of bounding error factor is sufficiently conservative for determining the bounding consequences for an accident analysis as well as for comparing with the radiological evaluation guidelines and release limits.

Identify Nominal and Bounding Values and Assign a Percentile to the Bounding Value. For each identified parameter of the product used in the calculation, an estimate of the nominal or median value, $X_{50\%}$ (i.e., the value with 50% chance of being exceeded) is determined. An estimate of the upper bounding value, say $X_{95\%}$ (i.e., the value with 5% chance of being exceeded) also is identified. An error factor is calculated by dividing the bounding value by the nominal value of the parameter (i.e., $EF = X_{95\%}/X_{50\%}$).

Calculate the Standard Normal Variable for Each Percentile. A confidence level is assigned to the bounding value for each identified parameter. The standard normal variable corresponding to the 95% confidence interval is 1.645. It would be 1.0 for the 84% confidence level, 1.28 for the 90% confidence level, and 2.32 for the 99% confidence level.

Estimate the Overall Median. The overall nominal value is the product of the individual nominal values.

Estimate the Overall Error Factor. The overall error factor for the 95% confidence level is the natural antilogarithm of the product of 1.645 times the square root of the sum of the squares of the natural logarithm of the individual error factors.

Estimate the Ninety-Fifth Percentile Upper Bound. The 95% upper bound value is the product of the overall nominal value times the overall error factor.

The use of this method to estimate the bounding value is a reasonable approximation for estimating uncertainty. This method is rigorously correct when (1) the consequence is a product of independent factors, (2) the factor uncertainties can be approximated by the lognormal distribution, and (3) the uncertainties in these factors are uncorrelated. In the CSB accident analyses, this method is applied to the terms used to calculate the accident source terms. This results in a 95% confidence source term, which is still highly conservative when combined with bounding meteorological conditions, dose conversion factors, and the other dose parameters to which this uncertainty methodology was not applied.

In the following example, this method is applied to determining the amount of particulate suspended inside an MCO by the shock impact of an MCO drop. The estimated amount of suspended material depends on the airborne release fraction (ARF), respirable fraction (RF), the MAR, and the leak path factor (LPF). Statistical descriptors for each of these quantities are estimated from the literature or from SNF Project documentation as appropriate.

If an MCO were dropped, the impact of the drop would shock and suspend some amount of particulate matter within the MCO. Unless the MCO were also breached, none of this material would be released. However, for a breached MCO, the gas from the blowdown of the MCO would carry some fraction of the suspended material outside the MCO. The amount of respirable particulate released can be estimated using the following equation:

$$M_{released} = ARF \times RF \times MAR \times LPF_{MCO}$$

where

$M_{released}$ = mass of material released
ARF = airborne release fraction
RF = respirable fraction
MAR = material at risk
LPF_{MCO} = leak path factor for MCO.

The ARF is the fraction of the particulate powder inside the MCO (UO_2 particulate) that is suspended by the drop. The RF is the fraction of the suspended powder that is respirable. DOE-HDBK-3010-94, *Airborne Release Fractions/Rates and Respirable Fractions/Rates for Nonreactor Nuclear Facilities* (Section 4.4.3.3, "Impact"), provides a measured median ARF of 4×10^{-4} and RF of 0.2 from the impact of structural debris on powder. The recommended bounding ARF is 1.0×10^{-3}, used in conjunction with an RF of 1.0, as the bounding value (assumed to be the 95th percentile). The resuspension of material in the MCO, either by drop impact, MCO handling, or internal or external hydrogen deflagrations, is assumed to use these bounding values.

The approximate time needed for the particulate to settle following an impact can be determined using a Stokes settling equation for a tranquil gas. For the gas and particulate in the CSB scenario, the terminal settling velocity of the particulate and then the time required to settle may be described by (Hinds 1982, Equation 3.13):

$$V_{TS} = \frac{\rho_p d^2 g}{18 \eta}$$

where

V_{TS} = terminal settling velocity (cm/s)
ρ_p = particle density (g/cm^3)
d = particle diameter (cm)
g = gravitational constant (cm/s^2)
η = viscosity of air (dyn·s/cm^2)

and

$$T_{settle} = \frac{H}{V_{TS}}$$

where

T_{settle} = time required to settle (s)
H = settling height (cm).

For 1-μm-diameter particulate of density 5 g/cm^3, the terminal settling velocity is given by

$$V_{TS} = (5 \text{ g/cm}^3)\ (1 \times 10^{-4} \text{ cm})^2\ (980 \text{ cm/s}^2) / (18 \times 1.81 \times 10^{-4} \text{ P}) = 0.015 \text{ cm/s}\ .$$

The corresponding time to settle a characteristic length of 2 ft in an MCO is

$$T_{settle} = (2 \text{ ft})\ (30.48 \text{ cm/ft}) / (0.015 \text{ cm/s}) = 4{,}100 \text{ s} \approx 1.1 \text{ h}\ .$$

For particulate larger than 1 μm in diameter, the settling time will be less than that calculated for 1 μm. One or two hours after the impact, the particulate will have settled so that it must be resuspended before it could be released.

The amount of material available for release depends on the amount of particulate mass generated in the MCO during processing. This quantity is a function of processing times and temperatures as well as of the condition of the fuel in the MCO (e.g., exposed surface area of fuel). HNF-SD-SNF-TI-015, *Spent Nuclear Fuel Project Technical Databook*, provides two estimates of this quantity: one for the safety basis, which is considered the bounding value, and the other for the design basis, which is considered the nominal value. When the MCO is received at the CSB, the safety basis value is 26.3 kg UO_2 (23.1 kg uranium) and the design value is 0.613 kg UO_2 (0.54 kg uranium) (HNF-SD-SNF-TI-015). After 40 years of storage at the CSB, the safety basis value is 34 kg UO_2 (30 kg uranium) and the design basis is 2.1 kg UO_2 (1.85 kg uranium) (HNF-SD-SNF-TI-015). The 40-year design basis value is used as the nominal value and the 40-year safety basis value is assumed to be the 99th percentile value.

The pressure in the MCO at the start of the blowdown determines the fraction of the suspended particulate that is released. The initial pressure varies from 1.50 atm (corresponding to the helium fill pressure of 22 lb/in^2 absolute at the CVDF) to a maximum pressure of 5.2 atm (as defined in the Technical Databook [HNF-SD-SNF-TI-015]). To allow for some additional margin in the calculation, a pressure of 2.0 atm is considered nominal (50th percentile) and corresponds to an LPF of 0.5, while a pressure of 6.0 atm is considered bounding (95th percentile) and corresponds to an LPF of 0.83.

Table 1-3 shows factors used in calculating the overall bounding value of material suspended, 1.2 g. If the individual bounding values for each of the factors were to be multiplied together, the product of the individual bounding values is 25 g. This is equivalent to an uncertainty or error factor of over 330 (equivalent to a confidence level of 99.97%) compared with the calculated uncertainty factor of 15.7 (for the 95th percentile). This methodology is applied to the calculation of the source term for each of the DBAs as appropriate.

For both the onsite and offsite receptors at all accident frequency categories, the radiological effects are greater than the toxicological effects of an airborne emission. Therefore, the toxicological consequences of the postulated airborne releases will not require mitigating features beyond those required by the radiological consequences.

No routine chemical processes will be conducted in the CSB. Purging and backfilling the MCOs will involve the use of an inert gas (helium). Some chemicals, such as those used for equipment decontamination, may be used occasionally according to HNF-SD-SNF-CM-001, *Spent Nuclear Fuel Project Configuration Management Plan*. However, there are no chemical inventories of concern for safety analysis considerations.

Table 1-3. Example of Input Factors and Calculation for Determining Release of Particulate Suspended in Multi-Canister Overpack by Shock Impact.

Factor	Individual median values	Individual bounding values			EF	ln(EF)	ln(EF)/SNV
		Bounding	Percentile	SNV[a]			
MAR	1.85 kg U	30 kg U	99	2.326	16.22	2.79	1.198
ARF	4.00 E-04	1.00 E-03	95	1.645	2.50	0.92	0.557
RF	0.20	1.00	95	1.645	5.00	1.61	0.978
LPF_{MCO}[b]	0.50	0.83	95	1.645	1.67	0.51	0.311
Square root {sum of $[\ln(EF)/SNV]^2$}							1.673
Overall EF(95%) = exp(1.645 × square root {sum of $[\ln(EF)/SNV]^2$})							15.7
Overall median = product of the individual median values							7.4 E-02 g
Overall bounding (95%) = EF(95%) × overall median							1.2 g
Product of individual bounding values							25 g
Percentile of product of individual bounding values							99.97

[a]The standard normal variable corresponding to the 95% upper confidence limit is1.645. For the 99% upper confidence limit, the corresponding value is 2.326.

[b]LPF_{MCO} = (MCO pressure - 1 atm) / (MCO pressure). At a nominal MCO pressure of 2.0 atm, the LPF_{MCO} is 0.5, and at a bounding MCO pressure of 6.0 atm, the LPF_{MCO} is 0.83.

ARF = airborne release fraction.
EF = error factor (i.e., bounding value divided by nominal value).
ln(EF) = natural log of EF.
LPF = leak path factor.
MAR = material at risk.
MCO = multi-canister overpack.
RF = respirable fraction.
SNV = standard normal variable.

1.2.2 Consequence Analysis

Radiological inhalation dose consequences for each accident analyzed are based on the following factors:

- Mass of respirable airborne material released (M)
- Material at risk (MAR)
- Respirable fraction (RF)

- Airborne release fraction (ARF) or airborne release rate (ARR) and exposure duration
- Leak path factor (LPF)
- Atmospheric transport factor (χ/Q')
- Breathing rate (BR)
- Dose per unit mass of uranium (UD).

Some of these parameters are CSB-specific and are discussed below; others are based on common methods, assumptions, or methodology for the SNF Project and are fully described in Chapter 3.0 of HNF-3553, *Spent Nuclear Fuel Project Final Safety Analysis Report*.

The mass of respirable airborne material released (M) is determined by the specific CSB accident scenario. The quantity (M) is a function of the MAR, the ARF or ARR and RF, and the LPF of any passive structural enclosure that may cause deposition of an airborne release before the release enters the atmosphere. The LPF is based on a time-integrated calculation of aerosol deposition within and release from an enclosure of given dimensions with specified leakage area, pressure, and temperature differentials. The specific value of each parameter is determined in the individual DBA analysis and based on the physical phenomena of the accident; thus they are specific to CSB.

The atmospheric transport factor (χ/Q') is based on specific release conditions (e.g., ground level or elevated, long or short duration) and the receptor's distance from the release. While the methodology is common to the SNF Project, the atmospheric transport factor is the time-integrated normalized air concentration at the receptor's location, which is a measured distance from the CSB. The transport factor includes the dilution of an airborne contaminant caused by atmospheric mixing and turbulence. The air transport values used in this report have been generated using GXQ, which is described in WHC-SD-GN-SWD-30002, *GXQ Program User's Guide*. GXQ is a FORTRAN program for calculating atmospheric dispersion using site-specific wind data. It uses the Gaussian straight line model for both instantaneous and continuous releases. Several models are available that modify parameters within the Gaussian plume model to account for phenomena such as plume depletion, building wake, plume meander, gravitational settling, and plume rise. The building wake model from NRC Regulatory Guide 1.145, *Atmospheric Dispersion Models for Potential Accident Consequence Assessments at Nuclear Power Plants*, was use to model CSB building effects (see Appendix 1A for GXQ input and output data used in building wake calculation). The treatment of site wind data is also subject to user controls to allow various frequencies of exceedance to be computed. GXQ is intended to be used by individuals who understand the limits and applicability of the models implemented. According to WHC-SD-GN-SWD-30003, *GXQ Program Verification and Validation*, the program has been tested and verified to implement its calculational models correctly. Table 1-4 contains the atmospheric transport values used to determine onsite and offsite consequences.

Table 1-4. Atmospheric Transport Factors Used in Accident Analyses for the Canister Storage Building.

Receptor location description	Air transport factors[a] Acute Less than 1 hour[b]
Onsite worker (100 m)	3.41 E-02
Onsite worker (100 m) with building wake effect	1.14 E-02
Highway 240 (9,280 m W)	2.36 E-05
Hanford Site boundary (17, 390 m E)	1.30 E-05

[a]Units for these values are seconds per cubic meter. In all cases the releases are assumed to be point sources at ground level to maximize the dose consequences.

[b]No adjustment for plume meander (HNF-SD-SNF-TI-059, 1999, *A Discussion on the Methodology for Calculating Radiological and Toxicological Consequences for the Spent Nuclear Fuel Project at the Hanford Site*, Rev. 2, Fluor Daniel Hanford, Incorporated, Richland, Washington.).

Atmospheric transport factors were calculated using methods found in NRC Regulatory Guide 1.145. In each wind direction the observed frequencies of particular wind speed and stability class combinations were used to compute χ/Q'. For the accident analysis, the higher of either the 99.5% sector-dependent or the 95% overall value was used. This was repeated for all 16 compass directions to determine the worst-case location.

Exposures to the collocated worker onsite are calculated for the individual at the 100-m location. The risk evaluation guidelines apply to this individual. For assessment purposes, DOE has directed in Letter 96-SFD-113, *Clarification of Site Boundary for Spent Nuclear Fuel Project (SNFP) Work in or near K Basins* (Sellers 1996), that the Hanford Site boundary be considered the location of the offsite receptor. Consequences for a receptor located on Highway 240 are included for information only.

None of the accidents analyzed in this document adjusts the air transport factors for the elevation of the release above ground level (the stack is not high enough relative to the operation building to justify using elevated release). It is always conservative to ignore stack effects because the stack effect serves to disperse the release such that the collocated worker and the offsite receptor will receive a lower estimated dose if the effect is included. As an additional conservatism, all accidents were evaluated using the air transport factors calculated for less than 1 hour as provided in HNF-SD-SNF-TI-059, *A Discussion on the Methodology for Calculating Radiological and Toxicological Consequences for the Spent Nuclear Fuel Project at the Hanford Site*. Section 1.4.1.2.8 of HNF-3553 provides additional information on the calculation of the air transport factors.

The breathing rate (BR) depends on individual activity factors and exposure duration. This methodology is common to the SNF Project facilities and is described in Chapter 3.0 of the SNF Project FSAR.

The dose per unit mass of uranium (UD) is the 50-year dose commitment for all relevant exposure pathways per gram of uranium released (HNF-SD-SNF-TI-059). The major radiation exposure pathway for the identified accidents is inhalation of radioactive material. This methodology is common to the SNF Project facilities and is described in Chapter 3.0 of the SNF Project FSAR.

The dose per unit intake is the 50-year dose commitment for all relevant exposure pathways per gram of radioactive material released (HNF-SD-SNF-TI-059). The major radiation exposure pathway for the identified accidents is inhalation of radioactive material. Dose contributions from the submersion pathway were calculated and found to be negligible with respect to the total dose for the radionuclides of interest (HNF-SD-SNF-TI-059). Doses from groundshine also are expected to be negligible because most of the radionuclides of interest are alpha emitters. Therefore, the doses from groundshine and submersion are not included in the radiological dose calculations.

Potential doses from the ingestion pathway are not considered because DOE, state, and federal emergency preparedness plans limit ingestion of contaminated food in the event of an accident. DOE/RL-94-02, *Hanford Emergency Response Plan*, governs emergency response for all Hanford Site facilities. The primary determinant of exposure from the ingestion pathway is the effectiveness of public health measures (i.e., interdiction) rather than the severity of the accident itself. Ingestion, if it occurs, involves a relatively slow-to-develop pathway and is not considered an immediate threat to an exposed population in the same sense as the inhalation pathway. In addition, calculations in HNF-SD-SNF-TI-059 show that the contribution of ingestion to the total dose is negligible compared to the inhalation contribution.

Table 1-5 shows the composition of the K Basins fuel used to determine the committed effective dose equivalent per gram of respirable release. Nuclides with minor contributions (less than 0.1 mrem/g) are not shown. Isotopes of plutonium, americium, and curium constitute 99.5% of the total inhalation dose. The specific dose for the safety analysis inventory is 4.38×10^5 rem/g. The values shown for the dose per unit respirable radioactive material inhaled (UD) are the product of the activity and the dose conversion factor found in EPA Federal Guidance Report Number 11, *Limiting Values of Radionuclide Intake and Air Concentration and Dose Conversion Factors for Inhalation, Submersion, and Ingestion*. The dose conversion factor for tritium was increased by 50% to account for skin absorption (ICRP Publication 30). The committed effective dose equivalent for ^{85}Kr is the submersion dose factor from EPA Federal Guidance Report Number 12, *Manual of Protective Action Guides and Protective Actions for Nuclear Incidents*, divided by the light activity breathing rate.

Table 1-5. Composition of K Basins Fuel and the Dose per Unit of Intake. (2 sheets)

Radionuclide	Activity (Ci/MTU)[a]	CEDE per unit intake[b] (rem/g)
^{3}H	2.61 E+01	2.5 E-03
^{14}C	5.53 E-01	1.2 E-03
^{60}Co	2.09 E+00	4.6 E-01
^{85}Kr	3.70 E+02	4.9 E-04
^{90}Sr[c]	6.93 E+03	1.7 E+03
^{99}Tc	2.19 E+00	1.8 E-02
^{113m}Cd	2.78 E+00	4.3 E+00
^{134}Cs	6.47 E+00	3.0 E-01
^{137}Cs[c]	9.66 E+03	3.1 E+02
^{147}Pm	1.09 E+02	4.3 E+00
^{151}Sm	1.02 E+02	3.1 E+00
^{152}Eu	8.45 E-01	1.9 E-03
^{154}Eu	1.13 E+02	3.2 E+01
^{155}Eu	1.06 E+01	4.4 E-01
^{234}U	3.84 E-01	5.1 E+01
^{235}U[c]	1.27 E-02	1.6 E+00
^{236}U	7.16 E-02	9.0 E+00
^{238}U[c]	3.31 E-01	3.9 E+01
^{237}Np[c]	4.66 E-02	2.5 E+01
^{238}Pu	1.33 E+02	5.2 E+04
^{239}Pu	1.73 E+02	7.4 E+04
^{240}Pu	1.37 E+02	5.9 E+04
^{241}Pu[c]	6.82 E+03	5.6 E+04
^{242}Pu	8.71 E-02	3.6 E+01
^{241}Am	4.34 E+02	1.9 E+05
^{242m}Am[c]	3.72 E-01	1.6 E+02
^{243}Am[c]	2.78 E-01	1.2 E+02

Table 1-5. Composition of K Basins Fuel and the Dose per Unit of Intake. (2 sheets)

Radionuclide	Activity (Ci/MTU)[a]	CEDE per unit intake[b] (rem/g)
^{244}Cm	4.47 E+00	1.1 E+03
^{55}Fe	5.41 E-01	1.5 E-03
^{63}Ni	3.47 E+00	2.2 E-02
^{79}Se	6.54 E-02	6.4 E-04
^{93}Zr	2.95 E-01	9.5 E-02
^{93m}Nb	1.93 E-01	5.6 E-02
^{106}Ru[c]	2.56 E-02	1.2 E-02
^{107}Pd	1.56 E-02	2.0 E-04
^{121m}Sn[c]	6.27 E-02	7.2 E-04
^{126}Sn[c]	1.29 E-01	1.3 E-02
^{129}I	5.16 E-03	9.0 E-04
^{135}Cs	6.04 E-02	2.8 E-04
^{144}Ce[c]	7.91 E-04	3.0 E-04
^{244}Cm	4.47 E+00	1.1 E+03
Total	—	4.38 E+05

[a]Combined K Basins inventories decayed to May 31, 1998: 1.0 Ci = 3.7 x 10^{10} Bq.

[b]Fifty-year committed effective dose equivalent. The total was calculated by spreadsheet retaining three significant figures.

[c]The following short-lived progeny nuclides are not shown in the table: ^{90}Y, ^{137m}Ba, ^{106}Rh, ^{121}Sn, ^{126m}Sb, ^{144m}Pr, ^{144}Pr, ^{231}Th, ^{234}Th, ^{233}Pa, ^{234}Pa, ^{234m}Pa, ^{237}U, ^{238}Np, ^{242}Am, and ^{242}Cm. These nuclides are found in secular equilibrium with the parent nuclide. Their dose contributions are included in the CEDE value shown for the parent nuclide.

MTU = metric ton of uranium.
CEDE = committed effective dose equivalent.

1.2.3 Toxicological Effects

The SNF is primarily uranium metal, which is known to have adverse toxicological effects on humans. Plutonium and other transuranic heavy metals also are present in small quantities but add little to the overall toxicity of the fuel. For example, if the toxic air concentration limits for uranium are applied to neptunium, plutonium, americium, and curium, the "sum-of-fractions" indicator of toxicity increases about 0.2% (HNF-SD-SNF-TI-059). Thus, the uranium content of SNF controls the potential health impacts downwind following a postulated accident. Uranium acts like many heavy metals to damage one or more internal organs of individuals exposed to high air concentrations. The toxicity depends on the solubility of the uranium, with more soluble compounds being a greater hazard because they are transferred from the respiratory tract into the blood more quickly. The chemical form of radiological isotopes that is most soluble (toxic) was assumed when determining the toxicological effects.

Because any environmental release of SNF could have toxicological and radiological effects, both should be computed for comparison with consequence guidelines. A detailed comparison (HNF-SD-SNF-TI-059, Section 5.3) of the requirements for meeting the evaluation guidelines for toxicological and radiological effects of airborne emissions leads to the conclusion that toxicological effects are normally less severe than the radiological effects. The only exceptions are accidents in which new chemical forms are introduced into the CSB and then released into the air. If new chemicals are introduced at the CSB, they will be evaluated on a case-by-case basis.

No routine chemical processes are conducted in the SNF Project facilities. Purging and backfilling the MCOs involves the use of an inert gas (helium). Some chemicals, such as those used for equipment decontamination, may be used occasionally (HNF-SD-SNF-CM-001). However, there are no chemical inventories of concern for safety analysis considerations.

1.2.4 Risk Guidelines

The DOE-recommended radiological risk evaluation guidelines (Sellers 1997) are shown in Table 1-6. These criteria for identifying safety-class SSCs implement the guidance of DOE Order 6430.1A, *General Design Criteria*, Section 1300-1.4, "Guidance on Limiting Exposure of the Public," and are consistent with the graded approach to safety required by DOE Order 5480.23, *Nuclear Safety Analysis Reports*.

As stated in HNF-PRO-704, *Hazard and Accident Analysis Process*, satisfaction of its radiological evaluation guidelines meet the goals of SEN-35-91, *Nuclear Safety Policy*. However, the guidelines used by the SNF Project (Sellers 1997) are more conservative and are bounded by the guidelines specified in HNF-PRO-704, Table D-1. As such, satisfaction of the SNF Project radiological evaluation guidelines (Sellers 1997) will meet the goals of SEN-35-91.

Table 1-6. Radiological Evaluation Guidelines and Limits.

Event category	Frequency range (per year)	Onsite risk evaluation guidelines,* rem	Offsite accident release limits,* rem
Anticipated	1.0 E-01 to 1.0 E-02	1	0.5
Unlikely	1.0 E-02 to 1.0 E-04	10	5.0
Extremely unlikely	1.0 E-04 to 1.0 E-06	25	5.0

Note: All doses are committed effective dose equivalents.

*This terminology is consistent with Tables 1 and 2 of Sellers, E. D., 1997, *Risk Evaluation Guidelines (REGs) to Ensure Inherently Safer Designs* (Letter 97-SFD-172 to H. J. Hatch, Fluor Daniel Hanford, Incorporated, August 26), U.S. Department of Energy, Richland Operations Office, Richland, Washington. These SNF Project guidelines are more conservative than the values in HNF-PRO-705, *Safety Basis Planning, Documentation, Review, and Approval*, Fluor Hanford, Incorporated, Richland, Washington (shown in parentheses).

1.2.5 Design Basis Accident Analysis Assumptions

This section presents a summary of the key assumptions used in the DBA analyses for the CSB. The DBAs have been analyzed to quantify consequences and compare them with release limits for offsite consequences and evaluation guidelines for onsite consequences. All analyses have been performed based on the following MCO initial conditions defined in HNF-SD-SNF-TI-015:

1. Maximum particulate mass of aluminum hydroxide less than or equal to 9.47 kg in an MCO with bounding total particulate delivered to the CSB

   The bounding value is based on statistical analysis of good quality film thickness data at a 99% confidence level. To obtain this confidence level, a thickness of 1.8 times the actual mean of the measurements was used. This value was multiplied by the total assumed surface area and the theoretical density of aluminum hydroxide to obtain the bounding value. Additional information is documented in HNF-1527, *Estimates of Particulate Mass in Multi-Canister Overpacks*.

2. Maximum mass of uranium oxide hydrates less than or equal to 10.8 kg in an MCO delivered to the CSB

   Over 90% of this value is from sources that are quantified by analysis. The bounding values for these sources are based on fuel characterization data combined with very conservative assumptions of the amount of damaged fuel in the MCO and on literature data on hydrate decomposition. Less than 10% of the value is from canister particulate. To obtain this value, credit is taken for fuel cleaning, which must be validated by examination of a test batch of cleaned fuel assemblies and

confirmed by periodic examination of assemblies during the process. Additional information on the quantity of hydrates in a bounding MCO is provided in HNF-1527 and in HNF-1523, *K Basin Particulate Water Content, Behavior, and Impact*.

3. Maximum of two scrap baskets in an MCO delivered to the CSB

   This condition is controlled by TSR commitments in HNF-SD-WM-SAR-062, *K Basins Final Safety Analysis Report*. The safety of two scrap baskets has been demonstrated relative to all credible accident scenarios.

4. Maximum (not strongly adherent) UO_2 particulate less than or equal to 34 kg in an MCO after 40 years of storage at the CSB

   This is particulate that is generated after fuel cleaning. The requirement is met by bounding analysis that relies on TSR commitments in HNF-SD-WM-SAR-062 that limit the amount of scrap and damaged fuel in an MCO. This value is based on very conservative assumptions for both oxidation rates and elapsed time at various process steps. Additional information regarding the values for these process steps is documented in HNF-1527.

5. Maximum free water less than 200 g in an MCO delivered to the CSB

   This value is based on processing steps at the conclusion of cold vacuum drying with time, pressure, and temperature conditions that ensure sufficient water evaporation and removal even with very conservative assumptions of fuel cracking and trapped particulate. Analysis confirming the feasibility of limiting free water and the associated processing requirements at the CVDF is provided in HNF-1851, *Cold Vacuum Drying Residual Free Water Test Description*. This analysis is supported by whole-element characterization data and bounds the free water present in the MCO.

6. Leak rate of internal gas from MCO less than 10^{-5} standard cm^3/s

   Before the MCO is shipped from the CVDF to the CSB, the MCO's mechanical closure seal will have been demonstrated to meet a 10^{-5} standard cm^3/s total integrated leak test acceptance criterion as defined by ANSI N14.5-1987, *American National Standard for Radioactive Materials — Leakage Tests on Packages for Shipment*. The total integrated leakage criterion will be satisfied by a summation of test results for individual seals.

7. Maximum mass of uranium hydride (for heat and hydrogen generation) equal to 5.13 kg in an MCO delivered to the CSB and 9.08 kg after 40 years of storage at the CSB

   Two methods were used to estimate bounding and nominal hydride inventories. The first method assumed particulate generated by in-basin corrosion is partially composed of uranium hydride, as found in literature experiments. The second method assumed an element contains uranium hydride equivalent to observations reported in single-element drying tests. Similar estimates were obtained from both methods, but the estimate based on element drying data was used to develop the bounding estimate of uranium hydride inventory. Additional information is provided in HNF-3372, *Uranium Hydride in Multi-Canister Overpacks*.

8. Maximum of 6,339 kg of uranium per MCO (based on five Mark IV fuel baskets)

   The value is determined by the design of the MCO, which has room for five Mark IV fuel baskets. Each Mark IV fuel basket has positions for 54 fuel assemblies, and the maximum uranium mass in a Mark IV fuel assembly is 23.48 kg. The uranium mass in various fuel assemblies and the possible loading combinations are described in HNF-SD-SNF-TI-009.

9. Minimum inert gas pressure of 1.5 atm at 25 °C in an MCO delivered to the CSB.

   Before the MCO is shipped from the CVDF to the CSB, it will have been chilled in accordance with SNF-2356, *Spent Nuclear Fuel Project Cold Vacuum Drying Facility Operations Manual*, and backfilled with helium to between 1.65 atm and 1.85 atm absolute.

Combustible loading controls are presumed to be in place to preserve the combustible loadings assumed in HNF-SD-SNF-FHA-002, *Final Fire Hazard Analysis for the Canister Storage Building*. The fire hazard analysis was prepared in accordance with DOE Order 5480.7A, *Fire Protection*, and HNF-PRO-350, *Fire Hazard Analysis Requirements*. The analysis evaluated potential fire risks at the CSB to determine whether any undue hazards required mitigation to protect workers, property, the public, or the environment. The conclusion of the analysis is that the fire risks present in the facility are being mitigated through engineering design and administration of control of fuel packages (HNF-SD-SNF-FHA-002). This conclusion is consistent with the results of the accident hazard analysis prepared for this chapter (HNF-SD-SNF-HIE-001). Consequently, the accident analysis in this chapter has only evaluated the potential for the DBAs associated with deflagrations caused by hydrogen generation resulting from radiolysis and fuel corrosion. The fire hazard analysis (HNF-SD-SNF-FHA-002) and its implementation plan define the facility requirements related to combustible loadings and necessitate TSR controls.

1.3 REFERENCES

Apostolakis, G. E., 1974, *Mathematical Methods of Probabilistic Safety Analysis*, University of California, Los Angeles, California.

DOE-HDBK-3010-94, 1994, *Airborne Release Fractions/Rates and Respirable Fractions/Rates for Nonreactor Nuclear Facilities*, U.S. Department of Energy, Washington, D.C.

DOE Order 5480.7A, *Fire Protection*, U.S. Department of Energy, Washington, D.C.

DOE Order 5480.23, *Nuclear Safety Analysis Reports*, U.S. Department of Energy, Washington, D.C.

DOE Order 6430.1A, *General Design Criteria*, U.S. Department of Energy, Washington, D.C.

DOE/RL-94-02, 1995, *Hanford Emergency Response Plan*, U.S. Department of Energy, Richland Operations Office, Richland, Washington.

DOE-STD-3009-94, 1994, *Preparation Guide for U.S. Department of Energy Nonreactor Nuclear Facility Safety Analysis Reports*, U.S. Department of Energy, Washington, D.C.

EPA Federal Guidance Report Number 11, 1988, *Limiting Values of Radionuclide Intake and Air Concentration and Dose Conversion Factors for Inhalation, Submersion, and Ingestion*, EPA-520/1-88-020, U.S. Environmental Protection Agency, Washington, D.C.

EPA Federal Guidance Report Number 12, 1992, *Manual of Protective Action Guides and Protective Actions for Nuclear Incidents*, U.S. Environmental Protection Agency, Washington, D.C.

Hinds, W.C., 1982, *Aerosol Technology: Properties, Behavior, and Measurements of Airborne Particles*, John Wiley & Sons, New York, New York.

HNF-1523, 1998, *K Basin Particulate Water Content, Behavior, and Impact*, Rev. 1, Fluor Daniel Hanford, Incorporated, Richland, Washington.

HNF-1527, 1999, *Estimates of Particulate Mass in Multi-Canister Overpacks*, Rev. 2, Fluor Daniel Hanford, incorporated, Richland, Washington.

HNF-1851, 1999, *Cold Vacuum Drying Residual Free Water Test Description*, Rev. 2, Fluor Daniel Hanford, Incorporated, Richland, Washington.

HNF-3553, 2000, *Spent Nuclear Fuel Project Final Safety Analysis Report*, Rev. 0, Fluor Hanford, Incorporated, Richland, Washington.

HNF-PRO-350, *Fire Hazard Analysis Requirements*, Fluor Hanford, Incorporated, Richland, Washington.

HNF-PRO-704, *Hazard and Accident Analysis Process*, Fluor Hanford, Incorporated, Richland, Washington.

HNF-PRO-705, *Safety Basis Planning, Documentation, Review, and Approval*, Fluor Hanford, Incorporated, Richland, Washington.

HNF-SD-SNF-CM-001, 1997, *Spent Nuclear Fuel Project Configuration Management Plan*, Rev. 2, Fluor Daniel Hanford, Incorporated, Richland, Washington.

HNF-SD-SNF-FHA-002, 2000, *Final Fire Hazard Analysis for the Canister Storage Building*, Rev. 2, Fluor Hanford, Incorporated, Richland, Washington.

HNF-SD-SNF-HIE-001, 2000, *Canister Storage Building Hazard Analysis Report*, Rev. 3, Fluor Daniel Hanford, Incorporated, Richland, Washington.

HNF-SD-SNF-TI-009, 1998, *105-K Basin Material Design Basis Feed Description for Spent Nuclear Fuel Project Facilities*, Rev. 1, Fluor Daniel Hanford, Incorporated, Richland, Washington.

HNF-SD-SNF-TI-015, 1998, *Spent Nuclear Fuel Project Technical Databook*, Rev. 6, Fluor Daniel Hanford, Incorporated, Richland, Washington.

HNF-SD-SNF-TI-059, 1999, *A Discussion on the Methodology for Calculating Radiological and Toxicological Consequences for the Spent Nuclear Fuel Project at the Hanford Site*, Rev. 2, Fluor Daniel Hanford, Incorporated, Richland, Washington.

ICRP Publication 30, 1979, *Limits for Intake by Workers*, International Commission on Radiological Protection, Elmsford, New York.

NRC Regulatory Guide 1.145, 1982, *Atmospheric Dispersion Models for Potential Accident Consequence Assessments at Nuclear Power Plants*, U.S. Nuclear Regulatory Commission, Washington, D.C.

Sellers, E. D., 1996, *Clarification of Site Boundary for Spent Nuclear Fuel Project (SNFP) Work in or near K Basins* (Letter 96-SFD-113 to President, Westinghouse Hanford Company, May 22), U.S. Department of Energy, Richland Operations Office, Richland, Washington.

Sellers, E. D., 1997, *Risk Evaluation Guidelines (REGs) to Ensure Inherently Safer Designs* (Letter 97-SFD-172 to H. J. Hatch, Fluor Daniel Hanford, Incorporated, August 26), U.S. Department of Energy, Richland Operations Office, Richland, Washington.

SEN-35-91, 1991, *Nuclear Safety Policy*, U.S. Department of Energy, Washington, D.C.

SNF-4042, 2000, *Evaluation of Accident Frequencies at the Canister Storage Building*, Rev. 2, Fluor Hanford, Richland, Washington.

WHC-SD-GN-SWD-30002, 1995, *GXQ Program Users' Guide*, Rev. 1, Westinghouse Hanford Company, Richland, Washington.

WHC-SD-GN-SWD-30003, 1995, *GXQ Program Verification and Validation*, Rev. 1, Westinghouse Hanford Company, Richland, Washington.

APPENDIX 1A

GXQ INPUT AND OUTPUT FILES FOR CANISTER STORAGE BUILDING AND SUPPORT AREA STRUCTURE

This page intentionally left blank.

APPENDIX 1A

GXQ INPUT AND OUTPUT FILES FOR CANISTER STORAGE BUILDING AND SUPPORT AREA STRUCTURE

GXQ Version 4.0D
February 8, 1999

```
General Purpose Atmospheric Dispersion Code
Produced by Fluor Daniel Northwest, Inc.

Users Guide documented in WHC-SD-GN-SWD-30002 Rev. 1.
Validation documented in WHC-SD-GN-SWD-30003 Rev. 1.
Code Custodian is: Brit E. Hey
                   Fluor Daniel Northwest, Inc.
                   P.O. Box 1050
                   Richland, WA 99352-1050
                   (509) 376-2921


Run Date = 03/13/00
Run Time = 12:12:14.07


INPUT ECHO:
CSB Building Wake - Building Dimensions for Operating Area Structure (All Wind
c GXQ Version 4.0 Input File
c   mode
    1
c
c MODE CHOICE:
c mode = 1 then X/Q based on Hanford site specific meteorology
c mode = 2 then X/Q based on atmospheric stability class and wind speed
c mode = 3 then X/Q plot file is created
c
c LOGICAL CHOICES:
c   ifox  inorm icdf  ichk  isite ipop
    T     F     F     F     F     F
c ifox  = t then joint frequency used to compute frequency to exceed X/Q
c       = f then joint frequency used to compute annual average X/Q
c inorm = t then joint frequency data is normalized (as in GENII)
c       = f then joint frequency data is un-normalized
c icdf  = t then cumulative distribution file created (CDF.OUT)
c       = f then no cumulative distribution file created
c ichk  = t then X/Q parameter print option turned on
c       = f then no parameter print
c isite = t then X/Q based on joint frequency data for all 16 sectors
c       = f then X/Q based on joint frequency data of individual sectors
```

```
c ipop  = t then X/Q is population weighted
c       = f then no population weighting
c
c X/Q AND WIND SPEED ADJUSTMENT MODELS:
c   ipuff idep  isrc  iwind
    0     0     0     0
c DIFFUSION COEFFICIENT ADJUSTMENT MODELS:
c   iwake ipm   iflow ientr
    1     0     0     0
c EFFECTIVE RELEASE HEIGHT ADJUSTMENT MODELS:
c  (irise igrnd)iwash igrav
    0     0     0     0
c ipuff = 1 then X/Q calculated using puff model
c       = 0 then X/Q calculated using default continuous plume model
c idep  = 1 then plume depletion model turned on (Chamberlain model)
c isrc  = 1 then X/Q multiplied by scalar
c       = 2 then X/Q adjusted by wind speed function
c iwind = 1 then wind speed corrected for plume height
c iwake = 1 then NRC RG 1.145 building wake model turned on
c       = 2 then MACCS virtual distance building wake model turned on
c ipm   = 1 then NRC RG 1.145 plume meander model turned on
c       = 2 then 5th Power Law plume meander model turned on
c       = 3 then sector average model turned on
c iflow = 1 then sigmas adjusted for volume flow rate
c ientr = 1 then method of Pasquill used to account for entrainment
c irise = 1 then MACCS buoyant plume rise model turned on
c       = 2 then ISC2 momentum/buoyancy plume rise model turned on
c igrnd = 1 then Mills buoyant plume rise modification for ground effects
c iwash = 1 then stack downwash model turned on
c igrav = 1 then gravitational settling model turned on
c       = 0 unless specified otherwise, 0 turns model off
c
c PARAMETER INPUT:
c                 reference                    frequency
c   release       anemometer     mixing        to
c   height        height         height        exceed
c   hs(m)         ha(m)          hm(m)         Cx(%)
c   ------------  -------------  ------------  ------------
    0.00000E+00   1.00000E+01    1.00000E+03   5.00000E-01
c
c   initial       initial                                    gravitational
c   plume         plume          release       deposition    settling
c   width         height         duration      velocity      velocity
c   Wb(m)         Hb(m)          trd(hr)       vd(m/s)       vg(m/s)
c   ------------  -------------  ------------  ------------  ------------
    4.18000E+01   1.68000E+01    0.00000E+00   1.00000E-03   1.00000E-03
c
c                 initial        initial                     convective
c   ambient       plume          plume         release       heat release
c   temperature   temperature    flow rate     diameter      rate(1)
c   Tamb(C)       T0(C)          V0(m3/s)      d(m)          qh(w)
c   ------------  -------------  ------------  ------------  ------------
    2.00000E+01   2.20000E+01    1.00000E+00   1.00000E+00   0.00000E+00
c
```

```
c (1) If zero then buoyant flux based on plume/ambient temperature difference.
c
c   X/Q            Wind
c   scaling        Speed
c   factor         Exponent
c   c(?)           a(?)
c   ____________   ____________
    1.00000E+00    7.80000E-01
c
c RECEPTOR DEPENDENT DATA (no line limit)
c FOR MODE     make          RECEPTOR DEPENDENT DATA
c 1 (site specific)          sector distance receptor-height
c 2 (by class & wind speed) class windspeed distance offset receptor-height
c 3 (create plot file)       class windspeed xmax imax ymax jmax xqmin power
c
c RECEPTOR PARAMETER DESCRIPTION
c sector = 0, 1, 2... (all, S, SSW, etc.)
c distance = receptor distance (m)
c receptor height = height of receptor (m)
c class = 1, 2, 3, 4, 5, 6, 7 (P-G stability class A, B, C, D, E, F, G)
c windspeed = anemometer wind speed (m/s)
c offset = offset from plume centerline (m)
c xmax = maximum distance to plot or calculate to (m)
c imax = distance intervals
c ymax = maximum offset to plot (m)
c jmax = offset intervals
c xqmin = minimum scaled X/Q to calculate
c power = exponent in power function step size

MODE:
Site specific X/Q calculated.

LOGICAL CHOICES:
Joint frequency used to calculate X/Q based on frequency of exceedance.
No normalization of joint frequency.
X/Q calculated for single sector.

MODELS SELECTED:
NRC RG 1.145 building wake model selected.
Default Gaussian plume model selected.

WARNING/ERROR MESSAGES:

JOINT FREQUENCY DATA:
200 AREA (HMS) - 10 M - Pasquill A - G (1983 - 1991 Average)
Created 8/26/92 KR


CSB Building Wake - Building Dimensions for Operating Area Structure (All Wind D
```

SECTOR	DISTANCE (m)	RECEPT HEIGHT (m)	SECT. FREQ. (%)	POPULATION	TOTAL POPULATION SCALED X/Q (s/m3)	AVERAGE INDIVIDUAL SCALED X/Q (s/m3)	ATM. STAB. CLASS	WIND SPEED (m/s)
S	100	0	6.30	1	5.21E-03	5.21E-03	E	0.89
SSW	100	0	4.53	1	3.77E-03	3.77E-03	F	2.65
SW	100	0	2.93	1	4.04E-03	4.04E-03	F	2.65
WSW	100	0	2.72	1	4.06E-03	4.06E-03	F	2.65
W	100	0	4.80	1	9.32E-03	9.32E-03	G	2.65
WNW	100	0	3.98	1	5.33E-03	5.33E-03	G	4.70
NW	100	0	4.72	1	9.64E-03	9.64E-03	G	2.65
NNW	100	0	4.58	1	9.68E-03	9.68E-03	G	2.65
N	100	0	4.36	1	1.04E-02	1.04E-02	G	2.65
NNE	100	0	2.49	1	5.14E-03	5.14E-03	E	0.89
NE	100	0	3.90	1	5.24E-03	5.24E-03	E	0.89
ENE	100	0	6.17	1	8.41E-03	8.41E-03	G	2.65
E	100	0	14.05	1	1.14E-02	1.14E-02	F	0.89
ESE	100	0	18.80	1	1.08E-02	1.08E-02	F	0.89
SE	100	0	10.83	1	1.02E-02	1.02E-02	G	2.65
SSE	100	0	4.78	1	5.25E-03	5.25E-03	G	4.70

```
CSB Building Wake - Building Dimensions for Operating Area Structure (All Wind
Directions Except North)
c GXQ Version 4.0 Input File
c   mode
    1
c
c MODE CHOICE:
c mode = 1 then X/Q based on Hanford site specific meteorology
c mode = 2 then X/Q based on atmospheric stability class and wind speed
c mode = 3 then X/Q plot file is created
c
c LOGICAL CHOICES:
c   ifox  inorm icdf  ichk  isite ipop
    t     f     f     f     f     f
c ifox  = t then joint frequency used to compute frequency to exceed X/Q
c       = f then joint frequency used to compute annual average X/Q
c inorm = t then joint frequency data is normalized (as in GENII)
c       = f then joint frequency data is un-normalized
c icdf  = t then cumulative distribution file created (CDF.OUT)
c       = f then no cumulative distribution file created
c ichk  = t then X/Q parameter print option turned on
c       = f then no parameter print
c isite = t then X/Q based on joint frequency data for all 16 sectors
c       = f then X/Q based on joint frequency data of individual sectors
c ipop  = t then X/Q is population weighted
c       = f then no population weighting
c
c X/Q AND WIND SPEED ADJUSTMENT MODELS:
c   ipuff idep  isrc  iwind
    0     0     0     0
c DIFFUSION COEFFICIENT ADJUSTMENT MODELS:
c   iwake ipm   iflow ientr
    1     0     0     0
c EFFECTIVE RELEASE HEIGHT ADJUSTMENT MODELS:
c  (irise igrnd)iwash igrav
    0     0     0     0
c ipuff = 1 then X/Q calculated using puff model
c       = 0 then X/Q calculated using default continuous plume model
c idep  = 1 then plume depletion model turned on (Chamberlain model)
c isrc  = 1 then X/Q multiplied by scalar
c       = 2 then X/Q adjusted by wind speed function
c iwind = 1 then wind speed corrected for plume height
c iwake = 1 then NRC RG 1.145 building wake model turned on
c       = 2 then MACCS virtual distance building wake model turned on
c ipm   = 1 then NRC RG 1.145 plume meander model turned on
c       = 2 then 5th Power Law plume meander model turned on
c       = 3 then sector average model turned on
c iflow = 1 then sigmas adjusted for volume flow rate
c ientr = 1 then method of Pasquill used to account for entrainment
c irise = 1 then MACCS buoyant plume rise model turned on
c       = 2 then ISC2 momentum/buoyancy plume rise model turned on
c igrnd = 1 then Mills buoyant plume rise modification for ground effects
c iwash = 1 then stack downwash model turned on
c igrav = 1 then gravitational settling model turned on
```

```
c       = 0 unless specified otherwise, 0 turns model off
c
c PARAMETER INPUT:
c                    reference                        frequency
c   release          anemometer      mixing           to
c   height           height          height           exceed
c   hs(m)            ha(m)           hm(m)            Cx(%)
c   _____________    _____________   _____________    _____________
    0                10              1000             .5
c
c   initial          initial                                           gravitational
c   plume            plume           release          deposition       settling
c   width            height          duration         velocity         velocity
c   Wb(m)            Hb(m)           trd(hr)          vd(m/s)          vg(m/s)
c   _____________    _____________   _____________    _____________    _____________
    41.8             16.8             0               0.001            0.001
c
c                    initial         initial                           convective
c   ambient          plume           plume            release          heat release
c   temperature      temperature     flow rate        diameter         rate(1)
c   Tamb(C)          T0(C)           V0(m3/s)         d(m)             qh(w)
c   _____________    _____________   _____________    _____________    _____________
    20               22              1                1                0
c
c (1) If zero then buoyant flux based on plume/ambient temperature difference.
c
c   X/Q              Wind
c   scaling          Speed
c   factor           Exponent
c   c(?)             a(?)
c   _____________    _____________
    1                .78
c
c RECEPTOR DEPENDENT DATA (no line limit)
c FOR MODE     make          RECEPTOR DEPENDENT DATA
c 1 (site specific)          sector distance receptor-height
c 2 (by class & wind speed) class windspeed distance offset receptor-height
c 3 (create plot file)       class windspeed xmax imax ymax jmax xqmin power
c
c RECEPTOR PARAMETER DESCRIPTION
c sector = 0, 1, 2... (all, S, SSW, etc.)
c distance = receptor distance (m)
c receptor height = height of receptor (m)
c class = 1, 2, 3, 4, 5, 6, 7 (P-G stability class A, B, C, D, E, F, G)
c windspeed = anemometer wind speed (m/s)
c offset = offset from plume centerline (m)
c xmax = maximum distance to plot or calculate to (m)
c imax = distance intervals
c ymax = maximum offset to plot (m)
c jmax = offset intervals
c xqmin = minimum scaled X/Q to calculate
c power = exponent in power function step size
0  100    0
```

```
                    GXQ Version 4.0D
                    February 8, 1999

General Purpose Atmospheric Dispersion Code
Produced by Fluor Daniel Northwest, Inc.

Users Guide documented in WHC-SD-GN-SWD-30002 Rev. 1.
Validation documented in WHC-SD-GN-SWD-30003 Rev. 1.
Code Custodian is: Brit E. Hey
                   Fluor Daniel Northwest, Inc.
                   P.O. Box 1050
                   Richland, WA 99352-1050
                   (509) 376-2921


Run Date = 03/13/00
Run Time = 12:14:07.33


INPUT ECHO:
CSB Building Wake - Support Building Dimensions for North Wind Direction Only
c GXQ Version 4.0 Input File
c   mode
    1
c
c MODE CHOICE:
c mode = 1 then X/Q based on Hanford site specific meteorology
c mode = 2 then X/Q based on atmospheric stability class and wind speed
c mode = 3 then X/Q plot file is created
c
c LOGICAL CHOICES:
c   ifox  inorm icdf  ichk  isite ipop
    T     F     F     F     F     F
c ifox  = t then joint frequency used to compute frequency to exceed X/Q
c       = f then joint frequency used to compute annual average X/Q
c inorm = t then joint frequency data is normalized (as in GENII)
c       = f then joint frequency data is un-normalized
c icdf  = t then cumulative distribution file created (CDF.OUT)
c       = f then no cumulative distribution file created
c ichk  = t then X/Q parameter print option turned on
c       = f then no parameter print
c isite = t then X/Q based on joint frequency data for all 16 sectors
c       = f then X/Q based on joint frequency data of individual sectors
c ipop  = t then X/Q is population weighted
c       = f then no population weighting
c
c X/Q AND WIND SPEED ADJUSTMENT MODELS:
c   ipuff idep  isrc  iwind
    0     0     0     0
c DIFFUSION COEFFICIENT ADJUSTMENT MODELS:
c   iwake ipm   iflow ientr
```

```
    1     0     0     0
c EFFECTIVE RELEASE HEIGHT ADJUSTMENT MODELS:
c  (irise igrnd)iwash igrav
    0     0     0     0
c ipuff = 1 then X/Q calculated using puff model
c       = 0 then X/Q calculated using default continuous plume model
c idep  = 1 then plume depletion model turned on (Chamberlain model)
c isrc  = 1 then X/Q multiplied by scalar
c       = 2 then X/Q adjusted by wind speed function
c iwind = 1 then wind speed corrected for plume height
c iwake = 1 then NRC RG 1.145 building wake model turned on
c       = 2 then MACCS virtual distance building wake model turned on
c ipm   = 1 then NRC RG 1.145 plume meander model turned on
c       = 2 then 5th Power Law plume meander model turned on
c       = 3 then sector average model turned on
c iflow = 1 then sigmas adjusted for volume flow rate
c ientr = 1 then method of Pasquill used to account for entrainment
c irise = 1 then MACCS buoyant plume rise model turned on
c       = 2 then ISC2 momentum/buoyancy plume rise model turned on
c igrnd = 1 then Mills buoyant plume rise modification for ground effects
c iwash = 1 then stack downwash model turned on
c igrav = 1 then gravitational settling model turned on
c       = 0 unless specified otherwise, 0 turns model off
c
c PARAMETER INPUT:
c                   reference                       frequency
c   release         anemometer      mixing          to
c   height          height          height          exceed
c   hs(m)           ha(m)           hm(m)           Cx(%)
c   ____________    ____________    ____________    ____________
    0.00000E+00     1.00000E+01     1.00000E+03     5.00000E-01
c
c   initial         initial                                         gravitational
c   plume           plume           release         deposition      settling
c   width           height          duration        velocity        velocity
c   Wb(m)           Hb(m)           trd(hr)         vd(m/s)         vg(m/s)
c   ____________    ____________    ____________    ____________    ____________
    4.57000E+01     4.90000E+00     0.00000E+00     1.00000E-03     1.00000E-03
c
c                   initial         initial                         convective
c   ambient         plume           plume           release         heat release
c   temperature     temperature     flow rate       diameter        rate(1)
c   Tamb(C)         T0(C)           V0(m3/s)        d(m)            qh(w)
c   ____________    ____________    ____________    ____________    ____________
    2.00000E+01     2.20000E+01     1.00000E+00     1.00000E+00     0.00000E+00
c
c (1) If zero then buoyant flux based on plume/ambient temperature difference.
c
c   X/Q             Wind
c   scaling         Speed
c   factor          Exponent
c   c(?)            a(?)
c   ____________    ____________
    1.00000E+00     7.80000E-01
```

```
c
c RECEPTOR DEPENDENT DATA (no line limit)
c FOR MODE     make          RECEPTOR DEPENDENT DATA
c 1 (site specific)          sector distance receptor-height
c 2 (by class & wind speed) class windspeed distance offset receptor-height
c 3 (create plot file)       class windspeed xmax imax ymax jmax xqmin power
c
c RECEPTOR PARAMETER DESCRIPTION
c sector = 0, 1, 2... (all, S, SSW, etc.)
c distance = receptor distance (m)
c receptor height = height of receptor (m)
c class = 1, 2, 3, 4, 5, 6, 7 (P-G stability class A, B, C, D, E, F, G)
c windspeed = anemometer wind speed (m/s)
c offset = offset from plume centerline (m)
c xmax = maximum distance to plot or calculate to (m)
c imax = distance intervals
c ymax = maximum offset to plot (m)
c jmax = offset intervals
c xqmin = minimum scaled X/Q to calculate
c power = exponent in power function step size

MODE:
Site specific X/Q calculated.

LOGICAL CHOICES:
Joint frequency used to calculate X/Q based on frequency of exceedance.
No normalization of joint frequency.
X/Q calculated for single sector.

MODELS SELECTED:
NRC RG 1.145 building wake model selected.
Default Gaussian plume model selected.

WARNING/ERROR MESSAGES:

JOINT FREQUENCY DATA:
200 AREA (HMS) - 10 M - Pasquill A - G (1983 - 1991 Average)
Created 8/26/92 KR
```

CSB Building Wake - Support Building Dimensions for North Wind Direction Only

SECTOR	DISTANCE (m)	RECEPT HEIGHT (m)	SECT. FREQ. (%)	POPULATION	TOTAL POPULATION SCALED X/Q (s/m3)	AVERAGE INDIVIDUAL SCALED X/Q (s/m3)	ATM. STAB. CLASS	WIND SPEED (m/s)
S	100	0	6.30	1	7.12E-03	7.12E-03	E	0.89
SSW	100	0	4.53	1	5.42E-03	5.42E-03	E	0.89
SW	100	0	2.93	1	5.58E-03	5.58E-03	E	0.89
WSW	100	0	2.72	1	5.61E-03	5.61E-03	E	0.89
W	100	0	4.80	1	9.37E-03	9.37E-03	G	2.65

WNW	100	0	3.98	1	8.13E-03	8.13E-03	G	2.65
NW	100	0	4.72	1	9.64E-03	9.64E-03	G	2.65
NNW	100	0	4.58	1	9.68E-03	9.68E-03	G	2.65
N	100	0	4.36	1	1.04E-02	1.04E-02	G	2.65
NNE	100	0	2.49	1	6.18E-03	6.18E-03	E	0.89
NE	100	0	3.90	1	6.96E-03	6.96E-03	E	0.89
ENE	100	0	6.17	1	8.99E-03	8.99E-03	G	2.65
E	100	0	14.05	1	1.14E-02	1.14E-02	F	0.89
ESE	100	0	18.80	1	1.08E-02	1.08E-02	F	0.89
SE	100	0	10.83	1	1.02E-02	1.02E-02	G	2.65
SSE	100	0	4.78	1	7.48E-03	7.48E-03	E	0.89

```
CSB Building Wake - Support Building Dimensions for North Wind Direction Only
c GXQ Version 4.0 Input File
c   mode
    1
c
c MODE CHOICE:
c mode = 1 then X/Q based on Hanford site specific meteorology
c mode = 2 then X/Q based on atmospheric stability class and wind speed
c mode = 3 then X/Q plot file is created
c
c LOGICAL CHOICES:
c   ifox  inorm icdf  ichk  isite ipop
    t     f     f     f     f     f
c ifox  = t then joint frequency used to compute frequency to exceed X/Q
c       = f then joint frequency used to compute annual average X/Q
c inorm = t then joint frequency data is normalized (as in GENII)
c       = f then joint frequency data is un-normalized
c icdf  = t then cumulative distribution file created (CDF.OUT)
c       = f then no cumulative distribution file created
c ichk  = t then X/Q parameter print option turned on
c       = f then no parameter print
c isite = t then X/Q based on joint frequency data for all 16 sectors
c       = f then X/Q based on joint frequency data of individual sectors
c ipop  = t then X/Q is population weighted
c       = f then no population weighting
c
c X/Q AND WIND SPEED ADJUSTMENT MODELS:
c   ipuff idep  isrc  iwind
    0     0     0     0
c DIFFUSION COEFFICIENT ADJUSTMENT MODELS:
c   iwake ipm   iflow ientr
    1     0     0     0
c EFFECTIVE RELEASE HEIGHT ADJUSTMENT MODELS:
c  (irise igrnd)iwash igrav
    0     0     0     0
c ipuff = 1 then X/Q calculated using puff model
c       = 0 then X/Q calculated using default continuous plume model
c idep  = 1 then plume depletion model turned on (Chamberlain model)
c isrc  = 1 then X/Q multiplied by scalar
c       = 2 then X/Q adjusted by wind speed function
c iwind = 1 then wind speed corrected for plume height
c iwake = 1 then NRC RG 1.145 building wake model turned on
c       = 2 then MACCS virtual distance building wake model turned on
c ipm   = 1 then NRC RG 1.145 plume meander model turned on
c       = 2 then 5th Power Law plume meander model turned on
c       = 3 then sector average model turned on
c iflow = 1 then sigmas adjusted for volume flow rate
c ientr = 1 then method of Pasquill used to account for entrainment
c irise = 1 then MACCS buoyant plume rise model turned on
c       = 2 then ISC2 momentum/buoyancy plume rise model turned on
c igrnd = 1 then Mills buoyant plume rise modification for ground effects
c iwash = 1 then stack downwash model turned on
c igrav = 1 then gravitational settling model turned on
c       = 0 unless specified otherwise, 0 turns model off
```

```
c
c PARAMETER INPUT:
c                    reference                          frequency
c    release         anemometer      mixing             to
c    height          height          height             exceed
c    hs(m)           ha(m)           hm(m)              Cx(%)
c    ____________    ____________    ____________       ____________
     0               10              1000               .5
c
c    initial         initial                                          gravitational
c    plume           plume           release            deposition    settling
c    width           height          duration           velocity      velocity
c    Wb(m)           Hb(m)           trd(hr)            vd(m/s)       vg(m/s)
c    ____________    ____________    ____________       ____________  ____________
     45.7            4.9             0                  0.001         0.001
c
c                    initial         initial                          convective
c    ambient         plume           plume              release       heat release
c    temperature     temperature     flow rate          diameter      rate(1)
c    Tamb(C)         T0(C)           V0(m3/s)           d(m)          qh(w)
c    ____________    ____________    ____________       ____________  ____________
     20              22              1                  1             0
c
c (1) If zero then buoyant flux based on plume/ambient temperature difference.
c
c    X/Q             Wind
c    scaling         Speed
c    factor          Exponent
c    c(?)            a(?)
c    ____________    ____________
     1               .78
c
c RECEPTOR DEPENDENT DATA (no line limit)
c FOR MODE     make          RECEPTOR DEPENDENT DATA
c 1 (site specific)          sector distance receptor-height
c 2 (by class & wind speed) class windspeed distance offset receptor-height
c 3 (create plot file)       class windspeed xmax imax ymax jmax xqmin power
c
c RECEPTOR PARAMETER DESCRIPTION
c sector = 0, 1, 2... (all, S, SSW, etc.)
c distance = receptor distance (m)
c receptor height = height of receptor (m)
c class = 1, 2, 3, 4, 5, 6, 7 (P-G stability class A, B, C, D, E, F, G)
c windspeed = anemometer wind speed (m/s)
c offset = offset from plume centerline (m)
c xmax = maximum distance to plot or calculate to (m)
c imax = distance intervals
c ymax = maximum offset to plot (m)
c jmax = offset intervals
c xqmin = minimum scaled X/Q to calculate
c power = exponent in power function step size
0  100   0
```

2.0 MECHANICAL DAMAGE OF MULTI-CANISTER OVERPACK

2.1 PURPOSE AND OBJECTIVES

If the multi-canister overpack (MCO) or the cask–MCO were to be subjected to an accidental drop, impact, or shear force of sufficient magnitude, the MCO or the cask–MCO could be damaged in such a way as to breach the MCO or to substantially compromise its internal geometry. A number of potential accidents that could cause mechanical damage to the MCO have been identified at the Canister Storage Building (CSB). These potential accidents are listed in Section 2.2. While some of the cases could lead to a breach and potential radiological dose consequences, a criticality is not credible because of the lack of a credible water source even if the internal geometry of the MCO were substantially compromised. Consequence analysis for breaches is contained in HNF-3553, *Spent Nuclear Fuel Project Final Safety Analysis Report*, Annex A, "Canister Storage Building Final Safety Analysis Report," Section A3.4.2.1.3.

2.2 SCENARIO DEVELOPMENT

At the CSB the MCO is hoisted by both the receiving crane and the MCO handling machine (MHM). The MCO could be dropped, either when it is inside the transportation cask or when it is outside the cask. Objects (e.g., the transportation cask lid) also are hoisted above the MCO, creating the potential for a drop onto the MCO. Other building equipment could move and collide with the MCO or the transportation cask. Several different scenarios that could cause mechanical damage to the MCO were considered, all of which were considered potentially serious hazards to the MCO in HNF-SD-SNF-HIE-001, *Canister Storage Building Hazard Analysis Report*. These scenarios are listed in Table 2-1.

The translational movement of the CSB receiving crane and the MHM, and the rotational movement of the MHM turret provide mechanisms for applying lateral or shear forces to the side of the MCO. The MHM is operated with interlocks that are designed to prevent drop, rotational, or translational forces from damaging the MCO. The lack of a credible water source prevents scenarios involving breaches from becoming criticality concerns. In general, there is no need to consider internal geometry effects because no variation of internal geometry can credibly cause criticality without the presence of water.

Frequency calculations for all scenarios identified in Table 2-1 are documented in SNF-4042, *Evaluation of Accident Frequencies at the Canister Storage Building*. Three classifications of accidents have been selected for evaluation: drop of the MCO or cask–MCO, shear of the MCO by the MHM, and impacts to the MCO other than drops or shears. Engineering calculations have been performed to determine the extent of any mechanical damage to the MCO following any of the possible drop, shear, or impact scenarios identified in Table 2-1. Based on the results of the frequency calculations and the engineering calculations, controls have been selected to meet the requirements for radiological dose releases.

Table 2-1. Multi-Canister Overpack Process Steps and Possible Drop, Shear, or Impact Scenarios. (3 sheets)

Process step or event	Drop, shear	Scenario identifier	Drop, shear, or impact description
Cask–MCO arrival at CSB	1	--	None
Cask–MCO moved by the receiving crane to the cask receiving pit	2	D1	Drop cask–MCO onto trailer edge with horizontal slap-down onto floor Drop height: 60 in.
	3	D1	Drop cask–MCO vertically directly onto concrete floor Drop height: 60 in.
	4	D1	Drop cask–MCO onto edge of cask receiving pit with slap-down
	5	D1	Drop cask–MCO onto edge of cask receiving pit spanning the pit
	6	D1	Drop cask–MCO onto edge of cask receiving pit with cask impact on opposite edge of service pit
	7	D2	Drop cask–MCO into cask receiving pit
	8	S1	Shear of cask–MCO by moving receiving crane while cask–MCO is partially lowered into pit
	9a	D3	Drop cask–MCO onto edge of or into maintenance pit
	9b	D3	Drop cask–MCO onto edge of or into FFTF pit
	10	S1	Shear of MCO because of collision between the crane and cask–MCO as the MCO is lowered into the cask receiving pit
Cask yoke removal	11	O1	Drop yoke onto cask lid
Cask lid removal using gantry hoist	12	O1	Drop cask lid onto MCO
Seismic event	13	O2	CSB facility structure falls on MCO
MCO retrieved from cask in cask receiving pit into the MHM	14	O3	Drop cask receiving pit plug onto MCO
	15	D4	Drop MCO onto edge of cask (eccentric drop at cask receiving pit)
	16	D5	Drop MCO back into cask (concentric drop at cask receiving pit)
	17a	S2	Shear MCO by turret rotation with MCO only partially retrieved into the MHM cask
MCO retrieved from cask in cask receiving pit into the MHM (continued)	17b	S3	Shear MCO by moving MHM with MCO only partially retrieved into the MHM cask

Table 2-1. Multi-Canister Overpack Process Steps and Possible Drop, Shear, or Impact Scenarios. (3 sheets)

Process step or event	Drop, shear	Scenario identifier	Drop, shear, or impact description
Seismic event	18	S4	Shear MCO while MCO is partially inserted into cask receiving pit, weld station, or storage tube during DBE
	19	O4	MHM fall onto operating deck, resulting in major structural damage to deck
MCO transported to storage tube or sampling/weld station	20	S2	Shear MCO by rotating turret with MCO only partially retracted into MHM cask
	21	D6	Drop MCO within MHM MCO cask tube onto MHM turret deck
	22	D7	Drop MCO onto CSB operating floor
	23	D7	Drop MCO onto storage covers for CSB vaults 2 or 3
	24	D8	Drop MCO onto or into maintenance pit or tube plug exchange facility
	25	D9	Drop MCO onto or into FFTF maintenance pit
Intermediate impact absorber installed on MCO	26	O5	Drop intermediate impact absorber on MCO damaging MCO
MCO placed in storage tube or sampling/weld station	27	S5	Shear MCO by moving MHM with MCO only partially retrieved into the MHM cask
	28	S2	Shear MCO by rotating turret with MCO only partially retracted into MHM cask
	29	D10	Drop MCO onto impact absorber in storage tube or sampling/weld station
	30	--	Combined with 29
	31	D11	Drop MCO onto another MCO in storage tube (no intermediate impact absorber)
	32	--	Combined with 31
	33	D12	Drop MCO onto storage tube plug because of inadvertent turret rotation
	34	D13	Drop MCO onto edge of storage tube(eccentric drop)
	35	D14	Drop MCO onto edge of sampling/weld station (eccentric drop)
	36	O3	Drop storage tube plug onto MCO

Table 2-1. Multi-Canister Overpack Process Steps and Possible Drop, Shear, or Impact Scenarios. (3 sheets)

Process step or event	Drop, shear	Scenario identifier	Drop, shear, or impact description
MCO placed in storage tube or sampling/weld station (continued)	37	*	MHM collision with sampling/weld station

*Shear of sample lines is addressed in other design basis accidents (e.g., gaseous release).

CSB = Canister Storage Building.
DBE = design basis earthquake.
FFTF = Fast Flux Test Facility.
MCO = multi-canister overpack.
MHM = multi-canister overpack handling machine.

2.2.1 Drop of a Multi-Canister Overpack

At the CSB the MCO is moved by both the receiving crane and the MHM. The MCO could be dropped, either when it is inside the transportation cask or when it is outside the cask. Several different scenarios that could cause an MCO drop have been considered. All of these drop scenarios are considered potentially serious hazards to the MCO in the CSB hazard analysis (HNF-SD-SNF-HIE-001):

D1 Cask–MCO drop from receiving crane onto receiving area

D2 Cask–MCO drop from receiving crane into cask receiving pit

D3 Cask–MCO drop from receiving crane into Fast Flux Test Facility (FFTF) pit or MHM maintenance pit

D4 Drop of MCO by MHM onto edge of cask receiving pit

D5 Drop of MCO by MHM back into cask

D6 Drop of MCO within MHM turret onto MHM turret deck

D7 Drop of MCO from MHM onto CSB operating area floor or onto storage tube covers of vault 2 or vault 3 in CSB

D8 Drop of MCO from MHM onto or into MHM maintenance pit or tube plug exchange facility

D9 Drop of MCO from MHM onto or into FFTF pit

D10 Drop of MCO by MHM into storage tube or sampling/weld station

D11 Drop of MCO by MHM onto another MCO located in the bottom of a storage tube (no intermediate impact absorber involved)

D12 Drop of MCO by MHM onto storage tube plug because of inadvertent turret rotation

D13 Drop of MCO by MHM onto edge of storage tube

D14 Drop of MCO by MHM onto edge of sampling/weld station.

D1 — Cask–Multi-Canister Overpack Drop from Receiving Crane onto Receiving Area. The receiving crane is used to lift the cask–MCO from the transport trailer using a yoke. The crane is then translated to place the cask–MCO above the cask receiving pit, and the cask–MCO is lowered into the pit. The cask–MCO could be dropped from the receiving crane at any location through which the crane travels with the suspended cask–MCO. The CSB receiving

crane has been designated a safety-significant and important-to-safety piece of equipment. The crane is not single-failure-proof but is rated for twice the load required for a safety-significant hoist.

Cask–MCO drops from the receiving crane could occur because of a failure in the lift system (e.g., the hook, hoist rope, cask yoke) or as a result of improper connection of the load to the hoist. Because the crane is designed to select criteria of ASME NOG-1, *Rules for Construction of Overhead and Gantry Cranes (Top Running Bridge, Multiple Girder)*, Type I, the crane load remains suspended during and after a design basis earthquake (DBE) event. The following five scenarios involving 60-in. drops from the receiving crane have been analyzed in WMTS-RPT-037, *Canister Storage Building Multi-Canister Overpack Cask and Multi-Canister Overpack Impact Analysis*.

1. Cask–MCO Slapdown Drop onto the Concrete Deck. (This case corresponds to scenario 2 in Table 2-1.) In this case, two drop orientations of the cask–MCO are evaluated: a center-of-gravity over corner orientation and a shallow angle (15°) orientation. In both orientations, the cask–MCO is assumed to be suspended initially from the crane with the impacting corner of the cask–MCO 60 in. from the floor. The rigging then fails in a manner such that the cask–MCO is subjected to an oblique drop and slapdown onto the concrete deck of the CSB. For both orientations, the primary impacts are simulated as corner drops and the slapdowns are simulated separately as flat horizontal drops from heights that account for the additional rotational velocity of the cask center of gravity at impact.

2. Cask–MCO End (Vertical) Drop onto the Concrete Deck. (This case corresponds to scenario 3 in Table 2-1.) In this case, the cask–MCO is assumed to be suspended initially from the crane with the bottom of the cask–MCO 60 in. from the floor. The rigging then fails in a manner such that the cask–MCO is subjected to a flat bottom-end drop onto the concrete deck and does not tip over.

3. Cask–MCO Drop onto Edge of Cask Receiving Pit with Slapdown. (This case corresponds to scenario 4 in Table 2-1.) This case is the same as case 1 except the initial oblique drop is on the edge of the cask receiving pit with slapdown (both shallow angle and center-of-gravity over corner orientations). This slapdown is simulated by a horizontal side drop from an increased height that accounts for the rotational velocity of the center of gravity of the cask.

4. Cask–MCO Drop Spanning Cask Receiving Pit. (This case corresponds to scenario 5 in Table 2-1.) In this case, the cask–MCO is assumed to drop from a height of 60 in. onto the cask receiving pit. The drop is assumed to be a horizontal side drop with the center of gravity of the cask over the geometric center of the pit.

5. Shallow Angle Cask–MCO Drop into the Cask Receiving Pit with Cask Impacting on Opposite Edge of Vault Pit. (This case corresponds to scenario 6 in Table 2-1.) In this case, the cask–MCO is assumed to drop into the pit at a shallow angle off the

horizontal (approximately 15°). Initially the cask–MCO is assumed to be suspended from the crane with the impacting corner of the cask–MCO 60 in. from the floor. The rigging then fails in a manner such that the cask–MCO is subjected to a shallow angle drop into the pit and subsequent slapdown onto the concrete deck near the edge of the vault pit. The primary impact is simulated as a shallow angle drop impacting the opposite edges of the pit and the slapdown is simulated separately as flat horizontal drops from heights that account for the rotational velocity of the cask center of gravity at impact. The slapdown sequence is that the cask initially impacts on its bottom corner in the pit and the top end closure slaps down on the vault pit edge.

Using U.S. Nuclear Regulatory Commission and commercially accepted practices, the cask in these cases is considered to be a rigid body impacting a yielding surface. The concrete and soil are considered real surfaces that absorb the energy of impact. This is predicated on the shipping cask being much harder and stiffer than a concrete surface. Consequently, the concrete and underlying soil act to decelerate the cask.

Numerical simulations using the ABAQUS/Explicit computer program were used to develop the average inertial load factors and inertial load factor time histories for the various scenarios involving cask–MCO drops onto concrete surfaces at the CSB. Since the cask has a natural frequency in excess of 33 Hz, the cask was modeled as a rigid body in the numerical impact simulations. The impacted CSB concrete surfaces and soil subgrades were modeled as real targets. The slope of the velocity time history profiles was used to determine the average inertial load factors.

Quasi-static methods were used for structural evaluation of the cask–MCO closure. This quasi-static method is based on D'Alembert's principle of substituting an equivalent static force for the inertial force created by impact. These inertial forces represented in the calculation as equivalent static loads were determined by multiplying the weight of the cask by the average inertial load factor of the cask. In addition, this average inertial load factor was multiplied by the maximum dynamic load factor to account for the dynamic response of the cask.

Given the robustness of the cask and cask closure lid, the most vulnerable components of the cask relative to loss of confinement during and after a free drop impact are the closure lid bolts. The bolts were evaluated by classical linear elastic methods by the evaluation approach specified in NUREG/CR-6007, *Stress Analysis of Closure Bolts for Shipping Casks*. For conservatism, the closure system was considered a protected lid with the weight of the closure lid applying a shear load to the bolts at the threads.

The loading evaluation for these cases (WMTS-RPT-037) shows that stresses in the bolts are below the allowable limits specified in NUREG/CR-6007 for accident conditions. This is demonstrated by the positive margins of safety based on the allowable stress intensity limits in all cases. Results show that margins of safety on the reduced shank of the bolt are positive and the margins of safety of the shear ring are large. During a flat bottom end drop, the only loading on the closure lid bolts is the fixed edge moments and forces applied by the closure lid inertia. This results in an average tensile load on the bolt that, when compared with the allowable stress

intensity limits, results in a margin of safety of 7.38. Initial oblique bottom impact loads on the bolts were treated as axial and radial vector components of the impact force. In these cases, the inertial load factors were relatively low compared with the horizontal side drop and bottom end drop. As a result, the margins of safety on the closure bolts are large. Consequently, as demonstrated by the positive margins of safety, the cask closure lid bolts, reduced bolt shank, and shear ring remain elastic and maintain confinement in the various scenarios involving a drop of the cask–MCO onto the CSB floor and floor structures.

To be conservative, a breach of the MCO as well as a breach of the cask following this drop is assumed. Unmitigated, this event has been determined to be in the unlikely category (SNF-4042). The gas leaving the MCO contains considerable hydrogen so a flammable mixture of hydrogen, helium, and air forms in the space between the outside of the MCO and the inside of the cask. This flammable mixture ignites, but the resulting pressure increase is not expected to damage the cask (see Chapter 5.0).

D2 — Cask–Multi-Canister Overpack Drop from Receiving Crane into Cask Receiving Pit. (This case corresponds to scenario 7 in Table 2-1.) The cask receiving pit is fitted with an impact absorber designed to control the dynamics of dropping an MCO cask containing an MCO into an empty cask (i.e., to limit the deceleration). The impact absorber mitigates the damage to the MCO following the drop accident. The impact absorber is required to limit the deceleration of a maximum weight MCO dropped from the maximum height to less than 35 *g*. The MCO and internal baskets are designed to maintain confinement under drops with decelerations limited below 35 *g*. The impact absorber for the cask receiving pit is designed for a drop height of 281 in. The maximum height of the cask receiving pit impact absorber is 45 in. The impact absorber design was developed through a combination of both calculations and static and dynamic tests.

To be conservative, a breach of the MCO as well as a breach of the cask following this drop is assumed. Unmitigated, this event has been determined to be in the unlikely category (SNF-4042). Full-scale prototypic tests of the impact absorber were performed and are documented in TR-003, *Test Report for the CSB Prototypic Impact Absorbers*. The tests used video records to demonstrate acceptable deceleration. While a direct crush measurement of the impact absorber indicated a deceleration load that was higher than expected and higher than the design criteria, this was attributed to energy transferred to the ground upon impact.

HNF-SD-SNF-DR-003, *Multi-Canister Overpack Design Report*, demonstrates that the MCO will meet design criteria. The design calculation shows that the Mark 1A MCO's internals can withstand the design basis conditions of a 35 *g* vertical drop or a 101 *g* horizontal drop. The MCO cask containing an MCO will not be damaged following a drop into the cask receiving pit.

D3 — Cask–Multi-Canister Overpack Drop from Receiving Crane into Fast Flux Test Facility Pit or Multi-Canister Overpack Handling Machine Maintenance Pit. (This case corresponds to scenarios 9a and 9b in Table 2-1.) When the receiving crane is moving the cask–MCO from the transport trailer to the cask receiving pit, the cask–MCO is not to be moved over the FFTF or maintenance pits. The receiving crane resolver tracks the east–west position of

the receiving crane. Before the receiving crane reaches the west side of the FFTF pit, the interlock removes power from the drive motors. Power may only be restored to the crane by both the use of a supervisor-controlled fortress key at a remote station and the operator depressing an override button on the crane. While this interlock does not reduce the drop frequency, it does reduce the frequency of drops into the FFTF or maintenance pits.

However, given certain errors, the cask–MCO could mistakenly be moved over the FFTF or maintenance pits where it would be vulnerable to a potential drop into the pit. The consequences of a cask–MCO drop by the receiving crane (from a height greater than 60 in.) into the FFTF or maintenance pit with a slapdown have not been determined. While definitive supporting calculations do not exist, no radiological releases or associated onsite or offsite dose consequences are expected from such an accident because of the structural protection provided by the cask. A breach of the MCO as well as a breach of the cask following this drop is assumed. Unmitigated, this event has been determined to be in the unlikely category (SNF-4042). The gas leaving the MCO contains considerable hydrogen so a flammable mixture of hydrogen, helium, and air forms in the space between the outside of the MCO and the inside of the cask. This flammable mixture ignites, but the resulting pressure increase is not expected to damage the cask (see Chapter 5.0).

D4 — Drop of a Multi-Canister Overpack by the Multi-Canister Overpack Handling Machine onto Edge of the Cask Receiving Pit. (This case corresponds to scenario 15 in Table 2-1.) If the MHM were to drop an MCO, the MCO would impact the slope of the shield hatch and MCO guide assembly because of the shield hatch and MCO guide assembly design and the centering guide installed in the MHM. The shield hatch has a 75° incline, which would greatly reduce the impact force. The centering guide would limit MCO tilt, which would ensure the impact area was always on the shield hatch incline.

An engineering analysis using the ABAQUS/Explicit computer code has been performed to address dropping an MCO onto the edge of the cask receiving pit (eccentric drop); the analysis is documented in SNF-5204, *Analysis for Eccentric Multi-Canister Overpack Drops at the Canister Storage Building (CSB-S-0073)*. This analysis predicted accelerations, plastic strain, and stress distributions, and identifies failure modes. The structural numerical models addressed nonlinear material behavior as well as impact dynamics. The weight of the MCO used in the analysis was 20,000 lb, and the drop height was conservatively assumed to be 90 in. The maximum equivalent MCO strain was found to be 18% and occurred on the MCO bottom near the point of impact. Since the failure strain is above 80%, it is not likely that through-the-wall cracking would occur although removal of local surface metal may occur. The maximum predicted equivalent plastic strain at the MCO lower weld was 0.4% during a drop into the standard storage tube. This is well below a 13% failure strain. The maximum tensile principal strain was in a radial direction, so any failure would be by spalling or flaking rather than through-the-wall cracking.
The deceleration of the MCO baskets was shown to be about 20 *g* or less, well within the design allowable of 35 *g*.

To be conservative, a breach of the MCO following this drop is assumed. Unmitigated, this event has been determined to be in the unlikely category (SNF-4042).

D5 — Drop of Multi-Canister Overpack by the Multi-Canister Overpack Handling Machine Back into Cask. (This case corresponds to scenario 16 in Table 2-1.) An engineering analysis has been performed to address dropping an MCO back into the cask; the analysis is documented in SNF-5276, *Analysis for SNF MCO Drop into the Cask from the MHM with Air Cushion*. The MCO was assumed to drop from a height of 8.2 ft above the cask, enter the cask concentrically, and fall the additional 12.83 ft to the cask bottom. The MCO's fall would be slowed by air entrapment and the interface fit between the MCO and the cask. The shipping cask was assumed to be resting on the cask receiving impact absorber at the time of impact, and the energy absorbing properties of the cask receiving pit impact absorber were included in the analysis.

The engineering analysis (SNF-5276) showed that an MCO drop into the cask produces very large impact reactions on the MCO and its internals. Plastic strains were shown to occur in the bottom of the MCO, the sides of the MCO near the weld area, the basket support plates, the outside basket support posts, and the basket center support post. Large amounts of energy were absorbed during the impact by these components.

The maximum equivalent plastic strain in the bottom of the MCO was 2.0%. This is below the calculated effective failure strain of 15%. The effective failure strain value was calculated based on the multi-axial stress state (triaxiality factor), temperature, and strain rate. Breaching of the MCO pressure boundary by through-wall cracking is not expected.

Equivalent plastic strains in the weld area at the juncture of the MCO walls and the MCO bottom were 2.1%. This is below the calculated 12.5% effective failure strain. The maximum equivalent plastic strain occurred at the inside surface of the MCO in the weld area. Breaching of the MCO pressure boundary by through-wall cracking in the weld area is also not expected.

To be conservative, a breach of the MCO following this drop is assumed. Unmitigated this event has been determined to be in the unlikely category (SNF-4042).

D6 — Drop of Multi-Canister Overpack within Multi-Canister Overpack Handling Machine Turret onto Multi-Canister Handling Machine Turret Deck. (This case corresponds to scenario 21 in Table 2-1.) When the MHM is traveling in the operating area with an MCO fully raised into the MCO cavity of the MHM turret, the MCO is vulnerable to a potential drop onto the MHM turret deck while partially rotated over the opening. Engineering analysis has been performed to evaluate an MCO drop onto the MHM turret deck (WMTS-RPT-037). As a worst case, it was assumed that the MCO dropped at a shallow angle of 1° off the vertical axis and onto a squared edge of the MHM turret base opening. The drop was assumed to result in an edge impact approximately one-eighth the diameter in from the edge of the MCO.

The results show that the most vulnerable areas of the MCO are not breached and the MCO maintains confinement even at a metal temperature of 270 °F. The maximum equivalent strain (which is a true strain) is 15.5% at the impact point on the MCO bottom plate outside surface. The maximum equivalent strain at the inside surface on the bottom-end-plate-to-shell weld joint is

3.72%. Based on the CSB Expert Panel criteria adjusted for true strain (SNF-5276), the failure strain value at 270 °F is 6.7%. The margin of safety at the impact point for the base metal is 2.1, and in the weld area, the margin of safety is 0.8 (SNF-5276). The margin of safety used is calculated as follows:

(allowable value / calculated value) - 1 .

The allowable values for the MCO are ASME *Boiler and Pressure Vessel Code*, Section III, class 1 allowables for Service Level D (ASME 1995).

The maximum strain energy density at the impact point on the MCO bottom plate outside surface is 7,317 in-lbf/in^3, and the maximum strain energy density at the inside surface on the bottom-end-plate-to-shell weld joint is 1,258 in-lbf/in^3. For Type 304L stainless steel at 270 °F, the minimum yield strength is 19.6 ksi, and the minimum ultimate strength is 62.5 ksi at 40% strain, equating to a minimum rupture toughness of 16,420 in-lbf/in^3. Based on the material toughness criteria, the maximum allowable strain energy density of the base metal is 8,210 in-lbf/in^3. The maximum allowable strain energy density in the weld region is 4,105 in-lbf/in^3. The margin of safety of strain energy density is 0.12 at the impact point and 2.3 in the weld region.

The maximum equivalent plastic strain and strain energy density data show that at the contact locations, the outer surface of the bottom end closure of the MCO is dented. However, the data also show that this damage is only on the surface and does not extend into the inside surface of the bottom end closure plate. The maximum equivalent plastic strain at the weld joint between the MCO shell and bottom end closure plate is very low and well below the established limits for the material. In the weld joint region, the maximum equivalent plastic strain and strain energy density are on the inside surface of the confinement boundary.

To be conservative, a breach of the MCO following this drop is assumed. Unmitigated, this event has been determined to be in the unlikely category (SNF-4042).

D7 — Drop of Multi-Canister Overpack from Multi-Canister Overpack Handling Machine onto Canister Storage Building Operating Area Floor or onto Storage Tube Covers of Vault 2 or Vault 3 in Canister Storage Building. (This case corresponds to scenarios 22 and 23 in Table 2-1.) If errors are made in failing to replace the storage tube plug (or cover plug or center plate) when the MHM has finished raising an MCO into the MCO cavity in the MHM turret, and the MHM is inadvertently moved a short distance over the operating floor, the MCO is vulnerable to a potential drop onto the operating area floor from the fully raised position in the MCO cavity in the MHM turret when no credit is taken for the MHM interlocks. Anytime the MHM is carrying an MCO in the MCO cavity in the MHM turret and stops anywhere on the operating area, the MCO is vulnerable to a potential drop onto the operating area floor from the fully raised position in the MCO cavity in the MHM turret when the MHM is rotated to the MCO cavity of the MHM turret position, providing no credit is taken for the MHM interlocks. Whenever an MHM is carrying an MCO in the MCO cavity in the MHM turret and stops over vaults 2 or 3, the MCO is vulnerable to a potential drop onto the vault covers from the

fully raised position in the MCO cavity in the MHM turret when the MHM is rotated to the MCO cavity in the MHM turret position, providing no credit is taken for the MHM interlocks. A breach of the MCO following this drop is assumed. Unmitigated, this event has been determined to be in the extremely unlikely category (SNF-4042).

D8 — Drop of Multi-Canister Overpack from Multi-Canister Overpack Handling Machine onto or into Multi-Canister Overpack Handling Machine Maintenance Pit or Tube Plug Exchange Facility. (This case corresponds to scenario 24 in Table 2-1.) When the MHM is moving an MCO in the operating area, the MHM is not to be moved over the MHM maintenance pit. However, given certain errors, the MHM containing an MCO could mistakenly be moved over the MHM maintenance pit or tube plug exchange facility, where the MCO would be vulnerable to a potential drop into the pit providing no credit is taken for the MHM interlocks. A breach of the MCO following this drop is assumed. Unmitigated, this event has been determined to be in the extremely unlikely category (SNF-4042).

D9 — Drop of Multi-Canister Overpack from Multi-Canister Overpack Handling Machine onto or into Fast Flux Test Facility Pit. (This case corresponds to scenario 25 in Table 2-1.) When the MHM is moving an MCO in the operating area, the MHM is not to be moved over the FFTF pit. However, given certain errors, the MHM containing an MCO could mistakenly be moved over the FFTF pit, where the MCO would be vulnerable to a potential drop into the FFTF pit providing no credit is taken for the MHM interlocks. A breach of the MCO following this drop is assumed. Unmitigated, this event has been determined to be in the extremely unlikely category (SNF-4042).

D10 — Drop of Multi-Canister Overpack by Multi-Canister Overpack Handling Machine into Storage Tube or Sampling/Weld Station. (This case corresponds to scenario 29 in Table 2-1.) Each storage tube bottom is fitted with a bottom impact absorber of stainless steel tubes that has been designed to control the dynamics of dropping a single MCO into an empty storage tube. The bottom impact absorber will mitigate damage to an MCO following such a drop. These bottom impact absorbers are required to limit the deceleration of a maximum weight MCO dropped from the maximum height to less than 35 *g*. The MCO and its internal baskets are designed to maintain confinement under drops with decelerations limited below 35 *g* as specified in HNF-S-0426, *Performance Specification for Spent Nuclear Fuel Project, Multi-Canister Overpack*. Therefore, the MCO will not be damaged following a drop into the storage tube. The adequacy of the bottom impact absorber has been demonstrated by a full-scale test. To be conservative, a breach of the MCO following this drop is assumed. Unmitigated, this event has been determined to be in the unlikely category (SNF-4042).

An intermediate impact absorber is placed between two MCOs stacked in a storage tube. The intermediate impact absorber is designed to mitigate damage to both MCOs if the top MCO is accidentally dropped during storage tube loading. These intermediate impact absorbers are required to limit the deceleration of an MCO dropped on top of another MCO to less than 35 *g*. The MCOs will not be damaged following a drop on top of another MCO in the storage tube. The adequacy of the intermediate impact absorber has been demonstrated by a full-scale test.

Each sampling/weld station pit is fitted with an impact absorber of stainless steel tubes that has been designed to control the dynamics of dropping an MCO into the sampling/weld station rotating shield. The sampling/weld station impact absorber will mitigate damage to the MCO after such a drop. These impact absorbers are required to limit the deceleration of a maximum weight MCO dropped from the maximum height to less than 35 *g*. The MCO and its internal baskets are designed to maintain confinement under drops with decelerations limited below 35 *g* (HNF-S-0426). Therefore, the MCO will not be damaged following a drop into the sampling/weld station rotating shield. The design adequacy of the impact absorber has been demonstrated by a full-scale drop test.

D11 — Drop of Multi-Canister Overpack by Multi-Canister Overpack Handling Machine onto Another Multi-Canister Overpack Located in the Bottom of a Storage Tube (No Intermediate Impact Absorber Involved). (This case corresponds to scenario 31 in Table 2-1.) When the MHM is placing an MCO into a storage tube that contains one MCO but which has no intermediate impact absorber, each MCO would be vulnerable to a potential drop of the MCO hanging from the MHM.

A drop of an MCO onto another MCO already loaded into the storage tube would cause plastic deformation to the bottom of the dropped MCO and the top of the impacted shield plug, but the confinement functions of either MCO would not be jeopardized. The deceleration associated with such a drop would not damage the MCO internals. HNF-SD-SNF-DP-007, *Multi-Canister Overpack/Cask Drop Analysis File Documentation*, Appendix D, "Multi-Canister Overpack to Multi-Canister Overpack Drop Analysis," documents the simulation of a 31-ft drop of a loaded MCO onto another MCO. A bottom impact absorber is in place under the first MCO, but no intermediate impact absorber is in place between them. The analysis indicates that plastic deformation of the impacted shield plug seal and shoulder would be a maximum of 0.030 in. The impact absorber under the bottom MCO would be compressed 6 to 9 in. To be conservative, a breach of the MCO following this drop is assumed. Unmitigated, this event has been determined to be in the unlikely category (SNF-4042).

D12 — Drop of Multi-Canister Overpack by the Multi-Canister Overpack Handling Machine onto the Storage Tube Plug because of Inadvertent Turret Rotation. (This case corresponds to scenario 33 in Table 2-1.) Anytime an MHM is carrying an MCO in the MCO cavity in the MHM turret and stops over a storage tube plug, the MCO is vulnerable to a potential drop onto the storage tube plug pintle from the fully raised position in the MCO cavity in the MHM turret when the MHM is rotated to the MCO cavity in the MHM turret position providing no credit is taken for the MHM interlocks. A breach of the MCO following this drop is assumed. Unmitigated, this event has been determined to be in the extremely unlikely category (SNF-4042).

D13 — Drop of Multi-Canister Overpack by Multi-Canister Overpack Handling Machine onto Edge of Storage Tube. (This case corresponds to scenario 34 in Table 2-1.) The storage tube is supported off the floor. The lower flange of the tube is 4.5 in. thick and has a 45° incline to reduce any direct impact between a dropped MCO and the edge of the storage tube following an eccentric drop event. An engineering analysis (SNF-5204) has been performed to address dropping an MCO onto the edge of a storage tube (eccentric drop). The drop was

conservatively assumed to hit the lower flange of the storage tube (which has a 45° incline) not the guide funnel (which has a 75° incline). The weight of the MCO used in the analysis was 20,000 lb, and the drop height was conservatively assumed to be 90 in. The MCO was assumed to be tilted by no more than 2°21′ from vertical because of the MCO centering guide installed in the MHM. If a drop tilted more than 2°21′, the MCO would most likely hit the funnel placed above the upper flange. The funnel has a 75° entrance angle, and the impact would be less severe than an impact on the lower flange. The engineering analysis predicted accelerations, plastic strain, and stress distributions, and identified MCO failure modes. The structural numerical models address nonlinear material behavior as well as impact dynamics. The tube bellows, which has an insignificant effect, was not included in the model.

According to the analysis, the maximum equivalent MCO strain was 40% to 45% and occurred on the MCO bottom near the point of impact (SNF-5204). Since the failure strain is above 80%, it is not likely that through-the-wall cracking will occur although removal of local surface metal may occur. The maximum predicted equivalent plastic strain at the MCO lower weld was 2% during the drop into the standard storage tube. This is well below a 13% failure strain. The maximum tensile principal strain was in a radial direction, so any failure would be by spalling or flaking rather than through-the-wall cracking. The deceleration of the MCO baskets was shown to be about 20 *g* or less, well within the design allowable of 35 *g*. The deformations of the MCO and standard storage tube were less than the tube clearance, so no wedging of the MCO in the tube is expected. To be conservative, a breach of the MCO following this drop is assumed. Unmitigated, this event has been determined to be in the unlikely category (SNF-4042).

D14 — Drop of Multi-Canister Overpack by Multi-Canister Overpack Handling Machine onto Edge of a Sampling/Weld Station. (This case corresponds to scenario 35 in Table 2-1.) The MCO impacts a 75° inclined surface on the shield hatch ring at the cask receiving pit. The impact at the sampling/weld station is on a similar 75° inclined surface on the shield halves. The shield halves at the sampling/weld station is less massive and held in place less securely than the shield hatch ring of the cask receiving pit and will cause less damage to the MCO. Therefore, the results of an MCO drop onto the edge of the cask receiving pit bound those for a drop onto the edge of the sampling/weld station.

The MCO will impact the incline of the shield halves because of the design of the shield halves and the MCO centering guide installed in the MHM. The shield halves have a 75° incline, which will greatly reduce the impact force. The MCO centering guide will limit the MCO tilt, which ensures that the impact area is always on the incline of the shield halves. To be conservative, a breach of the MCO following this drop is assumed. Unmitigated, this event has been determined to be in the unlikely category (SNF-4042).

2.2.2 Shear of a Multi-Canister Overpack

At the CSB the MCO is hoisted by both the receiving crane and the MHM. The MCO could be sheared, either when it is inside the transportation cask or when it is outside the cask. Several different scenarios that could cause an MCO shear (which would be a localized breach or

tear and not a complete severance of the MCO) have been considered. All of these shear scenarios are considered potentially serious hazards to the MCO in the CSB hazard analysis (HNF-SD-SNF-HIE-001):

S1 Shear of cask–MCO by moving receiving crane while cask–MCO is partially lowered into cask receiving pit, or shear of cask–MCO because of collision between MHM and receiving crane as receiving crane lowers cask–MCO into cask receiving pit

S2 Shear of MCO by MHM turret rotation with MCO partially retrieved into MHM at cask receiving pit, storage tube, or sampling/weld station

S3 Shear of MCO by MHM translational movement with MCO only partially retrieved into MHM at cask receiving pit

S4 Shear of MCO while MCO is partially retrieved from or inserted into cask receiving pit, storage tube, or sampling/weld station during significant seismic event

S5 Shear of MCO by MHM translational movement with MCO only partially retrieved into MHM turret at storage tube or sampling/weld station.

S1 — Shear of Cask–Multi-Canister Overpack by Moving Receiving Crane while Cask–Multi-Canister Overpack is Partially Lowered into Cask Receiving Pit, or Shear of Cask–Multi-Canister Overpack because of Collision between Multi-Canister Overpack Handling Machine and Receiving Crane as Receiving Crane Lowers Cask–Multi-Canister Overpack into Cask Receiving Pit. (This case corresponds to scenarios 8 and 10 in Table 2-1.) When the receiving crane is lowering the cask–MCO into the cask receiving pit and the cask–MCO is partially inserted into the cask receiving pit, the cask–MCO is vulnerable to a potential shear of the cask between the pit wall and the cask wall if the receiving crane were to be moved at this time. The shear forces from accidental movement of the receiving crane are bounded by those from collision of the MHM with the receiving crane and are therefore insufficient to breach the cask–MCO. No breach of the MCO following this collision is predicted by analysis. Unmitigated, this event has been determined to be in the anticipated category (SNF-4042).

When the receiving crane is lowering the cask–MCO into the cask receiving pit and the cask–MCO is partially inserted into the cask receiving pit, design features preclude the MHM from colliding with the crane. It is conservative to assume that the cask–MCO is vulnerable to a potential shear of the cask from the MHM colliding with the receiving crane and subsequently with the cask; the cask provides confinement. Analysis documented in FDT-137, *MHM Impact with Cask/MCO during Insertion into CSB Transfer Pit* (Petersen 1998), has shown that a collision would not breach the cask–MCO. MHM interlock P5, which inhibits receiving crane and MHM interaction, was not credited in the frequency calculation (SNF-4042); it is considered part of the defense-in-depth measures.

S2 — Shear of Multi-Canister Overpack by Multi-Canister Overpack Handling Machine Turret Rotation with Multi-Canister Overpack Partially Retrieved into Multi-Canister Overpack Handling Machine at Cask Receiving Pit, Storage Tube, or Sampling/Weld Station. (This case corresponds to scenarios 17a, 20, and 28 in Table 2-1.) When the MHM is raising the MCO into the MHM turret and the MCO is partially removed from the transportation cask, the storage tube, or sampling/weld station, the MCO is vulnerable to a potential shear from premature MHM turret rotation.

Analysis documented in SNF-5930, *Structural Analysis of Multi-Canister Overpack for Accidental Movement of Multi-Canister Overpack Handling Machine during Multi-Canister Overpack Lifting Operations*, demonstrates that a shear of the MCO is not possible using the turret rotation motor. For a turret rotational speed of 2 rpm, the kinetic energy is 1,300 ft-lbf. A locked rotor torque of 63 lb-ft results in a force on the MCO of 10,000 lbf. This force applied over a distance of 0.2 in. (penetration to fracture) increases the total energy to 1,470 ft-lbf. The energy required to initiate puncture of the MCO shell is 3,000 ft-lbf; therefore, the shell will not puncture from the inertial effects of the rotating turret combined with the drive motor effects. The peak force required to initiate puncture is 270,000 lbf. This value is roughly 27 times the 10,000 lbf the motor and gearing are capable of applying to the MCO at a locked rotor torque of 63 lb-ft. No breach of the MCO following turret rotation is predicted by analysis. Unmitigated, this event has been determined to be in the anticipated category (SNF-4042).

S3 — Shear of Multi-Canister Overpack by Multi-Canister Overpack Handling Machine Translational Movement with Multi-Canister Overpack only Partially Retrieved into Multi-Canister Handling Machine at Cask Receiving Pit. (This case corresponds to scenario 17b in Table 2-1.) When the MHM is raising the MCO into the MHM turret and the MCO is partially removed from the transportation cask, the MCO is vulnerable to a potential shear from premature MHM translational motion. A breach of the MCO following the forces from MHM translational movement is assumed. Unmitigated, this event has been determined to be in the unlikely category (SNF-4042). To be conservative, breach of the MCO was assumed for this shear, which is considered to be an unlikely event. Analysis documented in SNF-5930 shows that the internal geometry of the Mark IA baskets remain intact (no rearrangement of internal geometry).

S4 — Shear of Multi-Canister Overpack while Multi-Canister Overpack is Partially Retrieved from or Inserted into Cask Receiving Pit, Storage Tube, or Sampling/Weld Station during Significant Seismic Event. (This case corresponds to scenario 18 in Table 2-1.) When the MHM is raising the MCO into the MHM turret and the MCO is partially removed from the shipping cask, the MCO is vulnerable to a potential shear from a seismic event. This shear event includes the potential shear caused by turret rotation or the potential shear caused by translational movement of the MHM. This shear event is prevented by the bridge and trolley seismic restraints as well as by the turret locking pin and base locking pin. Calculations have been performed to demonstrate the design adequacy of the seismic restraints and locking pins for seismic events with forces up to those of the DBE. To be conservative, a breach of the MCO following the shear forces from MHM translational movement during a significant seismic event is assumed. Unmitigated, this event has been determined to be in the unlikely category (SNF-4042).

S5 — Shear of Multi-Canister Overpack by Multi-Canister Overpack Handling Machine Translational Movement with Multi-Canister Overpack only Partially Retrieved into Multi-Canister Overpack Handling Machine Turret at Storage Tube or Sampling/Weld Station. (This case corresponds to scenario 27 in Table 2-1.) When the MHM is raising the MCO into or lowering the MCO from the MHM turret and the MCO is partially removed from the storage tube or sampling/weld station pit, the MCO is vulnerable to a potential shear from premature MHM translational motion.

Analysis shows that the internal geometry of the Mark IA baskets remain intact (SNF-5930). To be conservative, a breach of the MCO following the shear forces from MHM translational movement is assumed. Unmitigated, this event has been determined to be in the unlikely category (SNF-4042).

2.2.3 Impacts Other than Shears and Drops of a Multi-Canister Overpack

At the CSB impacts to the MCO or to the cask–MCO could also be caused by events other than shears and drops. Several different scenarios that could cause an impact to the MCO have been considered. All of these impact scenarios are considered potentially serious hazards to the MCO in the CSB hazard analysis (HNF-SD-SNF-HIE-001):

O1 Drop of receiving crane yoke onto cask lid, or drop of cask lid onto MCO

O2 Collapse of CSB structure and impact to MCO during seismic event

O3 Drop of cask receiving pit shield hatch and MCO guide assembly's shield hatch plate by MHM onto MCO, or drop of storage tube plug or sampling/weld station enter shield plate by MHM onto MCO in storage tube or sampling/weld station

O4 MHM fall or damage caused by a seismic event

O5 Drop of intermediate impact absorber onto MCO.

O1 — Drop of Receiving Crane Yoke onto Cask Lid, or Drop of Cask Lid onto Multi-Canister Overpack. (This case corresponds to scenarios 11 and 12 in Table 2-1.) When the receiving crane is raising the cask–MCO yoke away from the cask–MCO in the cask receiving pit, the cask lid is vulnerable to a potential drop of the yoke. In the case of the lifting yoke and crane rigging falling onto the MCO cask lid, the acceptable performance criterion is the cask lid not being punctured. Acceptable performance of the MCO cask lid is demonstrated by a quantitative comparative analysis based on a cask puncture test (WMTS-RPT-037).

For this scenario, the impact energy of the lifting yoke, crane rigging, and hook dropping onto the cask–MCO lid was compared with the cask–MCO puncture resistance analysis documented in *Design Analysis Report for the TN-WHC Cask and Transportation System* (TN 1996). The following assumptions were made in the comparative energy evaluation:

- Crane two-blocking causes the lifting yoke and crane hook and rigging to drop onto the cask–MCO lid while the cask is in the cask receiving pit.
- The total weight of the lifting yoke and crane hook and rigging is 6,200 lb.
- The cask–MCO is elevated to a working height, therefore the closure bolts are at CSB floor level.
- For conservatism, the protection provided by the lifting brackets and trunnions is not considered.
- The crane hook impacts the cask lid.

Based on the above assumptions, the drop height of the lifting yoke, crane hook, and rigging is 28 ft. The top of the cask closure lid, excluding the trunnion brackets, is 11 in. off the floor. This results in a drop height of 27 ft, 1 in. onto the closure lid. The potential energy from such a drop is 168 kip-ft.

The top end cask puncture evaluation (TN 1996) was performed in accordance with Title 10, *Code of Federal Regulations*, Part 71, "Packaging and Transportation of Radioactive Materials," Section 71.73, "Hypothetical Accident Conditions" (10 CFR 71). The evaluation (TN 1996) determined that the loaded cask–MCO could survive a 40-in. drop onto a 6-in. solid vertical cylinder (puncture bar) mounted on an unyielding surface.

The impact energy of the lifting yoke and crane hook and rigging was calculated as being approximately 19% less than the impact energy evaluated in the Transnuclear (TN 1996) design analysis report. Therefore, there is margin of safety of 19% based on the cask puncture bar test. This is in addition to cask–MCO margin of safety in resisting puncture of 6.07 shown in the Transnuclear (TN 1996) evaluation.

The tent gantry hoist in the load-in/load-out area will be used to remove the cask lid from the cask–MCO. When the tent gantry hoist is raising the cask lid away from the cask–MCO in the cask receiving pit, the MCO is vulnerable to a potential drop of the cask lid. An analysis has been performed to evaluate cask lid drops (HNF-SD-SNF-DP-007). The analysis concluded that the MCO maintains confinement of all spent nuclear fuel during and after a 1.5-m (approximately 60 in.) drop of a cask lid. A drop of the cask lid from the tent gantry hoist onto the MCO would cause only local cosmetic damage at the point of impact, but the MCO would maintain its confinement functions. Local plastic damage would only be found by close inspection of the hardware after the event. If the receiving crane were used to remove the cask lid from the cask, the reliability of the receiving crane makes the consequences of the cask lid drop acceptable for the likelihood of a receiving crane drop. No breach of the MCO following a drop of the cask lid by the tent gantry hoist is predicted by analysis. A breach of the MCO following drop of the cask lid by the receiving crane is assumed. Unmitigated, this breach event has been determined to be in the unlikely category (SNF-4042).

O2 — Collapse of Canister Storage Building Structure and Impact to Multi-Canister Overpack during Seismic Event. (This case corresponds to scenario 13 in Table 2-1.) Given a seismic event occurs, there is potential for the CSB facility to structurally fail and fall to the operating area deck and to strike an MCO exposed at the cask receiving pit or the sampling/weld station pit. The CSB has been designed to withstand the DBE.

O3 — Drop of Cask Receiving Pit Shield Hatch and MCO Guide Assembly's Shield Hatch Plate by Multi-Canister Overpack Handling Machine onto Multi-Canister Overpack, or Drop of Storage Tube Plug or Sampling/Weld Station Center Shield Plate by Multi-Canister Overpack Handling Machine onto Multi-Canister Overpack in Storage Tube or Sampling/Weld Station. (This case corresponds to scenarios 14 and 36 in Table 2-1.) When the MHM is raising the cask receiving pit shield hatch and MCO guide assembly's shield hatch plate, it is possible that the MHM could drop the shield hatch plate toward the MCO in the cask. However, it is physically impossible for a dropped shield hatch plate to make contact with the top of an MCO because of the dimensions of the shield hatch plate and depth of the top of the MCO below the shield hatch and MCO guide assembly.

When the MHM is raising or lowering a storage tube plug or sampling/weld station center shield plate with the tube plug grapple, it is possible that the MHM could drop the storage tube plug or sampling/weld station center shield plate toward the MCO in the storage tube or the sampling/weld station pit. However, it is physically impossible for a dropped tube plug or cover plug to make contact with the top of an MCO because of the dimensions of the plug and depth of the top of the MCO below the storage tube embed or the sampling/weld station shielding.

O4 — Multi-Canister Overpack Handling Machine Fall or Damage Caused by a Seismic Event. (This case corresponds to scenario 19 in Table 2-1.) Evaluations documented in SNF-5984, *Multi-Canister Overpack Handling Machine Trolley Seismic Uplift Constraint Design Loads*, were performed to study the behavior of the MHM during a DBE. These evaluations considered the effects on the MHM both with and without the seismic restraints and without the rail stops. All cases studied demonstrate that the MHM will not tip over or collapse during a DBE. For the unrestrained seismic event, the MHM trolley seismic uplift restraints exceed the ASME-NOG-1 allowables. The design of the MHM will be strengthened to meet ASME-NOG-1 requirements, and this modification will be incorporated before implementation of the CSB Final Safety Analysis Report. A potential MHM tip-over caused by the rail stops (if the MHM is near the rail stops without seismic restraints) during a DBE was not analyzed. The postulated scenario was judged to have very low likelihood because the MHM is rarely located close to the rail stops without the seismic restraints applied.

O5 — Drop of Intermediate Impact Absorber onto Multi-Canister Overpack. (This case corresponds to scenario 26 in Table 2-1.) The acceptable performance criterion for the intermediate impact absorber impacting the top of an MCO is that the critical confinement boundaries of the MCO remain below yield under the impact loading.

A comparative qualitative analysis of an intermediate impact absorber drop onto the top of an MCO was performed based on HNF-SD-SNF-DP-007, the impact energy, and the design and weight of the intermediate impact absorber (WMTS-RPT-037).

The evaluation demonstrates that the MCO after a free drop impact of the intermediate impact absorber onto the MCO maintains confinement. Analysis documented in HNF-SD-SNF-DP-007 shows the MCO maintains confinement after the impact from a 31-ft free fall of another fully loaded MCO onto the top of a stationary MCO in the CSB storage tube. It was assumed that the MCO canister cover was not installed and the MCO shield plug area was exposed to the impact (HNF-SD-SNF-DP-007). The comparative analysis shows that based on the difference in weight of the MCO (20,000 lb) and the intermediate impact absorber (630 lb), the impact energy of the intermediate impact absorber is significantly less than the impact of a fully loaded MCO (620 kip-ft versus 19.5 kip-ft) (WMTS-RPT-037). Consequently, the MCO, with or without the cover cap, will maintain confinement after a free fall drop of the intermediate impact absorber onto a stationary MCO in the CSB storage tube.

2.3 SOURCE TERM ANALYSIS

The quantity of particulate released following an MCO breach caused by mechanical damage depends on the initial aerosol concentration, which includes that generated by the mechanical accident forces, and subsequent particulate entrainment. The potential sources of particulate entrainment come from venting of pressurized powder and aerodynamic entrainment. Both of these sources represent the effects of local gas velocities to entrain particles. The key difference between two entrainment sources is that the powder venting source is intended to represent a situation in which the gas flow field is predominantly through the particle bed, while the aerodynamic entrainment source is intended to represent a situation in which the gas flow field is predominantly outside the bed.

The amount of material available for release depends on the amount of particulate mass generated in the MCO during processing. This quantity is a function of processing times and temperatures as well as of the condition of the fuel in the MCO (e.g., exposed surface area of fuel). HNF-SD-SNF-TI-015, *Spent Nuclear Fuel Project Technical Databook*, provides two estimates of this quantity: one for the safety basis, which is considered the bounding value, and the other for the design basis, which is considered the nominal value. When the MCO is received at the CSB, the safety basis value is 23.1 kg uranium and the design value is 0.54 kg uranium (HNF-SD-SNF-TI-015). After 40 years of storage at the CSB, the safety basis, or bounding, value is 30 kg uranium and the design basis, or nominal, value is 1.85 kg uranium (HNF-SD-SNF-TI-015). Because of the conservative methodology used to calculate the bounding value, 30 kg is considered representative of the 99th percentile.

The MCO blowdown scenario features films of particles, not deep powder beds. While it is true that there is some gas flow through particle layers during a blowdown, experiments documented in *Technical Report 11.6: Resuspension of Deposited Aerosols Following Primary System or Containment Failure* (IDCOR 1984) clearly show that this is a trivial effect.

Experiments that underlie the powder venting source term feature a pressurized cylinder packed with powder. During depressurization, the flow velocity is zero at the bottom of the particle bed when there is no underlying gas plenum, and the velocity increases to its maximum at the exit, which is at the top. The gas velocity at the top of the bed must be enough to fluidize the bed locally and to entrain the particles. When the particle bed height was decreased in these experiments, the velocity at the top of the bed decreased in linear proportion to the distance, and there was a bed height at which little or no entrainment could occur. In such a situation, there was gas flow through the bed during depressurization, but the local velocity was simply not sufficient for entrainment (IDCOR 1984). Therefore, for application to the MCO blowdown accident scenarios, in which particle layers are thin and relatively well-distributed throughout the MCO, the pressurized powder venting source term is not applicable, and a source term based upon aerodynamic entrainment should be used.

DOE-HDBK-3010-94, *Airborne Release Fractions/Rates and Respirable Fractions/Rates for Nonreactor Nuclear Facilities*, documents airborne release rates (ARRs) and respirable fractions (RFs). Based on the data reported in DOE-HDBK-3010-94, a bounding (95th percentile) ARR of 4×10^{-5}/h and an RF of 1.0 were selected. The contents of the MCO are intact fuel elements tightly packed in fuel baskets and pieces of fuel elements housed in scrap baskets. Particulate matter swept upward by streams of flowing gas within the MCO must take a tortuous path through the MCO to exit the MCO. For shielded powder, where the aerodynamic stresses are reduced by debris or exposure to static conditions, DOE-HDBK-3010-94 recommends an ARR of 4×10^{-6}/h and an RF of 0.2. These values were selected as nominal (50th percentile).

The duration of the blowdown depends on the flow area of the leak and the initial MCO pressure. The MCO depressurizes to atmospheric pressure in less than 1 minute, even for an MCO pressure of about 150 lb/in^2 gauge and a 0.25-in. hole. The MCO depressurizes in a much shorter time for lower pressures and larger leak paths. For the calculation of the source term, a nominal (50th percentile) value of 10 seconds and a bounding (95th percentile) time of 60 seconds were selected.

Using the methodology described in Chapter 1.0 and the bounding and nominal values identified above, the bounding (95th percentile) value for the material released through aerodynamic entrainment is calculated to be 2.0×10^{-4} g, as shown in Table 2-2.

Table 2-2. Aerodynamic Entrainment Source Term for Mechanical Damage of the Multi-Canister Overpack.

	Nominal	Bounding	EF	Percentile	SNV	ln(EF)/SNV
MAR	1.85 kg	30 kg	16.22	99	2.326	1.198
ARR	4.00 E-06/h	4.00 E-05/h	10.00	95	1.645	1.400
Time	10 s	60 s	6.00	95	1.645	1.089
RF	0.20	1.00	5.00	95	1.645	0.978
M	4.1 E-6 g[a]	2.0 E-04 g[b]	48[c]	95	1.645	2.353

Note: The 1.645 is the standard normal variable corresponding to the 95% upper confidence limit. For the 99% upper confidence limit, the corresponding value is 2.326.

[a] $\text{Nominal}_{\text{overall}}\ M = \text{MAR}_{\text{nominal}} \times \text{ARR}_{\text{nominal}} \times \text{RF}_{\text{nominal}} \times \text{time}_{\text{nominal}}$.

[b] $\text{Bounding}_{\text{overall}}\ M = (\text{EF}_{\text{overall}})\ (\text{nominal}_{\text{overall}}\ M)$.

[c] $$\text{EF}_{\text{overall}} = \exp\left(\text{SNV}_{95\%}\left(\sum_i\left[\frac{\ln(\text{EF}_i)}{\text{SNV}_i}\right]^2\right)^{\frac{1}{2}}\right)$$.

ARR = airborne release rate.
EF = error factor (i.e., bounding value divided by nominal value).
ln(EF) = natural log of EF.
M = mass of material released.
MAR = material at risk.
RF = respirable fraction.
SNV = standard normal variable.

The aerosol concentration inside the MCO at the time of the release depends on prior MCO handling conditions and the mechanical forces exerted on the MCO structure by the accident. The powder in the MCO at rest could be ejected into the gas volume by the response of the underlying solid MCO and fuel substrate to vibration or jolting induced by impact or falling debris. According to DOE-HDBK-3010-94, the value of the airborne release fraction (ARF) under such circumstances should exceed the value of the ARF for aerodynamic suspension alone but be less than the ARF for the free fall of powder. The powder undergoing vibration shock is bounced into the gas while subject to the same gas velocities as those for aerodynamic entrainment. Based on the discussion in DOE-HDBK-3010-94, a bounding (95th percentile) ARF of 1×10^{-3} and an RF of 1.0 were chosen for the suspension of powder-like surface contamination by shock vibration. A nominal (50th percentile) value of 4×10^{-4} was chosen for the ARF and a nominal (50th percentile) value of 0.2 was chosen for the RF based on evaluation of the discussion in DOE-HDBK-3010-94. The pressure in the MCO at the start of the blowdown determines the fraction of the suspended particulate that is released. The range in initial pressure varies from 1.50 atm (corresponding to the helium fill pressure of 22 lb/in^2 absolute at the Cold Vacuum Drying Facility) to a maximum pressure of 5.2 atm (as defined in the Technical Databook

[HNF-SD-SNF-TI-015]). To allow for some additional margin in the calculation, a pressure of 2.0 atm is considered nominal (50th percentile) and corresponds to a leak path factor (LPF) of 0.5, while a pressure of 6.0 atm is considered bounding (95th percentile) and corresponds to an LPF of 0.83.

Using the methodology described in Chapter 1.0 and the bounding and nominal values identified above, the bounding (95th percentile) value for the material released by impact is calculated to be 1.2 g, as seen in Table 2-3.

Table 2-3. Initial Aerosol Concentration Source Term for Mechanical Damage of the Multi-Canister Overpack.

	Nominal	Bounding	EF	Percentile	SNV	ln(EF)/SNV
MAR	1.85 kg	30 kg	16.22	99	2.326	1.198
ARF	4.00 E-04	1.00 E-03	2.50	95	1.645	0.557
RF	0.20	1.00	5.00	95	1.645	0.978
LPF_{MCO}[a]	0.50	0.83	1.67	95	1.645	0.311
M	7.4 E-02 g[b]	1.2 g[c]	15.7[d]	95	1.645	1.673

Note: The 1.645 is the standard normal variable corresponding to the 95% upper confidence limit. For the 99% upper confidence limit, the corresponding value is 2.326.

[a]LPF_{MCO} = (MCO pressure - 1 atm) / (MCO pressure). At a nominal MCO pressure of 2.0 atm, the LPF_{MCO} is 0.5, and at a bounding MCO pressure of 6.0 atm, the LPF_{MCO} is 0.83.

[b]$Nominal_{overall}\ M = MAR_{nominal} \times ARF_{nominal} \times RF_{nominal} \times LPF_{MCO}$.

[c]$Bounding_{overall}\ M = (EF_{overall})\ (nominal_{overall}\ M)$.

[d]$$EF_{overall} = \exp\left(SNV_{95\%}\left(\sum_i\left[\frac{\ln(EF_i)}{SNV_i}\right]^2\right)^{\frac{1}{2}}\right)$$

ARF = airborne release fraction.
EF = error factor (i.e., bounding value divided by nominal value).
ln(EF) = natural log of EF.
LPF = leak path factor.
M = mass of material released.
MAR = material at risk.
MCO = multi-canister overpack.
RF = respirable fraction.
SNV = standard normal variable.

The bounding source term for the gaseous release is 1.2 g, which is the sum of 2.0×10^{-4} g from the aerodynamic entrainment of particulate and 1.2 g from vibration and shock.

2.4 CONSEQUENCE ANALYSIS

The dose calculation equation and data from Chapter 1.0 are used to calculate the dose to the onsite receptor.

$$D_{onsite} = M \times \frac{\chi}{Q'} \times BR \times UD \times LPF_{building}$$

$$= (1.2 \text{ g U})(1.14 \times 10^{-2} \text{ s/m}^3)(3.33 \times 10^{-4} \text{ m}^3/\text{s})(4.38 \times 10^{5} \text{ rem/g U})(1.0)$$

$$= 1.9 \text{ rem } (1.9 \times 10^{-2} \text{ Sv}).$$

where

D_{onsite} = committed effective dose equivalent (rem)
M = mass of respirable airborne material released (g U)
χ/Q' = time-integrated atmospheric transport factor (s/m^3)
BR = breathing rate (m^3/s)
UD = dose per unit mass of uranium (rem/g U)
$LPF_{building}$ = 1.0.

The dose consequences at the remaining receptor sites are calculated in the same manner and are shown in Table 2-4.

Table 2-4. Dose Calculation Summary for Mechanical Damage of a Multi-Canister Overpack.

Receptor location (distance, direction)	Duration (hours)	Unmitigated dose[a] rem (Sv)	Evaluation guideline[b]/ release limits rem (Sv) unlikely[c]	Mitigated dose rem (Sv)
Onsite (with building effects) (100 m)	<1	1.9 (1.9 E-02)	10 (1.0 E-01)	--
Highway 240[d] (9,280 m W)	<1	4.0 E-03 (4.0 E-05)	--	--
Hanford Site boundary (17,390 m E)	<1	2.2 E-03 (2.2 E-05)	5 (5.0 E-02)	--

[a]Fifty-year committed effective dose equivalent.
[b]Evaluation guideline for onsite (100 m) receptor only.
[c]Unmitigated frequency for these events is unlikely ($>10^{-4}$ to $\leq 10^{-2}$ per year) or less.
[d]Provided for information only.

Because the consequences of the unmitigated accident do not exceed offsite release limits, no mitigated consequences were calculated for the offsite doses. No mitigated dose calculation was performed for the onsite receptor because the onsite consequences are within the evaluation guidelines for an unlikely event.

2.5 REFERENCES

10 CFR 71, 1995, "Packaging and Transportation of Radioactive Materials," Section 71.73, "Hypothetical Accident Conditions," *Code of Federal Regulations*.

ASME, 1995, *Boiler and Pressure Vessel Code*, American Society of Mechanical Engineers, New York, New York.

ASME NOG-1, 1989, *Rules for Construction of Overhead and Gantry Cranes (Top Running Bridge, Multiple Girder)*, American Society of Mechanical Engineers, New York, New York.

DOE-HDBK-3010-94, 1994, *Airborne Release Fractions/Rates and Respirable Fractions/Rates for Nonreactor Nuclear Facilities*, U.S. Department of Energy, Washington, D.C.

HNF-3553, 2000, *Spent Nuclear Fuel Project Final Safety Analysis Report*, Annex A, "Canister Storage Building Final Safety Analysis Report," Rev. 0, Fluor Hanford, Richland, Washington.

HNF-S-0426, 1997, *Performance Specification for Spent Nuclear Fuel Multi-Canister Overpack*, Rev. 3, Fluor Daniel Hanford, Incorporated, Richland, Washington.

HNF-SD-SNF-DP-007, 1997, *Multi-Canister Overpack/Cask Drop Analysis File Documentation*, Rev. 0, Fluor Daniel Hanford, Incorporated, Richland, Washington.

HNF-SD-SNF-DR-003, 1998, *Multi-Canister Overpack Design Report*, Rev. 2, Fluor Daniel Hanford, Incorporated, Richland, Washington.

HNF-SD-SNF-HIE-001, 2000, *Canister Storage Building Hazard Analysis Report*, Rev. 3, Fluor Hanford, Richland, Washington.

HNF-SD-SNF-TI-015, 1998, *Spent Nuclear Fuel Project Technical Databook*, Rev. 6, Fluor Daniel Hanford, Incorporated, Richland, Washington.

IDCOR, 1984, *Technical Report 11.6: Resuspension of Deposited Aerosols Following Primary System or Containment Failure*, Fauske & Associates, Incorporated, Burr Ridge, Illinois.

NUREG/CR-6007, 1993, *Stress Analysis of Closure Bolts for Shipping Casks*, prepared for the U.S. Nuclear Regulatory Commission by Lawrence Livermore National Laboratory and Kaiser Engineering, Livermore, California.

Petersen, S. L., 1998, *Simulation of MCO Handling Machine Impact with Cask/MCO during Insertion into the Transfer Pit* (Transmittal FDT-137 to A. S. Daughtridge, D&ES Hanford, November 30), Fluor Daniel Hanford, Incorporated, Richland, Washington.

SNF-4042, 2000, *Evaluation of Accident Frequencies at the Canister Storage Building*, Rev. 2, Fluor Hanford, Richland, Washington.

SNF-5204, 1999, *Analysis for Eccentric Multi-Canister Overpack Drops at the Canister Storage Building (CSB-S-0073)*, Rev. 0, Fluor Daniel Hanford, Incorporated, Richland, Washington.

SNF-5276, 2000, *Analysis for SNF MCO Drop into the Cask from the MHM with Air Cushion*, Rev. 0, Fluor Hanford, Incorporated, Richland, Washington.

SNF-5930, 2000, *Structural Analysis of Multi-Canister Overpack for Accidental Movement of Multi-Canister Overpack Handling Machine during Multi-Canister Overpack Lifting Operations*, Rev. 0, Fluor Hanford, Incorporated, Richland, Washington.

SNF-5984, 2000, *Multi-Canister Overpack Handling Machine Trolley Seismic Uplift Constraint Design Loads*, Rev. 0, Fluor Hanford, Incorporated, Richland, Washington.

TN, 1996, *Design Analysis Report for the TN-WHC Cask and Transportation System*, Transnuclear, Incorporated, Hawthorne, New York.

TR-003, 1999, *Test Report for the CSB Prototypic Impact Absorbers*, Rev. 0, PacTec, Tacoma, Washington.

WMTS-RPT-037, 2000, *Canister Storage Building Multi-Canister Overpack Cask and Multi-Canister Overpack Impact Analysis*, Rev. 1, Waste Management Technical Services, Richland, Washington.

3.0 CALCULATIONS FOR GASEOUS RELEASE FROM THE MULTI-CANISTER OVERPACK

3.1 PURPOSE AND OBJECTIVES

This chapter evaluates events that may result in releases of radioactive materials to the Canister Storage Building (CSB) caused by loss of the multi-canister overpack (MCO) confinement pressure boundary. The potential for hydrogen deflagrations caused by loss of confinement is discussed in Chapter 5.0. MCOs are backfilled with helium to a prescribed pressure just before being sealed at the Cold Vacuum Drying Facility (CVDF) for shipment from the CVDF to the CSB. The integrity of the mechanical seal also is checked and verified at the CVDF before the MCO is shipped to the CSB. The uncontrolled release of the MCO internal gas pressure, referred to as a pressurized gaseous release accident, results from failure of the MCO pressure boundary to confine the MCO gases at the CSB. A pressurized gaseous release would lead to the entrainment and release of fuel particulate from the MCO and the creation of a radiological hazard. The gases released from the MCO in this event are those in the MCO after it is processed at CVDF and those generated in the MCO at the CSB. These gases include helium, hydrogen, water vapor, and possibly some small concentration of oxygen.

Based on the results documented in HNF-SD-SNF-HIE-001, *Canister Storage Building Hazard Analysis Report*, the potential for gaseous releases from an MCO can be the result of operations at the CSB, chemical properties of the spent nuclear fuel (SNF), or a breach of confinement caused by drops or impacts. The potential for a breach of the MCO caused by a drop of the MCO or cask–MCO or by MCO or cask–MCO impacts has been addressed in Chapter 2.0. Therefore, the bounding accident scenarios addressed in this chapter include overpressurization caused by radiolytic decomposition and gaseous releases caused by sampling system equipment failures or operator error during sampling and backfilling operations at the CSB. The scenarios considered in this accident analysis are assumed to not result in a deflagration of the gases within the MCO. Internal and external deflagrations are addressed in Chapters 4.0 and 5.0.

3.2 SCENARIO DEVELOPMENT

3.2.1 Overpressurization Due to Radiolytic Decomposition

MCOs arrive at the CSB from the CVDF in a mechanically sealed configuration with no pressure relief. Following operations at the CVDF the MCO is transported to the CSB. During the period encompassing closure at CVDF and awaiting transport to the CSB, transport to the CSB, and receipt at the CSB awaiting closure, there is the potential for the MCO to pressurize from radiolytic decomposition. This scenario assumes that the MCO overpressurizes (i.e., pressure caused by radiolytic decomposition is sufficient to fail the mechanical seal) and releases gases and particulate to the CSB facility.

As discussed in HNF-3553, *Spent Nuclear Fuel Project Final Safety Evaluation Report*, Annex A, "Canister Storage Building Final Safety Analysis Report," Chapter A2.0, the MCO's mechanical seal is designed to withstand pressures up to 150 lb/in^2 (18.3 atm). The initial pressure within an MCO is 22 lb/in^2 absolute (1.5 atm). According to HNF-SD-SNF-TI-040, *MCO Internal Gas Composition and Pressure during Interim Storage*, internal MCO pressures following 40 years of storage could be as high as 76 lb/in^2 absolute (5.2 atm), which is well below the design pressure of the MCO. Therefore, insufficient pressures will be generated within the MCO to fail the mechanical seal (receipt condition or condition during sampling operations) or the welded seal (long-term or 40-year storage condition). Thus it can be concluded that insufficient pressures will be generated within an MCO from radiolytic decomposition to overpressurize an MCO and result in a release upon receipt at the CSB.

3.2.2 Gaseous Release at the Sampling/Weld Station

A gaseous release could occur at the CSB because of operator error during sampling and backfilling operations. This scenario assumes the incorrect installation or removal of the sampling and backfilling equipment or a failure of the equipment resulting in a direct path for leakage into the CSB facility. Dropping of an object onto the sampling/weld station components is another potential initiator for a leak from the sampling system. A drop could shear the sampling system piping or otherwise fail the confinement capability of the sampling system pressure boundary. A confinement failure could also result from the sampling/weld station gantry crane, the MCO handling machine (MHM), or some other equipment moving horizontally into the sampling/weld station components and shearing the piping.

Gaseous Release during Sampling Operations The sampling process begins when the MHM lowers the selected MCO into the sampling/weld station pit. The surface temperature of the MCO is monitored. If the surface of the top of the MCO is not sufficiently cool, the MCO is cooled using the sampling/weld station cooling cap to reduce the exposed portions of the MCO to a temperature consistent with standard industrial safety regulations. After removing temporary radiation shields and guard rails, the sampling hood is installed on the MCO to confine possible airborne contamination generated by an accidental release during sampling. The MCO sampling cart is connected to the local distributed control system and inert gas system. Piping on the sample cart connects to the sample gas accumulator through the sampling hood high-efficiency particulate air (HEPA) filter outlet using a quick-disconnect attachment. The flexible hose of the sample cart vent is connected to the sampling hood discharge, which dumps to the exhauster. This exhaust system fan establishes negative pressure within the hood relative to the operating area pressure to maintain air contamination control and air flow around the top of the MCO.

For MCO sampling, an MCO process valve operator is installed on the short tube port (port 2) of the MCO after the cover plate is removed. The process valve operator is connected with a quick-disconnect coupling to a flexible hose that connects to the inlet of the sample line HEPA filter. The remainder of the sample system piping is the flexible piping that connects the outlet of the sample line HEPA filter to the sample cart and the rigid piping in the sample cart that goes to the sample valve and the sample accumulator. This piping is used to draw a sample of gas

from the MCO and to pressurize the MCO using helium from the 120 lb/in^2 gauge CSB helium supply system. The sampling system piping between the refill valve and the MCO is pressurized during the MCO refill operation. The entire sampling process is a manual operation; the technician taking the sample is present at all times during sampling.

After completion of the sampling activities, the MCO is backfilled with helium if necessary to maintain internal pressure. The same equipment and process lines used during sampling are used to backfill the MCO. However, the sample valve is closed and the helium backfill valve is opened.

The following scenario involves a failure of this process line while it is connected to the MCO with the MCO process valve open, leading to a blowdown of the gases inside the MCO. With only one process line connected to the MCO, no flow path through the MCO can exist to continuously remove particulate from the MCO for an extended period of time. To get a release, the break in a section of process piping must be upstream of the sample line HEPA filter. A release from a piping failure downstream of the sample line HEPA filter requires failure of the sample system HEPA filter as well. A release also is possible if the MCO valve operator is inadvertently removed before the process port is closed.

A leak within the confines of the sample hood would be quickly exhausted through the sampling/weld station HEPA filter to the CSB exhaust system plenum and out to the environment through the CSB stack. Leaks from the sample system outside of the sample hood would be to the CSB operating air.

The effective leak flow area is bounded by the flow area of the path through the MCO shield plug (1.0-in.-diameter). All of the sampling system piping outside of the sampling hood is less than 0.75-in. inside diameter except the sample line to the cart, which is 1 in. in diameter. The flexible hose inside the sample hood and the associated fittings have inside diameters less than 1.0 in. If the valve operator body is improperly secured to the top of the MCO, then the leak path flow area around the valve could be large enough to make the flow area of the shield plug the limiting flow area. Therefore, the largest leak path flow area possible would be for a leak into the sample hood. Sampling system leaks outside of the sample hood would have smaller flow area paths and would have traveled through the sample line HEPA filter.

Gaseous Release during Reinerting Operations. In addition to the gaseous release accident at the sampling/weld station, the overpressurization of the MCO by the inert gas system during reinerting of a monitored MCO after sampling also is considered. This accident is initiated by failure of the pressure regulator on the helium supply system while an MCO is in the sampling/weld station undergoing the MCO helium backfill operation. This scenario assumes the helium supply pressure is sufficient to breach the MCO shield plug seal. As with the sampling process, the entire backfilling process is a manual operation and the technician is present at all times.

3.3 SOURCE TERM ANALYSIS

For the gaseous release accident, the particulate available for release depends on the amount of particulate generated between the time the fuel is washed at the K Basins and the time of the accident. The MCO gaseous release accident could only occur during the time the MCO sampling program is being conducted. HNF-SD-SNF-TI-015, *Spent Nuclear Fuel Project Technical Databook*, states that the safety basis or bounding value for the mass of particulate in the MCO is 34.0 kg of uranium dioxide, which contain 30.0 kg of uranium. Because of the conservative methodology used to calculate the bounding value, 30 kg is considered representative of the 99th percentile. HNF-SD-SNF-TI-015 also states that the design or nominal value is 2.1 kg of uranium dioxide, which contain 1.85 kg of uranium.

The quantity of particulate actually released during a gaseous release accident depends on the initial aerosol concentration and subsequent particulate entrainment. The pressurized powder venting source term is not applicable, and a source term based upon aerodynamic entrainment, as described in Chapter 1.0, is used.

Based on the data reported in DOE-HDBK-3010-94, *Airborne Release Fractions/Rates and Respirable Fractions/Rates for Nonreactor Nuclear Facilities*, a bounding (95th percentile) airborne release rate (ARR) of 4×10^{-5} per hour and a respirable fraction (RF) of 1.0 were selected. The contents of the MCO are intact fuel elements tightly packed in fuel baskets and pieces of fuel elements housed in scrap baskets. Particulate matter swept upward by streams of flowing gas within the MCO must take a tortuous path through the MCO and through the MCO shield plug to exit the MCO. For shielded powder, where the aerodynamic stresses are reduced by debris or exposure to static conditions, DOE-HDBK-3010-94 recommends an ARR of 4×10^{-6} per hour and an RF of 0.2. These values were selected as nominal (50th percentile).

The pressurized gaseous release from the MCO occurs close to the MCO through a leak path with a flow area greater than or equal to the flow area through the MCO shield plug. Such a leak could be caused by complete severance of the pipe or flexible tubing within the sampling/weld station sample hood or by failure to tighten the hold down bolts on the MCO port valve operator. The duration of the blowdown depends on the flow area of the leak and the initial MCO pressure. The MCO depressurizes to atmospheric pressure in less than 1 minute, even for an MCO pressure of about 150 lb/in^2 gauge and a 0.25-in. hole. The MCO depressurizes in a much shorter time for lower pressures and larger leak paths. For the calculation of the source term, a nominal (50th percentile) value of 10 seconds and a bounding (95th percentile) time of 60 seconds were selected.

Using the methodology described in Chapter 1.0 and the bounding and nominal values identified above, the bounding (95th percentile) value for the material released through aerodynamic entrainment is calculated to be 2×10^{-4} g, as shown in Table 3-1.

Table 3-1. Aerodynamic Entrainment Source Term for the Gaseous Release from the Multi-Canister Overpack.

	Nominal	Bounding	EF	Percentile	SNV	ln(EF)/SNV
MAR	1.85 kg	30 kg	16.22	99	2.326	1.198
ARR	4.00 E-06/h	4.00 E-05/h	10.00	95	1.645	1.400
Time	10 s	60 s	6.00	95	1.645	1.089
RF	0.20	1.00	5.00	95	1.645	0.978
M	4.1 E-06 g[a]	2.0 E-04 g[b]	48[c]	95	1.645	2.353

Note: The 1.645 is the standard normal variable corresponding to the 95% upper confidence limit. For the 99% upper confidence limit, the corresponding value is 2.326.

[a] $\text{Nominal}_{\text{overall}}\ M = \text{MAR}_{\text{nominal}} \times \text{ARR}_{\text{nominal}} \times \text{RF}_{\text{nominal}} \times \text{time}_{\text{nominal}}$.

[b] $\text{Bounding}_{\text{overall}}\ M = (\text{EF}_{\text{overall}})\ (\text{nominal}_{\text{overall}}\ M)$.

[c] $$\text{EF}_{\text{overall}} = \exp\left(\text{SNV}_{95\%}\left(\sum_i\left[\frac{\ln(\text{EF}_i)}{\text{SNV}_i}\right]^2\right)^{\frac{1}{2}}\right)$$

ARR = airborne release rate.
EF = error factor (i.e., bounding value divided by nominal value).
ln(EF) = natural log of EF.
M = mass of material released.
MAR = material at risk.
RF = respirable fraction.
SNV = standard normal variable.

The aerosol concentration inside the MCO at the time of the release depends on prior MCO handling conditions. The powder in the MCO at rest could be ejected into the gas volume and suspended by the response of the underlying solid MCO and fuel substrate to vibration or jolting induced by impact or falling debris. According to DOE-HDBK-3010-94, the value of the airborne release fraction (ARF) under such circumstances should exceed the value of the ARF for aerodynamic suspension alone but be less than the ARF for the free fall of powder. The powder undergoing vibration shock is bounced into the gas while subject to the same gas velocities as those for aerodynamic entrainment. Based on the discussion in DOE-HDBK-3010-94, a bounding (95th percentile) ARF of 1×10^{-3} and an RF of 1.0 were chosen for the suspension of powder-like surface contamination by shock vibration. A nominal (50th percentile) value of 4×10^{-4} was chosen for the ARF and a nominal value of 0.2 was chosen for the RF based on evaluation of the discussion in DOE-HDBK-3010-94. The pressure in the MCO at the start of the blowdown determines the fraction of the suspended particulate that is released. The range in initial pressure varies from 1.50 atm (corresponding to the helium fill pressure of 22 lb/in^2 absolute at the CVDF) to a maximum pressure of 5.2 atm (as defined in HNF-SD-SNF-TI-015). To allow for some additional margin in the calculation, a pressure of 2.0 atm is considered

nominal (50th percentile) and corresponds to a leak path factor (LPF) of 0.5, while a pressure of 6.0 atm is considered bounding (95th percentile) and corresponds to an LPF of 0.83.

Unlike in a drop event, there is no clear mechanism identified in this accident to provide the impact to suspend particulate within the MCO. However, normal handling of the MCO by the MHM during transport from the storage tube to the sampling/weld station will produce some vibration and jostling of the fuel and suspend some material. For the purposes of this analysis, it is assumed that nominally 1% of the impact suspension concentration exists within the MCO at the start of sampling. Therefore a value of 1% is assumed for the 50th percentile. In addition, a value of 10% is assumed for the 95th percentile.

Using the methodology described in Chapter 1.0 and the bounding and nominal values identified above, the bounding (95th percentile) value for the material released by impact is calculated to be 2.7×10^{-2} g, as shown in Table 3-2.

The bounding source term for the gaseous release is 2.7×10^{-2} g, which is the sum of 2.0×10^{-4} g from the aerodynamic entrainment of particulate and 2.7×10^{-2} g from vibration and shock.

3.4 CONSEQUENCE ANALYSIS

The radiological dose is calculated using the dose calculation equation and data from Chapter 1.0.

The dose to the onsite receptor is calculated as follows:

$$D_{onsite} = M \times \frac{\chi}{Q'} \times BR \times UD \times LPF_{building}$$

$$= (0.027 \text{ g U})(1.14 \times 10^{-2} \text{ s/m}^3)(3.33 \times 10^{-4} \text{ m}^3/\text{s})(4.38 \times 10^{5} \text{ rem/g U})(1.0)$$

$$= 4.5 \times 10^{-2} \text{ rem } (4.5 \times 10^{-4} \text{ Sv}) .$$

where

D_{onsite} = committed effective dose equivalent (rem)
M = mass of respirable airborne material released (g U)
χ/Q' = time-integrated atmospheric transport factor (s/m^3)
BR = breathing rate (m^3/s)
UD = dose per unit mass of uranium (rem/g U)
$LPF_{building}$ = 1.0.

Table 3-2. Initial Suspended Material Source Term for the Gaseous Release from the Multi-Canister Overpack.

	Nominal	Bounding	EF	Percentile	SNV	ln(EF)/SNV
MAR	1.85 kg	30 kg	16.22	99	2.326	1.198
ARF	4.00 E-04	1.00 E-03	2.50	95	1.645	0.557
RF	0.20	1.00	5.00	95	1.645	0.978
Settling	1%	10%	10.00	95	1.645	1.400
LPF_{MCO}[a]	0.50	0.83	1.67	95	1.645	0.311
M	7.4 E-04 g[b]	2.7 E-02 g[c]	36[d]	95	1.645	2.181

Note: The 1.645 is the standard normal variable corresponding to the 95% upper confidence limit. For the 99% upper confidence limit, the corresponding value is 2.326.

[a]LPF_{MCO} = (MCO pressure - 1 atm) / (MCO pressure). At a nominal MCO pressure of 2.0 atm, the LPF_{MCO} is 0.5, and at a bounding MCO pressure of 6.0 atm, the LPF_{MCO} is 0.83.

[b]$Nominal_{overall}\ M = MAR_{nominal} \times ARF_{nominal} \times RF_{nominal} \times settling \times LPF_{MCO}$.

[c]$Bounding_{overall}\ M = (EF_{overall})\ (nominal_{overall}\ M)$.

[d]$$EF_{overall} = \exp\left(SNV_{95\%}\left(\sum_i\left[\frac{\ln(EF_i)}{SNV_i}\right]^2\right)^{\frac{1}{2}}\right)$$

ARF = airborne release fraction.
EF = error factor (i.e., bounding value divided by nominal value).
ln(EF) = natural log of EF.
LPF = leak path factor.
M = mass of material released.
MAR = material at risk.
MCO = multi-canister overpack.
RF = respirable fraction.
SNV = standard normal variable.

The actual duration of the release is expected to be less than 1 hour for all receptors, therefore the applied χ/Q' value is conservatively chosen for a 1-hour duration. The estimated bounding doses to receptors at several locations have been calculated and the results summarized in Table 3-3.

Table 3-3. Dose Calculation Summary for a Bounding Gaseous Release Event at the Sampling/Weld Station.

Receptor location (distance, direction)	Release Duration (hours)	Unmitigated dose[a] rem (Sv)	Evaluation guideline[b]/ release limits rem (Sv) anticipated[c]	Mitigated dose rem (Sv)
Onsite (with building effects) (100 m)	<1	4.5 E-02 (4.5 E-04)	1.0 (1.0 E-02)	--
Highway 240[d] (9,280 m W)	<1	9.3 E-05 (9.3 E-07)	--	--
Hanford Site boundary (17,390 m E)	<1	5.1 E-05 (5.1 E-07)	0.5 (5.0 E-03)	--

[a]Fifty-year committed effective dose equivalent.
[b]Evaluation guideline for onsite (100 m) receptor only.
[c]Unmitigated frequency for this event is anticipated (>0.01 to ≤0.1 per year).
[d]Provided for information only.

3.5 REFERENCES

DOE-HDBK-3010-94, 1994, *Airborne Release Fractions/Rates and Respirable Fractions/Rates for Nonreactor Nuclear Facilities*, U.S. Department of Energy, Washington, D.C.

HNF-3553, 2000, *Spent Nuclear Fuel Project Final Safety Analysis Report*, Annex A, "Canister Storage Building Final Safety Analysis Report," Rev. 0, Fluor Hanford, Incorporated, Richland, Washington.

HNF-SD-SNF-HIE-001, 2000, *Canister Storage Building Hazard Analysis Report*, Rev. 3, Fluor Hanford, Richland, Washington.

HNF-SD-SNF-TI-015, 1998, *Spent Nuclear Fuel Project Technical Databook*, Rev. 6, Fluor Daniel Hanford, Incorporated, Richland, Washington.

HNF-SD-SNF-TI-040, 1999, *MCO Internal Gas Composition and Pressure During Interim Storage*, Rev. 3, Fluor Daniel Hanford, Incorporated, Richland, Washington.

4.0 CALCULATIONS FOR MULTI-CANISTER OVERPACK INTERNAL HYDROGEN DEFLAGRATION

4.1 PURPOSE AND OBJECTIVES

Three events have been identified that could result in formation of flammable mixtures of hydrogen and oxygen inside a multi-canister overpack (MCO) while at the Canister Storage Building (CSB). These are described in Section 4.2. The first identified event is radiolytic decomposition of oxygen-containing compounds, such as aluminum hydroxide and uranium oxide (hydrate). The second event is the charging of an MCO with a gas containing oxygen at the sampling/weld station. The third event is an ingress of air to an MCO that has been breached at the CSB.

4.2 SCENARIO DEVELOPMENT

In the postulated accidents, hydrogen is generated and accumulates in the MCO due to either radiolytic decomposition or corrosion of uranium in a moist environment. The general sequence of events leading to a hydrogen explosion is shown in SNF-4042, *Evaluation of Accident Frequencies at the Canister Storage Building*. Two conditions necessary for radiolytic production of hydrogen and oxygen in the MCO are (1) enough aluminum hydroxide, uranium oxide (hydrated), or free water and (2) a high enough radiation level, which is indicated by the thermal power of the fuel. Two conditions necessary for production of hydrogen by reaction with uranium inside the MCO are adequate amounts of exposed uranium metal and water vapor.

Radiolytic production of hydrogen and oxygen occurs slowly, and the hydrogen is produced at several times the rate of the oxygen. Thus, the mixture is not combustible until the oxygen concentration exceeds the minimum necessary.

Charging the MCO with oxygen at the sampling/weld station would occur early in the storage period because sampling will take place then. Hydrogen accumulates from fuel corrosion (uranium–water reaction) rather quickly inside the MCO; adding oxygen creates a flammable mixture that then could burn. Because it takes very little energy to begin the hydrogen–oxygen combustion, it has been assumed that ignition sources (e.g., static charge accumulated by moving gases, uranium hydride decomposition) are always present. The specific accident scenarios evaluated are described in the following subsections.

4.2.1 Hydrogen Deflagration Caused by Radiolysis during Storage

Radiolytic decomposition of aluminum hydroxide, aluminum, iron and uranium hydrate, and free water will lead to a mixture of hydrogen and oxygen in an MCO. Hydrogen would be produced at a higher rate than the oxygen, making oxygen the limiting reactant. A deflagration cannot occur until the oxygen concentration exceeds the minimum necessary.

Because oxygen gas reacts with uranium in damaged fuel elements, it is assumed that there is no exposed uranium surface. This is the minimum area assumption for safety basis calculations provided in HNF-SD-SNF-TI-017, *Fuel Surface Area*. With minimum exposed uranium, there is minimum hydrated water bound in the uranium oxides. Most of the oxygen comes from the aluminum hydroxide. See Appendix 4A for a discussion on the basis for nonstoichiometric production of radiolytic oxygen.

4.2.2 Hydrogen Deflagration Following Oxygen Addition at the Sampling/Weld Station

At the sampling/weld station, the MCO is connected to the sample cart and a small gas sample is taken from the MCO. If required, inert gas is added to the MCO to raise the internal pressure. Two methods for charging oxygen into the MCO have been postulated. One requires failing to purge air from the helium line so that air is forced into the MCO rather than helium. The other requires that the helium be contaminated with oxygen.

The helium line runs from the storage tank on the north side of the CSB to the sampling/weld station on the south side of the CSB. Because of its length, this pipe contains a significant volume of air initially. It is possible for this line to be filled with air during a sampling sequence by omission of the helium purge steps.

By either method, oxygen is charged into an MCO with a bounding hydrogen concentration. The deflagration is expected to occur shortly after the oxygen enters the MCO. Combustion temperatures and pressures are high enough that the hot gases forced from the MCO cause the sample line to fail. The compromise of the confinement boundary of the MCO leads to a release of particulate matter at the sampling/weld station. An event tree is provided in SNF-4042.

4.2.3 Hydrogen Deflagration Following an Air Ingress

It is assumed that the MCO is breached. Gases inside the MCO can escape, and gases outside the MCO can diffuse into the MCO. At some point there will be a flammable mixture in the MCO. The resulting deflagration leads to a gaseous release of particulate matter.

4.3 SOURCE TERM ANALYSIS

The mathematical analysis of the postulated accidents focuses on the hydrogen and oxygen concentrations in an MCO. Mixtures of hydrogen in air are flammable in the range of 4% to 75% hydrogen by volume at atmospheric pressure. According to NUREG/CR-2726, *Light Water Reactor Hydrogen Manual*, significant shock waves may be produced if the hydrogen concentration is between 18 and 58 vol% in air. The stoichiometric ratio (2 moles hydrogen per 1 mole of oxygen) corresponds to 29.6% hydrogen in air. The presence of helium changes the stoichiometric ratio because it displaces oxygen. For example, if there are equal volume percents

of hydrogen and helium, then the stoichiometric hydrogen concentration is reduced to 22.8%. The minimum oxygen concentration needed for combustion is 4% (NUREG/CR-2726). For a given oxygen and hydrogen concentration at higher initial gas pressures, the reaction is slowed by the increased amount of nonreacting atoms. The overall effect is to raise the minimum concentrations.

4.3.1 Basis for Hydrogen Deflagration Caused by Radiolysis

HNF-SD-SNF-TI-040, *MCO Internal Gas Composition and Pressure during Interim Storage*, predicts the possible range of MCO internal gas composition and pressure during a defined 40-year storage period at the CSB. Internal gas composition is a primary focus because of flammability concerns; pressure is a secondary focus because of a priori knowledge that the MCO design pressure will not be exceeded. Gas compositions are affected by CSB temperature, MCO decay power, the MCO inventory of gas-releasing compounds, and reactive surface area in an MCO. Uncertainties exist in the rates of decomposition of gas-releasing compounds and reaction rates between exposed uranium metal and gases. HNF-SD-SNF-TI-040 describes the expected range for each of the factors that influence gas composition and provides results for gas concentrations and total pressures for situations of greatest interest. The ranges and results are summarized in this section. For simplicity, HNF-SD-SNF-TI-040 focused on the time period when oxygen was present in an MCO and did not address subsequent H_2O and H_2 gettering when oxygen was depleted.

During storage of MCOs in the CSB, gas composition will evolve as a consequence of competing rates of gas formation by radiolysis (chiefly H_2 and O_2) and thermal decomposition (chiefly H_2O), and rates of gas depletion by reactions with fuel (H_2, O_2, and H_2O). The potential for formation of flammable mixtures is therefore of interest, in particular for cases in which an MCO is at relatively low temperature or has relatively little reactive surface area. An oxygen content of 4% is recommended as the flammability limit for H_2-O_2-He mixtures. According to HNF-1523, *K Basin Particulate Water Content, Behavior, and Impact*, MCO pressure can be expected to be below design limits.

The gas-releasing compounds considered are $Al(OH)_3$ and uranium oxide hydrates. $Al(OH)_3$ is found to decompose only by radiolysis under CSB conditions. Only about 4% of the $Al(OH)_3$ cladding film inventory of an average power MCO can decompose over the 40-year storage period, and about 10% of the $Al(OH)_3$ in canister particulate can decompose radiolytically. Uranium oxide hydrates can potentially partially thermally decompose from $UO_3 \cdot 2H_2O$ to $UO_3 \cdot H_2O$ with further decomposition by radiolysis, but water vapor from free water evaporation would limit thermal decomposition. It is possible that thermal decomposition of $UO_3 \cdot H_2O$ may also occur, but the rate may be comparable to that of radiolysis. In any event, it is conservative to assume radiolytic decomposition because this allows oxygen formation and yields more moles gas per mole solid. Fifty percent of the $UO_3 \cdot 2H_2O$ in an average power MCO can decompose by radiolysis over 40 years.

Water vapor and oxygen react with uranium at rates that have been measure and correlated but are subject to a range of uncertainty. N Reactor fuel has been observed to react at a rate up to 100 times the literature value for dry air at low temperature, but rate law enhancements to literature correlations, or "rate law multipliers," are not considered. Oxygen is depleted before net water vapor depletion occurs, so all weight gain, applying literature correlations to MCO conditions at the CSB, corresponds to net oxygen consumption.

Hydrogen reactions with clean uranium are observed to be as fast as oxygen reactions, but the rate is substantially decreased for oxidized uranium surfaces (otherwise hydrogen would not be an observed reaction product of water vapor and the metal) and is essentially unquantified. Hydrogen will react with fuel only after oxygen and water vapor are nearly depleted; hence this reaction may be neglected to calculate oxygen concentration and maximum pressure.

Reaction rates vary strongly with temperature, but it is shown in HNF-SD-SNF-TI-040 that only about 20% to 50% increases in the time-average reaction rate occur when annual and diurnal variations are rigorously considered. Therefore, reaction rates may be simply specified by the lifetime average temperature experienced by an MCO; a conservatively small vault annual temperature variation of ± 12 °C was employed.

Reaction rates are correlated per unit area, and the reactive surface area in an MCO is an uncertain parameter. The presence of a scrap basket in an MCO, if actually filled with scrap rather than intact fuel, ensures a best-estimate reactive area of about 1.9 m^2, of which 1.7 m^2 are from scrap and 0.2 m^2 are from fuel baskets. A range of fuel and scrap areas is considered for MCO configurations with zero, one, and two scrap baskets.

The inventory of water-bearing compounds is uncertain and varies with the number of scrap baskets. Reference bounding and best-estimate water masses are used in various cases. Only some MCOs from the K West Basin will contain $Al(OH)_3$, which would be present as a cladding surface film. The amount of uranium oxide hydrate varies from assembly to assembly but increases with increasing fuel damage. The uranium oxide hydrate is quantified in HNF-SD-SNF-TI-040 using 0.05 kg/m^2 of water from the adhering particulate source as a best estimate and 0.10 kg/m^2 as a bounding value for sensitivity.

The key result of calculations in HNF-SD-SNF-TI-040 is that when reference $g(O_2)$ values are used, the MCO oxygen concentration at 40 years is below the 4% flammability limit for best-estimate cases. This is true for any possible MCO power and a reactive area of at least 0.1 m^2. For more information, see Appendix 4A.

Configurations with no scrap baskets were considered because of the potential for low reactive area. There was no combination of high MCO power, water content, and 0.0 m^2 reaction area that led to oxygen concentrations above 4% after 40 years, given nominal helium backfill. For best-estimate water inventories, the worst case was 0.75% oxygen at the low-bound (non-zero) area. All one and two scrap basket configurations examined had less than 4% oxygen at 40 years, even with bounding high water and bounding low area.

Detailed results in HNF-SD-SNF-TI-040 indicate that the net rate of oxygen production can change significantly during storage. In particular it is possible for no oxygen to be present for many years, and then for oxygen to suddenly appear. This is because oxygen consumption declines faster than oxygen production in most cases, so at some point in time the net rate of production becomes positive.

The best-estimate MCO pressure at 40 years is 2.1 atm (for an MCO having one scrap basket, average power, average reactive area, and 25% $Al(OH)_3$ assemblies). The bounding MCO pressure at 40 years is 5.2 atm (for an MCO having two scrap baskets, 770 W*, 7.7 m^2 reactive area, zero $Al(OH)_3$ assemblies, bounding canister, and adhering particulate), which is well below the design pressure of 30 atm (450 lb/in^2 gauge).

4.3.2 Basis for a Hydrogen Deflagration Caused by Oxygen in the Helium System

The composition of the gas inside the MCO shortly after it arrives at the CSB is assumed to be only helium and hydrogen. The hydrogen is generated primarily by reaction between exposed fuel and water vapor. The radiolytic decomposition of water and hydroxides adds very little and is not considered. For a reaction to occur rapidly, there must be a large, exposed fuel surface area. The MCO with two scrap baskets is bounding.

The bounding hydrogen content of an MCO with two scrap baskets will be estimated assuming the water reactions with uranium metal and uranium hydride occur at the same rate. From HNF-SD-SNF-TI-015, *Spent Nuclear Fuel Project Technical Databook*, the enhancement factor for the metal reaction is 10 while the enhancement factor for the hydride reaction is 12. In addition, the metal reaction produces 1 mole of hydrogen gas for every mole of water reacted, but the hydride reaction produces 1.75 moles hydrogen for every mole of water reacted. The combined effect is that the hydrogen generation increases by the factor

$$\frac{(10)(1) + (12)(1.75)}{10 + 12} = 1.409$$

over the amount expected from the uranium metal reaction alone.

The hydrogen gas that could be generated from the uranium metal is limited by the amount of water available to react. The bounding free water estimate is 200 g in crevices and cracks. In addition, uranium oxide dihydrate will lose one of the water molecules at normal MCO temperatures (HNF-1523). Much of this loss may occur during drying at the Cold Vacuum Drying Facility but, to maximize the hydrogen generation after drying, none will be assumed for

*The bounding power is 776 W and the average power is 403 W (HNF-SD-SNF-TI-015). Calculation inputs used 770 W and 396 W as bounding and nominal, respectively. These differences have no impact on conclusions.

this calculation. The bounding hydrated water estimate for two scrap baskets is 1,190 g water (HNF-SD-SNF-TI-015). Half of this amount is available to react with uranium fuel to form hydrogen. The total water mass of 795 g is equivalent to 44 moles of water. The hydride enhancement described above leads to the bounding production of 62 moles of hydrogen in the MCO. From the ideal gas law, this hydrogen has a volume of 1,520 L at reference conditions.

The initial low helium inventory is 22.5 moles (conservative fill pressure of 1.1 atm). Thus, the gas in the MCO is 27% helium and 73% hydrogen. Chapter 5.0 shows that the reaction producing this hydrogen can proceed rather quickly so that by the time an MCO is sampled it is reasonable to assume the above hydrogen inventory has been realized.

An MCO containing the bounding hydrogen gas inventory is vented at the sampling/weld station and assumed to be completely depressurized so that recharge with helium is necessary. However, instead of charging the MCO with helium, a gas mixture containing oxygen is added and creates a flammable mixture of hydrogen and oxygen in the MCO.

When the MCO is depressurized, the relative amounts of helium and hydrogen remain unchanged. The gas mixture is still 27% helium and 73% hydrogen. At a pressure of 1 atm and a temperature of 50 °C (122 °F), the MCO inventory is 18.9 moles total, or 13.9 moles hydrogen and 5.0 moles helium. This is below the bounding temperature to maximize the mass of hydrogen in the MCO at the time of gas recharge.

Adding a helium and oxygen mixture to the MCO increases the pressure in the MCO to 129 kPa (1.27 atm or 4.0 lb/in^2 gauge). The amount of gas added is calculated from the ideal gas law to be 5.1 moles. The final total in the MCO is 24.0 moles. The hydrogen concentration decreases from 73% to 58%. The oxygen concentration in the MCO depends on the oxygen concentration in the added gas. From the ideal gas law, the oxygen concentration in the MCO follows the absolute pressures. Thus, the final oxygen concentration is 0.27/1.27, which is 0.213 times the concentration of the added gas. If the added gas were 60% oxygen, then the oxygen concentration in the MCO would be 12.8%.

To achieve a flammable mixture at atmospheric pressure, the oxygen concentration must exceed 4.0% in the MCO. Thus, the oxygen concentration of the added gas must be greater than 19%. Note the oxygen concentration in air is 21%. To achieve a mixture in the MCO that will produce shock waves, the oxygen concentration in the MCO must be at least 9%. Thus, the flammable mixture in the MCO does not become very damaging until the oxygen concentration in the added gas exceeds 42%.

4.3.3 Basis for Hydrogen Deflagration after an Air Ingress

As discussed in Section 4.3.2, the low helium MCO contains a mixture of 73% hydrogen and 27% helium. When this mixes with air containing 21% oxygen and 79% nitrogen, the stoichiometric mixture of hydrogen and oxygen is reached after about 67% of the gas in the MCO

has been replaced with air. The final mixture is 5% helium, 28% hydrogen, 14% oxygen, and 53% nitrogen. These determine the peak pressure during combustion.

4.3.4 Estimating Peak Pressures Caused by Hydrogen Combustion

When the hydrogen and oxygen react, water vapor is formed and energy is released. To be conservative, it is assumed that the energy released stays in the gas and none is lost to the MCO components. The heat capacity of the gases allows the final temperature to be computed. This final temperature, together with the number of moles of gases in the MCO and the ideal gas law, is used to calculate the final pressure resulting from the combustion.

The heat of water vapor formation from hydrogen and oxygen gas is 57,800 cal/mole at a temperature of about 300 K (27 °C). The heat capacity of various gases is calculated from a quadratic formula as listed in Table 4-1.

Table 4-1. Parameters to Determine Heat Capacities.

Gas	A	B	C
H_2	4.959	-1.96 E-04	4.76 E-07
N_2	4.470	1.39 E-03	-6.90 E-08
O_2	4.130	3.17 E-03	-1.01 E-06
H_2O	5.149	2.64 E-03	4.59 E-08
He	3.020	0	0

Note: The heat capacity at constant volume (in cal/mole/K) is computed from the formula $Cv = A + B \cdot T + C \cdot T^2$, where T is the temperature of the gas. The heat capacities apply to the temperature range from 300 K (27 °C) to 1,500 K (1,227 °C). At higher temperatures the heat capacities are overestimated.

The final temperature of the gas mixture is found using the following formula (see Appendix 5A for details). The integration is between the initial temperature of the gas mixture before combustion and the final temperature of the gas mixture after combustion. The summation is over the types of gases present in the MCO after combustion. Because the final gas temperature is unknown but determines the heat capacities, the temperature must be solved by an iterative process.

$$(H_F)(N_{H2O}) = \int_{T_o}^{T_f} \left(\sum (Cvi)(Ni) \right) \quad (dT)$$

where

H_F = heat of formation of water from hydrogen and oxygen, 57,800 cal/mole formed as a vapor

N_{H2O} = number of moles of water formed; computed as the smaller of the number of moles of hydrogen and twice the number of moles of oxygen (before combustion)

T_o = temperature of the gas mixture before combustion, in degrees Kelvin

T_f = temperature of the gas mixture after combustion, in degrees Kelvin

Cvi = heat capacity at constant volume of gas "I"; depends on the temperature of the gas (represented as a quadratic equation)

Ni = number of moles of gas "I" after the oxygen and hydrogen react.

For a deflagration at the sampling/weld station resulting from air in the helium line, the gas added to the MCO is 21% oxygen and 79% nitrogen. The composition of the gas before combustion is 5.0 gmoles helium, 13.9 gmoles hydrogen, 1.1 gmoles oxygen, and 4.0 gmoles nitrogen. The MCO pressure is 129 kPa (1.27 atm or 4.0 lb/in^2). The MCO gas temperature is 323 K (50 °C).

The combustion reaction uses 1.1 gmoles oxygen together with 2.2 gmoles hydrogen. This produces 2.2 gmoles water vapor. The final gas mixture in the MCO is 5.0 gmoles helium, 11.7 gmoles hydrogen, 2.2 gmoles water vapor, and 4.0 gmoles nitrogen. The energy liberated by the formation of the water vapor is 124,000 cal.

By an iterative process, the final temperature of the gas mixture is 1,408 K (1,134 °C) see Appendix 5A for iterative process methodology). The corresponding pressure in the MCO is 536 kPa (5.29 atm or 63 lb/in^2 gauge). This is well below the MCO design pressure of 450 lb/in^2. In addition, the sample line and connection are designed to withstand even greater pressure. However, the sample line could fail from the high gas temperatures. When the explosion occurs, the sample line can melt to the point that gases in the MCO rush out and carry particulate matter into the environment.

For an explosion at the sampling/weld station resulting from impure helium, if the gas added to the MCO is 60% oxygen, then the composition of the MCO gas before combustion is 7.1 moles helium, 13.9 moles hydrogen, and 3.0 moles oxygen. The MCO pressure at this time is 129 kPa (1.27 atm or 4.0 lb/in² gauge). The MCO gas temperature is 323 K (50 °C).

The combustion reaction at the sampling/weld station uses 3.0 moles of oxygen, together with 6.0 moles of hydrogen. This produces an additional 6.0 moles of water vapor. The final gas mixture in the MCO is 7.1 moles helium, 7.9 moles hydrogen, and 6.0 moles water vapor. The energy liberated by the formation of the water vapor is 355,000 cal.

By an iterative process, the final temperature of the gas mixture is about 3,060 K (2,790 °C). The corresponding pressure in the MCO is 1,060 kPa (10.5 atm or 140 lb/in² gauge). According to *SFPE Handbook of Fire Protection Engineering*, the average pressure is a factor of 2 higher because the oxygen concentration is high enough to form shock waves. Before welding, the MCO design pressure is 150 lb/in^2; therefore, the MCO is not expected to be damaged by the worst-case explosion. An MCO with mechanical closure is stable to an internal loading of 340 lb/in^2, and the after welding rated pressure is 450 lb/in^2. In addition, the sample line and connection are designed to withstand even greater pressure. However, the sample line is assumed to fail from the high gas temperatures. When the explosion occurs, the sample line can melt enough that gases in the MCO rush out and carry particulate matter into the environment.

The air ingress accident leads to a similar environmental release. When the gas mixture in the MCO burns, the adiabatic flame temperature reaches 2,910 K (2,640 °C). The pressure in the MCO is 785 kPa (7.7 atm or 99 lb/in² gauge). Because the oxygen concentration is high enough that shock waves may form, the average pressure is a factor of 2 higher (SFPE 1992). Because the MCO is already open to the environment, the gases rush through the opening and carry particulate matter into the environment.

4.3.5 Method Used to Determine Source Term

For the internal hydrogen deflagration, the material at risk (MAR) (i.e., particulate available for release) depends on the amount of particulate generated between the time the fuel is washed at the K Basins and the time of the accident. HNF-SD-SNF-TI-015 provides a bounding estimate of the MAR for any time during the 40-year life of the facility. HNF-SD-SNF-TI-015 identifies the safety basis or bounding value for the mass of particulate as 34.0 kg UO_2, which contains 30.0 kg of uranium. Because of the conservative methodology used to calculate the bounding value, 30 kg is considered representative of the 99th percentile. HNF-SD-SNF-TI-015 also identifies a design or nominal value of 2.1 kg UO_2, which contains 1.85 kg of uranium.

The quantity of particulate actually released during an accident depends on the initial aerosol concentration, which includes that generated by accident forces, and subsequent particulate entrainment. This blowdown scenario would feature films of particles rather than deep powder beds. In such a situation, there would still be gas flow through the bed during depressurization, but according to *Technical Report 11.6: Resuspension of Deposited Aerosols*

Following Primary System or Containment Failure (IDCOR 1984), the local velocity is simply not sufficient for entrainment. The pressurized powder venting source term is not applicable, and a source term based upon aerodynamic entrainment is used.

Based on the data reported in DOE-HDBK-3010-94, *Airborne Release Fractions/Rates and Respirable Fractions/Rates for Nonreactor Nuclear Facilities*, a bounding (95th percentile) airborne release rate (ARR) of 4×10^{-5} per hour and a respirable fraction (RF) of 1.0 were selected as bounding for the blowdown. The contents of the MCO are intact fuel elements tightly packed in fuel baskets and pieces of fuel elements housed in the scrap baskets. Particulate matter swept upward by streams of flowing gas within the MCO must take a tortuous path through the MCO and through the MCO shield plug to exit the MCO. For shielded powder, where the aerodynamic stresses are reduced by debris or exposure to static conditions, DOE-HDBK-3010-94 recommends an ARR of 4×10^{-6} per hour and an RF of 0.2 for powder under debris. These values were selected as nominal (50th percentile).

The initial pressure in the MCO at the start of the blowdown determines the fraction of the suspended particulate that is released. The range of pressure for an internal hydrogen deflagration varies with the composition of the initial flammable mixture. According to NUREG/CR-2726, the range of pressure from a hydrogen burn would be from 3 to 12 times the initial pressure. For the calculation of the source term, 5 atm is assumed to be the nominal pressure (50th percentile) with 12 atm used as the 95th percentile pressure. This results in a nominal (50th percentile) leak path factor (LPF) of 0.8 for the MCO and a 95th percentile LPF of 0.92.

The pressurized release from the MCO following the internal deflagration would flow most likely through a leak path with a flow area greater than or equal to the flow area through an MCO shield plug port. The duration of the blowdown depends on the flow area of the leak and the resultant pressure following the burn. The MCO depressurizes to atmospheric pressure in less than 1 minute, even for an MCO pressure of about 150 lb/in^2 gauge and a 0.25-in. hole. The MCO depressurizes in a much shorter time for lower pressures and larger leak paths. For the calculation of the source term, a nominal (50th percentile) value of 10 seconds and a bounding (95th percentile) time of 60 seconds were selected.

The material released by aerosol entrainment can be calculated using the methodology described in Chapter 1.0 and the bounding and nominal values identified above. The bounding (95th percentile) value for the material released by aerodynamic entrainment is 2.0×10^{-4} g, as shown in Table 4-2.

Table 4-2. Aerodynamic Entrainment Source Term for the Internal Deflagration Accident.

	Nominal	Bounding	EF	Percentile	SNV	ln(EF)/SNV
MAR	1.85 kg	30 kg	16.22	99	2.326	1.198
ARR	4.00 E-06/h	4.00 E-05/h	10.00	95	1.645	1.400
Time	10 s	60 s	6.00	95	1.645	1.089
RF	0.20	1.00	5.00	95	1.645	0.978
M	4.1 E-06 g[a]	2.0 E-04 g[b]	48[c]	95	1.645	2.353

Note: The 1.645 is the standard normal variable corresponding to the 95% upper confidence limit. For the 99% upper confidence limit, the corresponding value is 2.326.

[a] $\text{Nominal}_{\text{overall}}\ M = \text{MAR}_{\text{nominal}} \times \text{ARR}_{\text{nominal}} \times \text{RF}_{\text{nominal}} \times \text{time}_{\text{nominal}}$.

[b] $\text{Bounding}_{\text{overall}}\ M = (EF_{\text{overall}})\ (\text{nominal}_{\text{overall}}\ M)$.

[c] $$EF_{\text{overall}} = \exp\left(\text{SNV}_{95\%}\left(\sum_i\left[\frac{\ln(EF_i)}{\text{SNV}_i}\right]^2\right)^{\frac{1}{2}}\right)$$

ARR = airborne release rate.
EF = error factor (i.e., bounding value divided by nominal value).
ln(EF) = natural log of EF.
M = mass of material released.
MAR = material at risk.
RF = respirable fraction.
SNV = standard normal variable.

The blast and shock from the hydrogen deflagration would suspend some of the particulate within the MCO. The powder at rest in the MCO could be ejected into the gas volume by the response of the underlying solid MCO and fuel substrate to the vibration and jolting induced by deflagration. According to DOE-HDBK-3010-94, the value of the airborne release fraction (ARF) under such circumstances should exceed the value of the ARF for aerodynamic suspension alone but be less than the value of the ARF for the free-fall of powder. The powder undergoing vibration shock is bounced into the gas while subject to the same gas velocities as those for aerodynamic entrainment. Based on the discussion in DOE-HDBK-3010-94, a bounding (95th percentile) ARF of 1×10^{-3} and an RF of 1.0 were chosen for the suspension of powder-like surface contamination by blast and shock vibration. A nominal (50th percentile) value of 4×10^{-4} was chosen for the ARF and a nominal (50th percentile) value of 0.2 was chosen for the RF based on the evaluation of the discussion in DOE-HDBK-3010-94.

The material released by shock impact can be calculated using the methodology described in Chapter 1.0 and the bounding and nominal values identified above. The bounding (95th percentile) value for the material released by shock impact is 1.8 g, as shown in Table 4-3.

The bounding (95th percentile) source term for the internal hydrogen deflagration is 1.8 g, which is the sum of 1.8 g from vibration and shock and 2.0×10^{-4} g from aerodynamic entrainment.

Table 4-3. Initial Suspended Material Source Term for the Internal Deflagration Accident.

	Nominal	Bounding	EF	Percentile	SNV	ln(EF)/SNV
MAR	1.85 kg	30 kg	16.22	99	2.326	1.198
ARF	4.00 E-04	1.00 E-03	2.50	95	1.645	0.557
RF	0.20	1.00	5.00	95	1.645	0.978
LPF_{MCO}[a]	0.80	0.92	1.15	95	1.645	0.083
M	1.2 E-01 g[b]	1.8 g[c]	15[d]	95	1.645	1.646

Note: The 1.645 is the standard normal variable corresponding to the 95% upper confidence limit. For the 99% upper confidence limit, the corresponding value is 2.326.

[a] LPF_{MCO} = (MCO pressure - 1 atm) / (MCO pressure). At a nominal MCO pressure of 5 atm, the LPF_{MCO} is 0.80, and at a bounding MCO pressure of 12 atm, the LPF_{MCO} is 0.92.

[b] $Nominal_{overall}\ M = MAR_{nominal} \times ARF_{nominal} \times RF_{nominal} \times LPF_{MCO}$.

[c] $Bounding_{overall}\ M = (EF_{overall})\ (nominal_{overall}\ M)$.

[d] $$EF_{overall} = \exp\left(SNV_{95\%}\left(\sum_i\left[\frac{\ln(EF_i)}{SNV_i}\right]^2\right)^{\frac{1}{2}}\right)$$

ARF = airborne release fraction.
EF = error factor (i.e., bounding value divided by nominal value).
LPF = leak path factor.
ln(EF) = natural log of EF.
M = mass of material released.
MAR = material at risk.
MCO = multi-canister overpack.
RF = respirable fraction.
SNV = standard normal variable.

4.4 CONSEQUENCE ANALYSIS

The dose calculation equation and data from Section 3.4.1 of HNF-3553, *Spent Nuclear Fuel Project Final Safety Analysis Report*, are used to calculate the dose to the onsite receptor.

$$D_{onsite} = M \times \frac{\chi}{Q'} \times BR \times UD \times LPF_{building}$$

$$= (1.8 \text{ g U})(1.14 \times 10^{-2} \text{ s/m}^3)(3.33 \times 10^{-4} \text{ m}^3/\text{s})(4.38 \times 10^{5} \text{ rem/g U})(1.0)$$

$$= 3.0 \text{ rem } (0.03 \text{ Sv}).$$

where

D_{onsite} = committed effective dose equivalent (rem)
M = mass of respirable airborne material released (g U)
χ/Q' = time-integrated atmospheric transport factor (s/m^3)
BR = breathing rate (m^3/s)
UD = dose per unit mass of uranium (rem/g U)
$LPF_{building}$ = leak path factor from building.

The dose consequences at the remaining receptor sites are calculated in the same manner and are shown in Table 4-4.

Table 4-4. Dose Calculation Summary for a Bounding Internal Hydrogen Deflagration at the Sampling/Weld Station.

Receptor location (distance, direction)	Duration (hours)	Unmitigated dose[a] rem (Sv)	Evaluation guideline[b]/ release limits rem (Sv) unlikely[c]	Mitigated dose rem (Sv)
Onsite (with building effects) (100 m)	<1	3.0 (3.0 E-02)	10 (1.0 E-01)	--
Highway 240[d] (9,280 m W)	<1	6.1 E-03 (6.1 E-5)	--	--
Hanford Site boundary (17,390 m E)	<1	3.4 E-03 (3.4 E-05)	5.0 (5.0 E-02)	--

[a]Fifty-year committed effective dose equivalent.
[b]Evaluation guideline for onsite (100 m) receptor only.
[c]Unmitigated frequency for this event is unlikely ($>10^{-4}$ to $\leq 10^{-2}$ per year)
[d]Provided for information only.

4.5 REFERENCES

DOE-HDBK-3010-94, 1994, *Airborne Release Fractions/Rates and Respirable Fractions/Rates for Nonreactor Nuclear Facilities*, U.S. Department of Energy, Washington, D.C.

HNF-1523, 1998, *K Basin Particulate Water Content, Behavior, and Impact*, Rev. 1, Fluor Daniel Hanford, Incorporated, Richland, Washington.

HNF-3553, 2000, *Spent Nuclear Fuel Project Final Safety Analysis Report*, Rev. 0, Fluor Hanford, Richland, Washington.

HNF-SD-SNF-TI-015, 1998, *Spent Nuclear Fuel Project Technical Databook*, Rev. 6, Fluor Daniel Hanford, Incorporated, Richland, Washington.

HNF-SD-SNF-TI-017, 1998, *Fuel Surface Area*, Rev. 3, Fluor Daniel Hanford, Incorporated, Richland, Washington.

HNF-SD-SNF-TI-040, 1999, *MCO Internal Gas Composition and Pressure during Interim Storage*, Rev. 3, Fluor Daniel Hanford, Incorporated, Richland, Washington.

IDCOR, 1984, *Technical Report 11.6: Resuspension of Deposited Aerosols Following Primary System or Containment Failure*, Fauske & Associates, Incorporated, Burr Ridge, Illinois.

NUREG/CR-2726, 1983, *Light Water Reactor Hydrogen Manual*, Sandia National Laboratories, Albuquerque, New Mexico.

SFPE, 1992, *SFPE Handbook of Fire Protection Engineering*, Society of Fire Protection Engineers, Boston, Massachusetts.

SNF-4042, 2000, *Evaluation of Accident Frequencies at the Canister Storage Building*, Rev. 2, Fluor Hanford, Incorporated, Richland, Washington.

APPENDIX 4A

BASIS FOR USE OF NONSTOICHIOMETRIC PRODUCTION OF RADIOLYTIC OXYGEN FROM GAMMA IRRADIATION OF HYDRATED SOLIDS

This page intentionally left blank.

APPENDIX 4A

BASIS FOR USE OF NONSTOICHIOMETRIC PRODUCTION OF RADIOLYTIC OXYGEN FROM GAMMA IRRADIATION OF HYDRATED SOLIDS

The basis for use of nonstoichiometric production of radiolytic oxygen from gamma irradiation of hydrated solids is based on observations from solid materials in the literature. Examples of these observations are listed as follows.

- A. A. Garibov, M. M. Melikzade, M. Y. Bakirov, and M. K. Ramazanova, *Radiolysis of Adsorbed Water Molecules on the Oxides Al_2O_3, La_2O_3, Er_2O_3, and BeO*

  "Analysis of the radiolysis products showed that they contained a H_2 and O_2. The $[H_2]/[O_2]$ ratio of the products in all the samples was higher than the stoichiometric ratio, which indicates a trapping of the oxygen in the structures of the oxides."

- M. Nakashima and Y. Aratono, *Radiolytic Hydrogen Gas Formation from Water Adsorbed on Type A Zeolites*

  "In the 5A-water system, O_2 gas was not observed below 7×10^{18} eV/U.S. of absorbed energy. Above 2×10^{20} eV/U.S. the ratio of the amount of O_2 gas to that of H_2 gas (O_2/H_2 ratio) was far below the stoichiometric ratio of 0.5 and it increases with increase of the p-value [U.S. = unit sample containing 1 g of dried zeolite and p g of physisorbed water]. In 3A- and 4A-water system, this ratio smoothly decreased from about 0.4 at $p = 0.03$ to about 0.2 at $p = 0.21$, and seems to approach to a definite value near saturation amount of adsorbed water ($p = 0.29$). This tendency near saturation may be also the case in the 3A-water system, although the p-value dependence of the O_2/H_2 ratios was very different from that in the 4A-water system. Thus, radiolytic production of oxygen gas in these systems is really complicated, and a reasonable explanation cannot be given at the present moment for the difference of p-value dependence of O_2/H_2 ratio among these three A-type zeolite-water systems."

- M. Nakashima and E. Tachikawa, *Radiolytic Gas Production from Tritiated Water Adsorbed on Molecular Sieve 5A*

  "In the present experiments, O_2 gas was observed only in high-dose region of K-irradiation. The yields of O_2 gas evolved increased with energy absorbed by the entire system. The relative ratio of the amount of O_2 gas to that of H_2(HT) gas (O_2/H_2 ratio) is shown in Fig. 5 [this figure is found in Nakashima and Tachikawa (1987)]. The O_2/H_2 ratio increases with increase of the p-value and energy absorbed, but is far below the stoichiometric ratio of 0.5. The oxygen yield

extrapolated to the absorbed energy of 1×10^{19} eV per unit sample is less than 1×10^{15} molecules/g and the O_2/H_2 ratio is less than *0.1*. *Since this amount of* O_2 gas is far below the detection limit in the present experimental conditions, it is not clear whether O_2 gas is evolved in the low-dose region or not. However, these results at least indicate that reactions leading to oxygen formation gradually becomes pronounced with increase of energy absorbed and an appreciable amount of O_2 gas is evolved in high dose region." [An appreciable amount of O_2 gas still did not mean stoichiometric quantities.]

These observations indicate that the solid materials are capable of incorporating excess oxygen within the material crystal structure. Concern has been expressed that over long time periods, the crystal structure would "saturate," leading to stoichiometric production of oxygen at some point in the future. To investigate this concern, the projected stoichiometry of materials at the end of 40 years of storage was investigated.

The overall radiolysis stoichiometry can be described by the following general reactions:

$$Al_2O_3 \bullet 3H_2O \xrightarrow{\alpha,\beta,\gamma} Al_2O_{2+x-2y} \bullet (3-x)\,H_2O + x\,H_2 + y\,O_2$$

$$UO_2(OH)_2 \bullet H_2O \xrightarrow{\alpha,\beta,\gamma} UO_{2+2x-2y}(OH)_{2-2x} \bullet (1-z)\,H_2O + (x+z)\,H_2 + (y+\frac{z}{2})\,O_2$$

Based on the calculation methods in HNF-SD-SNF-TI-040, *MCO Internal Gas Composition and Pressure during Interim Storage*, the fraction decomposition of aluminum hydroxide in cladding films and canister particulate, and the hydrated uranium compounds in films and canister particulate, were estimated for a range of MCO heat loads. Each MCO was assumed to contain two scrap baskets. The quantity of hydrogen and oxygen evolved from the MCO over 40 years of storage was calculated, assuming no guttering and databook radiolysis G-values, to estimate the predicted overall decomposition stoichiometry. The results are shown in Table 4A-1 for an MCO containing 776 W (bounding heat load), 600 W (approximates the expected maximum heat load produced), or 396 W (nominal heat load) at the beginning of the storage period.

Table 4A-1. Fractional Decomposition of Hydrates in Multi-Canister Overpack Containing Two Scrap Baskets during Forty-Year Storage Period.

Material	MCO inventory		Effective fraction decomposed	Evolved gases (gmol)	
	kg	gmole		Hydrogen	Oxygen
776 W MCO					
$Al(OH)_3$, cladding film	9.47	121.41	0.06869	12.5	1.5
$Al(OH)_3$, canister particulate	0.24	3.08	0.18678	0.86	0.34
$UO_3 \cdot 2H_2O$	20.7	64.29	0.49012	63.0	11.0
600 W MCO					
$Al(OH)_3$, cladding film	9.47	121.41	0.05353	9.7	1.1
$Al(OH)_3$, canister particulate	0.24	3.08	0.14774	0.68	0.26
$UO_3 \cdot 2H_2O$	20.7	64.29	0.40596	52.2	9.0
396 W MCO					
$Al(OH)_3$, cladding film	9.47	121.41	0.03566	6.5	0.7
$Al(OH)_3$, canister particulate	0.24	3.08	0.10013	0.46	0.17
$UO_3 \cdot 2H_2O$	20.7	64.29	0.29088	37.4	6.4

Example calculation of mole ratios (based on 776 W MCO):

For $Al(OH)_3$, cladding film: $x = 2 \times 12.5/121.41 = 0.206$, $y = 2 \times 1.5/121.41 = 0.025$
(Note: 2 gmol $Al(OH)_3$/gmol $Al_2O_3 \cdot 3H_2O$)

For $Al(OH)_3$, canister particulate: $x = 2 \times 0.86/3.08 = 0.559$, $y = 2 \times 0.34/3.08 = 0.221$

For $UO_3 \cdot 2H_2O$: $(x + z) = 63/64.29 = 0.98$, $(y + z/2) = 11/64.29 = 0.171$;
therefore, for $z = 0$, $x = 0.98$, and $y = 0.171$, or for $y = 0$, $z = 0.342$, and $x = 0.638$.

This results in the overall radiolysis stoichiometry shown in Table 4A-2.

Table 4A-2. Estimated Overall Stoichiometry of Radiolysis in Multi-Canister Overpack Containing Two Scrap Baskets during Forty-Year Interim Storage.

Initial MCO heat load (W)	Material	Overall stoichiometry
776	$Al(OH)_3$ cladding film	$Al_2O_3 \bullet 3H_2O \xrightarrow{\gamma} Al_2O_{3.156} \bullet 2.794\,H_2O + 0.206\,H_2 + 0.025\,O_2$
	$Al(OH)_3$ canister particulate	$Al_2O_3 \bullet 3H_2O \xrightarrow{\alpha,\beta,\gamma} Al_2O_{3.117} \bullet 2.441\,H_2O + 0.559\,H_2 + 0.221\,O_2$
	$UO_3 \bullet 2H_2O$	$UO_2(OH)_2 \bullet H_2O \xrightarrow{\alpha,\beta,\gamma} UO_{3.618}(OH)_{0.04} \bullet H_2O + 0.98H_2 + 0.171O_2$ to $UO_2(OH)_2 \bullet H_2O \xrightarrow{\alpha,\beta,\gamma} UO_{3.276}(OH)_{0.724} \bullet 0.658\,H_2O + 0.98\,H_2 + 0.171\,O_2$
600	$Al(OH)_3$ cladding film	$Al_2O_3 \bullet 3H_2O \xrightarrow{\gamma} Al_2O_{3.124} \bullet 2.84\,H_2O + 0.16\,H_2 + 0.018\,O_2$
	$Al(OH)_3$ canister particulate	$Al_2O_3 \bullet 3H_2O \xrightarrow{\alpha,\beta,\gamma} Al_2O_{3.104} \bullet 2.558\,H_2O + 0.442\,H_2 + 0.169\,O_2$
	$UO_3 \bullet 2H_2O$	$UO_2(OH)_2 \bullet H_2O \xrightarrow{\alpha,\beta,\gamma} UO_{3.344}(OH)_{0.376} \bullet H_2O + 0.812H_2 + 0.14O_2$ to $UO_2(OH)_2 \bullet H_2O \xrightarrow{\alpha,\beta,\gamma} UO_{3.064}(OH)_{0.936} \bullet 0.72H_2O + 0.812H_2 + 0.14O_2$
396	$Al(OH)_3$ cladding film	$Al_2O_3 \bullet 3H_2O \xrightarrow{\gamma} Al_2O_{3.083} \bullet 2.893\,H_2O + 0.107\,H_2 + 0.012\,O_2$
	$Al(OH)_3$ canister particulate	$Al_2O_3 \bullet 3H_2O \xrightarrow{\alpha,\beta,\gamma} Al_2O_{3.077} \bullet 2.701\,H_2O + 0.299\,H_2 + 0.111\,O_2$
	$UO_3 \bullet 2H_2O$	$UO_2(OH)_2 \bullet H_2O \xrightarrow{\alpha,\beta,\gamma} UO_{2.964}(OH)_{0.836} \bullet H_2O + 0.582H_2 + 0.1O_2$ to $UO_2(OH)_2 \bullet H_2O \xrightarrow{\alpha,\beta,\gamma} UO_{2.764}(OH)_{1.236} \bullet 0.8\,H_2O + 0.582H_2 + 0.1O_2$

As indicated in Tables 4A-1 and 4A-2, complete decomposition of the hydrated materials is not projected over the 40-year storage period. As might be expected, the MCO containing the bounding heat load produces the largest quantity of excess oxygen that must be retained in the crystal structures due to the assumed nonstoichiometry G-values.

The 40-year storage period is projected to result in, at most, 5% oxygen within the crystal structure. The overall stoichiometry of aluminum hydroxide radiolysis appears to be similar to either dehydration or dehydroxylation. Partially dehydrated aluminum hydroxides not only reversibly adsorb water, but also anions, hydrated cations, and a number of organic compounds (Wefers and Misra 1987). Partial dehydroxylation is equivalent to preparation of activated alumina, which has the capability to catalyze certain chemical reactions and chemisorb a variety of molecular and ionic species. Fully dehydroxylated, crystaline I-Al_2O_3 is not active, nor are the well-ordered trihydroxides and oxide hydroxides of aluminum. Activity is directly related to the defect structure of the transition forms resulting from partial dehydroxylation (Wefers and Misra 1987). Based on these properties and the projected partial dyhydation, or dehydroxylation, over the 40-year storage period, it is concluded that nonstoichiometric production of hydrogen and oxygen from aluminum hydroxide radiolysis is feasible.

The ability of hydrated uranium compounds to incorporate oxygen in the crystal structure could be confused by the shorthand method of writing the chemical formula (e.g., $UO_3 \cdot 2H_2O$), which does not describe the actual molecule structure. The uranium hydrate shorthand formula is more completely described by $UO_2(OH)_2 \cdot H_2O$, which dehydrates to $UO_2(OH)_2$. As shown in Figure 4A-1, these compounds represent hydroxalation and hydration of the uranyl ion, which has the capacity to form multiple bounds with anions.

Table 4A-1 indicates that approximately 50% of the uranium hydrate is expected to decompose over the 40-year storage time. Much of this decomposition results from alpha and beta radiolysis, which has been projected to produce stoichiometric evolution of oxygen. The overall stoichiometry of radiolysis does not produce a large increase in oxygen that must be incorporated in the crystal structure. Therefore, it is concluded that the nonstoichiometric G-values for hydrated oxides can be sustained throughout the 40-year storage period.

REFERENCES

Chernyaev, I. I., 1964, *Complex Compounds of Uranium*, Academy of Sciences of the U.S.S.R., translated from Russian by L. Mandel, Israel Program for Scientific Translations, Jerusalem, 1966.

Garibov, A. A., M. M. Melikzade, M. Y. Bakirov, and M. K. Ramazanova, 1982, *Radiolysis of Adsorbed Water Molecules on the Oxides Al_2O_3, La_2O_3, Er_2O_3, and BeO*, Khimiya Vysokikh Énergii, Vol. 16, No. 3, pp. 225-227.

HNF-SD-SNF-TI-040, 1998, *MCO Internal Gas Composition and Pressure during Interim Storage*, Rev. 3, DE&S Hanford, Richland, Washington.

Nakashima, M., and Y. Aratono, 1993, *Radiolytic Hydrogen Gas Formation from Water Adsorbed on Type A Zeolites*, Radiat. Phys. Chem., Vol 41, No. 3, pp.461-465.

Nakashima, M., and E. Tachikawa, 1987, *Radiolytic Gas Production from Tritiated Water Adsorbed on Molecular Sieve 5A*, Journal of Nuclear Science and Technology, 24[1], pp. 41-46.

Wefers, K., and C Misra, 1987, *Oxides and Hydroxides of Aluminum*, Alcoa Technical Paper No. 19, Revised, Alcoa Laboratories, Aluminum Company of America.

Figure A-1. Structure of Hydrated Uranyl Ions.

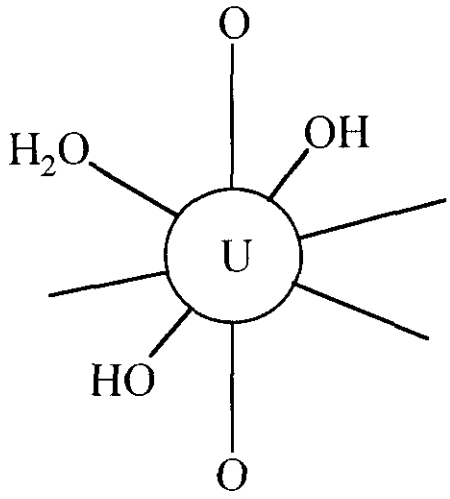

(a) $UO_2(OH)_2 \cdot H_2O$ (Simplified formula: $UO_3 \cdot 2\ H_2O$)

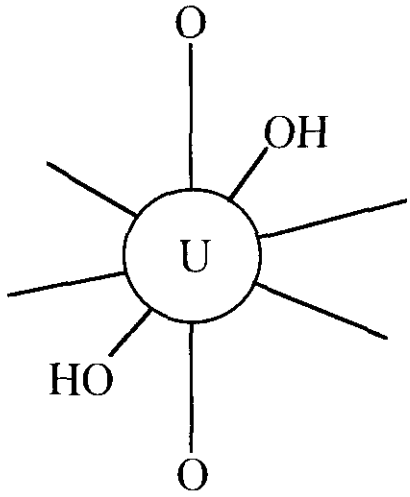

(b) $UO_2(OH)_2$ (Simplified formula: $UO_3 \cdot H_2O$)

Note: This figure is based on I. I. Chernyaev, 1964, *Complex Compounds of Uranium*, Academy of Sciences of the U.S.S.R., translated from Russian by L. Mandel, Israel Program for Scientific Translations, Jerusalem, 1966.

5.0 CALCULATIONS FOR MULTI-CANISTER OVERPACK EXTERNAL HYDROGEN DEFLAGRATION

5.1 PURPOSE AND OBJECTIVES

The potential consequences of hydrogen deflagrations outside the multi-canister overpack (MCO) are evaluated in this chapter. There are potential accident conditions during the handling of a cask–MCO in the Canister Storage Building (CSB) in which concentrations of hydrogen outside an MCO could be significant enough to lead to a deflagration.

No thermal constraints on extended duration storage at the CSB have been identified beyond those identified in Chapter 7.0. HNF-SD-SNF-SARR-005, *Multi-Canister Overpack Topical Report*, identifies a 234-hour window for shipping from the Cold Vacuum Drying Facility (CVDF) to the CSB. This chapter identifies this as an external cask–MCO hazard when the internal atmosphere of the cask is vented at the CSB. Analysis has shown that the hazards of this event are prevented by slow venting of the cask after positive pressure is detected within the cask.

5.2 SCENARIO DEVELOPMENT

In all postulated accident scenarios, hydrogen accumulates in an MCO because of processing delays, equipment malfunctions, or catastrophic events. The general sequence of events leading to a hydrogen deflagration is shown in SNF-4042, *Evaluation of Accident Frequencies at the Canister Storage Building*. The accident sequence begins with the presence of enough hydrogen inside an MCO to form a flammable mixture with air outside the MCO. Three conditions necessary for hydrogen accumulation inside an MCO within a reasonable time frame are uranium metal and hydrides, water, and high temperatures. The uranium and water are reactants, and the elevated temperature speeds the reaction.

In all external hydrogen deflagration scenarios, the accumulated hydrogen escapes the MCO and mixes with air to form a combustible mixture of hydrogen and oxygen. The mixture is then ignited. Because it takes very little energy to begin the hydrogen–oxygen combustion, it is assumed that ignition sources are present in the mixture. The combustion could be initiated by static electricity in ventilation ducting, a small particle of uranium hydride, static electricity in the spray nozzles in the water storage tanks, and other sources. The specific accident scenarios are described in the following subsections.

5.2.1 Hydrogen Deflagration Caused by Drop from Transportation Trailer

The cask–MCO is dropped while being removed from the transportation trailer. The cask is not damaged by this drop, but the MCO may be damaged. It is assumed that the MCO is breached and loses pressure. The gas leaving the MCO has considerable hydrogen so that a flammable mixture of hydrogen, helium, and air forms in the space between the outside of the

MCO and the inside of the cask. This flammable mixture ignites but the resulting pressure increase is not expected to damage the cask.

5.2.2 Hydrogen Deflagration during Multi-Canister Overpack Cask Venting

MCOs are transported from the CVDF to the CSB in sealed transportation casks. When a cask–MCO first arrives at the CSB, the MCO contains helium and hydrogen, and the cask contains air in the void space. The hydrogen in the MCO is liberated primarily by the reaction of water vapor with uranium and uranium hydrides and also by the radiolytic decomposition of water-containing compounds in the MCO.

Hydrogen produced inside the MCO will increase the MCO pressure and could leak into the space between the MCO and the transportation cask. Rough handling or some other failure at the CVDF is assumed to cause a mechanically sealed MCO to leak much faster than the maximum allowed rate (e.g., 10,000 times faster than allowed). Within 4 days, enough hydrogen forms and leaks from the MCO and into the cask void volume to raise the gas pressure in the transportation cask. When the initial pressure check at the CSB discloses excessive pressure, the mobile service station tent is placed over the cask for contamination control. The excessive pressure required initiation of recovery action. Very little contamination will be release from the MCO to the cask with a leak this size. HNF-SD-SNF-HIE-001, *Canister Storage Building Hazard Analysis Report*, identified this event as a worker safety concern only.

5.2.3 Hydrogen Deflagration from Receiving a Wet Cask–Multi-Canister Overpack

A hydrogen deflagration from receiving a wet cask–MCO is a variation on the deflagration during cask venting in that the source of hydrogen in the cask is wet corrosion of the fuel. When a cask–MCO is ready to leave the CVDF and go to the CSB, it looks the same as a cask–MCO that has just arrived at the CVDF for drying operations. It has been assumed that at the CVDF, one cask–MCO is dry and ready for shipment to the CSB at about the same time a water-filled cask–MCO arrives from K Basins. A process interruption causes the two casks to be mistaken, and the water-filled cask–MCO is sent to the CSB. An event tree for this scenario is provided in SNF-4042. This is a very low probability event. It will be recognized during the initial pressure check at the CSB and will therefore initiate a recovery action. The MCO full of water will release little contamination. The hazard analysis (HNF-SD-SNF-HIE-001) identified this event as a worker safety concern only.

5.2.4 Hydrogen Deflagration during Multi-Canister Overpack Handling

The MCO handling machine (MHM) transports MCOs within the CSB. The space inside the MHM is filled with air and ventilated by a high-efficiency particulate air (HEPA) filtered exhauster located on the turret. The HEPA filter units are located at the same level as the operating platform. If there were a major equipment breakdown that trapped a leaking MCO in

the MHM for an extended period of time, then significant hydrogen could accumulate in the air around the MCO.

A mechanically sealed MCO must leak significantly more than the maximum allowed rate following the MHM malfunction to be of concern. After a few days, enough hydrogen has leaked from the MCO that potential flammable concentrations of hydrogen exist in the MHM. A flammable mixture of air and hydrogen would also exists in the exhaust ducts and HEPA filter.

A spark would lead to a deflagration in the ducts and HEPA filter. Any personnel nearby could be injured. A deflagration also could lead to environmental release of the radioactivity accumulated on the MHM HEPA filter. The projected radiation dose to any individual downwind does not exceed the dose criteria.

5.2.5 Hydrogen Deflagration during Interim Storage

MCOs are expected to be in interim storage for about 40 years. Welded MCOs have a maximum allowable leak rate of 1×10^{-7} cm^3/s, and mechanically sealed MCOs have a higher maximum allowable leak rate (1×10^{-5} cm^3/s). Over a long period of time, a high leak rate (greater than the maximum allowable) could produce flammable concentrations of hydrogen and air in the storage tube.

Rough handling or some other failure is assumed to cause an MCO to leak much faster than the maximum allowed rate. Within a few weeks enough hydrogen has leaked from the MCO into the storage tube to create flammable concentrations. A deflagration of this mixture could damage the storage tube, but it is unlikely to exceed any safety criteria.

5.2.6 Hydrogen Deflagration during Multi-Canister Overpack Gas Sampling

Cover cap welding on selected MCOs will be delayed to allow for gas sampling at the CSB. An MCO that is to be sampled is moved to the sampling pit, and a sampling hood is placed over the MCO. Connections are made to the MCO sample port, and MCO gas is collected using the positive pressure of the MCO. If the connection to the MCO were to fail and discharge MCO gas into the sampling hood, a potentially explosive mixture of hydrogen and air could be formed in the hood. Because personnel normally are near the hood during this time, it is probable that an explosion in the sampling hood would cause a significant injury to the operator opening the MCO vent valve. An event tree for this scenario is provided in SNF-4042. This event is the design basis accident scenario presented in HNF-3553, *Spent Nuclear Fuel Project Final Safety Analysis Report*, Annex A, "Canister Storage Building Final Safety Analysis Report," for external hydrogen deflagrations.

5.3 SOURCE TERM ANALYSIS

The mathematical analysis of the identified postulated hydrogen deflagration accidents focuses on hydrogen concentration in a transportation cask, the MHM, or in a CSB storage tube. Before describing the accidents in detail, some general information relevant to all the external hydrogen accidents will be presented.

5.3.1 Hydrogen Accumulation and Other Parameters

Parameters and assumptions common to all, or most, of the postulated accidents are presented here. The values presented include gas volumes, helium inventory in the MCO, air inventory in the transportation cask, hydrogen content of the MCO after all the available free and hydrated water has reacted with the uranium, the corresponding MCO pressure, the MCO leak rate, and the peak overpressures due to hydrogen combustion.

5.3.1.1 Volumes. The volumes of accumulated hydrogen are listed in Table 5-1. Because the shapes are somewhat irregular, the volumes are approximate. However, the conclusions are not sensitive to minor changes in the estimated volume.

Table 5-1. Volumes Assumed for Hydrogen Accumulation.

Location	Volume, L	Volume, ft^3
Free volume inside MCO	500	17.7
Free volume of cask	125	4.4
Free volume of MHM	1,170	41.3
Storage tube - one MCO	2,890	102.1
Storage tube - two MCOs	1,530	54.0
Sampling hood	600	21.2

Note: These are approximate values due to the irregular shapes. More exact volumes will have no effect on the conclusions.

MCO = multi-canister overpack.
MHM = multi-canister overpack handling machine.

5.3.1.2 Helium and Air Inventory in the Multi-Canister Overpack. Before leaving the CVDF, the MCO is pressurized with helium. According to HNF-SD-SNF-TI-015, *Spent Nuclear Fuel Project Technical Databook*, the MCO pressure after filling is 1.5 atm with a temperature of 25 °C. From the ideal gas law, for an MCO volume of 500 L, 30.7 gmoles of helium are required to pressurized the MCO. The cask is filled at the CVDF with air at atmospheric pressure and a

temperature of 20 °C. With a cask annulus volume of 125 L, this corresponds to 5.20 gmoles of air (see Section 5.3.2).

5.3.1.3 Bounding Hydrogen Gas in the Multi-Canister Overpack. The composition of the gas inside the MCO when it is received at the CSB is based on the assumption that there is only helium and hydrogen. The hydrogen is generated primarily by corrosion of fuel and reaction with uranium hydride. The radiolytic decomposition of water and hydroxides adds very little and has not been considered.

The bounding hydrogen content of an MCO with two scrap baskets will be estimated assuming the water reactions with uranium metal and uranium hydride occur at the same rate. From HNF-SD-SNF-TI-015, the enhancement factor for the metal reaction is 10, while the enhancement factor for the hydride reaction is 12. In addition, the metal reaction produces 1 mole of hydrogen gas for every mole of water reacted, but the hydride reaction produces 1.75 moles of hydrogen for every mole of water reacted. The combined effect is that the hydrogen generation increases by the factor

$$\frac{(10)(1) + (12)(1.75)}{10 + 12} = 1.409$$

over the amount expected from the uranium metal reaction alone.

The hydrogen gas that could be generated from the uranium metal is limited by the amount of water available to react. The bounding free water estimate is 200 g in crevices and cracks. In addition, uranium oxide dihydrate will lose one of the water molecules at normal MCO temperatures according to HNF-1523, *K-Basins Particulate Water Content, Behavior, and Impact*. Much of this loss may occur during drying at CVDF, but to maximize the hydrogen generation after drying none will be assumed. The bounding hydrated water estimate for two scrap baskets is 1,190 g (HNF-SD-SNF-TI-015). Half of this amount is available for temperatures less than 100 °C to react with uranium fuel to form hydrogen.

5.3.1.4 Multi-Canister Overpack Leak Rate Calculation. Because of an off-normal condition, the MCO is assumed to leak much faster than the bounding leak rate for a mechanically sealed MCO. According to HNF-2155, *Multi-Canister Overpack Combustible Gas Management Leak Test Acceptance Criteria*, the bounding leak rate is 1.0×10^{-5} cm^3/s (8.64×10^{-4} L/d) at reference conditions. Reference conditions are defined as an inside pressure of 101.3 kPa (14.7 lb/in^2) and an outside pressure of 1.013 kPa (0.147 lb/in^2), both at a temperature of 25 °C. The reference leak rate is based on volumes inside the container. A bounding formula follows to represent the leak rate at the postulated conditions outside the container. Note that no distinction is made between hydrogen and helium leak rates. The hydrogen is lighter than helium and could diffuse more rapidly through a small leak. The formula comes from the observation that the leakage rate is proportional to the pressure difference inside and outside the cask and also the density, which is represented as pressure. The temperature adjustment is included to adjust for

density change and to be consistent with the method used in the derivation of the leak rate criteria (HNF-2155).

$$L_{MCO,out} = L_x \frac{\left(P_{MCO,in} - P_{MCO,out}\right)\left(P_{MCO,ave}\right)\left(T_{MCO,out}\right)}{\left(P_{MCO,out}\right)\left(T_{MCO,in}\right)}$$

where

$L_{MCO,out}$ = leak rate at the postulated conditions outside the MCO, in L/d (or L/h)

L_x = proportionality constant based on the leak rate at reference conditions, in L/d (or L/h) per kPa

$P_{MCO,in}$ = pressure inside the MCO at postulated conditions, in kPa

$P_{MCO,out}$ = pressure outside the MCO at postulated conditions, in kPa

$P_{MCO,ave}$ = average pressure, $(P_{MCO,in} + P_{MCO,out})/2$, in kPa

$T_{MCO,in}$ = temperature inside the MCO at postulated conditions, in degrees Kelvin

$T_{MCO,out}$ = temperature outside the MCO at postulated conditions, in degrees Kelvin.

The constant, L_x, takes the place of more complex parameters described in HNF-2155. These parameters mainly depend on the leak diameter and are weakly dependent on gas temperature. The value for L_x can be obtained using reference conditions inside the container. This is shown as

$$L_x = L_{ref,in} \frac{\left(P_{ref,in}\right)}{\left(P_{ref,in} - P_{ref,out}\right)\left(P_{ref,ave}\right)} = L_{ref,in}\left(0.01975\ \text{kPa}^{-1}\right)$$

where

L_x = proportionality constant, in L/d (or L/h) per kPa
$L_{ref,in}$ = leak rate at reference conditions inside, in L/d (or L/h)
$P_{ref,in}$ = pressure inside the MCO at reference conditions, 101.3 kPa
$P_{ref,out}$ = pressure outside the MCO at reference conditions, 1.013 kPa
$P_{ref,ave}$ = average pressure, $(P_{ref,in} + P_{ref,out})/2 = 51.16$ kPa.

The leak rates modeled with the described formulas are very low. Since small leak rates are associated with very small holes or cracks, the associated matter released due to suspended or entrained particulate is very small and will be ignored in the analysis of external hydrogen accidents.

5.3.1.5 Pressures Due to Hydrogen Deflagration. Mixtures of hydrogen in air are flammable in the range of 4% to 75% hydrogen by volume at atmospheric pressure and room temperature. Higher pressures and temperatures change the flammable concentration range, but these limits will be assumed for simplicity. According to NUREG/CR-2726, *Light Water Reactor Hydrogen Manual*, higher pressure shock waves may be produced if the hydrogen concentration is between 18 and 58 vol% in air. The stoichiometric ratio (2 moles hydrogen per 1 mole of oxygen) corresponds to 29.6% hydrogen in dry air. The presence of helium changes the stoichiometric ratio because it displaces oxygen. For example, if there are equal volume percents of hydrogen and helium, then the stoichiometric hydrogen concentration is reduced to 22.8%.

When the hydrogen and oxygen react, water vapor is formed and energy is released. To be conservative, it is assumed that the energy released stays in the gas and none is lost to the MCO components. The heat capacity of the gases allows the final temperature to be computed. This final temperature, together with the number of moles of gases in the MCO and the ideal gas law, is used to calculate the final pressure resulting from the combustion.

The heat of formation of water vapor from hydrogen and oxygen gas is 57,800 cal/mole at a temperature of about 27 °C. The heat capacity of various gases can be calculated from a quadratic formula as listed in Table 5-2.

Table 5-2. Parameters to Determine Heat Capacities.

Gas	A	B	C
H_2	4.959	-1.96 E-04	4.76 E-07
N_2	4.470	1.39 E-03	-6.90 E-08
O_2	4.130	3.17 E-03	-1.01 E-06
H_2O	5.149	2.64 E-03	4.59 E-08
He	3.020	0	0

Values for the heat capacity at constant volume (in cal/mole/K) are computed from the formula $Cv = A + B \cdot T + C \cdot T^2$, where T is the temperature of the gas. This method and parameter values are given in Whitwell and Toner, 1969, *Conservation of Mass and Energy*, Blaisdell Publishing Company, Waltham, Massachusetts.

The heat capacity parameters shown on this table apply to the temperature range of 300 K (27 °C) to 1,500 K (1,230 °C). At higher temperatures, the heat capacities are over-estimated.

The final temperature of the gas mixture is found using the following formula. (The integration is between the initial temperature of the gas mixture before combustion and the final temperature of the gas mixture after combustion. The summation is over the types of gases present in the MCO after combustion. Because the final gas temperature is unknown but determines the heat capacities, it must be solved by an iterative process.)

$$(H_F)(N_{H2O}) = \int_{T_o}^{T_f} \left(\sum (Cvi)(Ni) \right) \quad (dT)$$

where

H_F = heat of formation of water from hydrogen and oxygen, 57,800 cal/mole formed as a vapor

N_{H2O} = number of moles of water formed; computed as the smaller of the number of moles of hydrogen and twice the number of moles of oxygen (before combustion)

T_o = temperature of the gas mixture before combustion, in Kelvin

T_f = temperature of the gas mixture after combustion, in Kelvin

Cvi = heat capacity at constant volume of gas "I"; depends on the temperature of the gas (represented as a quadratic equation)

Ni = number of moles of gas "I" after the oxygen and hydrogen react.

The pressure pulse from a hydrogen explosion exists for only a fraction of a second, but may do considerable damage to the vessel containing it. An estimate of how long this pressure exists can be obtained from the following formula for the rate of pressure increase from *SFPE Handbook of Fire Protection Engineering* (SFPE 1992).

$$(dP/dt)_{max} = (K_G)/(V^{1/3})$$

where

$(dP/dt)_{max}$ = maximum rate of pressure increase, kPa/s

K_G = parameter measured for explosions in spherical containers; for hydrogen this is 66,000 kPa·m/s (SFPE 1992)

V = volume of the container with the burning gases, m^3.

Dividing the final pressure rise by the maximum rate of pressure rise leads to a bound on the shortest possible time in which the pressure could reach the peak. This minimum time is useful for estimating the motion of objects affected by the pressure pulse. As an example, an explosion in a storage tube could lift the storage tube plug.

The momentum imparted to an object affected by the pressure pulse is computed as the time-integral of the force acting on the object. As a simple approximation, the pressure is assumed to rise linearly to the peak and then fall linearly back to where it started. The total time is twice the value for t_{min} given above. The force on the object is the product of the affected surface area and the pressure. Therefore, the momentum imparted to an object is the product of the peak pressure increase (P_x-P_o), the affected surface area, and the time for the pressure to rise to the peak (t_{min}). The final speed of the object is this momentum divided by its mass:

$$U = (P_x\text{-}P_o)(A)(t_{min})/(M)$$

where

U = speed of object affected by the pressure pulse, in m/s
P_x = maximum pressure after completion of combustion of M_H, in kPa
P_o = starting pressure before combustion, 101.3 kPa is used
A = surface area affected by the pressure pulse, in m^2
t_{min} = minimum time for the pressure to rise to the peak value (P_x), in units of milliseconds
M = mass of object affected by the pressure pulse, in kg.

In the case of storage tube explosions, the speed of the object can be used to estimate how high the storage tube plug could rise following a hydrogen explosion (see Section 5.3.4). In the case of an explosion in the sampling hood, this speed could indicate the maximum velocity at which the hood view port could move toward the operator as a result of the explosion (see Section 5.3.5).

5.3.2 Basis for Hydrogen Deflagration Caused by Drop from Transportation Cask

Each of the assumed temperatures and pressures used in the analysis of this event has an allowable range. Values chosen are intended to maximize combustion and generate pressure in the cask. The calculation begins with assumptions about the amount of helium and hydrogen in the MCO at the time of the accident and the amount of air in the space between the cask and MCO. It also is assumed that 100% of the hydrogen is burned. The resulting pressure is calculated using a standard adiabatic model.

The initial amount of helium in the MCO depends on the filling pressure and temperature. It is assumed that the filling pressure is 1.5 atm and the gas temperature after filling is 298.15 K. The amount of helium in the 500-L MCO is calculated as follows.

$$\text{He gmoles} = \frac{(1.5 \text{ atm})\ (500 \text{ L})}{(0.082057 \text{ L·atm/gmole/K})\ (298.15 \text{ K})}$$

$$= 30.7 \text{ gmoles helium}.$$

The amount of hydrogen in the MCO at the time it arrives at the CSB is assumed to be the number of moles of hydrogen that would be formed by the reaction of 800 g of water (200 g of free water plus approximately 600 g of water from uranium hydrate [see Section 4.3.1]) with uranium metal to form uranium dioxide and hydrogen gas. The amount of hydrogen formed, including the hydride enhancement factor, is as shown below.

$$H_2 \text{ gmoles} = \frac{(800 \text{ g } H_2O)\ (1 \text{ gmole } H_2)}{(18.015 \text{ g/gmole})\ (1 \text{ gmole } H_2O)} \times 1.409$$

$$= 62.6 \text{ gmoles } H_2.$$

The average temperature of the gas inside MCO when it arrives at the CSB is assumed to be 60 °C (333.15 K). The total number of moles of gas in the MCO is the sum of the moles of helium and hydrogen, 93.2 gmoles.

From the ideal gas law, the pressure is calculated as shown below.

$$\text{MCO pressure} = \frac{(93.2 \text{ gmole})\ (0.082057 \text{ L·atm/gmole/K})\ (333 \text{ K})}{500 \text{ L}}$$

$$= 5.1 \text{ atm}.$$

The cask was filled with air at the CVDF at atmospheric pressure and a temperature of 20 °C (293.15 K). The volume of the space between the outside of the MCO and the inside of the cask is assumed to be about 125 L based on information provided in HNF-SD-SNF-SARR-005. Thus the cask initially contains 5.20 gmoles of air. The composition of the air is shown in Table 5-3.

Table 5-3. Composition of Air in the Cask Before the Accident.

Type of gas	Percent by volume	Amount (gmoles)
H_2O vapor	0.46%	0.02
N_2	77.76%	4.04
O_2	20.85%	1.08
Ar	0.93%	0.05
Total	100.00%	5.20

The assumed relative humidity is 20%. At 20 °C, the saturated pressure of water vapor is 2.3388 kPa (0.02308 atm).

At the time of the cask drop accident, the temperature of the air in the cask will have increased to 30 °C (303 K), as shown in Table 5-4. Using the ideal gas law, the pressure is calculated to have increased to 0.5 lb/in^2 gauge (1.034 atm). The MCO leak causes the MCO pressure to relieve to the cask. Eventually the pressures inside and outside the MCO are equal. This condition determines what fraction of the MCO gas inventory leaks into the cask.

Table 5-4. Composition of the Multi-Canister Overpack and Cask before the Drop.

	Volume	Temperature	Pressure	H_2	O_2	H_2O	N_2	He	Ar
MCO	500 L	333 K	5.1 atm	62.57 gmoles	0.00 gmoles	0.00 gmoles	0.00 gmoles	30.66 gmoles	0.00 gmoles
				67.12 vol%	0.00 vol%	0.00 vol%	0.00 vol%	32.88 vol%	0.00 vol%
Shipping cask	125 L	303 K	1.0 atm	0.00 gmoles	1.08 gmoles	0.02 gmoles	4.04 gmoles	0.00 gmoles	0.05 gmoles
				0.00 vol%	20.85 vol%	0.46 vol%	77.76 vol%	0.00 vol%	0.93 vol%

MCO = multi-canister overpack.

The equilibrium pressure (equalized pressure in cask and MCO) was found to be 4.2 atm, as shown in the calculation below and in Table 5-5.

$$P_{eq} = \left[\frac{V_{MCO} P_{MCO}}{T_{MCO}} + \frac{V_{cask} P_{cask}}{T_{cask}} \right] \left[\frac{V_{MCO}}{T_{MCO}} + \frac{V_{cask}}{T_{cask}} \right]^{-1}$$

$$= \frac{\left[\frac{(500\ L)(5.1\ atm)}{(333\ K)} + \frac{(125\ L)(1.03\ atm)}{(303\ K)} \right]}{\left[\frac{(500\ L)}{(333\ K)} + \frac{(125\ L)}{(303\ K)} \right]}$$

$$= 4.2\ atm\ .$$

P_{MCO}, V_{MCO}, and T_{MCO} are the pressure (5.1 atm), volume (500 L), and temperature (333 K) of the MCO.

P_{cask}, V_{cask}, and T_{cask} are the pressure (1.03 atm), volume, (123 L), and temperature (303 K) of the cask.

P_{eq} is the pressure in the cask and MCO after equalization.

Table 5-5. Composition of the Multi-Canister Overpack and Cask after the Drop.

	Volume	Temperature	Pressure	H_2	O_2	H_2O	N_2	He	Ar
MCO	500 L	333 K	4.2 atm	51.82 gmoles	0.00 gmoles	0.00 gmoles	0.00 gmoles	25.39 gmoles	0.00 gmoles
				67.12 vol%	0.00 vol%	0.00 vol%	0.00 vol%	32.88 vol%	0.00 vol%
Shipping cask	125 L	303 K	4.2 atm	10.75 gmoles	1.08 gmoles	0.02 gmoles	4.04 gmoles	5.27 gmoles	0.05 gmoles
				50.7 vol%	5.1 vol%	0.1 vol%	19.0 vol%	24.8 vol%	0.2 vol%

MCO = multi-canister overpack.

The composition of the gas in the cask after it burns is shown in Table 5-6. All of the oxygen is assumed to react with the hydrogen to form water vapor.

Table 5-6. Composition of the Multi-Canister Overpack and Cask after Combustion.

	Volume	Temperature	Pressure	H_2	O_2	H_2O	N_2	He	Ar
MCO	500 L	333 K	4.2 atm	51.82 gmoles	0.00 gmoles	0.00 gmoles	0.00 gmoles	25.39 gmoles	0.00 gmoles
				67.12 vol%	0.00 vol%	0.00 vol%	0.00 vol%	32.88 vol%	0.00 vol%
Shipping cask	125 L	1,548 K	20.5 atm	8.58 gmoles	0.00 gmoles	2.19 gmoles	4.04 gmoles	5.27 gmoles	0.05 gmoles
				42.6 vol%	0.0 vol%	10.9 vol%	20.1 vol%	26.2 vol%	0.2 vol%

MCO = multi-canister overpack.

The heat of formation of water vapor is 57,800 cal/gmole. Since 2.17 gmoles of hydrogen react to form 2.17 gmoles of water vapor, the energy liberated is

$$(2.17 \text{ gmole})\ (57{,}800 \text{ cal/gmole}) = 125{,}000 \text{ cal}\ .$$

This energy raises the temperature of the post-combustion gas mixture to 1,550 K at most. The calculation of the final temperature is carried out by an iterative process described in Appendix 5A. At this temperature, the gas pressure is about 290 lb/in^2 gauge. This pressure exceeds the design pressure of the cask (150 lb/in^2 gauge). However, according to SNF-5679, *Maximum Pressure Load Determination for Multi-Canister Overpack Cask (WMTS-ECAL-010)*, the cask is not expected to rupture because the design pressure includes a safety margin of at least 2. The pressure in the cask rapidly decreases as gas is forced back into the MCO, the gases cool, and the steam condenses. All of the oxygen in the cask is consumed by the burn and no further combustion is possible in either the cask or the MCO. Thus the mixing of MCO and cask gases will not lead to a flammable mixture.

5.3.3 Hydrogen Deflagration during Multi-Canister Overpack Handling

Soon after arrival at the CSB, the pressure in the bounding MCO reaches about 5.1 atm if the MCO vapor space is oxygen free. The gas in the MCO is 67% hydrogen and 33% helium. It has been assumed that some accident occurs while an MCO is being transported from one location to another inside the CSB. The MHM is immobilized with the MHM ventilation system out of service. In addition, the MCO begins to leak much faster than the leak rate criteria.

As gas slowly leaves the MCO, the pressure decreases. It is assumed that the gases leave the MCO at a rate proportional to their concentration. Diffusion effects are considered minimal compared to convective flow effects. The air space around the MCO is ventilated by natural circulation only. Thus, clean air continually enters the MHM air space while a mixture of air, hydrogen, and helium continually leaves. The representation of gas concentrations in the MHM

uses the equations below. Note that all volumes have been converted to reference temperature and pressure conditions.

According to HNF-SD-TP-SARP-017, *Safety Analysis Report for Packaging (Onsite) Multicanister Overpack Cask*, the maximum leak rate from the MCO is 2.0×10^{-4} cm^3/s at 5 atm. This is equivalent to 0.017 L/day. The volume of the MHM is 1,170 L. One air exchange per day with the MHM would five a flow rate of 1,170 L/day. The rate of change in volume fraction of H_2 in the MHM can be describe with the following equation:

$$\frac{dx_{H2}(t)}{dt} = \frac{L_{MCO}}{V_{MHM}} - \frac{\left(L_{MCO} + L_{MHM}\right) x_{H2}}{V_{MHM}}$$

where

x_{H2} = volume fraction of hydrogen in the MHM
L_{MCO} = MCO leak rate
L_{MHM} = MHM inflow rate
V_{MHM} = MHM volume
t = time.

Use of a constant leak rate from the MCO overestimates the hydrogen concentration because it ignores the decrease in MCO pressure and the corresponding decrease in the leak rate.

$$x_{H2}(t) = \frac{H_2 L_{MCO}}{L_{MCO} L_{MHM}} \left(1 - \exp\left[\frac{\left(L_{MCO} + L_{MHM}\right) t}{V_{MHM}} \right] \right) .$$

where

H2 = volume fraction of hydrogen in MCO.

The maximum hydrogen concentration in the MHM is found at large times:

$$x_{H2}^{(\infty)} = \frac{H_2 L_{MCO}}{L_{MCO} + L_{MHM}} .$$

For a natural circulation rate of 100% per day and the maximum MCO leak rate of 0.017 L per day, the maximum H_2 concentration is

$$\frac{H_2 L_{MCO}}{L_{MCO} + L_{MHM}} = \frac{(0.67)\ (0.017\ L/day)}{(0.017\ L/day + 1{,}170\ L/day)} = 0.001\% .$$

Higher leak rates and lower natural circulation rates are needed to reach flammable concentrations in the MHM (see Table 5-7). It is assumed that the MHM is filled with air initially to provide the oxygen.

Table 5-7. Peak Hydrogen Concentrations for Various Multi-Canister Overpack Leak Rates and Multi-Canister Overpack Handling Machine Circulation Rates.

MHM natural circulation (L/day)	Peak hydrogen concentration (vol%)		
	MCO leak rate × 1,000 (17 L/day)	MCO leak rate × 3,000 (52 L/day)	MCO leak rate × 10,000 (173 L/day)
1,170	0.97%	2.8%	8.6%
351	3.1%	8.6%	22%
117	8.6%	20%	40%

MCO = multi-canister overpack.
MHM = multi-canister overpack handling machine.

Thirty hours after the start of the worst case in Table 5-7, the hydrogen concentration in the MHM would be about 10%. Thus, the mass of hydrogen present would be 9.6 g, which is equivalent to 274 g of TNT. Again, the damage from hydrogen is lower because of the greater volume affected and the slower rate of combustion. The adiabatic flame temperature is 1,370 K (1,100 °C), which leads to a maximum pressure of 436 kPa (48 lb/in² gauge).

A hydrogen deflagration in the MHM would cause transitory high pressures that would damage the MHM. Because the MCO would not be damaged, the only available source of radioactivity is the HEPA filter units on the MHM turret. These could fill with the hydrogen–air mixture and be affected by the deflagration. For personnel protection reasons, the pair would read less than 50 mR/h on contact. Thus, the worst-case explosion near them would have consequences no worse than the rupture of the containment tent exhauster during MCO venting. The potential for personnel injury exists because personnel normally are located near the MHM turret to operate the MHM.

5.3.4 Hydrogen Deflagration during Interim Storage

While an MCO is inside a storage tube at the CSB, an abnormal leakage rate could lead to flammable concentrations of hydrogen and air in the storage tube. The same equations derived to model the hydrogen accumulation in the MHM apply to the storage tube with the exception of differences in volume of the storage tube and ventilation rate. First, a storage tube containing a single, mechanically sealed MCO has a free volume of about 2,890 L. Second, the natural ventilation rate for the storage tube comes from the value for volumetric changes due to barometric pressure variations during the year. WHC-EP-0651, *Barometric Pressure Variations*, gives the following value for this rate.

$$dV_{air}/dt/V_{storage\ tube} = 1.69 \text{ per year} = 0.463\% \text{ per day}.$$

As with the MHM, it will be assumed that the storage tube is initially filled with air so that oxygen is present to react with the hydrogen leaking from the MCO. Because the ventilation rate is fixed, higher leak rates lead to higher peak concentrations of hydrogen in the storage tube. A summary of peak concentrations and times to reach those concentrations are shown in Table 5-8.

Table 5-8. Peak Storage Tube Concentrations for Various Multi-Canister Overpack Leak Rates.

MCO leakage rate (L/day)	Factor	Peak hydrogen concentration (%)
0.017	× 1	0.09
0.207	× 12	1.0
0.864	× 50	4.0

Note: The MCO leakage factor times 1 E-05 cm^3/s is the leak rate at reference conditions.

MCO = multi-canister overpack.

It can be seen from Table 5-8 that a leak rate 50 times greater than the maximum is required to reach a flammable mixture in the storage tube.

5.3.5 Hydrogen Deflagration during Multi-Canister Overpack Sampling

To determine the composition of gases in an MCO, selected MCOs are moved from the storage tubes to the sampling/weld station for analysis. A sampling hood is placed over the MCO. The hood is connected to the HEPA-filtered exhaust system, and the flow rate through the hood is between 47 L/s and 118 L/s. Gas is vented from the MCO via a sampling line attached to the

MCO. If this connection were to fail, hydrogen and helium in the MCO would be vented to the hood and the exhauster.

Higher flow rates will lead to greater hydrogen concentrations. The excess gas (air, hydrogen, and helium) is being forced out of the hood. Flow rates that are lower lead to lower hydrogen concentrations. The value chosen simply illustrates a flow rate that produces flammable mixtures in the hood.

$$\dot{Q}_{choke} = C_{dis} A P_{MCO} \sqrt{\frac{\gamma g M}{R T_{MCO}} \left(\frac{2}{\gamma + 1} \right)^{(\gamma+1)/(\gamma-1)}}$$

where

Q_{choke} = mass flow rate out the hole, in lbm/s

C_{dis} = discharge coefficient, which is assumed to be 1.0

A = cross-sectional area of the hole, in $in.^2$

g = conversion factor, 32.17 lbm-ft/s^2/lbf

M = average molecular weight of the escaping gas, 2.67 lbm/lb-mole

R = ideal gas constant, 1,545 ft-lbf/lb-mole/°R

T_{MCO} = absolute temperature of the gas in the MCO, 627 °R (75 °C)

P_{MCO} = absolute pressure of the gas in the MCO, 78 lbf/in^2

γ = the ratio of the heat capacities at constant pressure and volume for the hydrogen-helium mixture. For monatomic gases like helium, γ is 1.67; while for diatomic gases like hydrogen and air, γ is 1.40. The weighted average γ was computed for the hydrogen-helium mixture using the number of moles of each as the weighting factor, giving a value of 1.49.

Under the above conditions, the peak hydrogen concentration in the hood is 16.7%, which is reached in 27 seconds. The lower flammability limit (4% hydrogen) is reached in 2.0 seconds. Notice the time scale is now in seconds rather than days.

If the hydrogen concentration in the sampling hood were 10% at the time of the explosion, the hood would contain 4.9 g of hydrogen, which releases a thermal energy equivalent to 140 g of TNT. Again, the damage from hydrogen is lower because of the greater volume affected and the slower rate of combustion. The adiabatic flame temperature is 1,370 K, which leads to a

maximum pressure of 442 kPa (49 lb/in² gauge). Based on conservative assumptions, this pressure is high enough to damage the hood and injure any personnel nearby. The potential for personnel injury exists because personnel normally are located near the sampling hood during sampling operations.

To quantify the potential hazard to personnel, consider the effect of the explosion on the viewing window in front of the operator. Using the viewing window dimensions of 30 in. wide by 18 in. tall, the peak pressure increase of 49 lb/in² applies a force of 26,700 lb to the viewing window. Assuming the window is 0.5 in. thick and has a density of 1,100 kg/m³, then its mass is 4.87 kg (10.7 lb). The peak pressure is reached in 4.4 milliseconds using the method presented in Section 5.3.1.5. If no energy is lost to breaking the window free of its mounts, the speed of the window is 106 m/s (237 mi/h). If the hood window were to strike a nearby operator, the impact could possibly cause a fatality. If half the energy were needed to free the window, the speed would still be 71% of the maximum. Thus, there is a real possibility of serious injury or death from an explosion in the sampling hood.

In addition to personnel injury, the hydrogen explosion in the sampling hood may break the sample line, resulting in a rapid depressurizing of the MCO. Radioactive contamination in the MCO and sampling hood HEPA filter can be released to the environment. The primary sources of radioactivity are (1) the HEPA filter near the sampling hood, (2) the dry particulate matter suspended inside the MCO by the explosion, and (3) the entrained particulate matter resuspended and carried out with the gases leaving the MCO. Of these three, the third source is estimated to provide nearly all of the activity released. Estimates of the amounts released are provided in Section 5.4.

5.3.6 Method Used to Determine Source Term

The material at risk (MAR) (i.e., the particulate available for release) depends on the amount of particulate generated between the time the fuel is washed at the K Basins and the time of the accident. HNF-SD-SNF-TI-015 provides a bounding estimate of the MAR for any time during the 40-year life of the facility. HNF-SD-SNF-TI-015 identifies the safety basis or bounding value for the mass of particulate as 34.0 kg UO_2, which contains 30.0 kg of uranium. Because of the conservative methodology used to calculate the bounding value, 30 kg is considered representative of the 99th percentile. HNF-SD-SNF-TI-015 also identifies a design or nominal (50th percentile) value of 2.1 kg UO_2, which contains 1.85 kg of uranium.

In this accident, the MCO would blow down through the damaged sample line to relieve the pressure inside the MCO. However, such a blowdown scenario would feature films of particles rather than deep powder beds. In such a situation, there would still be gas flow through the bed during depressurization, but the local velocity is simply not sufficient for entrainment according to *Technical Report 11.6: Resuspension of Deposited Aerosols Following Primary System or Containment Failure* (IDCOR 1984). The pressurized powder venting source term is not applicable, and a source term based upon aerodynamic entrainment is used.

Based on the data reported in DOE-HDBK-3010-94, *Airborne Release Fractions/Rates and Respirable Fractions/Rates for Nonreactor Nuclear Facilities*, a bounding (95th percentile) airborne release rate (ARR) of 4×10^{-5} per hour and a respirable fraction (RF) of 1.0 were selected. The contents of the MCO are intact fuel elements tightly packed in fuel baskets and pieces of fuel elements housed in the scrap baskets. Particulate matter swept upward by streams of flowing gas within the MCO must take a tortuous path through the MCO and through the MCO shield plug to exit the MCO. For shielded powder, where the aerodynamic stresses are reduced by debris or exposure to static conditions, DOE-HDBK-3010-94 recommends an ARR of 4×10^{-6} per hour and an RF of 0.2 for powder under debris. These values were selected as nominal (50th percentile).

The pressurized release from the MCO following the external deflagration would flow mostly likely through a leak path with a flow area greater than or equal to the flow area through an MCO shield plug port. The duration of the blowdown depends on the flow area of the leak and the resultant pressure following the burn. The MCO depressurizes to atmospheric pressure in less than 1 minute, even for an MCO pressure of about 150 lb/in^2 gauge and a 0.25-in. hole. The MCO depressurizes in a much shorter time for lower pressures and larger leak paths. For the calculation of the source term, a nominal (50th percentile) value of 10 seconds and a bounding (95th percentile) time of 60 seconds were selected.

The material released by aerosol entrainment can be calculated using the methodology described in Chapter 1.0 and the bounding and nominal values identified above. The bounding (95th percentile) value for the material released by aerodynamic entrainment is 2×10^{-4} g, as shown in Table 5-9.

A blast and shock could suspend some of the particulate within the MCO. The powder at rest in the MCO could be ejected into the gas volume by the response of the underlying solid MCO and fuel substrate to the vibration and jolting induced by deflagration. According to DOE-HDBK-3010-94, the value of the airborne release fraction (ARF) under such circumstances should exceed the value of the ARF for aerodynamic suspension alone but be less than the value of the ARF for the free-fall of powder. The powder undergoing vibration shock is bounced into the gas while subject to the same gas velocities as those for aerodynamic entrainment. Based on the discussion in DOE-HDBK-3010-94, a bounding (95th percentile) ARF of 1×10^{-3} and an RF of 1.0 were chosen for the suspension of powder-like surface contamination by blast and shock vibration. A nominal (50th percentile) value of 1×10^{-4} was chosen for the ARF and a nominal (50th percentile) value of 0.2 was chosen for the RF based on the evaluation of the discussion in DOE-HDBK-3010-94.

Table 5-9. Aerodynamic Entrainment Source Term for the External Hydrogen Deflagration Accident.

	Nominal	Bounding	EF	Percentile	SNV	ln(EF)/SNV
MAR	1.85 kg	30 kg	16.22	99	2.326	1.198
ARR	4.00 E-06/h	4.00 E-05/h	10.00	95	1.645	1.400
Time	10 s	60 s	6.00	95	1.645	1.089
RF	0.20	1.00	5.00	95	1.645	0.978
M	4.1 E-06 g[a]	2.0 E-04 g[b]	48[c]	95	1.645	2.353

Note: The 1.645 is the standard normal variable corresponding to the 95% upper confidence limit. For the 99% upper confidence limit, the corresponding value is 2.326.

[a] $\text{Nominal}_{\text{overall}}\ M = \text{MAR}_{\text{nominal}} \times \text{ARR}_{\text{nominal}} \times \text{RF}_{\text{nominal}} \times \text{time}_{\text{nominal}}$.
[b] $\text{Bounding}_{\text{overall}}\ M = (\text{EF}_{\text{overall}})\ (\text{nominal}_{\text{overall}}\ M)$.

[c] $$\text{EF}_{\text{overall}} = \exp\left(\text{SNV}_{95\%}\left(\sum_i\left[\frac{\ln(\text{EF}_i)}{\text{SNV}_i}\right]^2\right)^{\frac{1}{2}}\right)$$

ARR = airborne release rate.
EF = error factor (i.e., bounding value divided by nominal value).
ln(EF) = natural log of EF.
M = mass of material released.
MAR = material at risk.
RF = respirable fraction.
SNV = standard normal variable.

As in the case of the gaseous release event, there is no clear dominating mechanism identified in this accident to provide the shock and impact to suspend particulate within the MCO. However, normal handling of the MCO by the MHM during transport from the storage tube to the sampling/weld station will produce some vibration and jostling of the fuel and suspend some material. For the purposes of this analysis, it is assumed that nominally 1% of the impact suspension concentration exists within the MCO at the start of sampling. Therefore a value of 1% is assumed for the 50th percentile. In addition, a value of 10% is assumed for the 95th percentile. The initial pressure in the MCO at the start of the blowdown determines the fraction of the suspended particulate that is released from the MCO. The range of MCO pressure for this scenario varies from a nominal (50th percentile) pressure of 2.0 atm to a maximum pressure of 6.0 atm, which is assumed to be the 95th percentile pressure. These pressures equate to a nominal (50th percentile) leak path factor (LPF) of 0.5 for the MCO and a 95th percentile LPF of 0.83.

The material released by shock impact can be calculated using the methodology described in Chapter 1.0 and the bounding and nominal values identified above. The bounding (95th percentile) value for the material released by shock impact is 2.7×10^{-2} g, as shown in Table 5-10.

Table 5-10. Initial Suspended Material Source Term for the External Deflagration Accident.

	Nominal	Bounding	EF	Percentile	SNV	ln(EF)/SNV
MAR	1.85 kg	30 kg	16.22	99	2.326	1.198
ARF	4.00 E-04	1.00 E-03	2.50	95	1.645	0.557
RF	0.20	1.00	5.00	95	1.645	0.978
Settling	1%	10%	10.00	95	1.645	1.400
LPF_{MCO}[a]	0.5	0.83	1.67	95	1.645	0.311
M	7.4 E-04 g[b]	2.7 E-02 g[c]	36[d]	95	1.645	2.181

Note: The 1.645 is the standard normal variable corresponding to the 95% upper confidence limit. For the 99% upper confidence limit, the corresponding value is 2.326.

[a] LPF_{MCO} = (MCO pressure - 1 atm) / (MCO pressure). At a nominal MCO pressure of 2.0 atm, the LPF_{MCO} is 0.5, and at a bounding MCO pressure of 6.0 atm, the LPF_{MCO} is 0.83.

[b] $\text{Nominal}_{\text{overall}}\ M = MAR_{\text{nominal}} \times ARF_{\text{nominal}} \times RF_{\text{nominal}} \times \text{settling} \times LPF_{MCO}$.

[c] $\text{Bounding}_{\text{overall}}\ M = (EF_{\text{overall}})\ (\text{nominal}_{\text{overall}}\ M)$.

[d] $$EF_{\text{overall}} = \exp\left(SNV_{95\%}\left(\sum_i\left[\frac{\ln(EF_i)}{SNV_i}\right]^2\right)^{\frac{1}{2}}\right)$$

ARF = airborne release fraction.
EF = error factor (i.e., bounding value divided by nominal value).
ln(EF) = natural log of EF.
LPF = leak path factor.
M = mass of material released.
MAR = material at risk.
MCO = multi-canister overpack.
RF = respirable fraction.
SNV = standard normal variable.

The external hydrogen deflagration also has the potential to damage the HEPA filters in the sample line and sampling hood exhaust system. For the HEPA filter blasts, the bounding release fraction is 0.01 with an RF of 1.0 (DOE-HDBK-3010-94, Section 5.2.2.2). The canister HEPA filter attached to the sampling hood is assumed to be bounded by 20 g of fuel (see Appendix 5B).

The amount of fuel released from the HEPA filter by the blast of the hydrogen deflagration is 0.2 g.

The bounding (95th percentile) source term for the external hydrogen deflagration is 0.23 g, which is the sum of 2.0×10^{-2} g from vibration and shock and 2.0×10^{-4} g from aerodynamic entrainment, plus an additional 0.2 g from the damage to the HEPA filter.

5.4 CONSEQUENCE ANALYSIS

The downwind doses for each accident are computed in the following subsections. During cask venting, the containment tent HEPA filter is ruptured and releases a portion of its activity into the air. A hydrogen explosion in a storage tube or in the MHM is not expected to produce meaningful offsite consequences because there is no radioactive contamination nearby. The hydrogen explosion in the sampling hood leads to much larger releases due to the depressurization of the MCO.

5.4.1 Consequences of Hydrogen Deflagration Caused by Drop from Transportation Trailer

As noted in the source term analysis in Section 5.3.2, the 290 lb/in^2 gauge combustion pressure exceeds the 150 lb/in^2 gauge design pressure of the cask but the combustion pressure is not expected to damage the cask (SNF-5679). Thus, there are no radioactive emissions from the cask.

5.4.2 Consequences of a Hydrogen Deflagration during Multi-Canister Overpack Handling

High pressures caused by a hydrogen deflagration in the MHM could damage the MHM. No environmental releases of radioactivity from the MCO are expected because the MCO would not be damaged. The only other sources of radioactivity are the HEPA filter units on the MHM turret. These filter units could fill with hydrogen–air mixture and be part of the deflagration. For personnel protection reasons, each filter would be expected to read less than 50 mR/h on contact. The onsite and offsite dose guidelines would not be exceeded. The potential for personnel injury exists because personnel will be located near the MHM turret to operate it. Therefore, safety-significant features may be required to mitigate this accident.

5.4.3 Consequences of a Hydrogen Deflagration during Interim Storage

The worst-case event in the storage tubes is when a tube containing a single MCO develops an explosive mixture of hydrogen and air. If this mixture were to detonate, it could seriously damage the storage tube and possibly lead to a misalignment that would prevent future removal of

the MCO by normal means. Any environmental release of radioactivity due to resuspension of surface contamination would be very small and would lead to onsite and offsite doses well below the guidelines for anticipated events.

5.4.4 Consequences of a Hydrogen Deflagration during Multi-Canister Overpack Sampling

High pressures caused by a hydrogen deflagration in the sampling hood could damage the sampling hood. A release of radioactivity from the MCO is expected because the sample line could also be damaged and allow the MCO to rapidly release its gaseous contents. Some particulate matter contained in the MCO could be resuspended by the explosion and entrained in the exiting gases.

The dose calculation equation and data from Section 3.4.1 of HNF-3553 are used to calculate the dose to the onsite receptor.

$$D_{onsite} = (M_{MCO} + M_{HEPA}) \times \frac{\chi}{Q'} \times BR \times UD \times LPF_{building}$$

$$= (0.23 \text{ g U})(1.14 \times 10^{-2} \text{ s/m}^3)(3.33 \times 10^{-4} \text{ m}^3/\text{s})(4.38 \times 10^5 \text{ rem/g U})(1.0)$$

$$= 0.38 \text{ rem } (3.8 \times 10^{-3} \text{ Sv}) .$$

where

D_{onsite}	= committed effective dose equivalent (rem)
M	= mass of respirable airborne material released (g U)
χ/Q'	= time-integrated atmospheric transport factor (s/m^3)
BR	= breathing rate (m^3/s)
UD	= dose per unit mass of radioactive material (rem/g U)
$LPF_{building}$	= leak path factor from building.

The dose consequences at the remaining receptor sites are calculated in the same manner and are shown in Table 5-11.

Table 5-11. Dose Calculation Summary for a Hydrogen Deflagration in the Sampling Hood.

Receptor location (*distance, direction*)	Duration (hours)	Unmitigated dose[a] rem (Sv)	Evaluation guideline[b]/ release limits rem (Sv) anticipated[c]	Mitigated dose rem (Sv)
Onsite (with building effects) (100 m E)	<1	0.38 (3.8 E-03)	1.0 (1.0 E-02)	--
Highway 240[d] (9,280 m W)	<1	7.8 E-04 (7.8 E-06)	--	--
Hanford Site boundary (17,390 m E)	<1	4.3 E-04 (4.3 E-06)	0.5 (5.0 E-03)	--

[a]Fifty-year committed effective dose equivalent.
[b]Evaluation guideline for onsite (100 m) receptor only.
[c]Unmitigated frequency for this event is anticipated (>0.01 to ≤0.1 per year).
[d]Provided for information only.

5.5 REFERENCES

DOE-HDBK-3010-94, 1994, *Airborne Release Fractions/Rates and Respirable Fractions/Rates for Nonreactor Nuclear Facilities*, U.S. Department of Energy, Washington, D.C.

HNF-1523, 1997, *K-Basins Particulate Water Content, Behavior, and Impact*, Rev. 0, Fluor Daniel Hanford, Incorporated, Richland, Washington.

HNF-2155, 1998, *Multi-Canister Overpack Combustible Gas Management Leak Test Acceptance Criteria*, Rev. 0, Fluor Daniel Hanford, Incorporated, Richland, Washington.

HNF-3553, 2000, *Spent Nuclear Fuel Project Final Safety Analysis Report*, Rev. 0, Fluor Hanford, Richland, Washington.

HNF-SD-SNF-HIE-001, 2000, *Canister Storage Building Hazard Analysis Report*, Rev. 3, Fluor Hanford, Incorporated, Richland, Washington.

HNF-SD-SNF-SARR-005, 1999, *Multi-Canister Overpack Topical Report*, Rev. 1, Flour Daniel Hanford, Incorporated, Richland, Washington.

HNF-SD-SNF-TI-015, 1998, *Spent Nuclear Fuel Project Technical Databook*, Rev. 6, Fluor Daniel Hanford, Incorporated, Richland, Washington.

HNF-SD-TP-SARP-017, 1998, *Safety Analysis Report for Packaging (Onsite) Multicanister Overpack Cask*, Rev. 1, Fluor Daniel Hanford, Incorporated, Richland, Washington.

IDCOR, 1984, *Technical Report 11.6: Resuspension of Deposited Aerosols Following Primary System or Containment Failure*, Fauske & Associates, Incorporated, Burr Ridge, Illinois.

NUREG/CR-2726, 1983, *Light Water Reactor Hydrogen Manual*, Sandia National Laboratories, Albuquerque, New Mexico.

SFPE, 1992, *SFPE Handbook of Fire Protection Engineering*, Society of Fire Protection Engineers, Boston, Massachusetts.

SNF-2770, 1999, *Cold Vacuum Drying Facility Design Basis Accident Analysis Documentation*, Rev. 3, Fluor Daniel Hanford, Incorporated, Richland, Washington.

SNF-4042, 2000, *Evaluation of Accident Frequencies at the Canister Storage Building*, Rev. 2, Fluor Hanford, Richland, Washington.

SNF-5679, 2000, *Maximum Pressure Load Determination for Multi-Canister Overpack Cask (WMTS-ECAL-010)*, Rev. 0, Fluor Hanford, Incorporated, Richland, Washington.

WHC-EP-0651, 1993, *Barometric Pressure Variations*, Westinghouse Hanford Company, Richland, Washington.

Whitwell, J. C., and R. K. Toner, 1969, *Conservation of Mass and Energy*, Blaisdell Publishing Company, Waltham, Massachusetts.

This page intentionally left blank.

APPENDIX 5A

CALCULATION OF ADIABATIC COMBUSTION PRESSURE

This page intentionally left blank.

APPENDIX 5A

CALCULATION OF ADIABATIC COMBUSTION PRESSURE

This appendix describes the calculation of adiabatic combustion pressure. First the temperature rise of the final mixture is estimated by calculating the heat energy absorbed by each component of the gas mixture as it heats from the initial temperature to some undetermined final temperature. The method for performing this calculation is given in Section 5.3.1.5. Since the increase of heat capacity with temperature is represented by a quadratic formula, the integral of the heat capacity can be solved for each gas. This is shown below.

$$H_X = [A_X \cdot (Tf - To) + B_X \cdot (Tf^2 - To^2)/2 + C_X \cdot (Tf^3 - To^3)/3] \cdot N_X$$

where

H_X = heat energy added to a gas in the post-combustion mixture, cal
A_X, B_X, C_X = quadratic constants for each gas from Table 5-2
To = initial gas temperature (before combustion), 303.15 K
Tf = final gas temperature (after combustion), 1,859 K
N_X = number of moles of a gas in the post-combustion mixture.

The heat energies added to each component of the final gas mixture are summed for comparison with the total heat energy released by the combustion reaction (97,600 cal). The determination of final gas temperature (Tf) is carried out by successive iterations until a final temperature is determined at which the energy liberated by combustion matches the energy absorbed by the gas. Three iterations of Tf assumptions are shown in Table 5A-1. The third case can be considered the solution.

Table 5A-1. Final Temperature in the Plume.

Gas	Stored heat energy (cal) for various final gas temperatures (Tf)		
	Tf= 1,800 K	Tf= 1,900 K	Tf= 1,859 K
H_2	0.0	0.0	0.0
He	26,015	27,753	27,041
H_2O	20,533	22,283	21,560
N_2	42,405	45,705	44,345
O_2	4,203	4,501	4,379
Ar	262	280	273
Total:	93,418	100,522	97,598

An illustration of how the absorbed energy is calculated for one gas (nitrogen) is shown below. The final gas temperature shown is the solution found by iteration.

$$H_{helium} = [(3.020)(1859 - 303.15) + (0.0)(1859^2 - 303.15^2)/2 + (0.0)(1859^3 - 303.15^3)/3](5.755 \text{ gmole})$$

$$= [(4{,}698.7) + (0.0) + (0.0)](5.755) = 27{,}041 \text{ cal}.$$

$$H_{water} = [(5.149)(1859 - 303.15) + (0.00264)(1859^2 - 303.15^2)/2 + (4.59\ E\text{-}08)(1859^3 - 303.15^3)/3](1.718 \text{ gmole})$$

$$= [(8{,}011.1) + (4{,}440.5) + (97.9)](1.718)$$

$$= (12{,}549.5)(1.718) = 21{,}560 \text{ cal}.$$

$$H_{nitrogen} = [(4.470)(1859 - 303.15) + (0.00139)(1859^2 - 303.15^2)/2 + (-6.90\ E\text{-}08)(1859^3 - 303.15^3)/3](4.849 \text{ gmole})$$

$$= [(6{,}954.3) + (2{,}338.0) + (-147.1)](4.849)$$

$$= (9{,}145.2)(4.849) = 44{,}345 \text{ cal}.$$

$$H_{oxygen} = [(4.130)(1859 - 303.15) + (0.00317)(1859^2 - 303.15^2)/2 + (-1.01\ E\text{-}06)(1859^3 - 303.15^3)/3](0.456\ gmole)$$

$$= [(6,425.7) + (5,331.9) + (-2,153.5)](0.456)$$

$$= (9,604.1)(0.456) = 4,379\ cal\ .$$

$$H_{argon} = [(3.020)(1859 - 303.15) + (0.0)(1859^2 - 303.15^2)/2 + (0.0)(1859^3 - 303.15^3)/3](0.058\ gmole)$$

$$= [(4,698.7) + (0.0) + (0.0)](0.058) = 273\ cal\ .$$

The total energy absorbed by the post-combustion gas mixture is the sum of the values shown above, namely, 97,598 cal. This is very close to the calculated energy release of 97,600 cal.

Note that the quadratic approximation for heat capacity is valid up to 1,500 K, but the final temperature is somewhat greater, 1,859 K. The extrapolation is still accurate because the mixture includes both overestimates and underestimates of energy absorbed, which tend to cancel out the departures from the true heat capacities. Hence, the final temperature of the post-combustion gas mixture is 1,859 K.

Using the ideal gas law, the final pressure of the gas mixture is calculated to be 177 lb/in^2 gauge (13.05 atm) as shown below.

$$Pf = (12.835\ gmoles)(0.082058\ L{\cdot}atm/gmole/K)(1859\ K)/(150\ L)$$
$$= 13.05\ atm\ .$$

This page intentionally left blank.

APPENDIX 5B

ISO-PC OUTPUT TO ESTIMATE HIGH-EFFICIENCY PARTICULATE AIR FILTER LOADING

This page intentionally left blank.

APPENDIX 5B

ISO-PC OUTPUT TO ESTIMATE HIGH-EFFICIENCY PARTICULATE AIR FILTER LOADING

Two high-efficiency particulate air (HEPA) filter units are of interest. The first is located on the portable exhauster. It is a 2-ft by 2-ft by 12-in.-thick HEPA filter. The second is located on the sampling/weld system hood. It is a cylinder 6 in. in diameter and 12 in. tall.

The dose rates near the filters were estimated using the safety/regulatory basis spent fuel composition from HNF-SD-SNF-TI-015, *Spent Nuclear Fuel Technical Databook*, and ISO-PC software Version 1.6. While this is not the current version of ISO-PC, WHC-SD-SQA-CSWD-303, *Validation of ISOSHLD-II*, documents the verification and validation tests that were completed. The program revisions since then have little effect on the computed dose rates for this geometry and shield thicknesses.

As input to the ISO-PC program, it was assumed that the portable HEPA filter held a total of 1.4 g of spent nuclear fuel (SNF). The filter medium was homogenized throughout its volume at a density of 0.16 g/cm^3, corresponding to a 2-ft by 2-ft by 12-in. filter weight of 18.1 kg (40 lb). Concrete was used to represent the medium. The second filter was modeled using the same material except the geometry was a cylinder with a radius of 3 in. and a height of 12 in. It was assumed to hold a total of 0.28 g SNF. The dose points for both filters were 2 in. to the side of the HEPA filter, corresponding to a likely dose rate measurement point for weekly surveys by radiation protection technicians. Dose rates are measured with an ion chamber instrument that reads out in units of milli-roentgen per hour (mR/h). Hence the calculated values are in milli-roentgen per hour also.

The ISO-PC result for both HEPA filters is 51 mR/h. The actual ISO-PC output file is listed at the end of this appendix. A major assumption regarding filter loading has been that the relative amounts of gamma-emitting and alpha-emitting nuclides are the same on the filters as they are in the fuel. Note that the gamma-emitting nuclides (e.g., ^{137}Cs) give essentially all of the measurable dose rate on the filters while the alpha-emitting nuclides (e.g., ^{241}Am) give essentially all of the internal dose when released into the environment. However, radioactive decay decreases the amount of cesium faster than the amount of alpha-emitters. In addition, it may be that the cesium dissolves more readily in water than the alpha emitters. Based on measured sludge compositions in the K Basins as well as various fuel compositions shown in HNF-SD-SNF-TI-009, *105-K Basin Material Design Basis Feed Description for Spent Nuclear Fuel Project Facilities*, Volume 1, "Fuel," and Volume 2, "Sludge," it is concluded that a factor of 10 will bound the observed cesium depletion factors (HNF-1777, Appendix B). Therefore, HEPA filter loadings will increase the ISO-PC value by a factor of 10.

In summary, the first HEPA filter must contain 14 g of SNF to read 50 mR/h, while the second HEPA filter must contain 2.8 g of SNF to read 50 mR/h.

```
Start run at  07:21:59  10/26/99

 ISOSHLD-PC    (RIBD removed)
 Version 1.6,  December 1989
 for IBM & Compatible Personal Computers
 Nuclear Safety & Radiological Analysis
 Westinghouse Hanford Company
 Richland, WA  99352
```

CSB Small HEPA Filters with SNF Fuel (Safety Source)

Table of Source Activity:

Scale Factor = 1.400E-06

Isotope Name	Initial Values	Final Curies
SR- 90	6.93E+03	9.702E-03
Y - 90	6.93E+03	9.702E-03
CD-113M	2.78E+00	3.892E-06
CS-134	6.47E+00	9.058E-06
CS-137	9.66E+03	1.352E-02
BA-137M	9.14E+03	1.280E-02
PM-147	1.09E+02	1.526E-04
SM-151	1.02E+02	1.428E-04
EU-154	1.13E+02	1.582E-04
EU-155	1.06E+01	1.484E-05
CO- 60	2.09E+00	2.926E-06

Shield Composition, g/cc

	Shield 1	Shield 2	Shield 3	Shield 4	Shield 5
ORDCONC	1.600E-01	0.000E+00	0.000E+00		
AIR	0.000E+00	1.200E-03	0.000E+00		
IRON	0.000E+00	0.000E+00	7.860E+00		

Group	Linear Attenuation Coefficients (last region is air)					
1	3.445E+00	4.106E-03	3.471E+02	4.424E-03	0.000E+00	0.000E+00
2	5.610E-01	6.072E-04	9.650E+01	6.542E-04	0.000E+00	0.000E+00
3	1.559E-01	3.252E-04	4.468E+01	3.504E-04	0.000E+00	0.000E+00
4	1.080E-01	2.520E-04	2.071E+01	2.715E-04	0.000E+00	0.000E+00
5	6.952E-02	2.232E-04	1.144E+01	2.405E-04	0.000E+00	0.000E+00
6	5.304E-02	2.086E-04	7.632E+00	2.247E-04	0.000E+00	0.000E+00
7	4.325E-02	1.984E-04	5.447E+00	2.137E-04	0.000E+00	0.000E+00
8	3.648E-02	1.902E-04	3.948E+00	2.049E-04	0.000E+00	0.000E+00

9	3.274E-02	1.842E-04	3.135E+00	1.985E-04	0.000E+00	0.000E+00
10	2.848E-02	1.601E-04	1.603E+00	1.725E-04	0.000E+00	0.000E+00
11	2.048E-02	1.368E-04	1.077E+00	1.474E-04	0.000E+00	0.000E+00
12	1.584E-02	1.218E-04	7.844E-01	1.312E-04	0.000E+00	0.000E+00
13	1.424E-02	1.098E-04	6.877E-01	1.183E-04	0.000E+00	0.000E+00
14	1.376E-02	1.038E-04	5.659E-01	1.118E-04	0.000E+00	0.000E+00
15	1.200E-02	8.340E-05	5.007E-01	8.986E-05	0.000E+00	0.000E+00
16	1.019E-02	7.620E-05	4.622E-01	8.210E-05	0.000E+00	0.000E+00
17	9.760E-03	6.876E-05	4.032E-01	7.408E-05	0.000E+00	0.000E+00
18	8.800E-03	6.180E-05	3.694E-01	6.658E-05	0.000E+00	0.000E+00
19	8.320E-03	5.736E-05	3.506E-01	6.180E-05	0.000E+00	0.000E+00
20	7.360E-03	5.400E-05	3.262E-01	5.818E-05	0.000E+00	0.000E+00
21	7.040E-03	5.100E-05	3.160E-01	5.495E-05	0.000E+00	0.000E+00
22	6.880E-03	4.884E-05	2.995E-01	5.262E-05	0.000E+00	0.000E+00
23	6.560E-03	4.644E-05	2.971E-01	5.004E-05	0.000E+00	0.000E+00
24	6.320E-03	4.440E-05	2.877E-01	4.784E-05	0.000E+00	0.000E+00
25	5.808E-03	4.068E-05	2.790E-01	4.383E-05	0.000E+00	0.000E+00

2'x 2' HEPA: 2" to the side

Source Shields Distance to Detector, X = 6.872E+01 cm
Slab Slab Volume = 1.116E+05 cc
Thickness = 6.100E+01 cm Height = 6.100E+01 cm Width = 3.000E+01 cm
Integration Specs: NTHETA = 19 NPSI = 27 DELR = 2.033E+00 cm
Total Intervals: 1.539E+04

Shield Thickness, cm 6.100E+01 2.540E+00 1.000E-01
Taylor Buildup Data for Shield 2 with Effective Atomic Number 7.0

Source Scale Factor was 1.400E-06

Group	Average Energy, Mev	Bremsstr. photons/sec	Source Total photons/sec	Energy Flux Mev/sq.cm/sec	Dose Rate R/hr
1	1.500E-02	1.262E+07	1.273E+07	3.486E-15	2.869E-19
2	2.500E-02	7.121E+06	7.270E+06	7.802E-04	1.350E-08
3	3.500E-02	4.237E+06	3.872E+07	1.951E+00	1.239E-05
4	4.500E-02	2.872E+06	2.977E+06	2.061E+00	6.761E-06
5	5.500E-02	2.073E+06	2.073E+06	4.674E+00	1.070E-05
6	6.500E-02	1.738E+06	1.747E+06	6.364E+00	1.203E-05
7	7.500E-02	1.555E+06	1.555E+06	7.087E+00	1.215E-05
8	8.500E-02	1.384E+06	1.560E+06	7.812E+00	1.263E-05
9	9.500E-02	1.231E+06	1.231E+06	6.683E+00	1.071E-05
10	1.500E-01	5.546E+06	7.880E+06	1.193E+02	2.062E-04
11	2.500E-01	1.809E+06	2.219E+06	5.609E+01	1.099E-04
12	3.500E-01	8.788E+05	8.788E+05	3.046E+01	6.276E-05
13	4.750E-01	6.557E+05	6.957E+05	3.234E+01	6.597E-05
14	6.500E-01	3.887E+05	4.285E+08	2.374E+04	4.938E-02
15	8.250E-01	1.435E+05	1.413E+06	9.023E+01	1.805E-04
16	1.000E+00	9.664E+04	1.894E+06	1.421E+02	2.743E-04
17	1.225E+00	4.916E+04	2.502E+06	2.250E+02	4.140E-04
18	1.475E+00	1.610E+04	6.726E+04	7.153E+00	1.259E-05
19	1.700E+00	3.675E+03	1.177E+05	1.453E+01	2.485E-05
20	1.900E+00	7.691E+02	7.691E+02	1.055E-01	1.751E-07

21	2.100E+00	4.474E+01	5.473E+02	8.235E-02	1.318E-07
22	2.300E+00	0.000E+00	0.000E+00	0.000E+00	0.000E+00
23	2.500E+00	0.000E+00	0.000E+00	0.000E+00	0.000E+00
24	2.700E+00	0.000E+00	0.000E+00	0.000E+00	0.000E+00
25	3.000E+00	0.000E+00	0.000E+00	0.000E+00	0.000E+00
TOTALS		4.442E+07	5.160E+08	2.449E+04	5.081E-02

Note that 5.081E-02 R/hr = 3.641E-09 amp/kg

Sample/Weld Hood HEPA: 2" to the side

Source Shields Distance to Detector, X = 1.320E+01 cm
Cylindrical Cylindrical Volume = 5.301E+03 cc
Source Length = 3.000E+01 cm Distance Along Cylinder, Y = 1.500E+01 cm
Integration Specs: NTHETA = 19 NPSI = 27 DELR = 5.000E-01 cm
Total Intervals: 7.695E+03

Shield Thickness, cm 7.500E+00 5.000E-01 1.000E-01
Taylor Buildup Data for Shield 2 with Effective Atomic Number 7.0

Source Scale Factor was 2.800E-07

Group	Average Energy, Mev	Bremsstr. photons/sec	Source Total photons/sec	Energy Flux Mev/sq.cm/sec	Dose Rate R/hr
1	1.500E-02	2.523E+06	2.546E+06	3.735E-15	3.074E-19
2	2.500E-02	1.424E+06	1.454E+06	1.893E-03	3.275E-08
3	3.500E-02	8.474E+05	7.745E+06	3.840E+00	2.438E-05
4	4.500E-02	5.744E+05	5.955E+05	3.513E+00	1.152E-05
5	5.500E-02	4.146E+05	4.146E+05	6.360E+00	1.457E-05
6	6.500E-02	3.476E+05	3.493E+05	7.422E+00	1.404E-05
7	7.500E-02	3.109E+05	3.109E+05	6.771E+00	1.160E-05
8	8.500E-02	2.769E+05	3.120E+05	5.613E+00	9.077E-06
9	9.500E-02	2.463E+05	2.463E+05	4.708E+00	7.546E-06
10	1.500E-01	1.109E+06	1.576E+06	1.248E+02	2.156E-04
11	2.500E-01	3.619E+05	4.438E+05	5.559E+01	1.090E-04
12	3.500E-01	1.758E+05	1.758E+05	2.947E+01	6.071E-05
13	4.750E-01	1.311E+05	1.391E+05	3.109E+01	6.342E-05
14	6.500E-01	7.774E+04	8.570E+07	2.365E+04	4.919E-02
15	8.250E-01	2.871E+04	2.826E+05	9.253E+01	1.851E-04
16	1.000E+00	1.933E+04	3.788E+05	1.469E+02	2.836E-04
17	1.225E+00	9.832E+03	5.005E+05	2.343E+02	4.312E-04
18	1.475E+00	3.220E+03	1.345E+04	7.492E+00	1.319E-05
19	1.700E+00	7.351E+02	2.355E+04	1.516E+01	2.593E-05
20	1.900E+00	1.538E+02	1.538E+02	1.102E-01	1.829E-07
21	2.100E+00	8.948E+00	1.095E+02	8.624E-02	1.380E-07
22	2.300E+00	0.000E+00	0.000E+00	0.000E+00	0.000E+00
23	2.500E+00	0.000E+00	0.000E+00	0.000E+00	0.000E+00
24	2.700E+00	0.000E+00	0.000E+00	0.000E+00	0.000E+00
25	3.000E+00	0.000E+00	0.000E+00	0.000E+00	0.000E+00
TOTALS		8.883E+06	1.032E+08	2.442E+04	5.067E-02

Note that 5.067E-02 R/hr = 3.631E-09 amp/kg

```
***>  This is the end of the small HEPA Cases !!


 Finish run at  07:22:09  10/26/99

 Contents of Input file, HEPA-CSB

0         2  CSB Small HEPA Filters with SNF Fuel (Safety Source)
2'x 2' HEPA:  2" to the side
 &Input  IGeom= 10,  SLTH= 30,  Y= 61,  T= 61,2.54,0.1,  X= 68.72,
  NShld= 3,  JBuf= 2,  NTheta= 19,  NPsi= 27,  DelR= 2.0,
  SFact= 1.4E-6,  Weight(472)= 2.09,  Next= 1,
  Weight(82)= 6930,0,6930,  Weight(206)= 2.78,
  Weight(319)= 6.47,  Weight(335)= 9660, 9140,
  Weight(388)= 109,   Weight(403)= 102,
  Weight(415)= 113,   Weight(418)= 10.6  &
  HEPA  16   0.16
  air    3          0.0012
1 duct   9                        7.86
Sample/Weld Hood HEPA:  2" to the side
 &Input  Next= 4,  IGeom= 7,  SLTH= 30,  Y= 15,
  SFact= 2.8E-7,  DelR= 0.5,  T= 7.5,0.5,  X= 13.2  &
This is the end of the small HEPA Cases !!
 &Input Next= 6  &

Note:  There is an air gap between the filter and the housing.
       The source activities are for one metric ton uranium (1E6 gU).
```

REFERENCES

HNF-1777, 1999, *K West Basin Integrated Water Treatment System Annular Filter Vessel Accident Calculations*, Rev. 4, Fluor Daniel, Incorporated, Richland, Washington.

HNF-SD-SNF-TI-009, 1998, *105-K Basin Material Design Basis Feed Description for Spent Nuclear Fuel Project Facilities*, Volume 1, "Fuel," and Volume 2, "Sludge," Rev. 2, Fluor Daniel Hanford, Incorporated, Richland, Washington.

HNF-SD-SNF-TI-015, 1998, *Spent Nuclear Fuel Technical Databook*, Rev. 6, Fluor Daniel Hanford, Incorporated, Richland, Washington.

WHC-SD-SQA-CSWD-303, 1989, *Validation of ISOSHLD-II*, Rev. 0, Westinghouse Hanford Company, Richland, Washington.

6.0 CALCULATIONS FOR THERMAL RUNAWAY REACTIONS INSIDE THE MULTI-CANISTER OVERPACK

6.1 PURPOSE AND OBJECTIVES

A thermal runaway reaction is only possible at the Canister Storage Building (CSB) if fuel temperatures are extremely high in combination with excessive water or oxygen available in the multi-canister overpack (MCO). Chemical reaction rates increase and produce more gases and heat as fuel temperatures increase. Pressure inside the MCO increases as a result. If pressure inside the MCO continues to increase to the point that the MCO pressure boundary is challenged, then the MCO could fail and release radioactive particulate and hydrogen gas into the surrounding environment.

The deterministic calculations summarized in this chapter demonstrate that a thermal runaway fuel reaction accident is not physically possible at the CSB if the MCOs satisfy dryness tests (<200 g of water) at the Cold Vacuum Drying Facility (CVDF) and if the aluminum hydroxide thermal decomposition data, based on an initial quantity of 9.47 kg provided in HNF-SD-SNF-TI-015, *Spent Nuclear Fuel Project Technical Databook*, for a two-scrap basket MCO, and decomposition rate of the aluminum hydroxide (Figure 6-1) remain valid and representative. Because these results indicate that high fuel temperatures (i.e., thermal runaway) do not occur, no detailed accident scenarios were documented. The bounding conditions used in this analysis are described. For these conditions, a thermal runaway event was determined not to occur at the CSB. It should be noted that with extreme ambient temperatures (MCO wall temperatures >115 °C) and complete shear of an MCO allowing large quantities of air as an oxidant, high fuel temperatures could occur in the upper MCO scrap basket.

6.2 SCENARIO DEVELOPMENT

There are two primary chemical reactions in an MCO at the CSB: (1) the reaction of water with uranium and uranium hydride (UH_3), and (2) the reaction of oxygen with uranium and uranium hydride.

There are two bounding scenarios involving the reaction of water with uranium and uranium hydride. The first scenario (Case 1) assumes all free water, including moisture in the MCO atmosphere, is available for reaction. The second scenario (Case 2) includes all free water plus the amount of water that is thermally freed from the aluminum hydroxide and therefore bounds the first scenario (Case 1). The analyses of Cases 1 and 2 are described in Section 6.2.1. No thermal runaways result in either case.

There are also two bounding scenarios involving the reaction of oxygen with uranium and uranium hydride. In the first scenario (Case 3), an MCO is accidentally injected with oxygen, and in the second scenario (Case 4), an MCO sustains a complete shear while at a high temperature (MCO wall temperatures equal to 115 °C). The analyses of Cases 3 and 4 are described in

Section 6.2.2. All oxygen scenarios are bounded by Case 4 with one exception. The exception is the extreme case of a completely sheared MCO with wall temperatures greater than 115 °C and the air temperature greater than 102 °C, which is discussed as a beyond design basis evaluation (Section 6.2.2.3). Case 3 describes an accident that is initiated when the MCO is accidentally filled with oxygen at the sampling/weld station. The MCO was determined not to overpressurize at bounding MCO temperatures. Because releases do not occur, offsite release limits and onsite evaluation guidelines are satisfied. The unmitigated scenario is brought to a stable state by ongoing MCO inerting and/or cooling at the sampling/weld station and the natural consumption of the oxygen. Case 4 evaluates the impact of a hypothetical complete shear of an MCO to initiate a thermal runaway reaction. However, Case 4 does not result in a thermal runaway, even though there is an unlimited supply of air to support the reaction.

6.2.1 Thermal Runaway Reaction from Water Reacting with Uranium and Hydride

In the following subsections, the chemical reactions from water are briefly described, the amount of water required to breach the MCO (depending on gas temperature and gas reaction) is estimated, and the amount of water available in an MCO for chemical reactions is detailed. Values show that there is not enough water to pressurize an MCO beyond its capable limits.

6.2.1.1 Chemical Reactions with Water. Depending on temperature and steam pressure, water (liquid or vapor) will react with uranium and form uranium dioxide particulate and hydrogen gas, liberating heat during the reaction:

$$U + 2 \cdot H_2O \rightarrow UO_2 + 2 \cdot H_2 + \text{heat}.$$

Water will also react with uranium hydride (UH_3) to form uranium dioxide and hydrogen, liberating heat during the reaction:

$$UH_3 + 2H_2O \rightarrow UO_2 + 3.5H_2 + \text{heat}.$$

6.2.1.2 Water Mass Required to Reach the Multi-Canister Overpack Pressure Rated Design Limit. According to HNF-SD-SNF-DR-003, *Multi-Canister Overpack Design Report*, the rated design pressure of an MCO before the cover cap is welded in place is 150 lb/in^2 (11.2 atm absolute). According to HNF-SD-SNF-SARR-005, *Multi-Canister Overpack Topical Report*, this rated pressure has a large margin to failure (i.e., no leakage is expected for even larger pressures) and is stable to internal loading of 340 lb/in^2 gauge. The design pressure of the mechanically sealed MCO is 450 lb/in^2 (31.6 atm absolute) after the cover cap is welded onto the MCO at the CSB sampling/weld station. According to HNF-3312, *MCO Monitoring Activity Description*, and HNF-3354, *MCO Monitoring Issue Closure Package*, six MCOs will be monitored and sampled and not have their cover caps welded. The MCOs reserved for sampling have significant time to pressurize before the MCO cover cap is welded in place, and all of the other MCOs have less time to pressurize.

According to SNF-2356, *Spent Nuclear Fuel Project Cold Vacuum Drying Facility Operations Manual*, each MCO is pressurized to approximately 1.5 atm with helium before leaving the CVDF. The average temperature of this helium is conservatively assumed to be 25 °C because the MCO wall temperature is cooled to 25 °C at the CVDF before the MCO is shipped to the CSB. Using the ideal gas law, the initial helium inventory in an MCO is estimated to be about 33 gmoles:

$$N_{He} = (P)(V)/(R)/(T)$$

where

N_{he} = number of gram-moles of helium in the MCO
P = helium pressure inside the MCO, 1.5 atm
V = gas volume of the MCO, 538 L
R = ideal gas law constant, 0.082057 L·atm/mole/K
T = temperature of the gas inside the MCO, 25 °C.

The number of moles of gas required to increase the MCO pressure (before the MCO and cover cap are welded together) to 11.2 atm (150 lb/in^2 gauge) and 31.6 atm (450 lb/in^2 gauge) also can be computed from the ideal gas law if a gas temperature is assumed. For an MCO gas temperature of 150 °C (423 K), which is very conservative and beyond the bounding value of 125 °C (HNF-SD-SNF-TI-015), about 173.5 moles of gas must be present in the MCO to achieve a pressure of 11.2 atm (150 lb/in^2 gauge). With about 33 moles of helium in an MCO at the time of arrival at the CSB, approximately 140.5 moles of other gases would need to be created at the CSB to reach 11.2 atm (150 lb/in^2 gauge) at an MCO gas temperature of 150 °C. A bounding 5.13 kg of uranium hydride are available at the CSB (HNF-SD-SNF-TI-015). Hence, the hydride mass would consume 765 g of water before being depleted, producing 74.5 moles of hydrogen. This leaves 66 moles of gas that need to be generated to reach 11.2 atm. For the uranium–water reaction, 66 moles of hydrogen gas are produced from 66 moles (1,190 g) of water consumed. Adding the water consumed by the two reactions (1,190 g plus 765 g) yields about 1.96 kg of water, which is the amount of free water needed to pressurize the MCO to 11.2 atm (150 lb/in^2 gauge) at a 150 °C MCO gas temperature.

The same simple calculation is performed for the 31.6 atm (450 lb/in^2 gauge) MCO pressure rated limit as well as for two lower gas temperatures. The results are shown in Table 6-1. After the water is consumed, hydrogen should react with uranium to form uranium hydride (hydrogen gettering). For purposes of this analysis, no hydrogen gettering is assumed to conservatively bound the MCO pressure.

Table 6-1. Water Mass Required to Pressurize Multi-Canister Overpack to 11.2 Atmosphere (150 lb/in^2 gauge) and 31.6 Atmospheres (450 lb/in^2 gauge) Versus Reaction and Gas Temperature.

Chemical reaction	High best estimate gas temperature, 100 °C	Bounding gas temperature, 125 °C	Beyond design basis gas temperature, 150 °C
Water mass required to reach 11.2 atm (150 lb/in^2 gauge)			
Hydride–water	1.69 kg	1.56 kg	1.45 kg
Uranium–water	2.95 kg	2.73 kg	2.53 kg
Bounding uranium-hydride mass* plus uranium	2.38 kg	2.15 kg	1.96 kg
Water mass required to reach 31.6 atm (450 lb/in^2 gauge)			
Bounding uranium-hydride mass* plus uranium	8.83 kg	8.20 kg	7.65 kg

*Assumes 765 g of water are used to react with a finite bounding uranium hydride mass of 5.13 kg (HNF-SD-SNF-TI-015, 1998, *Spent Nuclear Fuel Project Technical Databook*, Rev. 6, Fluor Daniel Hanford, Richland, Washington). The mass is consumed completely by hydride-water reaction.

Table 6-1 lists the total free water required to reach gas pressures of 11.2 atm (150 lb/in^2 gauge) and 31.6 atm (450 lb/in^2 gauge) for water reactions and their combined weighted average (weighted towards the uranium–water reaction) at three different MCO gas temperatures. The bounding uranium hydride mass is based on 0.765 kg of water is needed to consume the 5.13 kg of hydride, the bounding value for an MCO with two scrap baskets (HNF-SD-SNF-TI-015). The 125 °C gas temperature is the maximum MCO gas temperature anticipated for CSB storage (HNF-SD-SNF-TI-015).

If the newly created gas is a stoichiometric mixture of hydrogen and oxygen due to radiolysis of water and the gas temperature is 150 °C, only about 1.69 kg of water needs to be available for a pressure of 11.2 atm to be attained. The radiolysis process is very efficient in producing gas because it can generate up to 1.5 moles of gas for every mole of water. This production rate is not as efficient as the hydride–water reaction (1.75 moles of hydrogen per 1.0 mole of water) but is more efficient than the uranium–water reaction (1.0 mole hydrogen per 1.0 mole of water). However, HNF-SD-SNF-TI-040, *MCO Internal Gas Composition and Pressure During Interim Storage*, demonstrates that the radiolysis process is very slow, even for a period of 40 years. For a period of 1 year or less, the amount of water radiolytically decomposed has been shown to be less than 0.5% of the water available in the free and hydroxide phases and less than 5% of the water in uranium hydrate (1.19 kg) (see Chapter 5.0). Because this analysis focuses on thermal behavior and resulting high pressures of the MCO at the CSB during the first year, the slowly occurring radiolysis process is not considered. Radiolysis is considered in Chapter 5.0 for flammability potential and high pressure concerns over the entire 40-year projected storage period of an MCO at the CSB.

6.2.1.3 Bounding Water Mass and its Availability for Reactions in Multi-Canister Overpack. Water (HNF-SD-SNF-TI-015) in the bounding MCO can be classified into four groups: (1) free water (200 g), (2) water chemically bound in uranium hydrate (1.19 kg), (3) water chemically bound in aluminum hydroxide (3.32 kg) for MCOs containing fuel stored in aluminum canisters, and (4) water chemically bound in aluminum and iron hydrates (0.13 kg).

The projected bounding inventory of free water in an MCO received at the CSB is 200 g according to HNF-1851, *Cold Vacuum Drying Residual Free Water Test Description*, and HNF-SD-SNF-TI-015. The bounding MCO is assumed to be dried at the CVDF, with less than 200 g of free water remaining in cracks after the dryness tests at the CVDF. In addition to the 200 g of free water in an MCO with two scrap baskets and three fuel baskets, there is a bounding value of about 1.19 kg of water in the uranium hydrate that is part of the uranium oxide particulate matter, as reported in HNF-1523, *K-Basins Particulate Water Content, Behavior, and Impact*, and in HNF-SD-SNF-TI-015. However, this water would not be initially available to produce hydrogen. Some of the hydrate water would be removed at the CVDF. Based on information provided in FAI/98-40, *Hanford Spent Nuclear Fuel Safety Analysis Model HANSF 1.2: User's Manual*, water molecules bound in the uranium hydrate ($UO_3 \cdot 2H_2O$) are freed at temperatures above about 60 °C. Half the hydrate water (the first water molecule) liberates fairly easily, while the other half (the last water molecule) requires higher temperatures. Hydrate decomposition depends on the relative humidity as well as temperature in the surrounding gas, with dry gases promoting faster decomposition and saturated gases inhibiting decomposition. The reaction for the two stages of hydrate decomposition is

$$UO_3 \cdot 2H_2O \rightarrow UO_3 \cdot H_2O + H_2O \rightarrow UO_3 + 2H_2O.$$
(if temperature >60 °C) (if temperature >100 °C)

The MCO with the bounding water content contains two scrap baskets and three fuel baskets. Up to 3.32 kg of water are contributed by the bounding quantity of aluminum hydroxide on the fuel cladding with an additional 0.13 kg of water in aluminum and iron hydrates in the canister sludge (HNF-1523, HNF-SD-SNF-TI-015). Bound water, like the uranium hydrate water, is available initially. Very little of the hydroxide water is expected to be freed from the thermal decomposition of the aluminum hydroxide based on current data (about 5% of the water is freed for fuel temperatures less than 200 °C [HNF-1523, Rev. 1, Appendix B], and essentially no water is freed for fuel temperatures less than 150 °C). Earlier decomposition data from *Oxides and Hydroxides of Aluminum (*ALCOA 1987), reported in Revision 0 of HNF-1523, Appendix B, and reproduced in Figure 6-1, show more thermal decomposition at lower temperatures. This figure illustrates loss of water, porosity, internal surface area history, and change in density as a function of temperature. Weight loss is plotted on the right-hand side. About 20% of the hydroxide mass is lost (water) between 200 °C and 400 °C, and about another 10% is lost between 400 °C and 600 °C. The ALCOA (1987) thermal decomposition rates are more conservative at lower temperatures than the more recent data (HNF-1523, Rev. 1, Appendix B) and they are used for thermal decomposition. ALCOA (1987) decomposition data, expressed as water loss fraction of total hydroxide mass, which is 35% water, is converted to loss fraction of total water. At temperatures around 200 °C, the ALCOA (1987) data show the amount of water freed from decomposition is about 15% of the total water (5% of the total

hydroxide mass, Figure 6-1). For normal operations at the sampling/weld station, the MCO fuel temperatures will be less than 100 °C according to HNF-2256, *Simulation of Normal and Off-Normal Multi-Canister Overpack Behavior*. However, it is assumed that severe off-normal conditions at the station could result in MCO fuel temperatures above 100 °C. Hence, partial thermal decomposition of aluminum hydroxide is considered in the off-normal event calculations. The reaction is shown as:

$$2 \cdot Al(OH)_3 \rightarrow Al_2O_3 + 3 \cdot H_2O.$$
(if temperature >100 °C)

The bounding amounts of water in an MCO from all sources on arrival at the CSB and the availability of the water for reactions are shown in Table 6-2 as a function of fuel temperature. If the MCO fuel temperatures reach values close to 300 °C, then the thermal decomposition of aluminum hydroxide, along with hydrate decomposition and initial free water, could supply about 3.32 kg of water. This total is based on 57% thermal decomposition of the bound water from aluminum hydroxide and aluminum and iron hydrate (HNF-SD-SNF-TI-015), 100% thermal decomposition of the uranium hydrate, and 0.2 kg of free water. Because the iron and aluminum hydrate mass is small relative to aluminum hydroxide mass, both compounds are assumed to decompose at the same rate as the aluminum hydroxide.

The bounding water mass numbers in Table 6-3 are derived from the required water amounts identified in Table 6-1 and the available water amounts identified in Table 6-2. Table 6-3 shows the additional free water that would be needed at different gas temperatures for MCO pressures to increase to 11.2 and 31.6 atm (150 and 450 lb/in^2 gauge). It is assumed in Table 6-3 that the peak fuel temperatures will not be more than 50 °C higher than the gas temperatures, which has been shown in HNF-SD-SNF-CN-023, *Thermal Analysis of Cold Vacuum Drying of Spent Nuclear Fuel*, to be true for most conditions. The peak fuel temperatures occur on the innermost fuel assemblies or scrap and are less than 50 °C higher than the average gas temperature; whereas, the peripheral fuel elements or scrap are cooler than the average gas temperature. It is shown in Section 6.2.1.4 that if no fuel reactions are occurring (lack of oxidants), then the maximum fuel temperature is only 15 °C higher than the wall temperature.

Table 6-3 shows that, under normal conditions, at least 7.83 kg of additional free water are needed in an MCO at the CSB for the MCO pressure to reach the 31.6 atm (450 lb/in^2 gauge) design pressure after the cover cap is welded in place. Even under conditions that are beyond the bounding temperature causing more bound water to be liberated, at least 5.74 kg of additional free water would need to be available, which is more than the 4.84 kg total water that could be available in an MCO (HNF-SD-SNF-TI-015). Hence, if all the water (4.84 kg, Table 6-2) in the free, hydrate, and hydroxide phases were available for chemical reactions, the MCO pressure still would stay below the 450 lb/in^2 gauge design pressure after the cover cap is welded in place.

Table 6-2. Bounding Water Mass and Availability for Reactions in Multi-Canister Overpack for Thermal Runaway Reactions from Water.

Source of water	Total possible water mass (maximum free water is in an MCO with 2 scrap baskets and 3 fuel baskets)	Availability of water for reactions (Thermal decomposition, percent of total water mass)		
		Fuel T ≤ 100°C	Fuel T = 200°C	Fuel T = 300°C
Free water in cracks	0.20 kg	0.20 kg	0.20 kg	0.20 kg
Water in uranium hydrate	1.19 kg	0.60 kg (50 %)	1.19 kg (100 %)	1.19 kg (100 %)
Water in aluminum hydroxide*	3.32 kg	0.20 kg (6%)	0.50 kg (15 %)	1.90 kg (57 %)
Water in Al+Fe hydrates	0.13 kg	0.0 kg	0.02 kg (15 %)	0.07 kg (57 %)
TOTAL	4.84 kg	1.0 kg	1.91 kg	3.36 kg

*These data are from ALCOA, 1987, *Oxides and Hydroxides of Aluminum*, ALCOA Technical Paper No. 19, Revised, ALCOA Laboratories, Pittsburgh, Pennsylvania.

Table 6-3. Additional Water Mass Needed to Pressurize Multi-Canister Overpack to 11.2 Atmosphere (150 lb/in^2 gauge) and 31.6 Atmospheres (450 lb/in^2 gauge) for Different Gas Temperatures for Thermal Runaway Reactions from Water.

Water balance description	High best estimate gas temperature, 100 °C	Bounding MCO gas temperature, 125 °C (HNF-SD-SNF-TI-015)[a]	Beyond design basis gas temperature, 150 °C
11.2 atm (150 lb/in^2 gauge)			
Total water required to reach 150 lb/in^2 gauge (Table 6-1)	2.38 kg	2.15 kg	1.96 kg
Total free water available (Table 6-2)	1.0 kg[b]	<1.91 kg[c]	1.91 kg[c]
Additional water needed to reach 150 lb/in^2 gauge (water shortage at the CSB)	1.38 kg	>0.24 kg	0.05 kg
Safety margin	138%	>13%	3%
31.6 atm (450 lb/in^2 gauge)			
Total water required to reach 450 lb/in^2 gauge (Table 6-1)	8.83 kg	8.20 kg	7.65 kg
Free water available (Table 6-2)	1.0 kg[b]	1.91 kg[c]	1.91 kg[c]
Additional water needed to reach 450 lb/in^2 gauge (water shortage at the CSB)	7.83 kg	6.29 kg	5.74 kg
Safety margin	780%	329%	301%

[a]HNF-SD-SNF-TI-015, 1998, *Spent Nuclear Fuel Project Technical Databook*, Rev. 6, Fluor Daniel Hanford, Incorporated, Richland, Washington.

[b]Fuel T≤ 100 °C.

[c]Fuel T≤ 200 °C.

CSB = Canister Storage Building.

Table 6-3 shows there is insufficient water in the MCO to exceed the MCO rated pressure of 11.2 atm (150 lb/in^2 gauge) before the cover cap is welded in place. The additional water needed is 0.24 kg to pressurize the MCO to 11.2 atm at the CSB under bounding conditions. This indicates that activating the cooling system of the shield wall or removing the MCO from the sampling/weld station when the MCO temperature exceed 100 °C is prudent. There is additional margin in the MCO rated pressure of 11.2 atm, because no release is expected for pressures below 340 lb/in^2 gauge (HNF-SD-SNF-SARR-005).

6.2.1.4 Analysis Results of High-Temperature Scenarios. The HANSF code, Version 1.2 (FAI/98-40) was used to simulate four of the bounding events (Cases 1 through 4) with high temperature boundary conditions, as reported in HNF-SD-SNF-CN-023, *Thermal Analysis of Cold Vacuum Drying of Spent Nuclear Fuel*. The HANSF code has been used extensively for analyses of CVDF processes, and its quality assurance has been documented (HNF-SD-SNF-CN-023). The key parameters for these cases are identified in Appendix 6A. The newer HANSF version 1.3.2 (SNF-3650) is compared with HANSF version 1.2 in SNF-5226, *Comparison Cases Simulated with HANSF 1.3.2 that Supplement the Thermal Analyses Documented in HNF-SD-SNF-CN-023*. The comparison shows that the results from HANSF version 1.2 are more conservative than the results from HANSF version 1.3.2 for the cases in this analysis. The models developed for the code include the inner and outer fuel elements in each fuel assembly and 54 fuel assemblies per fuel basket. The models also include the scrap basket, which is physically modeled like a porous bed of gravel. HANSF version 1.3.2 was used to model the case related to air ingress (Case 5). The input parameters for this calculation are identified in SNF-5226.

The high-temperature scenario analysis was motivated by the high-temperature calculations documented in CSB-HV-0014, *Long Term MCO Temperature Without Cooling in the Sampling Station*. Those calculations analyzed an MCO in the sampling/weld station without active cooling for about two months. The MCO handling machine (MHM) also was assumed to be unable to remove the MCO from the sampling/weld station. For this unmitigated scenario, a 132 °C MCO wall temperature (design limit) was calculated to occur in about 40 days (CSB-HV-0014).

There were two high-internal MCO gas temperature cases with water-based reactions analyzed with Version 1.2 of the HANSF code (FAI/98-40). The key input parameters are given in Appendix 6A. The simulations used a bounding MCO with one scrap basket and four fuel baskets. However, to maximize the water content and available reactant for the thermal runaway reactor, the simulated water content of this MCO was equivalent to that of a bounding MCO with two scrap baskets and three fuel baskets. An MCO with two scrap baskets has the maximum hydrate water (1.19 kg) and total water (4.84 kg) in the free, hydrate, and hydroxide phases (see Table 6-2). The MCO with one scrap basket has more decay heat than the MCO with two scrap baskets because a fuel basket has more heat (or mass) than a scrap basket. To maximize the results and minimize the number of simulations, a hypothetical MCO was modeled with decay heat of an MCO with one scrap basket and the water content of an MCO with two scrap baskets. The temperature results of the single scrap basket represent the behavior of a second scrap basket. Five fuel baskets would have about 35 W of decay power more than four fuel baskets and one

scrap basket. However, 35 W of decay is insignificant when compared to the potential chemical heat rate in one scrap basket.

The total reaction surface area is not maximized for the entire MCO. The total reaction surface area is not important at the CSB because the reaction is limited by oxidants (water or oxygen), not by reaction rate or reaction area. After the CVDF, water is very limited and air is not present in an MCO. For air ingress scenarios, a single scrap basket with a 4.5 m^2 bounding surface area will determine the bounding temperature results for a second scrap basket, if present. The second scrap basket would compete with the first basket for oxidants such that the first basket would not heat as much, which is less conservative. All of the following results are obtained with this bounding, hypothetical MCO, except for the first two cases which use a lower decay power associated with aluminum hydroxide coated fuel.

6.2.1.4.1 Case 1 (CHOTSCEN). The MCO with the maximum water is one with aluminum hydroxide on the fuel cladding, which provides a potential water source. The bounding decay heat for aluminum hydroxide fuel is 528 W according to HNF-3035, *MCO Gas Composition for Low Reactive Surface Areas*. A bounding temperature MCO is in the sampling/weld station for at least 40 days without active cooling. The calculated fuel temperatures are consistent with the 132 °C MCO wall temperature. Simulations for this case assumed initial fuel temperatures of 125 °C and calculated the temperatures for two days. It was assumed that the 1.5 atm of helium injected at the CVDF included water. The water was assumed to be 2% (saturated steam at 25 °C) of the injected helium, which amounts to about 9 g of water mass. Steady-state temperatures for this case were attained in less than a day of simulated time (see Figures 6-2 and 6-3).

The fuel temperatures for Case 1 are shown in Figures 6-2 and 6-3 as a function of time. The hottest fuel temperature for Case 1 occurs on the inner fuel element nearest the center post of the MCO. This maximum temperature is about 145 °C for the fuel baskets and is steady. The hottest temperature for the scrap fuel is about 140 °C with a steady-state value of 135 °C. The scrap fuel is cooler than the fuel elements because the scrap basket copper fins effectively conduct heat toward the MCO wall and because some heat escapes from the scrap to the shield plug.

The MCO gas temperature reaches about 140 °C in the fuel baskets and about 132 °C in the scrap basket. The time in Figures 6-2 and 6-3 starts after the MCO wall temperature reaches 132 °C, which would be at least 40 days after the bounding MCO is placed in the sampling/weld station (CSB-HV-0014) with no active cooling for the shield wall. The initial helium temperature is 25 °C when it is injected into the MCO at a pressure of about 1.5 atm at the CVDF. In the simulation the gas heats up in about two or three minutes, due to the low heat capacity of the gas, and causes a rapid pressure increase. The MCO gas pressure reaches 7.0 atm in two days and is remaining steady. It is not expected that the fuel temperatures will heat up to these temperatures because the MCO wall temperatures were expected to be made cooler than 132 °C

6.2.1.4.2 Case 2 (CHOTSCR2). Case 2 investigates the effects of aluminum hydroxide water on MCO fuel reactions as a continuation of Case 1. Case 2 uses the final results of Case 1 for all initial conditions. This simulation adds 0.52 kg of water, which is about 15% of the water

contained in aluminum hydroxide and the aluminum and iron hydrates in the canister sludge (HNF-SD-SNF-TI-015, HNF-1523, Rev. 0). ALCOA data (ALCOA 1987) indicate that as much as 15% of the hydroxide water can be freed by thermal decomposition for temperatures up to 200 °C, and about 57% can be freed for temperatures up to 300 °C (HNF-1523, Rev. 0). In Case 1, the maximum fuel temperature was 146 °C, at which temperature less than 6% of the water in aluminum hydroxide is expected to be freed by thermal decomposition. Because thermal decomposition of aluminum hydroxide is not part of the HANSF code, additional water vapor (steam) was added as a source to simulate the water from aluminum hydroxide on temperatures and pressure. To be conservative, 15% or 0.52 kg of hydroxide water was added to the MCO fuel baskets over a 10,000 second interval. The kinetic disposition rate was not modeled explicitly because of the conservatism and the assumed rapid source rate.

In the simulation, the freed hydroxide water was added only to the fuel baskets, which is more conservative than evenly distributing the water to all the baskets. The added water from hydroxide causes the maximum fuel temperature to increase from 146 °C to about 155 °C in less than three hours (shown in Figure 6-4). All of the temperature and pressure results for this case are shown in Figures 6-4 and 6-5. The fuel and gas temperatures decrease after three hours because no more water is available to continue the chemical reactions. In less than two days, the maximum fuel temperature reaches a lower steady-state value of 145 °C. The hydroxide water-fuel reaction creates hydrogen gas, which has a very high thermal conductivity, and heat is removed from the MCO faster. The scrap fuel does not heat up, indicating that no steam enters the scrap basket from the top fuel basket. The MCO pressure rises to about 10.0 atm (133 lb/in^2 gauge), which is below the MCO design pressure of 11.2 atm (150 lb/in^2 gauge). The maximum fuel temperature does not rise above 155 °C and the gas temperature does not rise above 140 °C, indicating that the helium cover gas provides good thermal conductivity, thereby keeping the temperatures stable in the MCO at the CSB.

6.2.1.5 Conclusions and Conservatisms. The simulations show that MCO temperatures will remain stable even under very severe external thermal conditions. The maximum gas pressure will stay below 11.2 atm. This behavior occurs even with many conservatisms included in the evaluation. The main conservatisms used in the computer simulations are itemized in the following list.

- No hydrate water is removed at the CVDF, leaving all hydrate water available for thermal decomposition and reaction at the CSB.
- No hydride mass is consumed at the CVDF and the CSB, as the hydride reaction rate multiplier was kept at 12 (HNF-SD-SNF-TI-015) for all simulations at all times.
- MCO wall temperature is conservatively chosen to be 132 °C as the result of being in the sampling/weld station pit without active cooling for 40 days; whereas the wall temperature is only 126 °C at 40 days (CSB-HV-0014).
- Steam mass of 9 g is added to the MCO to account for the CVDF helium supply, possibly being contaminated with 2% steam.

- Fifteen percent of aluminum hydroxide water is released at fuel temperatures <150 °C instead of 200 °C (HNF-1523, Rev. 0) for Case 2, and this water is added only to the hotter fuel baskets instead of evenly distributing the water source over both scrap and fuel baskets.

- No hydrogen gettering takes place, which maximizes the gas pressure; if hydrogen gettering was allowed to take place, the hydrogen gas fraction in the MCO would be significantly reduced, thereby lowering the MCO pressure. Hydrogen gettering is expected to occur after all of the free water has been depleted; this process could lower the MCO pressure by as much as 80%.

6.2.2 Thermal Runaway Reaction from Oxygen Reacting with Uranium Hydride and Uranium

Heat also can be generated in an MCO when oxygen (or air) enters as the result of an off-normal event or as the result of radiolysis and reacts with the uranium metal fuel. This section examines the entrance of oxygen or air as the result of an off-normal event. Chapter 5.0 examines the long-term effects of radiolysis and flammability issues. Any oxygen that enters the MCO will react with uranium hydride and uranium to liberate heat, depending on the temperature (HNF-SD-SNF-TI-015). These reactions are as follows:

$$UH_3 + 1.75O_2 \rightarrow UO_2 + 1.5H_2O + \text{heat}$$

$$U + O_2 \rightarrow UO_2 + \text{heat}.$$

A high-pressure condition in an MCO is impossible with an air ingress event because pressure decreases when oxygen is consumed. However, as heat is liberated in these uranium-oxygen reactions, a thermal excursion may be possible with sufficient quantities of oxygen for reaction and sufficiently high fuel temperatures. Furthermore, because reactions with oxygen liberate heat and increase the fuel and gas temperatures, additional water could decompose from the uranium hydrate and aluminum hydroxide. This would increase the pressure and temperature in the MCO. The reactions with oxygen will be followed by the reactions with water after the oxygen is consumed. All of these reactions are coupled and interrelated. The HANSF code (FAI/98-40) was used to simulate the air ingress case.

The HANSF code (FAI/98-40), was used to evaluate the effect of competing reactions and to determine if a thermal runaway occurs for two different bounding air entry cases. Full realistic scenarios were not developed because no thermal runaways are expected even for very conservative or extremely off-normal conditions.

6.2.2.1 Case 3 (COXY2SC4). An MCO is charged with pure oxygen instead of helium at the CSB sampling/weld station during gas sampling (i.e., helium cylinders accidentally filled with oxygen or oxygen cylinders accidentally used in place of helium). In obtaining a gas sample from one of the monitored MCOs, the helium pressure in the MCO is accidentally reduced to 1.0 atm.

Hence, when oxygen, instead of helium, is accidentally injected into the MCO to 1.5 atm, 0.5 atm (about 33%) of the total pressure is due to oxygen. It is also assumed that only passive cooling is available in the sampling/weld station such that the air temperature and MCO wall temperature are both 132 °C. This maximum steady-state temperature is reached only after at least 40 days in the sampling/weld station with no active cooling (CSB-HV-0014). In the HANSF simulation, all fuel temperatures are conservatively assumed to be 153 °C, which is the maximum fuel temperature calculated for a 132 °C MCO wall and bounding decay power of 776 W for 5 fuel baskets (HNF-SD-SNF-TI-015).

A very high fuel temperature was used to assess margin. If oxygen reactions at high temperatures do not cause significant thermal excursion, then no thermal excursion would result for oxygen reactions at lower temperatures. This scenario is very conservative and may not be credible, but the maximum fuel temperature bounds the fuel temperatures in all air entry cases (except the complete shear of an MCO at elevated temperature MCO) and cases with helium bottles contaminated with air or oxygen. This case bounds all air ingress events, without complete shear, at the sampling/weld station because 100% oxygen is postulated to be injected and air has an oxygen content of only 21%. Air ingress through a single orifice (around 1 in. in diameter) cases are bounded by this scenario because very little air can flow into the MCO against the gas being generated within and flowing out of the MCO. A more representative air ingress case was simulated in Case 5 (Section 6.2.2.3). Also, no natural circulation with air ingress is possible at the CSB because natural circulation requires two openings, one for air entry and one for gas exit, and two openings are not available in the MCO at the CSB. However, the effects of one very large opening, such as in a complete shear is different (see Section 6.2.2.2). The complete shear scenario was simulated in Case 4 because it represents a physical situation with an unlimited amount of oxidant reaching the fuel.

The temperature and pressure results for Case 3 are shown in Figures 6-6 and 6-7. The design basis accident for air ingress was chosen to be Case 3, with oxygen instead of helium injected at the gas sampling station. For Case 3, the innermost fine scrap fuel has a thermal increase up to almost 440 °C before the oxygen is depleted in the scrap basket and the fuel cools rapidly (see Figure 6-6). This temperature increase occurs because the fine scrap fuel has a high surface-area-to-volume ratio and is initially conservatively at 153 °C. This is hot enough to rapidly oxidize the uranium hydride in the scrap fuel and dramatically increase the fine scrap temperature. The oxygen-hydride reaction at this high temperature rapidly consumes the oxygen, depleting it within an hour. There is not enough water available to continue the chemical reactions. As such, a sustained thermal runaway reaction does not occur. If aluminum hydroxide is included, only a small amount of water is expected to be freed by thermal decomposition because elevated temperatures exist for less than an hour and are restricted to only part of the innermost fine scrap, which represents less than 3% of the total fuel and cladding mass.

The maximum MCO pressure of about 6.2 atm is far below the 11.2 atm (150 lb/in^2 gauge) MCO rated pressure before the cover cap is welded in place. This maximum pressure is lower than that found in Cases 1 and 2, as expected, because the oxygen reactions do not produce as much gas as the water reactions. The pressure is also lower because the temperatures are

generally not as high and the hydrates do not completely decompose, providing less water for reaction.

6.2.2.2 Case 4 (CAIR2SC). In Case 4, the MCO is in the MHM without the MHM extract system cooling fan turned on. An analysis by the MHM manufacturer showed that the MCO wall temperature can reach a steady-state temperature of 115 °C and an MHM air temperature of 102 °C. Case 4 uses these temperatures and assumes that the MHM completely shears off the top, providing a large opening for air to enter the MCO. The scrap fuel and in-tact fuel assembly temperatures are conservatively assumed to be 125 °C. Under these hot conditions, the oxygen in the air reacts with both the uranium fuel and uranium hydride at a high enough rate to slowly increase the fuel temperatures. The scrap basket has better heat rejection than the fuel basket, especially because it is exposed to 102 °C air above it. Hence, the scrap fuel does not heat up as fast as the inner fuel elements, which reach high temperatures very rapidly after 18 hours (shown in Figure 6-8). The maximum temperature reached by the innermost fuel assemblies is about 540 °C, which is still below the uranium–iron eutectic temperature of 725 °C (HNF-SD-SNF-SARR-005).

To prevent a thermal excursion during a shear accident, the fuel temperatures must be kept below 125 °C. This can be achieved by keeping the MCO wall below 115 °C. Also, with interlocks, switches, and sensors in the MHM, shears are not credible.

6.2.2.3 Case 5 (AIRINGRS). Case 5 is a more credible air ingress scenario for a drop at the CSB than Case 3 or Case 4. The air enters the top of the MCO through a breach in the MCO. Air entry is maximized if the breach is located at the top of the MCO even though any potential breach would more likely be located toward the bottom of the MCO. The-cross sectional area of the air entry is conservatively taken to be 5.07×10^{-4} m^2, which is equivalent to an orifice with a diameter of 1 in. (0.0254 m). The MCO is stored in a storage tube at the CSB under hot weather conditions such that the storage tube air temperature is 92 °C and the MCO wall temperature is 108 °C (HNF-SD-SNF-TI-015). These temperatures were used to determine the initial fuel temperatures of the MCO at the start of the breach and air ingress. Version 1.3.2 of the HANSF code (SNF-3650) was used to simulate these initial conditions and the resulting air ingress scenario. As in the other cases, there is one scrap basket and four fuel baskets with 200 g of residual water plus the water from the uranium hydrates. After the breach of the MCO, the ambient outside air temperature is conservatively kept at 92 °C, which is the maximum storage tube air temperature under closed conditions.

Air enters through the top of breached MCO and reacts with the scrap fuel in the top basket. Even though hydrogen has accumulated in the top scrap basket (~49% of gas volume initially and around 40% immediately after breach), the oxygen starts reacting with the scrap fuel immediately and is almost completely consumed. As a result, the maximum oxygen content is always less than 0.5% of gas volume in the scrap basket, which is below flammable conditions (see Figure 6-9). The amount of hydrogen expelled from the MCO at the time of breach is about 40 g over a few seconds (see Figure 6-10). The consequences of the expelled hydrogen are bounded by the external hydrogen release in the sampling hood (see Chapter 5.0). More hydrogen is generated during the accident from the water freed during the thermal decomposition

of the uranium hydrate. All of the water vapor pressure shown in Figure 6-11 is from the dehydration water.

The air enters the MCO at a rate of about 16 mg/s about an hour after the initial blowdown release. The oxygen in this air, which is consumed by the scrap fuel, is enough to raise the maximum temperature of scrap fuel from about 120 °C to about 145 °C within 48 hours (see Figure 6-10). The temperature curves for each of the fuel baskets shown in Figures 6-10 and 6-11 indicate the fuel temperatures have essentially leveled off after 24 hours, and the scrap basket has the hottest fuel. The maximum fuel temperature in the all of non-scrap fuel baskets is below 145 °C. Since nitrogen enters the MCO and replaces the helium and hydrogen, the conductivity of the MCO gas decreases causing higher fuel temperatures, which reach an equilibrium value within 48 hours. Since some hydrogen is generated during the accident, the hydrogen concentration does not decline as much as the helium concentration. During the first few seconds after the blowdown, some oxygen gets past the scrap basket because of the blowdown cooling the gas left in the MCO, but the scrap basket consumes all of the entering oxygen after a few minutes. The amount of oxygen entering is enough to generate about 135 W of power from reacting with the fuel.

In summary, air ingress into the MCO if breached results in stable fuel temperatures and flammability conditions are not reached inside the MCO.

6.2.2.4 Beyond Design Basis Accident. In Case 4 at the MHM without its fan on, the air temperature is 102 °C, based on a previous analysis. Calculations for a complete shear of an MCO at MHM have shown that if the air temperature in the MHM was higher than 102 °C (e.g., 115 °C), then the scrap fuel would start burning rapidly within 8 hours of a complete shear and be completely oxidized in about 10 additional hours. This 100% scrap fuel burn (oxidation) generates about 1,000 kg of UO_2, which is the approximate material at risk in the scrap basket. This material at risk can produce an airborne source term of about 1 kg of UO_2, given the respirable airborne release fraction of 1×10^{-3} for oxidizing uranium provided in DOE-HDBK-3010-94, *Airborne Release Fractions/Rates and Respirable Fractions/Rates for Nonreactor Nuclear Facilities*. This source term results in an offsite dose of about 1 rem over a 12-hour period. The fuel in the MCO and the air in the MHM should never be hot enough ($\leq$102 °C) to cause a large fuel burn, as is demonstrated in Case 4. Hence, the conditions required for a large fuel burn are beyond the design basis accident for a complete shear providing unlimited oxidant for fuel reactions.

6.2.2.5 Conclusions and Conservatisms. Temperatures remain stable even under very severe external thermal conditions. However, the MCO pressure could get very close to the MCO pressure design limit. This could be a problem, but there are many conservatisms in the evaluation. The main conservatisms and/or margins over bounding parameter values assumed in the computer simulations are itemized as follows:

- No hydrate water is removed at the CVDF, leaving all hydrate water available for thermal decomposition at the CSB.

- No hydride mass is consumed at the CVDF and the hydride reaction rate multiplier was kept at 12 (HNF-SD-SNF-TI-015) for all times, which keeps the hydride-oxygen reaction going. In reality, much of the hydride would be consumed at the CVDF and not be available at the CSB.

- MCO wall temperature is 132 °C for Cases 1 through 4 because the MCO is placed in the sampling/weld station for 40 days without active cooling. MCO wall temperature is 108 °C for Case 5 because MCO is in storage tube.

- All fuel (center and peripheral) temperatures start at the maximum fuel temperature except in Case 5, which is initialized with a simulation.

Even with all of the above margins in the simulations, the calculated MCO gas pressure stays below the MCO design pressure of 11.2 atm (150 lb/in^2 gauge) before the cover cap is welded in place. The fuel temperatures also are stable after an increase in the innermost fine scrap fuel due to oxidization of the uranium hydride and the large area-to-volume ratio of the fine scrap. Even for a complete shear of a moderately high-temperature MCO, the fuel temperatures stay below guidelines (HNF-SD-SNF-SARR-005).

6.3 SOURCE TERM ANALYSIS

Detailed analyses show there is not enough heat, air, or water to have a credible thermal runaway reaction at the CSB.

Because there is no release expected even under severe off-normal conditions, no source term was estimated.

6.4 CONSEQUENCE ANALYSIS

Detailed analyses show there is not enough heat, air, or water to have a credible thermal runaway reaction at the CSB.

Because there is no release expected, even under severe off-normal conditions, the inhalation dose consequences are zero.

6.5 REFERENCES

ALCOA, 1987, *Oxides and Hydroxides of Aluminum*, ALCOA Technical Paper No. 19, Revised, ALCOA Laboratories, Pittsburgh, Pennsylvania.

CSB-HV-0014, 1998, *Long Term MCO Temperature Without Cooling in the Sampling Station,* Fluor Daniel Hanford, Incorporated, Richland, Washington.

DOE-HDBK-3010-94, 1994, *Airborne Release Fractions/Rates and Respirable Fractions/Rates for Nonreactor Nuclear Facilities*, U.S. Department of Energy, Washington, D.C.

FAI/98-40, 1998, *Hanford Spent Nuclear Fuel Safety Analysis Model HANSF 1.2: User's Manual*, Rev. 0, Fauske & Associates, Incorporated, Burr Ridge, Illinois.

HNF-1523, 1997, *K-Basins Particulate Water Content, Behavior, and Impact*, Rev. 0, Fluor Daniel Hanford, Incorporated, Richland, Washington.

HNF-1523, 1998, *K-Basins Particulate Water Content, Behavior, and Impact*, Rev. 1, Fluor Daniel Hanford, Incorporated, Richland, Washington.

HNF-1851, 1998, *Cold Vacuum Drying Residual Free Water Test Description*, Rev. 1, Fluor Daniel Hanford, Incorporated, Richland, Washington.

HNF-2256, 1998, *Simulation of Normal and Off-Normal Multi-Canister Overpack Behavior*, Rev. 1, Fluor Daniel Hanford, Incorporated, Richland, Washington.

HNF-3035, 1998, *MCO Gas Composition for Low Reactive Surface Areas*, Rev. 0B, Fluor Daniel Hanford, Incorporated, Richland, Washington.

HNF-3312, 1998, *MCO Monitoring Activity Description*, Rev. 0, Fluor Daniel Hanford, Incorporated, Richland, Washington.

HNF-3354, 1998, *MCO Monitoring Issue Closure Package*, Rev. 0, Fluor Daniel Hanford, Incorporated, Richland, Washington.

HNF-SD-SNF-CN-023, 1998, *Thermal Analysis of Cold Vacuum Drying of Spent Nuclear Fuel*, Rev. 1, Fluor Daniel Hanford, Incorporated, Richland, Washington.

HNF-SD-SNF-DR-003, 1999, *Multi-Canister Overpack Design Report*, Rev. 2, Fluor Daniel Hanford, Incorporated, Richland, Washington.

HNF-SD-SNF-SARR-005, 1999, *Multi-Canister Overpack Topical Report*, Rev. 1, Fluor Daniel Hanford, Incorporated, Richland, Washington.

HNF-SD-SNF-TI-015, 1998, *Spent Nuclear Fuel Project Technical Databook*, Rev. 6, Fluor Daniel Hanford, Incorporated, Richland, Washington.

HNF-SD-SNF-TI-040, 1998, *MCO Internal Gas Composition and Pressure During Interim Storage*, Rev. 2, Fluor Daniel Hanford, Incorporated, Richland, Washington.

SNF-2356, 1998, *Spent Nuclear Fuel Project Cold Vacuum Drying Facility Operations Manual*, Rev. 0A, Fluor Daniel Hanford, Incorporated, Richland, Washington.

SNF-3650, 1999, *HANSF 1.3.2: User's Manual*, Rev. 2, Fluor Daniel Hanford, Incorporated, Richland, Washington.

SNF-5226, 1999, *Comparison Cases Simulated with HANSF 1.3.2 that Supplement the Thermal Analyses Documented in HNF-SD-SNF-CN-023*, Rev. 0, Fluor Daniel Hanford, Incorporated, Richland, Washington.

Figure 6-1. Thermal Decomposition of Aluminum Hydroxide.

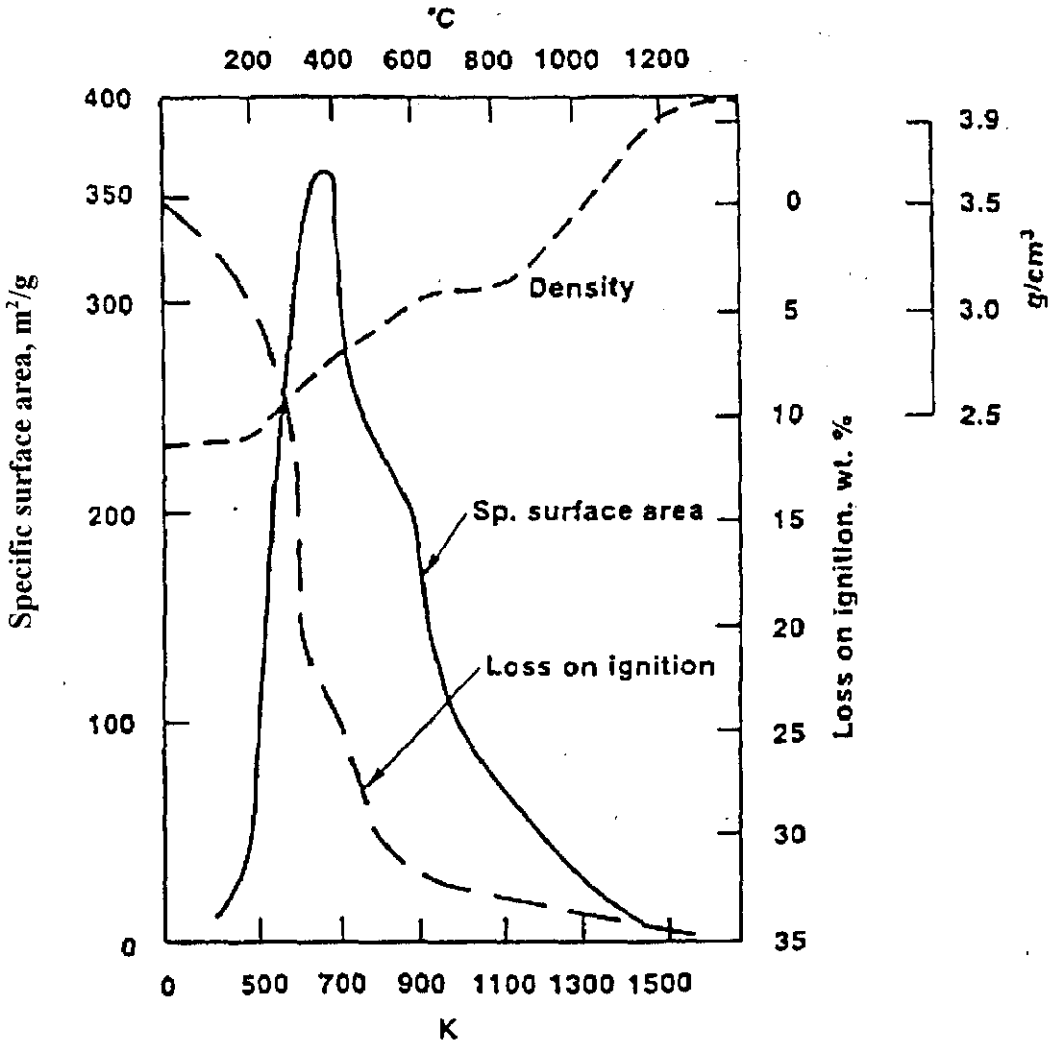

Note: This figure is based on Figure 4.4 in ALCOA, 1987, *Oxides and Hydroxides of Aluminum*, ALCOA Technical Paper No. 19, Revised, ALCOA Laboratories, Pittsburgh, Pennsylvania.

Figure 6-2. Temperature Versus Time for Multi-Canister Overpack Components for Case 1, CHOTSCEN.

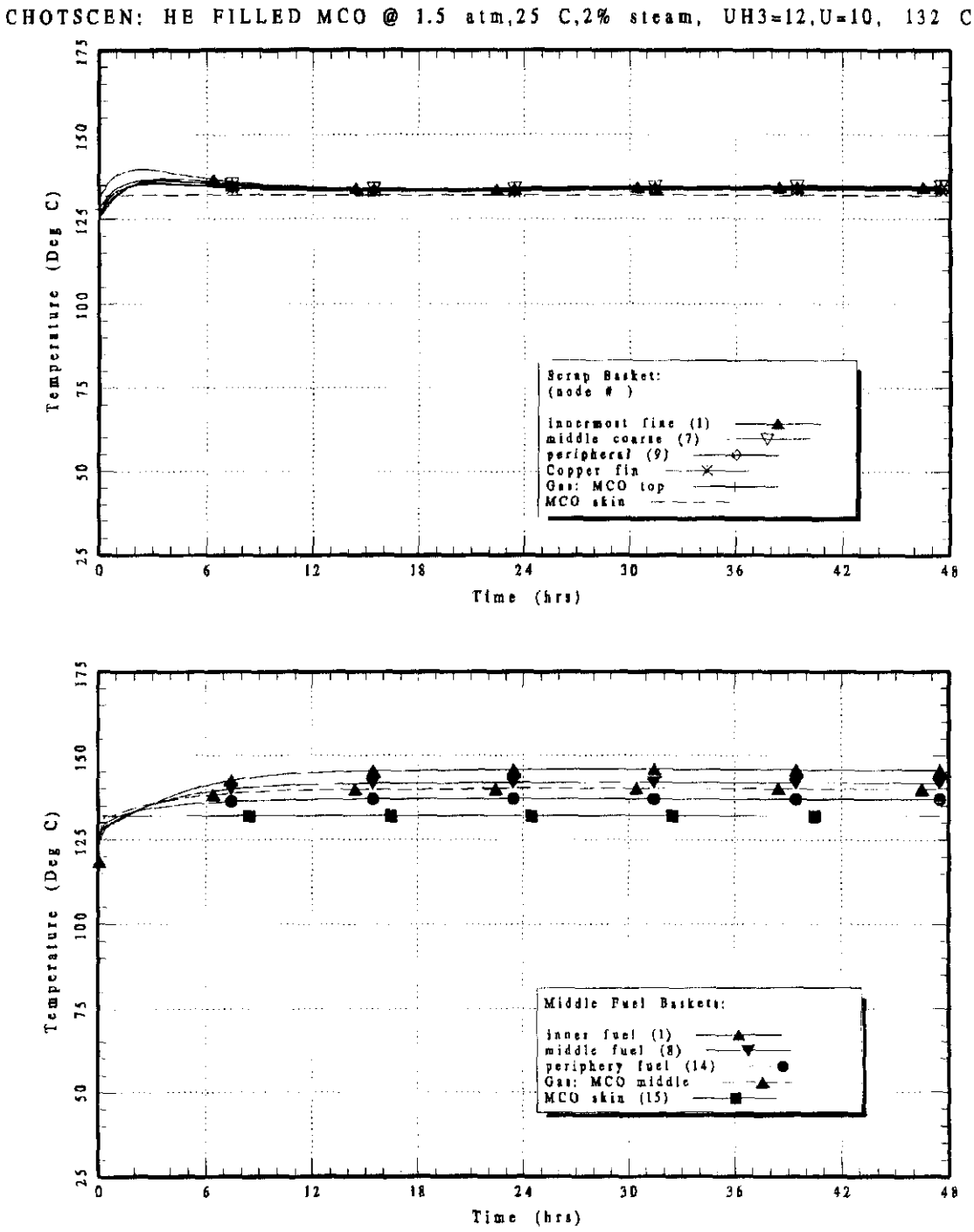

Figure 6-3. Temperature Versus Time for Multi-Canister Overpack Components in Bottom Fuel Basket and Pressure Versus Time for Case 1, CHOTSCEN.

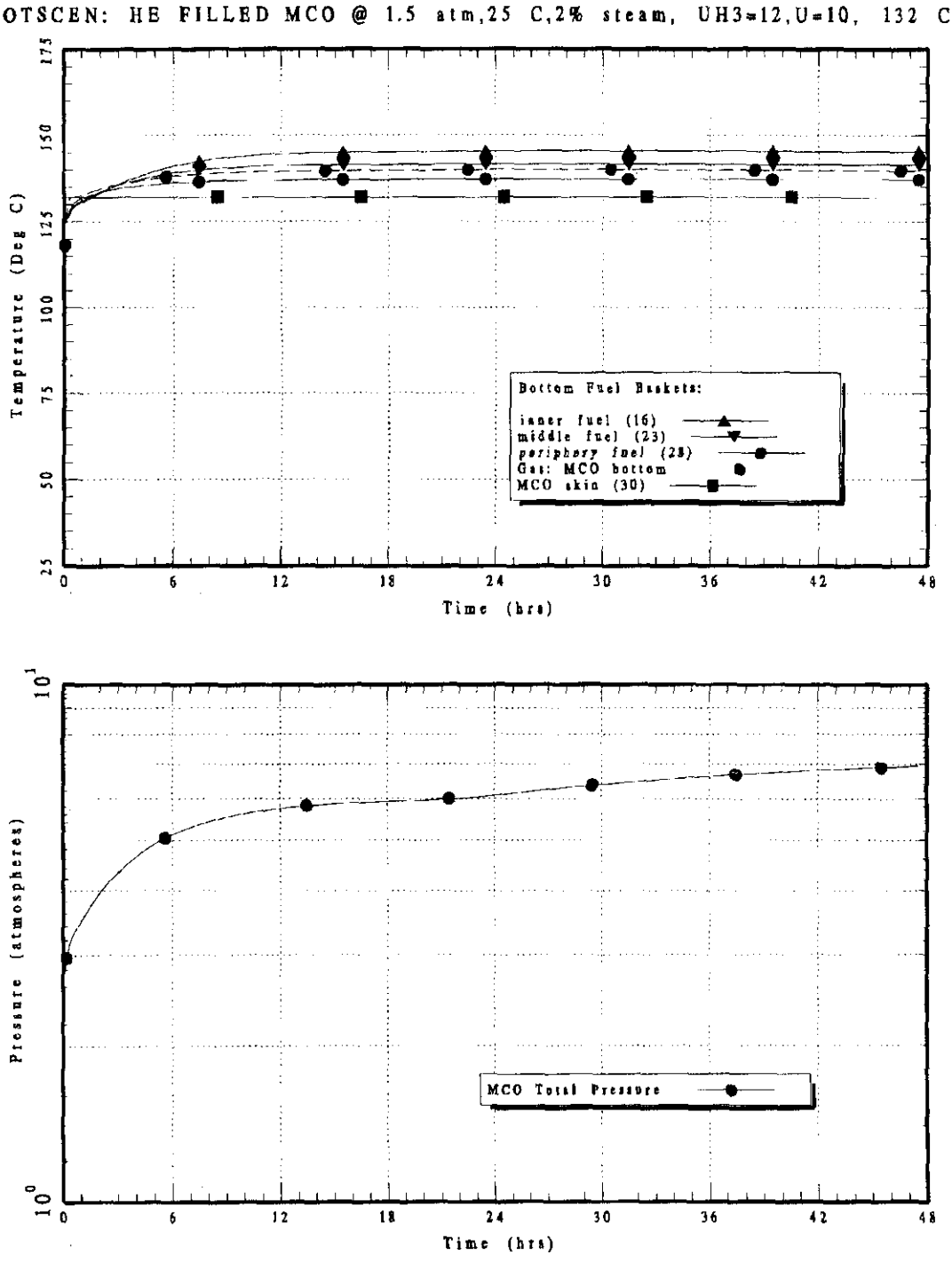

Figure 6-4. Temperature Versus Time for Multi-Canister Overpack Components for Case 2, CHOTSCR2.

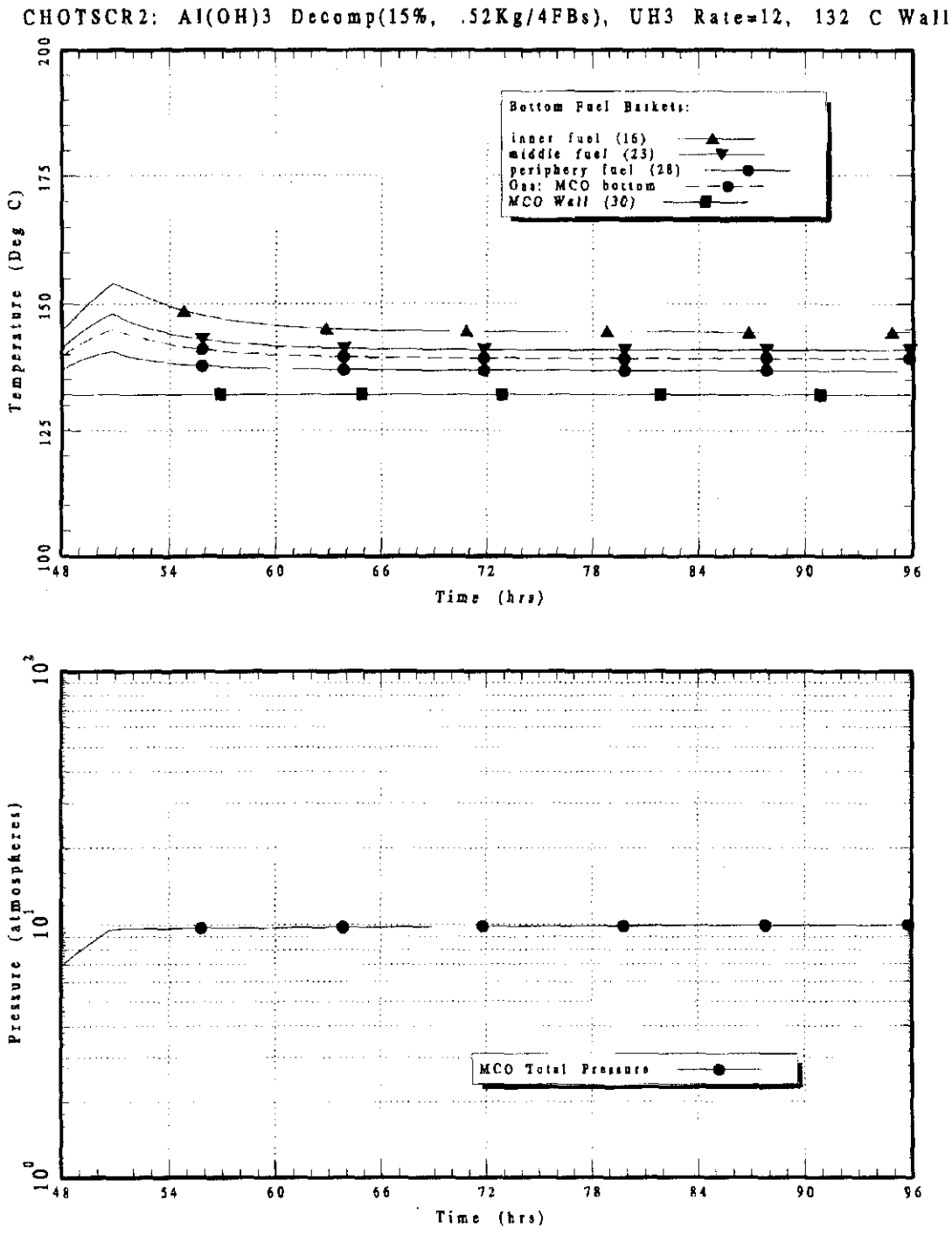

Figure 6-5. Temperature Versus Time for Multi-Canister Overpack Components in Bottom Fuel Basket and Pressure Versus Time for Case 2, CHOTSCR2.

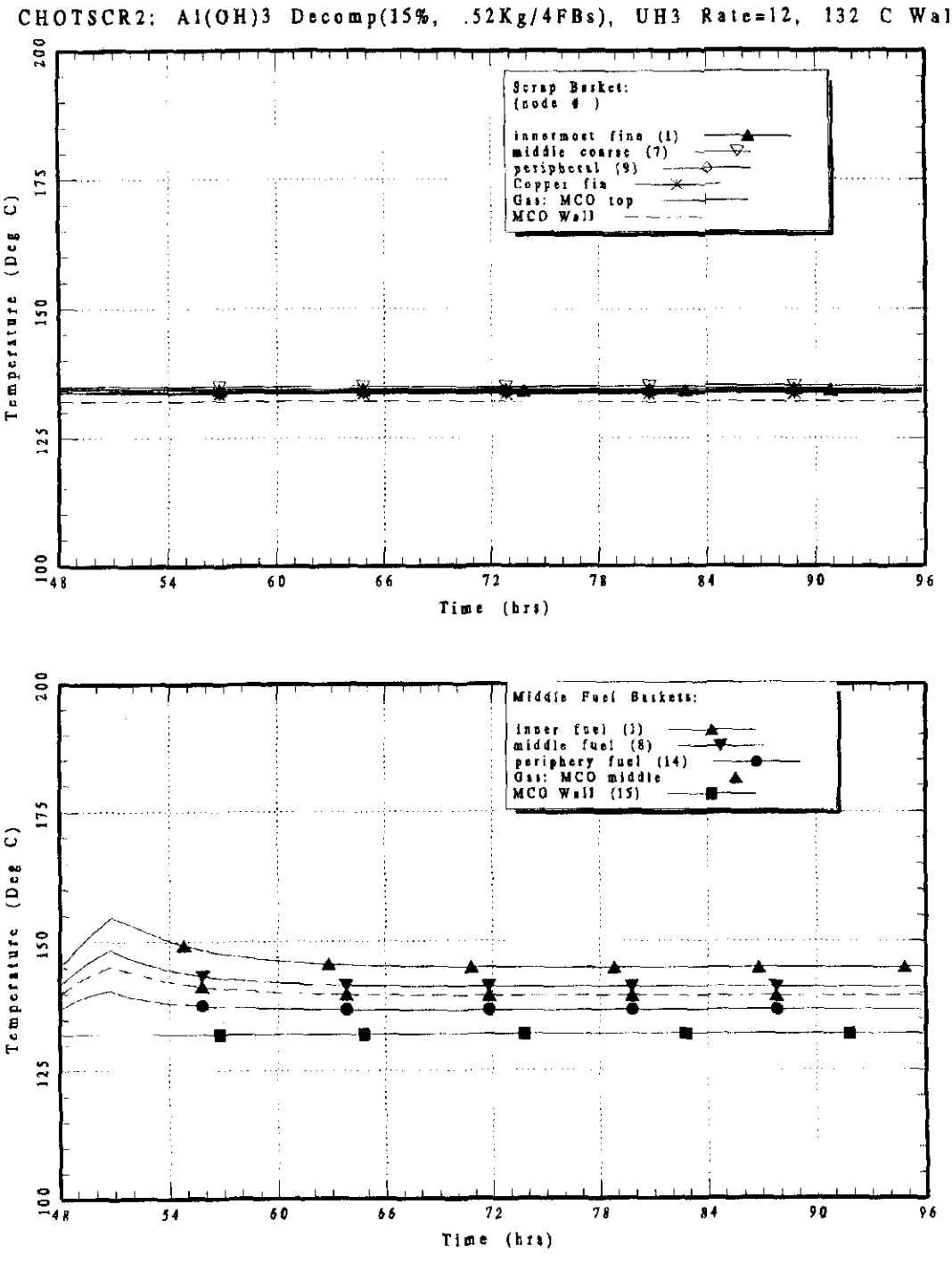

Figure 6-6. Temperature Versus Time for Multi-Canister Overpack for Case 3, COXY2SC4.

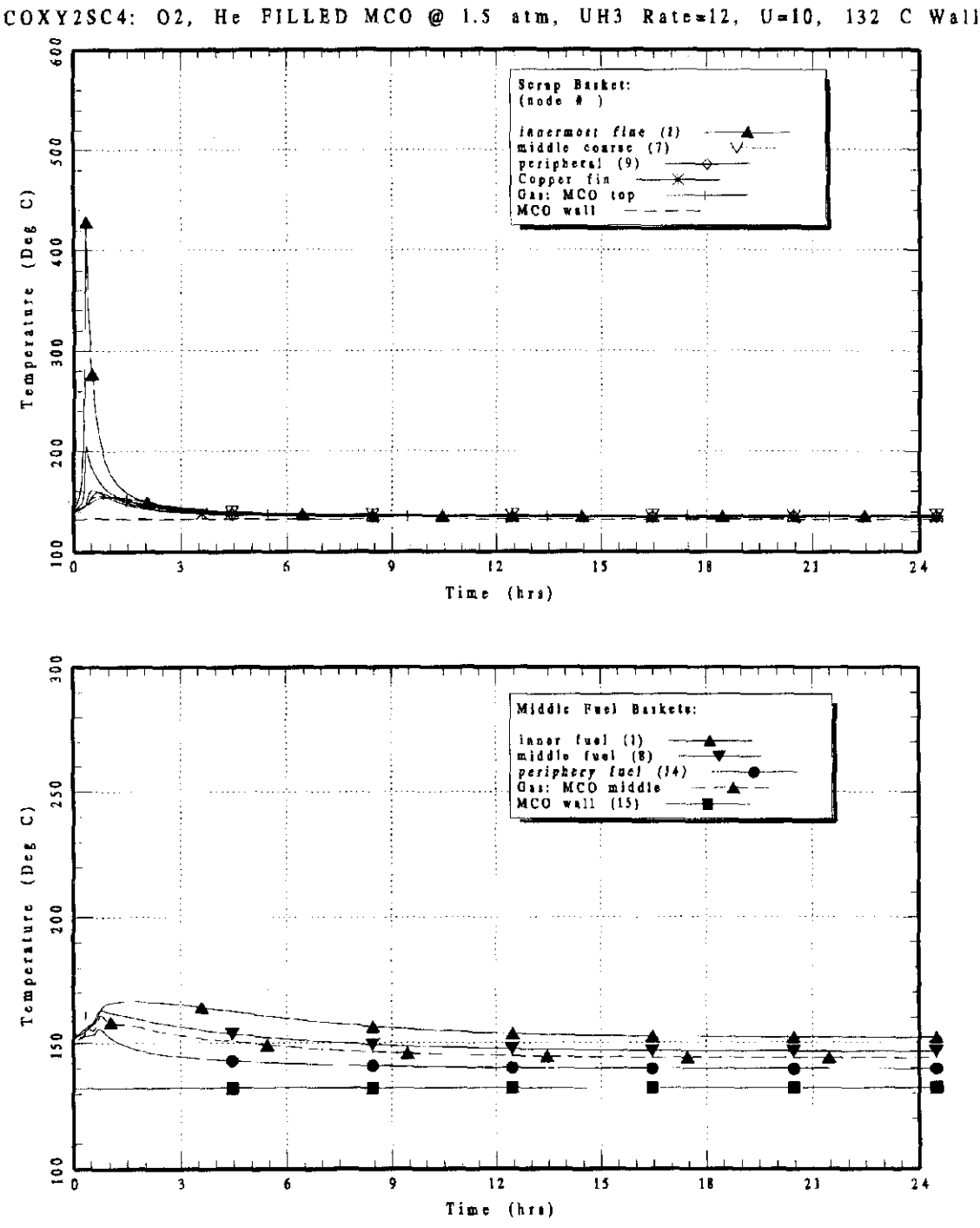

Figure 6-7. Temperature Versus Time for Multi-Canister Overpack Components in Bottom Fuel Basket and Pressure Versus Time for Case 3, COXY2SC4.

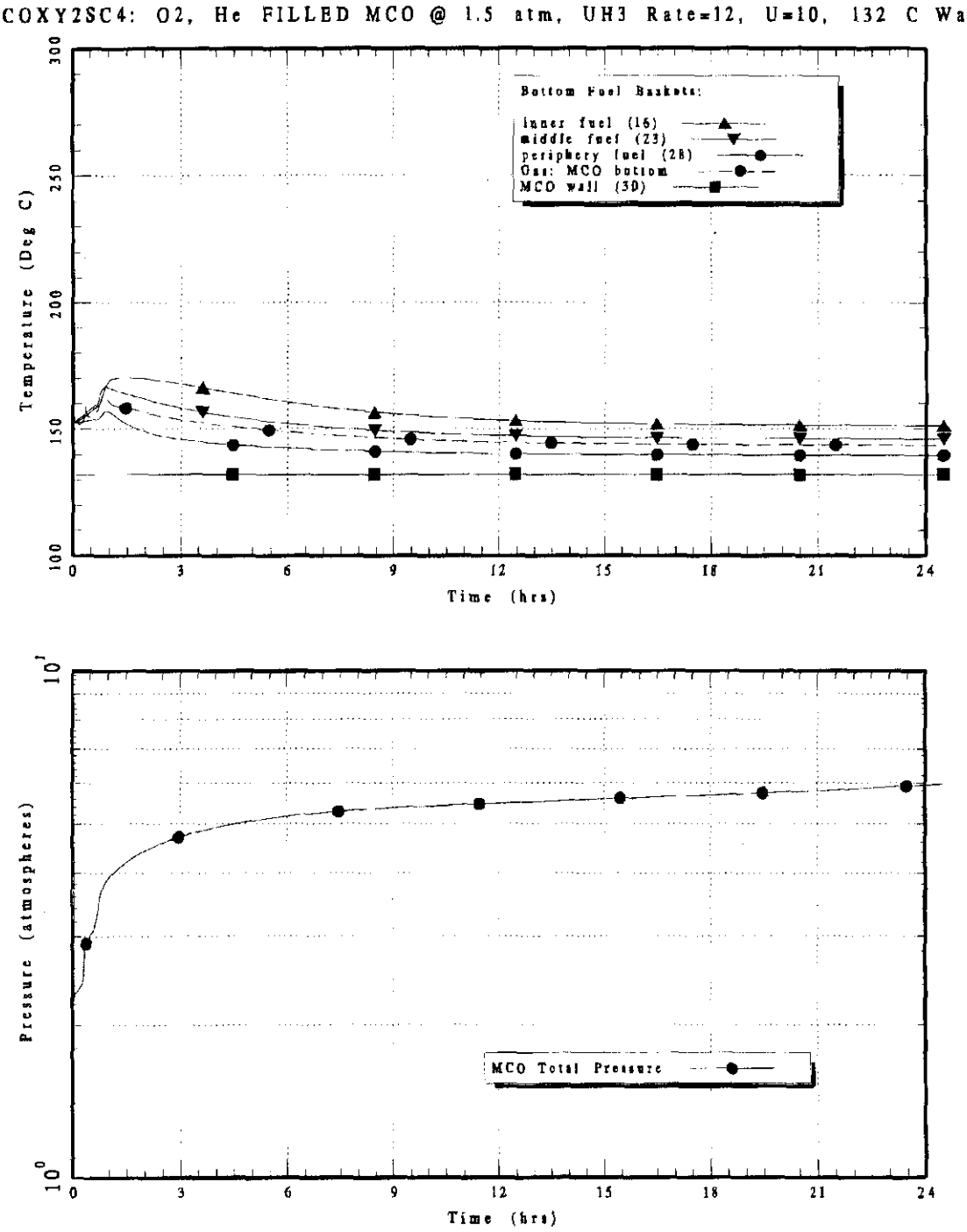

Figure 6-8. Pressure Versus Time for Multi-Canister Overpack
for Case 4, CAIR2SC.

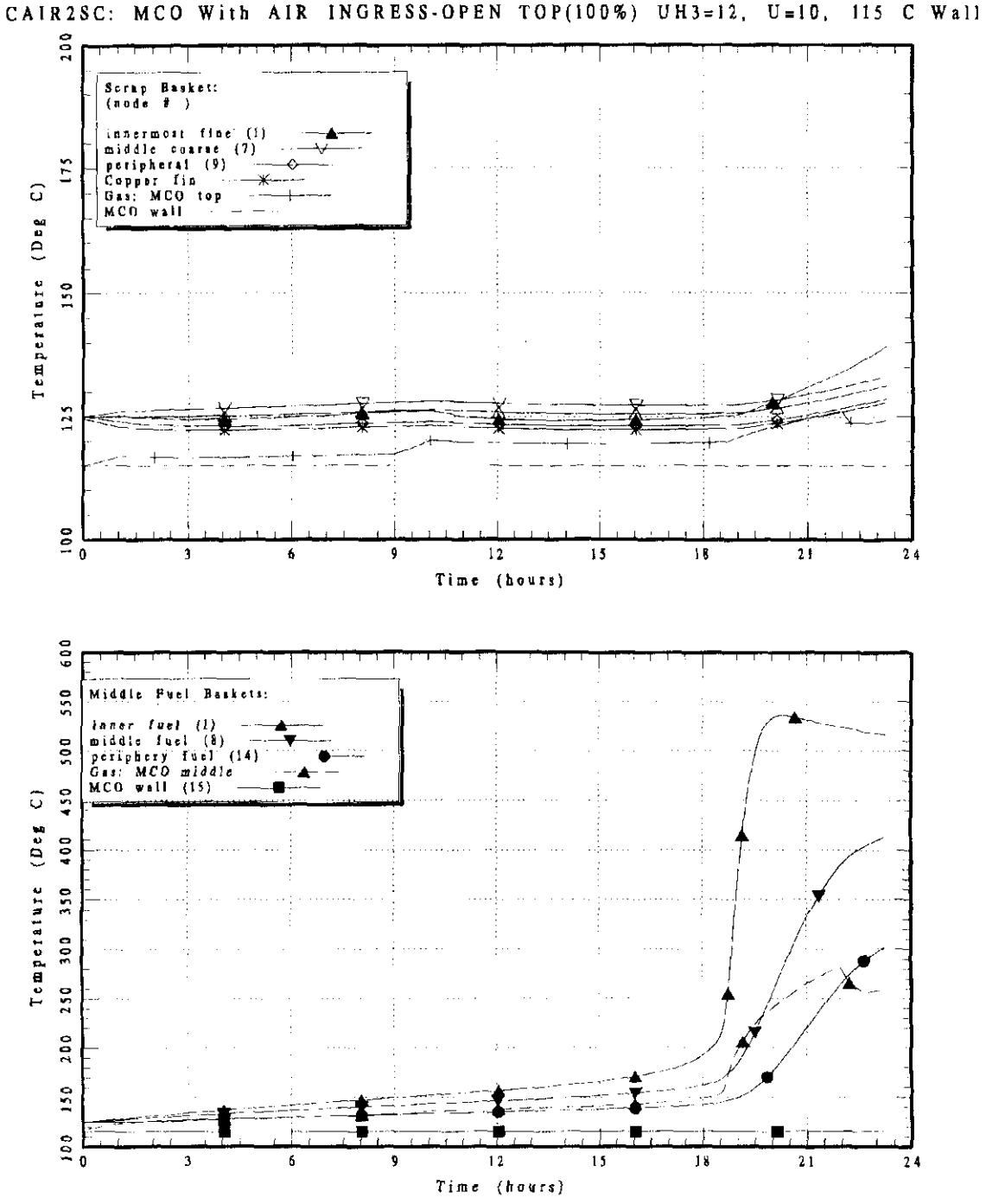

Figure 6-9. Gas Concentrations Versus Time for Multi-Canister Overpack for Case 5, AIRINGRS.

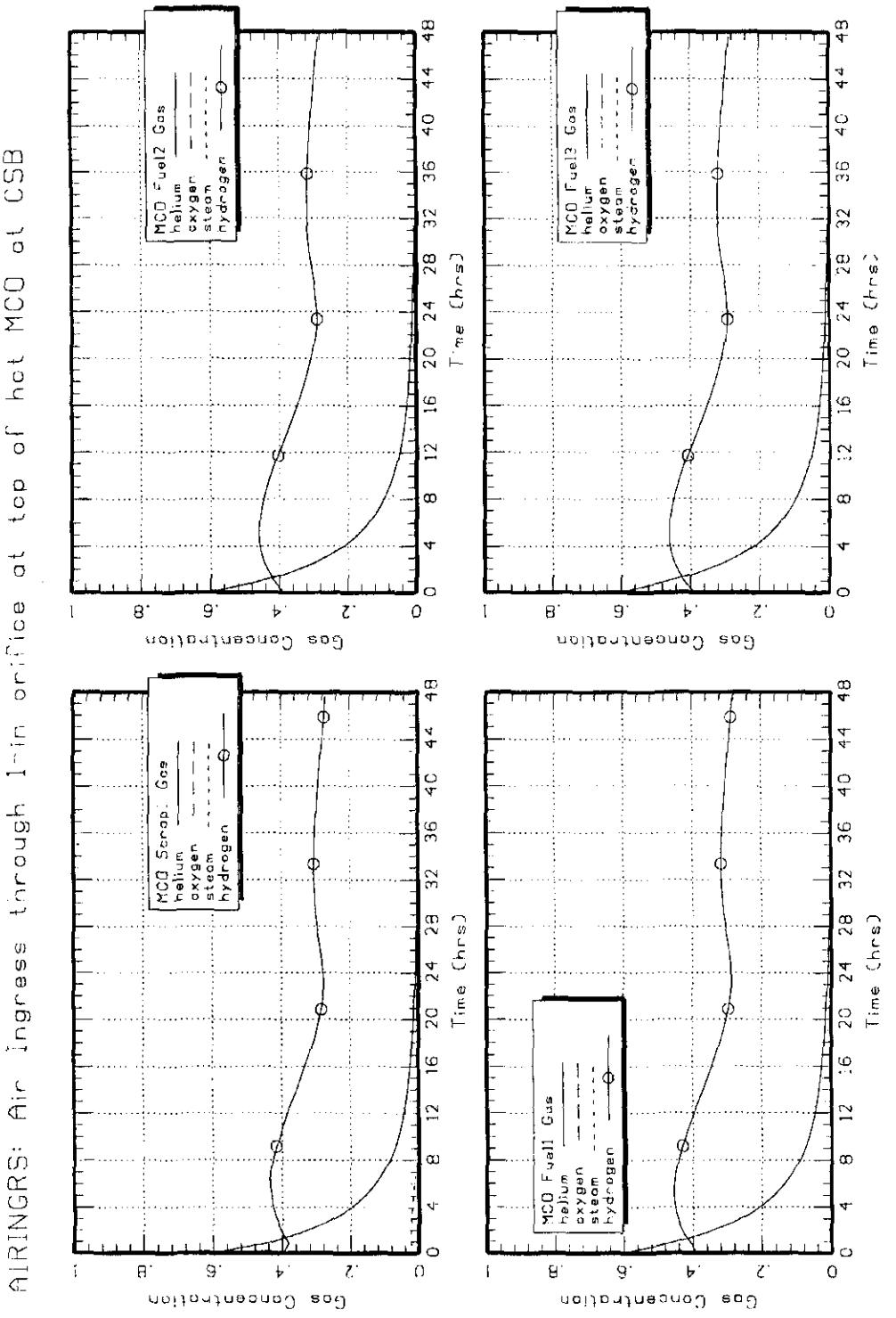

Figure 6-10. Gas Concentration, Purged Gases, and Temperatures Versus Time for Multi-Canister Overpack for Case 5, AIRINGRS.

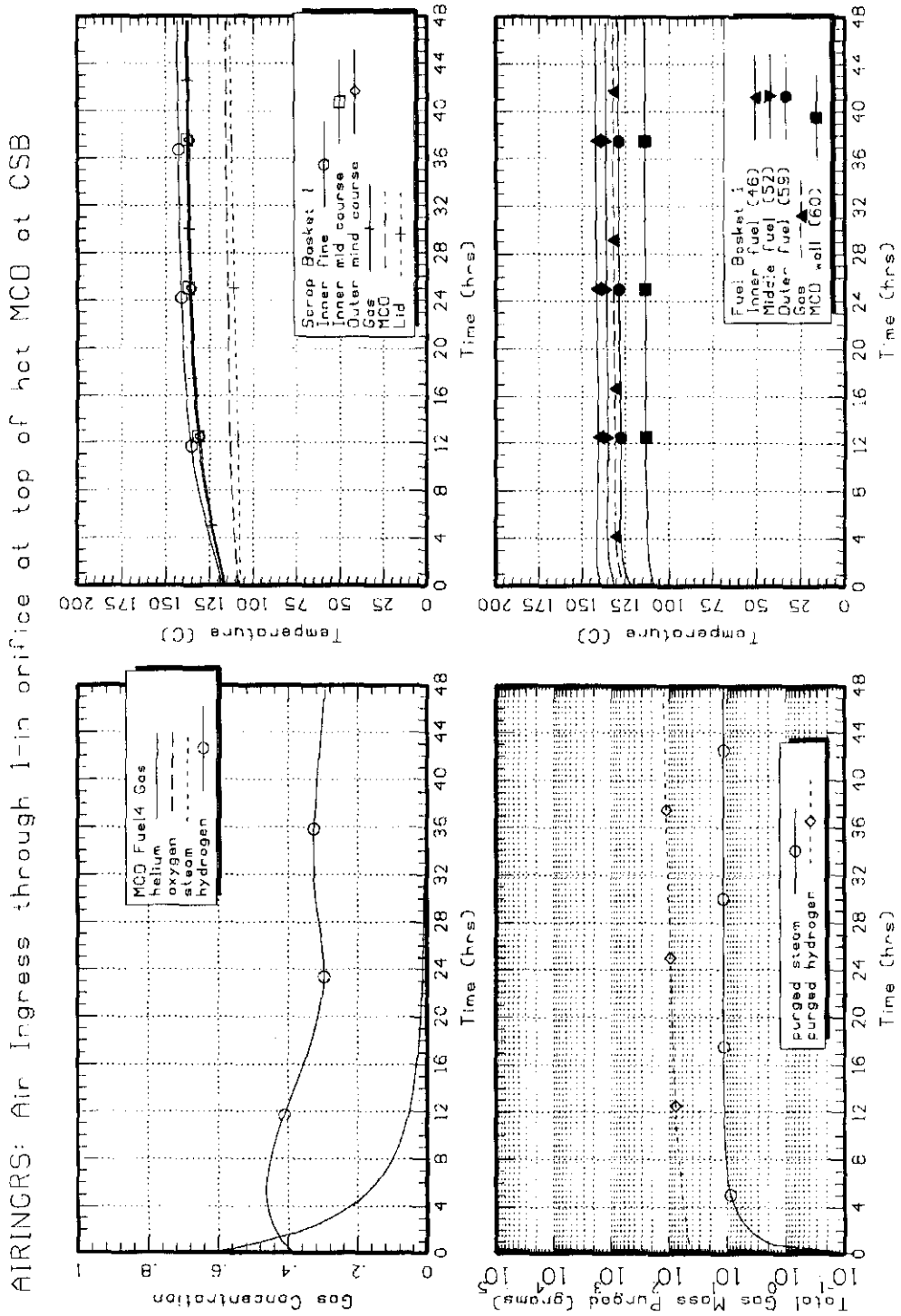

Figure 6-11. Temperatures and Pressures Versus Time for Multi-Canister Overpack for Case 5, AIRINGRS.

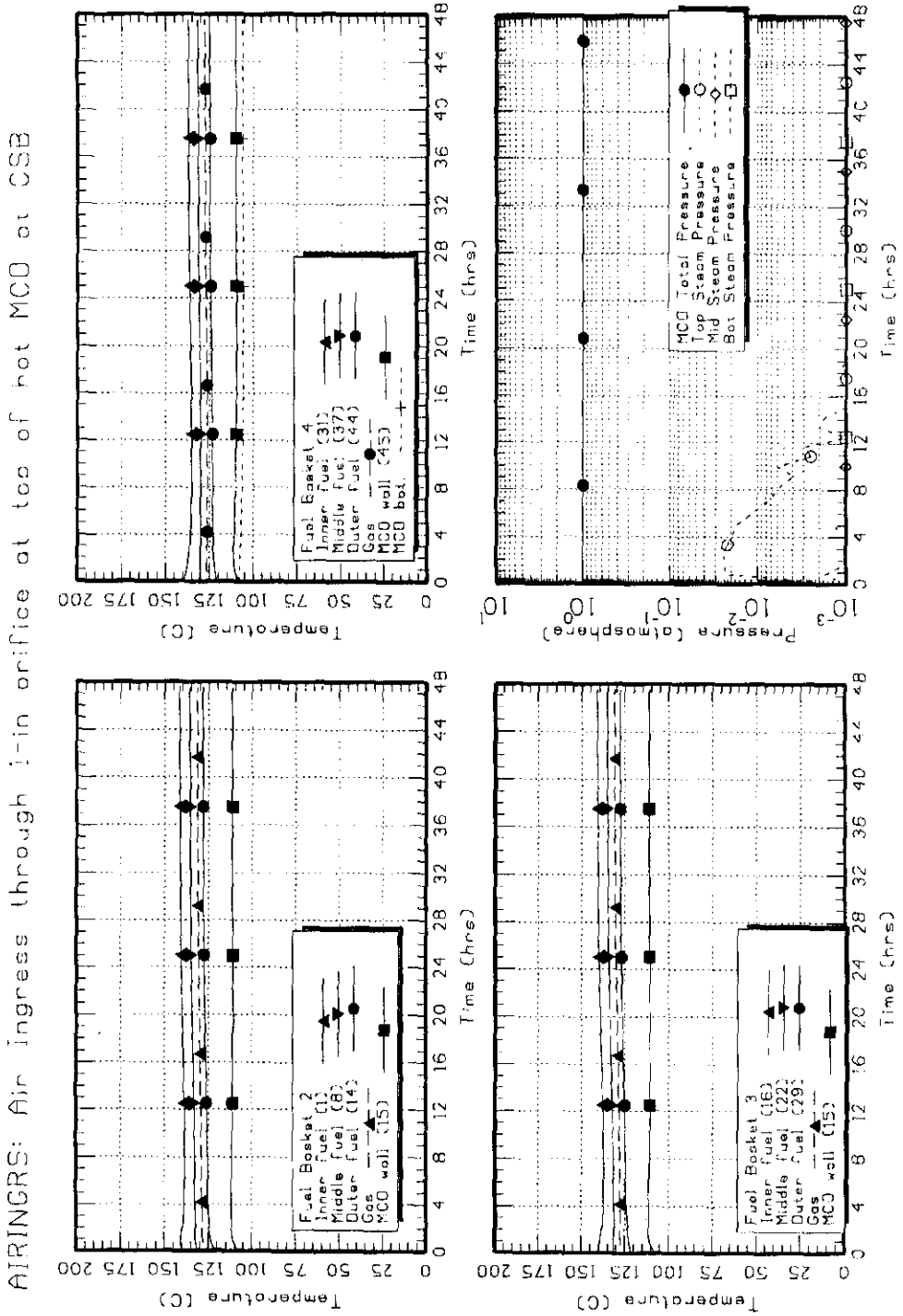

This page intentionally left blank.

APPENDIX 6A

KEY INPUT PARAMETERS FOR THERMAL RUNAWAY FUEL REACTIONS

This page intentionally left blank.

APPENDIX 6A

KEY INPUT PARAMETERS FOR THERMAL RUNAWAY FUEL REACTIONS

Key input parameters used in the analysis for the bounding multi-canister overpack (MCO) with Mark IV fuel under off-normal events at the Canister Storage Building (CSB) are shown in Table 6A-1. Notes are provided following the table. Most parameters are for one scrap basket and four fuel baskets, but some of the key data, like water content in the uranium hydrate, is for two scrap baskets and three fuel baskets in order to provide bounding MCO conditions.

Table 6A-1. Key Input Parameters for Canister Storage Building Thermal Runaway Analysis. (2 sheets)

Parameter	Value	Reference
HEAT GENERATION PARAMETERS: power, reaction area, reaction rate		
Bounding decay power (776 W for five fuel baskets)	740.8 W per MCO	HNF-SD-SNF-TI-015 Note 1
Scrap fuel reaction surface area	4.5 m^2	HNF-SD-SNF-TI-015
Fuel reaction area	3.16 m^2	HNF-SD-SNF-TI-015
Reaction rate multiplier	10	HNF-SD-SNF-TI-015
Rate multiplier for uranium hydride (bounding hydride mass for MCO with two scrap baskets)	Fuel basket: 12 Scrap basket: 12 (5.13 kg per MCO)	HNF-SD-SNF-TI-015 Note 2
RADIATION HEAT TRANSFER PARAMETERS: emissivity, view factors		
Scrap fuel emissivity	0.7	HNF-SD-SNF-TI-015
Cladding emissivity	0.43	HNF-SD-SNF-TI-015 Note 3
Inner shield plug emissivity	0.3	HNF-SD-SNF-TI-015
MCO wall emissivity	0.3	HNF-SD-SNF-TI-015
Cask, MCO bottom, and outer shield plug emissivity	0.25	FAI/98-40 Note 4
View factors and gap distances between fuel rods and MCO wall	8 by 8 matrix	FAI/98-40 Note 5
CONDUCTION HEAT TRANSFER PARAMETERS: mass, conductivity, specific heat, temperature		
Effective fuel–cladding mass density	18,573.3 kg/m^3	Note 6

Table 6A-1. Key Input Parameters for Canister Storage Building Thermal Runaway Analysis. (2 sheets)

Parameter	Value	Reference
Uranium (scrap) mass density at 100 °C	19,000 kg/m^3	Holden 1958 Note 7
Stainless steel mass density at 100 °C	8,000 kg/m^3	TID 26666 Note 8
Maximum fuel mass load (Mark IV fuel)	Scrap basket: 980 kg Fuel basket: 1,268 kg 6,052 kg per MCO	HNF-SD-SNF-TI-015
Effective fuel/clad thermal conductivity	24.2 W/m/K	Note 9
Stainless steel thermal conductivity	16.0 W/m/K	TID 26666
Effective fuel–cladding and uranium specific heat	122.67 J/kg/K	Note 10
Stainless steel specific heat	500.0 J/kg/K	TID 26666
Free residual water in cracks after cold vacuum drying, arriving at CSB	0.2 kg per MCO	HNF-SD-SNF-TI-015
Water in uranium hydrates, $UO_3 \cdot 2H_2O$	1.19 kg per MCO (two scrap baskets)	HNF-SD-SNF-TI-015 Note 11
Water in aluminum hydroxide, and aluminum+iron hydrates in sludge	3.32 kg per MCO (two scrap baskets)	HNF-SD-SNF-TI-015
Bounding MCO wall temperature	132 °C	CSB-HV-0014
CONVECTIVE HEAT AND MASS TRANSFER PARAMETERS: gas volume, flow area, flow rate		
Scrap basket gas volume	0.153 m^3	Note 12
Upper fuel (two fuel baskets) volume	0.186 m^3	Note 13
Lower fuel (two fuel baskets) volume	0.199 m^3	Note 14
Fine scrap porosity	0.40	Note 15
Course scrap porosity	0.723	Note 16
Flow area in scrap basket bottom	0.013 m^2	Note 17

CSB = Canister Storage Building.
MCO = multi-canister overpack.
SB = scrap basket.

Note 1 Bounding decay heat rate — The bounding decay power (i.e., decay heat rate) is given as 776 W per MCO with five Mark IV fuel baskets (155.2 W per fuel basket or

620.8 W for four fuel baskets), so the specific heat rate is 0.1224 W/kgU for Mark IV fuel (HNF-SD-SNF-TI-015). The scrap basket for Mark IV fuel has a maximum fuel loading of 980 kg (HNF-SD-SNF-TI-015), so the scrap basket has a maximum decay power of about 120 W (980 kgU × 0.1224 W/kgU). Hence, the bounding decay power (i.e., decay heat rate) is 740.8 W per MCO (620.8 W + 120 W) with four Mark IV fuel baskets and one Mark IV scrap basket.

Note 2 Rate multiplier for uranium hydride (UH_3) — Oxygen (and water) reacts faster with uranium hydride than with just uranium metal. The current hydride model (HNF-2256) calculates the enhanced reaction rate by increasing the effective surface area of reaction through the use of a rate multiplier. In the current hydride model, the hydrides in the MCO are strongly coupled thermally to the uranium fuel. Hence, any increase in hydride temperature is dissipated in the larger uranium fuel mass, resulting in a temperature increase for the entire fuel element. This analysis uses hydride rate multipliers that are shown in HNF-SD-SNF-TI-015, *Spent Nuclear Fuel Project Technical Databook*. The bounding mass loading of UH_3 in the MCO is 5.13 kg (1.97 kg in three fuel baskets, 3.16 kg in two scrap baskets) (HNF-SD-SNF-TI-015). The computer simulations used a constant rate multiplier of 12 in the simulations for all time, which means that the hydride mass consumption was turned off in the simulations in order to be conservative and not count on a depleting hydride mass for safety.

Note 3 Cladding emissivity — Cladding emissivity is used for the combined fuel–cladding composite heat element in the model because the cladding covers the fuel element on the outside, keeping the uranium fuel hidden. The emissivity of Zircaloy-2 ranges from 0.43 at high temperatures or thin oxide coating to 0.7 (HNF-SD-SNF-TI-015) at normal temperatures and thicker zirconium oxide layers. The more conservative lower value of 0.43 was chosen, which will cause less heat to radiate from the fuel–cladding heat elements to the wall.

Note 4 Cask, MCO bottom, and outer shield plug emissivity — The emissivity of the cask, MCO bottom plate, and the outer shield plug was decreased to 0.25 from 0.30 in HNF-SD-SNF-TI-015 in order to conservatively reduce the heat removal rate from the MCO (HNF-2256) and cask.

Note 5 View factors and gap distances between fuel rods and MCO wall — The view factors and gap distances between the fuel rods in the fuel basket and the MCO wall, which are used in the radiative heat transfer model and convection heat transfer model for an MCO fuel basket, are documented in the HANSF code document (FAI/98-40). However, the view factors used in this analysis differ slightly from those in the code document. The view factors for this analysis, and for the two-scrap basket report (HNF-2256), are described in detail in Appendix D of HNF-SD-SNF-CN-023, *Thermal Analysis of Cold Vacuum Drying of Spent Nuclear Fuel*.

Note 6 Effective fuel–cladding mass density — Since the cladding volume is merged with the fuel volume in the HANSF code (FAI/98-40), an effective mass density is needed for the combined fuel and cladding. To simplify the derivation, the inner fuel element and cladding are assumed to have the same effective mass density as the outer fuel element and its cladding. The total volume for the fuel elements and cladding in the HANSF code is 0.31752 m^3 (FAI/98-40). Since the maximum fuel mass for 216 Mark IV elements (four fuel baskets) is 5,072 kg (23.48 kg per element [HNF-SD-SNF-TI-015]), the volume of the fuel is about 0.26695 m^3, which is calculated by dividing the volume by the fuel density, 19,000 kg/m^3 at 100 °C (Holden 1958). The cladding volume is found by subtracting the fuel volume from the total volume:

$$V_{cladding} = V_{total} - V_{fuel} = 0.31752\ m^3 - 0.26695\ m^3 = 0.05057\ m^3 .$$

Multiplying the density of the Zircaloy-2 cladding, 6,541 kg/m^3 (UNI-M-61), by the volume of cladding gives a cladding mass of 330.8 kg:

$$M_{cladding} = 6{,}541\ kg/m^3 \times 0.26695\ m^3 = 330.8\ kg .$$

For thermal calculations, it is essential that the effective mass (and density) and specific heat product be conserved and, therefore, equal to the sum of the fuel and cladding parts:

$$(M \times C_p)_{eff} = M_{fuel} \times C_{p\text{-}fuel} + M_{cladding} \times C_{p\text{-}cladding}$$

where $C_{p\text{-}fuel}$ = 122.67 J/kg/K (HNF-SD-SNF-TI-015) and $C_{p\text{-}cladding}$ = 306.1 J/kg/K (WCAP-3269-41) .

For convenience, the effective specific heat is set equal to the specific heat of uranium and the effective mass calculated, which can be done since it's the product that must be conserved. Hence, the equation above becomes the following after dividing by the uranium specific heat:

$$M_{eff} = M_{fuel} + M_{cladding} \times C_{p\text{-}cladding}/C_{p\text{-}fuel}$$

$$= 5{,}072\ kg + 330.8\ kg \times (306.1\ J/kg/K \div 122.67\ J/kg/K)$$

$$= 5{,}897.4\ kg .$$

Since the Zircaloy-2 cladding has a higher heat capacity than uranium, the effective mass (in regards to mass times heat capacity product) is larger than just the sum of the masses. Using the calculated effective combined mass of the fuel and cladding above, the effective density of the fuel–cladding composite is simply the effective mass divided by the total volume:

$$\rho_{eff} = M_{eff}/V_{total}$$

$$= 5{,}897.4 \text{ kg}/0.31752 \text{ m}^3$$

$$= 18{,}573.3 \text{ kg/m}^3 .$$

The temperature dependence of densities, specific heats, and conductivities is ignored in the analysis because the HANSF code does not have the capability to handle temperature-dependent material properties (FAI/98-40). In order to be consistent, the material parameter values were chosen at around 100 °C and rounded off.

Note 7 Uranium mass density — The mass density of uranium is about 19,000 kg/m^3 at 100 °C. Since the HANSF code (FAI/98-40) does not include temperature-dependent material parameters, approximate values are used. The standard reference temperature of 100 °C was chosen because it's higher than normal operating temperatures but lower than most temperatures during off-normal conditions.

Note 8 Stainless steel mass density — The mass density of 304L stainless steel is about 8,000 kg/m^3 at 100 °C (TID 26666). See the discussion above in Note 10 about temperature-dependent material properties.

Note 9 Effective fuel–cladding thermal conductivity — Since the fuel elements and cladding are combined in the model, an effective thermal conductivity is needed to represent the combined materials. Although the cladding has a lower conductivity, the conductivity of both metals is high, so the calculation of an effective thermal conductivity is not important to the calculational results.

The effective thermal conductivity, K_{eff}, was estimated using the following equation, which is valid for conductors connected in series such as the fuel and cladding in the radial direction:

$$x_{total}/K_{eff} = x_{fuel}/K_{fuel} + x_{cladding}/K_{cladding}$$

where

K_{fuel} = thermal conductivity of spent fuel (26.9 W/m/K [Kaufman 1962])

$K_{cladding}$ = thermal conductivity of Zircaloy-2 cladding (13.4 W/m/K [WCAP-3269-41])

x_{total} = total radial thickness of fuel element and cladding ($x_{fuel} + x_{cladding}$) .

Since the cladding mass is about 7% of the spent fuel mass (HNF-SD-SNF-TI-015) and the cladding density is about one-third of the fuel density, the cladding was estimated to have about 20% (~7% × 3) of the combined fuel–cladding volume for

both inner and outer fuel elements on the average. The thickness is proportional to the volume, therefore the cladding thickness is estimated to be $0.2 \times x_{fuel}$, making the total thickness $1.2 \times x_{fuel}$. Substituting these values into the equation above, the value of K_{eff} is derived to be 24.2 W/m/K, which is close to fuel conductivity value.

Note 10 Effective fuel–cladding (and uranium) specific heat — As discussed in Note 9, which derived the effective mass density, the effective specific heat for the combined fuel and cladding elements was chosen to be equal to the uranium specific heat, 122.67 J/kg/K at 100 °C (Kaufman 1962). This choice was in conjunction with the effective mass density calculation since it is the product of mass density and specific heat that must be conserved (i.e., the specific heat of the cladding is included in the effective mass density [see Note 9]).

Note 11 The water in hydrates was increased to 1.16 kg for this report in order to provide extra margin over the hydrate water reported elsewhere (e.g., 0.65 kg [HNF-SD-SNF-TI-015]). However, for the "normal" suite of 13 runs, case 0, which simulates a complete drying cycle with tests, the hydrate water was reduced to 0.72 kg (HNF-1527) because the decomposing hydrates can affect the rebound pressure tests after vacuum drying.

Note 12 Scrap basket volume — Based on the latest design drawings (HNF-SD-SNF-DR-003), the scrap basket has a free volume of 0.153 m^3 when it contains 980 kg of uranium metal and no cladding. This volume includes the 0.0533-m (2.1-in) gap between the scrap basket and the bottom of the MCO assembly (below the shield plug) and 0.0159 m^3 void space (manifold) in the MCO assembly (HNF-2833) that is always open to the MCO on top. The scrap basket volume excludes the volume of the stainless steel parts, support post inner volumes, and insert inner volume. The total length of the inner MCO is 3.6 m (141.85 in.) which includes a 0.0533-m (2.1-in.) gap above the scrap basket and a 0.0381-m (1.5-in) gap between the bottom fuel basket and the top of MCO bottom plate. The inner radius of the MCO is 0.2921 m (11.5 in.).

Note 13 Upper fuel volume (two fuel baskets) — The two upper fuel baskets are combined into one control volume in the HANSF model (FAI/98-40). The free volume for the two fuel baskets, excluding the stainless steel volume and inner volume of support posts and insert, is 0.186 m^3 based on the design drawings (HNF-SD-SNF-DR-003).

Note 14 Lower fuel volume (two fuel baskets) — The bottom two fuel baskets have a combined free volume of 0.199 m^3. This volume includes the 0.0381-m (1.5-in) gap below the bottom fuel basket and above the MCO bottom plate with a volume of 0.013 m^3 and excludes the stainless steel volume and inner volume of support posts and insert.

Note 15 Fine scrap porosity — The porosity of the fine scrap fuel (0.25 in. to 1 in. maximum dimension) in the scrap basket is the void or gas space fraction (void volume divided

by total volume) in the total scrap volume when the scrap is completely dry. The porosity of porous media such as a course sand is about 0.35 to 0.45. The porosity of fine scrap was calculated to be in the same range (HNF-SD-SNF-CN-017). A fine scrap porosity of 0.40 was chosen for this analysis.

Note 16 Course scrap porosity — The largest dimension of the course scrap will not be less than 1 in. or greater than 3 in. The total open volume of an empty scrap basket is 0.16762 m^3 (total inner volume minus the insert and copper fin volumes). The fine scrap volume is 0.01592 m^3, and the course scrap volume is 0.1517 m^3. The total solid scrap volume is calculated by dividing the total bounding scrap mass, 980 kg, by the fuel mass density, 19,000 kg/m^3, resulting in a total solid volume of 0.05158 m^3. The solid (fuel) volume in the fine portion is 0.6 (1-porosity) times the total fine scrap volume, 0.01592 m^3, resulting in 0.009552 m^3. Hence, the coarse scrap solid volume is 0.05158 m^3 minus the fine scrap solid volume, 0.009552 m^3, for a value of 0.042028 m^3. Dividing the coarse scrap solid volume by the total coarse scrap volume gives the solid fraction of $0.042028\ m^3 \div 0.1517\ m^3 = 0.27707$ for the coarse portion. Hence, the porosity of the coarse scrap is just 1.0 - 0.27707 for a coarse scrap porosity value of 0.72293.

Note 17 Flow area in scrap basket bottom — The flow area at the bottom of the scrap basket is the only flow area available for the scrap and the total gas release out of the top of the MCO during vacuum drying. Since copper shims have been added between the outer scrap basket and MCO wall, the upward flow has nowhere to go except through the bottom of the scrap basket. The scrap basket bottom has 108 open 0.5-in. diameter holes (HNF-SD-SNF-DR-003) in it. Hence, the total flow area is calculated as follows:

$$A_{SB} = 108 \times 3.14159 \times (0.5 \times 0.0254/2)^2\ m^2$$

$$= 108 \times 1.2668 \times 10^{-4}\ m^2$$

$$= 0.0137\ m^2$$

which was truncated to 0.013 m^2 in order to constrict the gas flow through the scrap basket a little more to account for the wire screen covering part of the holes.

REFERENCES

CSB-HV-0014, 1998, *Long Term MCO Temperature Without Cooling in the Sampling Station,* Fluor Daniel Hanford, Incorporated, Richland, Washington.

FAI/98-40, 1998, *Hanford Spent Nuclear Fuel Safety Analysis Model HANSF 1.2: User's Manual*, Rev. 0, Fauske & Associates, Incorporated, Burr Ridge, Illinois.

HNF-1527, 1997, *Estimates of Particulate Mass in Multi-Canister Overpacks*, Rev. 0, Fluor Daniel Hanford, Incorporated, Richland, Washington.

HNF-2256, 1998, *Simulation of Normal and Off-Normal Multi-Canister Overpack Behavior*, Rev. 2, Fluor Daniel Hanford, Incorporated, Richland, Washington.

HNF-2833, 1998, *Inert Gas Requirements for Cask Loading*, Rev. 0, Fluor Daniel Hanford, Incorporated, Richland, Washington

HNF-SD-SNF-CN-017, 1998, *Fuel Surface Area,* ~~HNF-SD-SNF-CN-017,~~ Rev. 3, Fluor Daniel Hanford, Incorporated, Richland, Washington.

HNF-SD-SNF-CN-023, 1998, *Thermal Analysis of Cold Vacuum Drying of Spent Nuclear Fuel*, Rev. 1, Fluor Daniel Hanford, Incorporated, Richland, Washington.

HNF-SD-SNF-CSER-010, 1998, *Criticality Safety Evaluation Report for the K Basin Fuel Retrieval Subproject*, Rev. 0, Fluor Daniel Hanford, Incorporated, Richland, Washington.

HNF-SD-SNF-DR-003, 1998, *Multi-Canister Overpack Design Report*, Rev. 1, Fluor Daniel Hanford, Incorporated, Richland, Washington.

HNF-SD-SNF-TI-015, 1998, *Spent Nuclear Fuel Project Technical Databook*, Rev. 6, Fluor Daniel Hanford, Incorporated, Richland, Washington.

Holden, A. N., 1958, *Physical Metallurgy of Uranium*, Addison-Wesley Publishing Company, Reading, Massachusetts.

Kaufman, A. R., 1962, *Nuclear Reactor Fuel Elements*, Interscience Publication, New York, New York.

TID 26666, 1987, *Nuclear Systems Material Handbook*, Volume 1, "Design Data," Oak Ridge National Laboratory, Oak Ridge, Tennessee.

UNI-M-61, 1979, *Fuels Engineering Technical Handbook*, United Nuclear Industries, Richland, Washington.

WCAP-3269-41, 1965, *Physical and Mechanical Properties of Zircaloy-2 and 4*, Westinghouse Electric Corporation, Pittsburgh, Pennsylvania.

7.0 CALCULATIONS FOR VIOLATION OF DESIGN TEMPERATURE CRITERIA

7.1 PURPOSE AND OBJECTIVES

Heat is produced in the multi-canister overpack (MCO) from radioactive decay energy release and energy released from chemical reactions that occur between the fuel and water or gases. The MCO and Canister Storage Building (CSB) have been designed to provide for ample heat transfer away from the MCO so that an unacceptably high temperature will not be reached during normal handling and storage of the MCO at the CSB. This analysis investigates possible situations where normal heat conduction may be reduced in such a way or for such a length of time as to result in potential overheating of the MCO and/or surrounding structures.

7.2 SCENARIO DEVELOPMENT

Both radioactive decay and chemical reactions within the MCO generate heat. The bounding situation in which the heat transfer from the MCO to the outside environment is reduced enough to lead to a violation of temperature criteria have been identified by HNF-SD-SNF-HIE-001, *Canister Storage Building Hazard Analysis Report*. In this case, the natural convective cooling air flow to the vault is disrupted and the design temperature for the concrete vault structure is exceeded. This case bounds extended storage of an MCO and MCO effects due to convective heat transfer at other locations in the CSB. It should be noted that the loss of active cooling of an MCO at the weld station is not considered a serious hazard because there are no impacts for loss of cooling for more than 40 days.

7.2.1 Multi-Canister Overpack and Vault Concrete Temperatures During Vault Passive Cooling Disruption

Unacceptable wall temperatures may be reached if the passive cooling of the CSB vault is significantly reduced such that the MCOs in interim storage and vault structure overheat. If the vault intake and/or exhaust stacks are partially or fully blocked, the natural convection of air through the vault will be reduced or lost. Significant blockage of the flow could result from many different, unlikely causes, including debris being trapped in the inlet or frost forming over the inlet. Without the passive vault convective air cooling, temperatures within the vault will rise above design temperature criteria for the vault walls and ceiling and for the MCO centerline. High temperatures could cause the concrete operating deck and vault walls to suffer structural degradation, thereby compromising their safety functions. The MCO temperature could exceed design temperature criteria, which could cause loss of MCO safety functions to confine and control the geometry of the spent nuclear fuel.

ACI-349, *Code Requirements for Nuclear Safety Related Concrete Structures*, provides limitations for concrete temperatures during normal operation or any long-term period. The

temperatures shall not exceed 150 °F (66 °C) except for local areas, such as around penetrations, which are allowed to have increased temperatures not to exceed 200 °F (93 °C). For an accident duration or any short-term period, the concrete surface temperature shall not exceed 350 °F (177 °C).

Bounding calculations documented in CSB-HV-0003, *Spent Nuclear Fuel Vault Loss of Cooling Analysis*, assess the effect of loss or partial loss of vault convective cooling flow upon MCO and vault temperatures. These calculations assume that the vault is full of MCOs and that the corresponding total heat load is 191.6 kW as provided in HNF-SD-SNF-TI-015, *Spent Nuclear Fuel Project Technical Databook*. The outside air temperature available to cool the vault is assumed to be 115 °F (46 °C), and the surrounding ground temperature is assumed to be 60 °F (16 °C). Given these conditions, the maximum initial temperature of the MCO wall (with no blockage of vault air flow) is expected to be about 252 °F (122 °C) and the maximum vault concrete ceiling surface temperature is expected to be 132 °F (56 °C). Calculations in CSB-HV-0003 indicate that if the intake stack cross-sectional area is instantly reduced to 25% of normal (i.e., is 75% blocked), the MCO wall temperature would reach 268 °F (131 °C) and the ceiling temperature would reach 151 °F (66 °C) in 72 hours. Both temperatures continue to rise. If the vault inlet stack were somehow completely blocked, the MCO wall temperature would reach the 270 °F (132 °C) CSB limit in about 15 hours and would continue to rise in temperature at a rate of about 1 degree per hour. If 50% or less of the inlet area were blocked, the vault air flow rate and MCO and ceiling temperatures will be nearly equal to those expected for zero blockage.

The bottom of the inlet area of the vault intake structure is more than 19 m above the surrounding grade. A vertical grating surrounds the opening to the intake stack on four sides. This grating consists of a heavy gauge (0.13-in. wire diameter) interwoven stainless steel screen with 0.75-in. square openings supported by more widely spaced steel cross members. The overall dimensions of this grating are about 15.5 ft by 17 ft on two sides and 15.5 ft by 18 ft on two sides, giving a total flow area for all four vertical inlet grates of about 1,080 ft^2. Inlet air flows through this grating and down the inlet stack to a second horizontal grate inside the inlet stack that serves a safeguards and security function. This horizontal grating is composed of a metal lattice with perpendicular members spaced 6 in. apart. While it is possible for objects to partially block the intake by accumulating on either of these gratings, objects will not easily be able to reach and accumulate on them. Blowing debris, such as tumbleweeds or garbage, will occasionally be lifted to the height of the upper vertical grating and become lodged.

The intake stack horizontal cross-section is rectangular, with minimum interior dimensions of 16 ft by 10 ft, 8 in. producing a flow area of 172 ft^2. Because the intake outer grating is open on all sides and the opening is quite large, it is improbable that a significant portion (>50% blockage) of the intake could become blocked. Both the intake and exhaust are significantly above grade. Over a long period of time, it is conceivable that some debris could accumulate over the opening or pass through the outer grating and accumulate on the inner horizontal grating. Because the openings in the vertical inlet grate are significantly smaller than those of the horizontal grate, it is not considered possible for significant debris to accumulate on the horizontal grate. Because the vertical inlet grating has a total flow area that is more than 6 times that of the

horizontal cross-section of the inlet, about 92% of the vertical grating area must become fully blocked before more than 50% of the inlet cross-section area will be blocked. Given that such a large percentage of the four-sided vertical inlet must become fully blocked and that this inlet is located at such a great height above the existing grade, it is judged incredible for the inlet to block such that an unacceptable passive cooling condition will exist. While it would be prudent to have an infrequent but regular program to visually inspect the inlet for blockage caused by accumulated debris, no such inspection is relied upon. Such an inspection would also ensure that the vertical screen was still intact so that large debris could not pass into the stack.

7.2.2 Multi-Canister Overpack Temperature at the Sampling/Weld Station without Active Cooling

Another possible situation in which unacceptable temperatures may be reached is one in which the MCO is located at the sampling/weld station for an extended period of time without active cooling. Because the MCO is tightly confined at the sampling/weld station, the surrounding steel and concrete act to insulate it from adequate heat transfer once the thermal heat flux through the immediately surrounding materials has reached equilibrium. Calculations documented in CSB-HV-0014, *Long Term MCO Temperature Without Cooling in the Sample Station*, and CSB-S-0043, *HCSA Deck Design — Confirmation*, show that if the initial maximum temperature of the sampling/weld station pit shielding wall is 29 °C (85 °F), the design criteria temperature for the maximum heat generation MCO shell is exceeded in about 50 days and the design criteria temperature for the concrete is exceeded in about 40 days without active cooling.

It should be noted that if a bounding decay heat MCO is indefinitely left in the pit the maximum resulting wall temperature is not expected to exceed 138 °C (280 °F). No adverse effects to the MCO are expected from temperatures slightly above the MCO design temperature. From a safety perspective, wall temperatures above the MCO design temperature do not necessarily damage the safety function of the MCO outer wall or cause damage to MCO internals. See HNF-SD-SNF-SARR-005, *Multi-Canister Overpack Topical Report*, Chapter 4.0, for thermal limitations.

Calculation CSB-S-0043 evaluates the thermal effects on a concrete structure of an MCO left in the sampling/weld pit for 40 days. Using the thermal gradients shown in CSB-HV-0014, the deck and the pit meet all design criteria (worst-case demand–capacity ratio is 0.99 [vertical reinforcing on inside face of the tubular portion of the pit]). The calculation considered concrete strength degradation from thermal exposure by reducing the concrete strength from 4,000 lb/in^2 to 3,000 lb/in^2. This approach is conservative and has been used in other CSB structural calculations to account for concrete degradation.

Since the bounding decay heat MCO can remain in the weld station for more than 40 days without impact to the concrete or the MCO shell, this hazard has been evaluated as being bounded by the loss of vault cooling event.

7.3 SOURCE TERM ANALYSIS

The scenario described above could lead to the damage of safety-class equipment or structures such that their safety function could be compromised. DOE Order 6430.1A, *General Design Criteria*, indicates that safety-class controls are required to prevent conditions that would lead to the damage of safety-class equipment or structures that would impede their ability to perform their safety function. Because the development of radiological source term and dose consequences could not lead to more restrictive safety classification and controls, no source term is developed.

7.4 CONSEQUENCE ANALYSIS

Loss of the vault convective cooling could lead to temperature increases over a long period of time, resulting in potential gradual damage to the vault and operating deck concrete. Heat damage to the concrete would continue slowly once it began. Ample time would be available to identify and correct any loss of air flow condition in the vault. Because the outer vertical inlet screens are so large and are located so far above the existing grade, it is not considered credible for sufficient blockage of the inlet to occur and result in a temperature violation. These temperature criteria violation scenarios will be prevented so that no safety-class structures or equipment will be damaged.

7.5 REFERENCES

ACI-349, 1985, *Code Requirements for Nuclear Safety Related Concrete Structures*, American Concrete Institute, Farmington Hills, Michigan.

CSB-HV-0003, 1996, *Spent Nuclear Fuel Vault Loss of Cooling Analysis*, Fluor Daniel, Incorporated, Richland, Washington.

CSB-HV-0014, 1998, *Long Term MCO Temperature Without Cooling in the Sample Station*, Rev. 0, Fluor Daniel, Incorporated, Richland, Washington.

CSB-S-0043, 1996, *HCSA Deck Design - Confirmation*, Rev. 0, Fluor Daniel, Incorporated, Richland, Washington.

DOE Order 6430.1A, *General Design Criteria*, U.S. Department of Energy, Washington, D.C.

HNF-SD-SNF-HIE-001, 2000, *Canister Storage Building Hazard Analysis Report*, Rev. 3, Fluor Hanford, Incorporated, Richland, Washington.

HNF-SD-SNF-SARR-005, 1999, *Multi-Canister Overpack Topical Report*, Rev. 1, Fluor Daniel Hanford, Incorporated, Richland, Washington.

HNF-SD-SNF-TI-015, 1998, *Spent Nuclear Fuel Project Technical Databook*, Rev. 6, Fluor Daniel Hanford, Incorporated, Richland, Washington.

This page intentionally left blank.

8.0 PEER REVIEW CHECKLIST

PEER REVIEW CHECKLIST

Document Reviewed: SNF-3328, *Canister Storage Building Design Basis Accident Analysis Documentation*

Scope of Review: Changes made to Chapters 1.0, 2.0, 3.0, 4.0, 5.0, and 7.0 since last revision excluding derivation and applicability of statistical source term model and Appendixes 4A, 5A, and 5B. Review included consistency checks with HNF-3353, Annex A (Rev. 0). Calculations in Chap. 5 were checked by alternate hand calculations and all values matched. **

Author: R. D. Crowe, Y. J. Liu, M. G. Piepho, P. D. Rittmann (e.g., ideal gas law)

Yes	No	NA	
[X]	[ ]	[ ] *	Previous reviews complete and cover analysis, up to scope of this review, with no gaps.
[X]	[ ]	[ ]	Problem completely defined.
[X]	[ ]	[ ]	Accident scenarios developed in a clear and logical manner.
[X]	[ ]	[ ]	Necessary assumptions explicitly stated and supported.
[ ]	[ ]	[X]	Computer codes and data files documented.
[X]	[ ]	[ ]	Data used in calculations explicitly stated in document.
[X]	[ ]	[ ]	Data checked for consistency with original source information as applicable.
[X]**	[ ]	[ ]	Mathematical derivations checked including dimensional consistency of results.
[X]	[ ]	[ ]	Models appropriate and used within range of validity or use outside range of established validity justified.
[X]	[ ]	[ ]	Hand calculations checked for errors. Spreadsheet results should be treated exactly the same as hand calculations.
[ ]	[ ]	[X]	Software input correct and consistent with document reviewed.
[ ]	[ ]	[X]	Software output consistent with input and with results reported in document reviewed.
[ ]	[ ]	[X]	Limits/criteria/guidelines applied to analysis results are appropriate and referenced. Limits/criteria/guidelines checked against references.
[X]	[ ]	[ ]	Safety margins consistent with good engineering practices.
[X]	[ ]	[ ]	Conclusions consistent with analytical results and applicable limits.
[X]	[ ]	[ ]	Results and conclusions address all points required in the problem statement.
[ ]	[ ]	[X]	Format consistent with appropriate NRC Regulatory Guide or other standards
[ ]		[X] *	Review calculations, comments, and/or notes are attached.
[X]	[ ]	[ ]	**Document approved.**

frank A. medsker — Mark A. Medsker — 3/20/00

Reviewer (Printed Name and Signature) — Date

* Any calculations, comments, or notes generated as part of this review should be signed, dated and attached to this checklist. Such material should be labeled and recorded in such a manner as to be intelligible to a technically qualified third party.

CHECKLIST FOR PEER REVIEW

Document Reviewed: SNF-3328, *Canister Storage Building Design Basis Accident Analysis Documentation*

Scope of Review: Changes made to Chapter 5.0 since last revision

Author: P. D. Rittmann, R. D. Crowe

Yes	No	NA	
[ ]	[ ]	[X] *	Previous reviews complete and cover analysis, up to scope of this review, with no gaps.
[√]	[ ]	[ ]	Problem completely defined.
[√]	[ ]	[ ]	Accident scenarios developed in a clear and logical manner.
[√]	[ ]	[ ]	Necessary assumptions explicitly stated and supported.
[√]	[ ]	[ ]	Computer codes and data files documented.
[√]	[ ]	[ ]	Data used in calculations explicitly stated in document.
[√]	[ ]	[ ]	Data checked for consistency with original source information as applicable.
[√]	[ ]	[ ]	Mathematical derivations checked including dimensional consistency of results.
[√]	[ ]	[ ]	Models appropriate and used within range of validity or use outside range of established validity justified.
[√]	[ ]	[ ]	Hand calculations checked for errors. Spreadsheet results should be treated exactly the same as hand calculations.
[ ]	[ ]	[√]	Software input correct and consistent with document reviewed.
[ ]	[ ]	[√]	Software output consistent with input and with results reported in document reviewed.
[√]	[ ]	[ ]	Limits/criteria/guidelines applied to analysis results are appropriate and referenced. Limits/criteria/guidelines checked against references.
[√]	[ ]	[ ]	Safety margins consistent with good engineering practices.
[√]	[ ]	[ ]	Conclusions consistent with analytical results and applicable limits.
[√]	[ ]	[ ]	Results and conclusions address all points required in the problem statement.
[√]	[ ]	[ ]	Format consistent with appropriate NRC Regulatory Guide or other standards
[ ]		[√] *	Review calculations, comments, and/or notes are attached.
[√]	[ ]	[ ]	**Document approved.**

Yih Justin Liu 3/16/00

Reviewer (Printed Name and Signature) Date

* Any calculations, comments, or notes generated as part of this review should be signed, dated and attached to this checklist. Such material should be labeled and recorded in such a manner as to be intelligible to a technically qualified third party.

CHECKLIST FOR PEER REVIEW

Document Reviewed: SNF-3328, *Canister Storage Building Design Basis Accident Analysis Documentation*

Scope of Review: Changes made to Chapters 6.0 since last revision

Author: M. G. Piepho

Yes	No	NA	
[X]	[ ]	[ ] *	Previous reviews complete and cover analysis, up to scope of this review, with no gaps.
[X]	[ ]	[ ]	Problem completely defined.
[X]	[ ]	[ ]	Accident scenarios developed in a clear and logical manner.
[X]	[ ]	[ ]	Necessary assumptions explicitly stated and supported.
[X]	[ ]	[ ]	Computer codes and data files documented.
[X]	[ ]	[ ]	Data used in calculations explicitly stated in document.
[X]	[ ]	[ ]	Data checked for consistency with original source information as applicable.
[ ]	[ ]	[X]	Mathematical derivations checked including dimensional consistency of results.
[X]	[ ]	[ ]	Models appropriate and used within range of validity or use outside range of established validity justified.
[X]	[ ]	[ ]	Hand calculations checked for errors. Spreadsheet results should be treated exactly the same as hand calculations.
[X]	[ ]	[ ]	Software input correct and consistent with document reviewed.
[X]	[ ]	[ ]	Software output consistent with input and with results reported in document reviewed.
[ ]	[ ]	[X]	Limits/criteria/guidelines applied to analysis results are appropriate and referenced. Limits/criteria/guidelines checked against references.
[X]	[ ]	[ ]	Safety margins consistent with good engineering practices.
[X]	[ ]	[ ]	Conclusions consistent with analytical results and applicable limits.
[X]	[ ]	[ ]	Results and conclusions address all points required in the problem statement.
[X]	[ ]	[ ]	Format consistent with appropriate NRC Regulatory Guide or other standards
[ ]		[X] *	Review calculations, comments, and/or notes are attached.
[X]	[ ]	[ ]	**Document approved.**

RALPH D CROWE Ralph C 3/20/00

Reviewer (Printed Name and Signature) Date

* Any calculations, comments, or notes generated as part of this review should be signed, dated and attached to this checklist. Such material should be labeled and recorded in such a manner as to be intelligible to a technically qualified third party.

CHECKLIST FOR PEER REVIEW

Document Reviewed: SNF-3328, *Canister Storage Building Design Basis Accident Analysis Documentation*

Scope of Review: Derivation and applicability of statistical source term model

Author: R. D. Crowe

Yes	No	NA	
[X]	[ ]	[ ] *	Previous reviews complete and cover analysis, up to scope of this review, with no gaps.
[X]	[ ]	[ ]	Problem completely defined.
[X]	[ ]	[ ]	Accident scenarios developed in a clear and logical manner.
[X]	[ ]	[ ]	Necessary assumptions explicitly stated and supported.
[ ]	[ ]	[X]	Computer codes and data files documented.
[X]	[ ]	[ ]	Data used in calculations explicitly stated in document.
[X]	[ ]	[ ]	Data checked for consistency with original source information as applicable.
[X]	[ ]	[ ]	Mathematical derivations checked including dimensional consistency of results.
[X]	[ ]	[ ]	Models appropriate and used within range of validity or use outside range of established validity justified.
[X]	[ ]	[ ]	Hand calculations checked for errors. Spreadsheet results should be treated exactly the same as hand calculations.
RLG [X]	[ ]	[X]	Software input correct and consistent with document reviewed.
RLG [X]	[ ]	[X]	Software output consistent with input and with results reported in document reviewed.
[X]	[ ]	[ ]	Limits/criteria/guidelines applied to analysis results are appropriate and referenced. Limits/criteria/guidelines checked against references.
[X]	[ ]	[ ]	Safety margins consistent with good engineering practices.
[X]	[ ]	[ ]	Conclusions consistent with analytical results and applicable limits.
[X]	[ ]	[ ]	Results and conclusions address all points required in the problem statement.
[X]	[ ]	[ ]	Format consistent with appropriate NRC Regulatory Guide or other standards
[ ]		[X] *	Review calculations, comments, and/or notes are attached.
[X]	[ ]	[ ]	**Document approved.**

Richard L. Garrett 3/27/00

Reviewer (Printed Name and Signature) Date

* Any calculations, comments, or notes generated as part of this review should be signed, dated and attached to this checklist. Such material should be labeled and recorded in such a manner as to be intelligible to a technically qualified third party.

DISTRIBUTION SHEET

To	From	Page 1 of 1
Distribution	Nuclear Safety	Date 3/22/00
Project Title/Work Order		EDT No. N/A
SNF-3328, Rev. 2 Canister Storage Building Design Basis Accident Analysis Documentation		ECN No. 656349

Name	MSIN	Text With All Attach.	Text Only	Attach./ Appendix Only	EDT/ECN Only
B. J. Craig (5)	R3-26	X			
R. D. Crowe	R3-26	X			
R. L. Garrett	R3-26	X			
L. J. Garvin	R3-26	X			
Y. J. Liu	R3-26	X			
B. D. Lorenz	R3-26	X			
M.A. Medsker	R3-26	X			
M. G. Piepho	R3-26	X			
P. D. Rittmann	B4-43	X			
SNF Project Files	R3-11	X			